

Impact of amino acid side chain fluorination on proteolytic stability of peptides



Inaugural-Dissertation to obtain the academic degree
Doctor rerum naturalium (Dr. rer. nat.)

Submitted to the Department of Biology, Chemistry and Pharmacy
of Freie Universität Berlin

By

Vivian Asante

From Koforidua, Ghana

November 2014

1st Reviewer: Prof. Dr. Beate Koksch (Freie Universität Berlin)

2nd Reviewer: Prof. Dr. Rainer Haag (Freie Universität Berlin)

Date of defense: 10.02.2015

Erklärung

Die vorliegende Arbeit wurde auf Anregung und unter Anleitung von Frau Prof. Dr. Beate Kokschi in der Zeit von Oktober 2009 bis November 2014 an dem Institut für Chemie und Biochemie des Fachbereichs Biologie, Chemie, Pharmazie der Freien Universität Berlin angefertigt.

Hiermit versichere ich, dass ich die vorliegende Arbeit mit dem Titel "Impact of amino acid side chain fluorination on proteolytic stability of peptides", ohne Benutzung anderer als der zugelassenen Hilfsmittel selbstständig angefertigt habe. Alle angeführten Zitate sind als solche kenntlich gemacht. Die vorliegende Arbeit wurde in keinem früheren Promotionsverfahren angenommen oder als ungenügend beurteilt.

Berlin, November 2014,

Vivian Asante

Publication List

Peer-reviewed Major Publications: Journal Articles and Conference Proceedings

1. **Asante, V.**, Mortier, J., Wolber, G., Kokschi, B. (2014): Impact of fluorination on proteolytic stability of peptides: a case study with α -chymotrypsin and pepsin. Amino acids. DOI: <http://dx.doi.org/10.1007/s00726-014-1819-7>
2. **Asante, V.**, Mortier, J., Schlüter, H., Kokschi B., (2013): Impact of fluorination on proteolytic stability of peptides in human blood plasma. Bioorganic & Medicinal Chemistry 21: 3542-3546. DOI:10.1016/j.bmc.2013.03.051
3. Cadicamo, D.C., **Asante, V.**, Ammar, A.M., Borelli, C., Korting, C.H., Kokschi, B., (2009): Investigation of the synthetic route to pepstatin analogues by SPPS using O-protected and O-unprotected statine as building blocks. Journal of Peptide Science, 15: 272-277. DOI:10.1002/psc.1111
4. **Asante, V.**, Kokschi, B., (2013): Impact of fluorination on proteolytic stability of peptides; a case study using α -chymotrypsin and pepsin. 4th Annual Workshop of the Fluorine Graduate School "Fluorine as a Key Element" Potsdam, Germany, 10-11. 10.2013.
5. **Asante, V.**, (2012): Investigating the impact of side-chain fluorinated amino acids on proteolytic stability of peptides, Promotion Seminar of Rosa Luxemburg Stiftung, Berlin, Germany, 14-15.06. 2012.
6. **Asante, V.**, Kokschi, B., (2012): Impact of fluorination on the proteolytic stability of peptides towards alpha- chymotrypsin and pepsin, International Symposium on Fluorine Chemistry Kyoto, Japan, 22-27. 07.2012.
7. **Asante, V.**, Kokschi, B., (2012): Investigating the impact of side-chain fluorinated amino acids on proteolytic stability, 15. Deutschen Fluorotagung (15th German Fluorine day) Schmitten, Germany, 24-26. 09.2012.
8. **Asante, V.**, Kokschi, B., (2012): Impact of fluorination on proteolytic stability of peptides in human blood plasma, 3rd Annual Workshop of the Fluorine Graduate School "Fluorine as a Key Element" Spreewald, Germany, 22-23. 10.2012.
9. **Asante, V.**, Kokschi, B., (2012): Impact of fluorination on the proteolytic stability of peptides towards proteolytic enzymes and human blood plasma, Fluorine Graduate School Winter Semester 12/13 Berlin, Germany, 22-23. 11.2012.

Aus dieser Dissertation gingen bisher die Veröffentlichungen 1&2 hervor

Acknowledgements

I wish to express my utmost sincere gratitude and appreciation to Prof. Dr. Beate Kokschi who has been a friend and mentor, for the supervision of this study. I would like to thank her for her guidance, advice, support and comprehensive encouragement that enabled me to pursue my study to completion. I also wish to thank my second supervisor, Prof. Dr. R. Haag, for his support towards my study. I am greatly indebted to him for all the time and effort he committed to this study.

My sincere gratitude goes to Prof. Dr. Beate Röder of Humboldt-University of Berlin, Germany, for her motherly love and kindness. I also appreciate the continuous advice and assistance from Dr. Cosimo D. Cadicamo in the course of my study and Dr. Allison Ann Berger for her suggestions and careful editing of this thesis.

I would like to also express my sincere gratitude to Dr. Jérémie Mortier of FU Berlin, for the molecular modeling study which provided the in-depth interpretation of the results. I am grateful to Prof. Dr. Hartmut Schlüter and his group (University of Hamburg) for their collaboration and the supply of human blood plasma used in this study. My special thanks go to Dipl.-Biochem. Matthias Hakelberg for introducing me to this topic. I am grateful to Dr. Mario Salwiczek for his continuous advice and support in the course of my research. I also wish to thank all the members of the AG Kokschi group, for the competent advice and for the motivating working atmosphere in the laboratory.

I highly appreciate the support and advice from Prof Dr. Daniel Obeng-Ofori, Ghana and Mr. Udo Kummerow, Berlin.

Most of all, I would like to express special thanks to my husband (Dr. Charles Adarkwah, University of Development Studies, Temale, Ghana), our lovely children, Crystal and Jayson, my extended family members and all my friends for their love, care, support and understanding throughout my study. I am also grateful to my only brother Dr. Freeman Adane, Canada, for his support, advice and his brotherly love.

I am highly indebted to the Rosa Luxemburg Stiftung (RLS) for granting me a Ph.D. scholarship that supported my living in Germany. I also acknowledge the financial support extended to me by the Deutsche Forschungsgemeinschaft (Research Training Group “Fluorine as Key Element”).

Finally, I wish to thank all that I may not have mentioned, who supported me in many different ways for their material and moral support, advice and criticisms.

Dedication

This thesis is dedicated to all my family members who assisted me in my education especially Madam Theresa Osei-Nyarko (New York), Mr. Adjekum Asante (Nkawkaw) and the late Mr. Charles Baffour Anim (Nkawkaw).

“Life is like a book, each day is a new page.”

Abstract

Protease stability is a pivotal consideration in the development of peptide-based drugs. Improving the bioavailability of pharmacologically active peptides requires in-depth investigation into the noncovalent interactions between the protease and the peptide substrate under consideration. To this end, different strategies such as the use of unnatural building blocks and fluorinated amino acids have become standard approaches in protein engineering. The incorporation of fluorine into amino acids has attracted much interest in recent years due to the unique stereoelectronic properties of fluorine, which have already proven useful in the development of therapeutically active small molecules.

In this manner, the current thesis presents data on the systematic investigation of the influence of side chain fluorination on proteolytic stability of peptide sequences that are based on ideal protease substrates. Several model peptides were designed according to the specificities of serine and aspartic proteases; three different control sequences were modified by introducing either 2-aminobutyric acid (Abu) or one of its fluorinated derivatives at the P2, P1' or P2' positions. Through the use of an RP-HPLC assay with fluorescence detection, the proteolytic stabilities of these peptides toward α -chymotrypsin, pepsin, elastase, proteinase K and human blood plasma proteases were determined. Molecular modeling was used to support the interpretation of the structure-activity relationship based on the analysis of potential ligand-enzyme interactions.

In all cases, increases and decreases in proteolytic stability were observed for the different isolated enzymes and the human blood plasma, and these effects depend upon the particular peptide sequence, the fluorine content of the side chain, and the position of substitution relative to the cleavage site. Interestingly, in some cases fluorination leads to dramatic improvements in resistance to degradation: namely, TfeGly and DfeGly at the P2' position with pepsin; DfeGly at the P2 position with chymotrypsin; TfeGly and DfeGly at the P2 and P2' positions with proteinase K; and TfeGly at the P2 and P1' positions with elastase. Our observations indicate that although the fluorination of peptide substrates does not always have predictable effects on proteolytic stability, this strategy for developing more bioavailable peptide therapies is promising; in particular, part of this thesis was devoted to establishing an analytical approach for the identification of fluorinated peptide-based HIV-1 entry inhibitors.

Kurzzusammenfassung

Die Proteasestabilität ist ein wichtiges Kriterium bei der Entwicklung von Peptid-basierten Medikamenten. Daher umfasst die Verbesserung der Bioverfügbarkeit von pharmakologisch aktiven Peptiden eine gründliche Untersuchung der nichtkovalenten Interaktionen zwischen Protease und Peptidsubstrat. In diesem Zusammenhang gehören verschiedene Strategien, wie beispielsweise die Verwendung von nicht-natürlichen Aminosäuren mittlerweile zu etablierten Methoden im Protein Engineering. Der Einbau fluorierte Aminosäuren hat in den letzten Jahren besonders an Bedeutung gewonnen, da das Element Fluor über einzigartige stereoelektrische Eigenschaften verfügt, die sich bei der Entwicklung von Pharmazeutikern als nützlich erwiesen haben.

Die vorliegende Arbeit beschreibt die systematische Untersuchung des Einflusses von unterschiedlichen Fluormodifikationen auf die Proteasestabilität von Modelpeptiden, deren Sequenzen auf idealen Proteasesubstraten basieren. Die untersuchten Modelpeptide wurden dabei so entwickelt, dass sie für Serin- und Aspartatproteasen spezifisch sind. Die Peptide wurden so modifiziert, dass sie entweder α -Aminobuttersäure (Abu) oder dessen fluorierte Derivate in den Positionen P2, P1' oder P2' enthielten. Mit Hilfe eines RP-HPLC basierten Assays, welcher eine Fluoreszenzdetektion der Spaltprodukte nutzte, wurde die proteolytische Stabilität der jeweiligen Peptide gegenüber den isolierten Proteasen α -Chymotrypsin, Pepsin, Elastase, Proteinase K sowie in Anwesenheit von menschlichem Blutplasma ermittelt. Die Interpretation der Struktur-Wirkungsbeziehung wurde zusätzlich durch Molecular Modeling Simulationen unterstützt, welche auf den spezifischen Ligand-Enzym Wechselwirkungen basierten.

In allen untersuchten Fällen wurden sowohl höhere als auch geringere Proteasestabilitäten für die isolierten Enzyme sowie für das humane Blutplasma gefunden. Diese Effekte ergaben sich in Abhängigkeit von der Peptidsequenz, vom eingesetzten Enzym, von der jeweils substituierten Position relativ zur Schnittstelle des Enzyms und den jeweilig eingebauten fluorierten Aminosäuren, die einen unterschiedlichen Fluorgehalt in der Seitenkette aufweisen. Interessanterweise führt der Einbau fluorierte Aminosäuren in die Peptidsequenzen in einigen Fällen zu einer deutlich gesteigerten Proteasestabilität. Diese Effekt wurde in folgenden Fällen beobachtet: a) für den Einbau von TfeGly und DfeGly in P2' Position des Substrats mit Pepsin als Enzym; b) für DfeGly in P2 Position gegenüber α -Chymotrypsin; c) für TfeGly und DfeGly in den Positionen P2 und P2' in Anwesenheit von Proteinase K; und d) für TfeGly eingebaut in P2 und P1' Position mit dem Enzym Elastase. Unsere Ergebnisse zeigen, dass Fluormodifikationen einen unvorhersehbaren Effekt auf die proteolytische Stabilität von Peptiden haben können und somit eine viel versprechende Strategie für die Entwicklung von Peptidbasierten Therapeutikern sein können. Unter dieser Berücksichtigung wurde ein Teil dieser Arbeit der Etablierung eines analytischen Ansatzes für die Identifikation von fluorierten Peptiden gewidmet, welche als potentielle HIV1-Eintritts Inhibitoren Anwendung finden könnten.

ABBREVIATIONS

| | |
|-------------------|--|
| Å | Angstrom (1 Angstrom = 1.0×10^{-10} m) |
| AA | Amino acid |
| ACN | Acetonitrile |
| ADAMs | A disintegrin and metalloproteinases |
| AMP | Antimicrobial peptides |
| Boc | tert-Butyloxycarbonyl |
| CD | Circular dichroism |
| CHR | Carboxy-terminal heptad repeat |
| Da | Dalton |
| DBU | 1,8-diazabicyclo[5.4.0]undec-7-ene |
| DCM | Dichloromethane |
| DIC | Diisopropylcarbodiimide |
| DIPEA | N,N-diisopropyl ethylamine |
| DMF | Dimethylformamide |
| DMSO | Dimethylsulfoxide |
| DNA | Deoxyribonucleic acid |
| eq. | equivalent |
| ESI-ToF-MS | Electrospray ionization Time-of-Flight Mass Spectrometry |
| FDA | Food and Drug Administration) |
| Fmoc | 9-fluorenylmethyloxycarbonyl |
| GdnHCl | Guanidine hydrochloride |
| gp41 | glycoprotein 41 |
| HIV | Human immunodeficiency virus |
| HOAt | 1-hydroxy-7-azabenzotriazole |
| HOBt | 1-hydroxybenzotriazole |
| HPLC | High Performance Liquid Chromatography |
| IR | Infrared |
| MD | Molecular dynamics |
| MMPs | Matrix metalloproteinases |
| MW | Molecular weight |
| NHR | Amino-terminal heptad repeat |
| NMP | N-Methyl-2-pyrrolidinone |
| NMR | Nuclear magnetic resonance |
| PBS | Phosphate-Buffered Saline |
| PDB | Protein Data Bank |
| PEG | Polyethylene glycol |

| | |
|--------------------|---|
| pGlu | pyroglutamic acid |
| Pip | Piperidine |
| RP | Reversed phase |
| Rpm | Revolutions per minute |
| SEC | Size exclusion chromatography |
| SPPS | Solid phase-peptide synthesis |
| SPR | Surface plasmon resonance |
| TBTU | O-(benzotriazol-1-yl)-N,N,N',N'-tetramethyluronium tetrafluoroborate |
| <i>t</i>-Bu | <i>tert</i> -Butyl |
| Tert | tertiary |
| TFA | Trifluoroacetic acid |
| TIS | Triisopropylsilane |
| ToF | Time of flight |
| Tris | Tris-(hydroxymethyl)aminomethane |
| UV | Ultraviolet |
| vdW | van der Waals |
| Vis | Visible |

Abbreviations of the 20 canonical amino acids are consistent with the biochemical nomenclature proposed by the IUPAC-IUB commission (Eur. J. Biochem. **1984**, 138: 9-37).

Abbreviations of non-coded amino acids relevant to the present thesis are given below.

If not stated otherwise, the abbreviations correspond to the L-amino acids.

| | |
|---|---|
| 4³-F₃Ile | 4',4',4'-Trifluoroisoleucine; (2S,3R)-2-amino-3 trifluoromethyl)pentanoic acid |
| 4³-F₃Val | 4,4,4-Trifluorovaline; (<i>S</i>)-2-amino-3-(trifluoromethyl)butanoic acid |
| 5³,5³-F₆Leu | 5,5,5,5',5',5'-Hexafluoroisoleucine |
| 5³-F₃Ile | 5,5,5-Trifluoroisoleucine; (<i>S</i>)-2-amino-5,5,5-trifluoropentanoic acid |
| Abu | Aminobutyric acid; (<i>S</i>)-2-aminobutyric acid |
| Abz | ortho-aminobenzoic acid |
| Aib | Aminoisobutyric acid |
| DfeGly | Difluoroethylglycine; (<i>S</i>)-2-amino-4,4-difluorobutanoic acid |
| DfpGly | Difluoropropylglycine; (<i>S</i>)-2-amino-4,4-difluoropentanoic acid |
| HfV | 4,4,4,4',4',4'-Hexafluorovaline |
| MfeGly | Monofluoroethylglycine; (<i>S</i>)-2-amino-4-fluorobutanoic acid |

TfeGly

Trifluoroethylglycine; (*S*)-2-amino-4,4,4-trifluorobutanoic acid

TfmAla

Trifluoromethylalanine, 2-amino-2-(trifluoromethyl)propanoic acid

Table of Contents

Chapter 1

| | | |
|----|-------------------|---|
| 1. | Introduction..... | 1 |
|----|-------------------|---|

Chapter 2

| | | |
|---------|--|----|
| 2. | Theory / Literature | 3 |
| 2.1 | Proteases | 3 |
| 2.1.1 | Functions and importance of proteases..... | 3 |
| 2.1.2 | Classification of Proteases | 3 |
| 2.1.3 | Serine proteases | 6 |
| 2.1.3.1 | α -Chymotrypsin (EC 3.4.21.1) as a model enzyme..... | 7 |
| 2.1.4 | Aspartic proteases | 9 |
| 2.1.4.1 | Pepsin (EC 3.4.23.1) as a model enzyme..... | 9 |
| 2.2 | Nomenclature of proteases..... | 12 |
| 2.3 | Enzyme kinetics..... | 13 |
| 2.4 | Plasma..... | 16 |
| 2.4.1 | Protease stability in blood plasma..... | 16 |
| 2.4.2 | Chemical approaches used to enhance proteolytic stability and biological activity of peptides and proteins | 17 |
| 2.4.3 | Nonproteinogenic amino acids and unnatural amino acids in peptide modification | 19 |
| 2.4.4 | Types of nonproteinogenic amino acids | 20 |
| 2.4.4.1 | Inversion of configuration (D-amino acids)..... | 20 |
| 2.4.4.2 | Alkylation | 20 |
| 2.4.4.3 | Fluorination..... | 20 |
| 2.4.5 | Types of fluorinated amino acids used in peptide and protein modification | 21 |
| 2.4.6 | Fluoroalkyl amino acids and protease stability of fluorinated peptides and proteins | 25 |
| 2.4.7 | Protease catalyzed peptide synthesis with fluorinated amino acids..... | 28 |
| 2.4.8 | Use of fluorinated amino acids in enzyme/protease inhibitors | 31 |

Chapter 3

| | | |
|----|--------------------------|----|
| 3. | Aim and motivation | 35 |
|----|--------------------------|----|

Chapter 4

| | | |
|-------|--|----|
| 4. | Applied analytical methodologies..... | 37 |
| 4.1 | High Performance Liquid Chromatography (HPLC)..... | 37 |
| 4.1.1 | UV detection..... | 40 |
| 4.1.2 | Fluorescence detection..... | 42 |
| 4.1.3 | Coupling HPLC to a mass spectrometer (LC/MS) | 43 |
| 4.2 | Molecular modelling (molecular dynamics) | 45 |

| | |
|------------------|--|
| Chapter 5 | |
| 5. | Results and Discussion47 |
| 5.1 | Design of model peptides for proteolytic stability studies.....47 |
| 5.2 | Enzymatic assay and protease stability of peptides49 |
| 5.2.1 | Stability Measurements.....49 |
| 5.2.2 | Molecular modeling of FA variants with α -chymotrypsin and pepsin51 |
| 5.2.3 | Hydrolysis of peptides by α -Chymotrypsin (EC 3.4.21.1)52 |
| 5.2.3.1 | P2 variants.....52 |
| 5.2.3.2 | P1' variants.....61 |
| 5.2.3.3 | P2' variants.....62 |
| 5.2.4 | Hydrolysis of peptides by Pepsin (EC 3.4.23.1)66 |
| 5.2.4.1 | P2 variants.....66 |
| 5.2.4.2 | P1' FA peptide.....68 |
| 5.2.4.3 | P2' variants.....69 |
| 5.2.5 | Reaction of the peptides with proteinase K (EC 3.4.21.64).....72 |
| 5.2.6 | Comparing all control peptides with studied enzymes75 |
| 5.3 | Plasma studies.....77 |
| 5.3.1 | Plasma assay77 |
| 5.3.2 | Incubation of a substrate with the immobilized proteins77 |
| 5.3.3 | Nonimmobilized plasma reactions.....82 |
| 5.4 | Proteolytic stability of peptides towards Elastase (EC 3.4.21.36)87 |
| 5.4.1 | FA Analogues87 |
| 5.4.2 | Hydrolysis of the FK and FF peptides analogues88 |
| | |
| Chapter 6 | |
| 6. | Efforts toward protease stable and high affinity fluorinated HIV entry inhibitors 91 |
| | |
| Chapter 7 | |
| 7. | Conclusion101 |
| | |
| Chapter 8 | |
| 8. | Outlook105 |
| | |
| Chapter 9 | |
| 9. | Experimental part.....109 |
| 9.1 | General methods109 |
| 9.2 | Synthesis of fluorinated amino acids110 |
| 9.2.1 | Synthesis of (S)-2-amino-4,4,4- trifluoroethylglycine (TfeGly)110 |
| 9.2.1.1 | Synthesis of diethyl 2-acetamido-2-(2,2,2-trifluoroethyl) malonate (3a)110 |
| 9.2.1.2 | Synthesis of 2-amino-4,4,4- trifluoroethylglycine (3b)110 |
| 9.2.1.3 | Synthesis of 2-acetamido-4,4,4-trifluoroethylglycine (3c)111 |
| 9.2.1.4 | Synthesis of (S)-2-amino-4,4,4- trifluoroethylglycine (3d)111 |
| 9.2.1.5 | Synthesis of (S)-Fmoc-TfeGly (3e)112 |
| 9.2.2 | Synthesis of (S)-DfeGly.....113 |
| 9.3 | Solid-Phase Peptide Synthesis (SPPS)113 |
| 9.3.1 | Automated peptide synthesis114 |
| 9.3.2 | Manual peptide synthesis.....115 |

| | | |
|-------------------|--|-----|
| 9.3.3 | Capping of free α -amino groups | 115 |
| 9.3.4 | Cleavage of peptide from resin | 116 |
| 9.3.5 | Analytical HPLC | 116 |
| 9.3.6 | Preparative HPLC | 117 |
| 9.3.7 | Mass spectrometry analysis | 117 |
| 9.4 | Protease stability of peptides | 119 |
| 9.4.1 | Isolated enzyme assay | 119 |
| 9.4.2 | Determination of Michaelis Menten kinetics using HPLC | 121 |
| 9.4.3 | Inhibition assay | 121 |
| 9.5 | Plasma studies..... | 122 |
| 9.5.1 | Plasma preparation..... | 122 |
| 9.5.2 | Immobilization of plasma proteins onto CNBr-activated Sepharose Beads® | 122 |
| 9.5.2.1 | Preparation of the gel..... | 123 |
| 9.5.2.2 | Immobilization of plasma proteins | 123 |
| 9.5.2.3 | Incubation of the peptides with the immobilized proteins | 123 |
| 9.5.3 | Nonimmobilization of plasma proteins experiments | 124 |
| 9.6 | Molecular modeling..... | 124 |
| 9.7 | Synthesis of trivalent linker | 125 |
| 9.7.1 | Synthesis of tert-butyl 1-hydroxy-3,6,9,12-tetraoxapentadecan-15-oate{ 1 } | 125 |
| 9.7.2 | Synthesis of tert-butyl 1-(tosyloxy)-3,6,9,12-tetraoxapentadecan-15-oate{ 2 } | 126 |
| 9.7.3 | Coupling of tert-butyl 1-(tosyloxy)-3,6,9,12-tetraoxapentadecan-15-oate to Tris | 127 |
| 9.7.4 | Synthesis of N-Fmoc-tris(hydroxymethyl)aminomethane..... | 127 |
| Chapter 10 | | |
| 10. | References..... | 129 |

1. Introduction

Proteases are essential biological molecules that are found in all organisms. Since their identification, proteases have well been characterized and are known to carry out significant biological and physiological processes including digestion, haemostasis, apoptosis, signal transduction, reproduction and the immune response. Proteases are also well-known for their involvement in disease states such as cancer, viral infections, Alzheimer's disease, inflammatory and cardiovascular disorders.^[1,2] Over the past decades, proteases have found applications in the pharmaceutical and biotechnological industries^[3] and are now being used as drug targets and therapeutics. Several protease inhibitors have been approved by the U.S. FDA (Food and Drug Administration) and more are still in clinical studies, meaning that proteases will continue to represent a distinct curative class with various clinical applications.^[4]

Research in medicinal chemistry is increasingly being devoted to the exploration of peptide- and protein-based drugs, due to their incomparable selectivity among macromolecules. Natural peptides have numerous other advantages over small molecules, on the one hand, and antibodies, on the other hand, including affinity (multivalency) and membrane permeability, depending on the sequence. However, their use in pharmaceuticals or as drug candidates has been hampered by different factors such as serum sensitivity or short plasma half life, conformational flexibility, metabolic instability, low bioavailability, solubility and, in some cases, membrane permeability. Most peptide based drugs under production are unsuccessful due to toxicity, lack of efficacy, or poor bioavailability.^[5,6] Currently, a large number of biotherapeutics are now being marketed owing to newly improved chemical and biological synthetic strategies leading to improved bioavailability, reduced elimination and biodegradation and increased selectivity or affinity to the receptor or target.^[6]

Over the past few decades, a number of strategies have been employed to increase the enzymatic stability of peptides, including the introduction of nonproteinogenic amino acids such as β -amino acids, N-methylated amino acids, D-amino acids, PEGylated amino acids, and to a lesser extent, fluorinated analogues.^[7-9] In general, the introduction of non-canonical amino acids with newly designed side-chain functionalities serves as a powerful tool to improve kinetic and thermodynamic properties, proteolytic and structural stabilization of peptides and proteins in a way not possible using exclusively the repertoire of the 20 canonical amino acids.^[10-14]

INTRODUCTION

Due to its outstanding properties, fluorine has become an important element in various chemical industrial fields like agriculture, materials science, pharmaceuticals and mining.^[15,16] Substitution of fluorine in molecules has demonstrated a valuable improvement for therapeutic agents^[17,18] by enhancing hydrophobicity and metabolic stability, which in turn lead to improved bioactivity and bioavailability.^[19]

The involvement of fluorine in the design of artificial amino acids is now being explored in many peptide or protein therapeutics, a class of promising agents with high specificity but low metabolic stability.^[20] Studies on the protease-catalyzed incorporation of different fluoroalkyl-substituted amino acids and the impact of fluorinated building blocks on the structure, stability and activity of biologically active peptides have shown the importance of the fluorine content and the position of fluorination within an amino acid sequence of peptides and proteins.^[21-24] Recent research work has also indicated that the inclusion of fluorinated amino acids into peptides and globular proteins can have unpredictable effects on activity and stability.^[19,25-30] Thus, the properties of fluorine in protein and peptide environments still remain challenging to control and for this reason further systematic investigations are indispensable to generate modified peptides with the increased proteolytic properties and improved bioavailability required for pharmaceutical agents.

2. Theory / Literature

2.1 Proteases

Proteases, found in all organisms, are proteolytic enzymes comprising a group of structurally and functionally diverse proteins that have the ability to catalyze the hydrolysis of peptide bonds.^[31] They had been well characterized biochemically prior to becoming the subject of crystallographic studies.^[32] Proteases account for approximately 2% of the human genome and 1-5% of the genomes of infectious organisms.^[33] More recently, proteases have gained much interest in a wide variety of fields of chemistry due to their pivotal roles in digestion and the regulation of key physiological processes, and their numerous industrial applications.

2.1.1 Functions and importance of proteases

Proteases are involved in diverse physiological reactions, including controlling the activation, synthesis, and turnover of proteins, crucial regulatory roles in coagulation, conception, birth, digestion, growth, maturation, aging, inflammatory diseases and cell death. They also play an important role in host-pathogen interactions involving viruses, bacteria, fungi, and parasites.^[34-41]

Due to their important regulatory roles in the life cycle, they represent a largely untapped family of potential therapeutic targets for drug development. Proteases also have a wide range of industrial applications, including their use in laundry detergents, cheese making, bating (softening) leather, modifying food ingredients (e.g. soy protein whipping agents), meat tenderizers, and flavor development.^[42] They are also used in synthetic organic chemistry as biocatalysts. Finally, due to their ability to hydrolyze or synthesize peptide bonds with high specificity under mild conditions, they are widely used in proteomics and enzyme technology.^[43,44]

2.1.2 Classification of Enzymes and Proteases

Proteases have historically been classified as endoproteases, which target internal peptide bonds, or exopeptidases (aminopeptidases and carboxypeptidases), the action of which is directed by the NH₂ and COOH termini of their corresponding substrates.

However, the increasing availability of structural and mechanistic information has led to new classification schemes for proteases by the International Union of Biochemistry.^[45] These include serine, cysteine, aspartic, threonine, metalloproteases and glutamic acid proteases; it must be noted that glutamic acid proteases have not yet been identified in mammals. Each class has a characteristic set of functional amino acid residues arranged in a particular spatial distribution to form the active site. These classes are made up of diverse families that differ from each other in their amino acid sequence but have a similar mechanism of catalysis and active site geometry.^[46] Accordingly, Rawlings and Barrett grouped proteases into evolutionary clans and families based on the evidence of similar tertiary structures (clan), the order of catalytic residues in their sequences, or common sequence motifs (family) around the catalytic residues and thereby created a database of proteases (MEROPS).^[47-51] The database uses a hierarchical path to classify proteases and proteins into species, families (with their first character representing A, aspartic; C, cysteine; G, glutamic acid; M, metallo; S, serine; T, threonine; and U, unknown) and then clans. This classification framework aims to distinguish one protease from another by identifying the specificity of the peptidase in terms of proteolytic hydrolysis of the substrates and interaction with inhibitors.

In spite of their differences, there exist general mechanistic features among all classes of proteases: their active sites contain residues that serve as active nucleophile, general base, or general acid in the catalytic mechanism for substrate hydrolysis. The specificity for a particular amino acid in their active site leads to the nomenclature proposed by Schechter and Berger in 1967 (Figure 2.5).^[52]

To provide a broader context for these enzymes, it is important to note that different classes of enzymes and their subclasses are defined according to the chemical reaction they catalyze, and have been grouped by the Nomenclature Committee of IUBMB (International Union of Biochemistry and Molecular Biology) into a numbering scheme called the Enzyme Commission number (EC number).^[53] This numbering system divides reactions into six key groups and then subdivides these three more times yielding a unique four-digit identifier for each member (Table 2.1).

THEORY

Table 2.1 Six major classes of enzymes^[53]

| EC number | Class | Type of reaction | Example |
|-----------|-----------------|---|--|
| 1.1.y.z | Oxidoreductases | Oxidation-reduction | Lactate dehydrogenase |
| 2.1.y.z | Transferases | Group transfer | Nucleoside monophosphate kinase (NMP kinase) |
| 3.1.y.z | Hydrolases | Hydrolysis reactions (transfer of functional groups to water) | Chymotrypsin |
| 4.1.y.z | Lyases | Addition or removal of groups to form double bonds | Fumarase |
| 5.1.y.z | Isomerases | Isomerization (intramolecular group transfer) | Triose phosphate isomerase |
| 6.1.y.z | Ligases | Ligation of two substrates at the expense of ATP hydrolysis | Aminoacyl-tRNA synthetase |

Note: The first number represents the class of the enzyme, the second digit indicates the subclass, the third (y) gives the sub-subclass, and the fourth (z) is the serial number of the enzyme in its sub-subclass.

The threonine proteases consist of proteolytic enzymes that possess a threonine (Thr) residue within the active site. They are able to process misfolded and denatured proteins in a non-specific manner and play a vital role in the ubiquitin-dependent proteolytic pathway.^[54] The mechanism used to cleave peptide bonds involves the use of the secondary alcohol of the N-terminal threonine as a nucleophile by polarizing an ordered water which deprotonates the alcohol to increase its reactivity.^[55-59]

Metalloproteinases (metalloproteases) are a family of peptide-cleaving enzymes whose catalytic mechanism involves a metal (mostly zinc or calcium ion). They mainly consist of metzincin enzymes including serralysins, astacins, adamalysins (a disintegrin and metalloproteinase domain, ADAMs) and matrixins (matrix metalloproteinases, MMPs).^[60-62] The MMPs are usually involved in the release of growth factors from cell membranes, cleavage of growth factor receptors from the cell surface, shedding of cell adhesion molecules, and activation of other MMPs, among other non-catabolic functions.^[63-65] The ADAMs mainly function as extracellular domains cleaving many membrane proteins from the cell surface (ectodomain shedding).^[66-69] Like aspartic proteases, metalloproteinases use a metal ion (Zn) to activate a water molecule in a noncovalent catalysis mechanism in which the metal ion is coordinated to the protein via a glutamate residue and a histidine serves as base.^[60,67,70]

Cysteine proteases can be grouped into about 30 families based on their three dimensional structure. Papain, an enzyme purified from the fruit of the papaya, is the best-described member of the family of cysteine proteases; mammalian analogues of it, the cathepsins, have also been identified.^[71]

They utilize a mechanistic strategy similar to that of the chymotrypsin family. In principle, a cysteine residue, activated by a histidine residue, plays the role of the nucleophile that attacks the peptide bond in a manner quite analogous to that of the serine residue in serine proteases. The basic features of the mechanism include the formation of a covalent intermediate, the acyl-enzyme, resulting from nucleophilic attack of the active site thiol group on the carbonyl carbon of the scissile amide or ester bond of the bound substrate.^[72] Cysteine proteases are known to mediate functions such as intracellular protein catabolism and selective activation of signaling molecules (interleukin, enkephalin, protein kinase C) or extracellular protein degradation (bone resorption, macrophage function).^[73]

Serine and aspartic proteases are described in more detail in the following paragraph as they were applied in this doctoral dissertation.

2.1.3 Serine proteases

These enzymes form the largest group of known proteases.^[47-50] They are found in eukaryotes, prokaryotes, archaea and viruses and play pivotal roles in many vital physiological processes, including digestion (trypsin and chymotrypsin), the immune response (complement factors B, C, D), blood coagulation (factors VIIa, IXa, Xa, XIIa), fibrinolysis (urokinase, tissue plasminogen activator, plasmin, kallikrein) and reproduction (acrosin).^[74,75]

Since its mechanism was first reported in the 1960s by Bender and his co-workers,^[76] many studies enabled the details to be established: three amino acid residues (histidine, aspartic acid, and serine), the catalytic triad, which function in a “charge relay” system in the active site upon hydrolysis of a peptide bond.^[74-88] Generally, the serine acts as the nucleophile, histidine acts as the general base or acid, and the aspartate helps to orient the histidine residue and neutralize the charge that develops on the histidine. According to this scheme a proton is exchanged from Ser195 to His57 and from His57 to Asp102 (double proton transfer).^[88] Studies from different groups using different methods of analysis, such as nuclear magnetic resonance (NMR) and neutron diffraction studies have confirmed a single proton exchange from Ser195 O γ to the His57N ϵ 2.^[58,89-93] Well-studied members with three dimensional structures are chymotrypsin, trypsin, elastase, and subtilisin.^[93-96]

However, it has also been reported that there are other serine proteases that carry out catalysis/hydrolysis with other catalytic residue arrangements other than the canonical triad and are described as atypical serine proteases. They use novel triads such as Ser/His/Glu, Ser/His/His, or Ser/Glu/Asp, dyads such as Ser/Lys or Ser/His, or a single Ser catalytic residue.^[58,97] Chymotrypsin and trypsin are two of the best studied serine proteases of this family, and these achieve catalysis through the Ser/His/Asp triad.

2.1.3.1 α -Chymotrypsin (EC 3.4.21.1) as a model enzyme

α -chymotrypsin a serine endopeptidase that is initially synthesized in the pancreas as the inactive zymogen chymotrypsinogen, and converted to the active enzyme in the intestine by tryptic cleavage. It has 245 residues and is arranged in two six-stranded beta barrels. There are several crystal structures of chymotrypsin-ligand complexes reported in the protein data base (PDB, Figure 2.1), and they reveal three domains; the catalytic, the substrate recognition and the zymogen activation domains.^[86] The active site region is composed of the substrate binding groove, the substrate specificity binding pockets, the catalytic Ser/His/Asp triad, and the oxyanion hole.^[58]

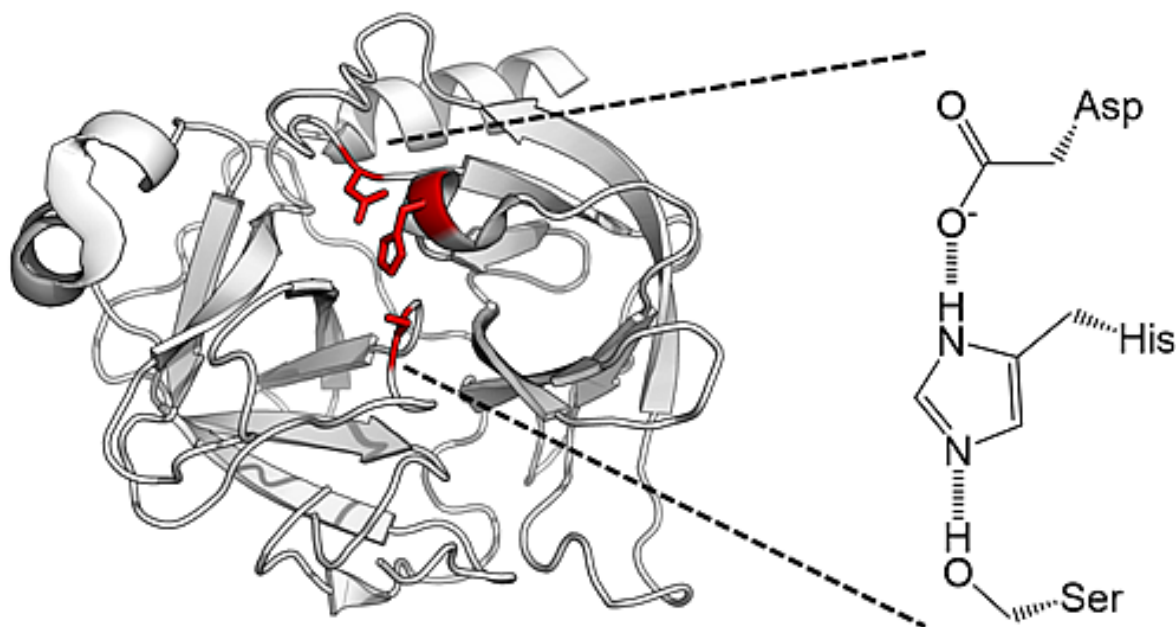


Figure 2.1 Crystal structure of α -chymotrypsin showing the catalytic residues (Asp-His-Ser). PDB ID: 4CHA

THEORY

The well-known mechanism involves the imidazole ring of histidine (His57), which, with the aid of the proton-withdrawing aspartate (Asp102), deprotonates the serine hydroxyl (Ser195), enabling nucleophilic attack on the substrate carbonyl carbon (Figure 2.2a) resulting in a tetrahedral intermediate bearing an oxyanion (Figure 2.2b). The oxyanion hole stabilizes this tetrahedral transition state through interaction with the backbone -NH groups of glycine193 and serine195 as hydrogen bond donors.^[58,60,86,87,97,98]

The resulting tetrahedral intermediate then collapses, leading to the loss of the C-terminal peptide which in turn gives rise to the covalent acyl enzyme intermediate (Figure 2.2c).

Next, an activated water molecule attacks the acyl intermediate which results in the second tetrahedral intermediate (Figure 2.2d) that subsequently collapses leading to the release of the N-terminal peptide.^[58]

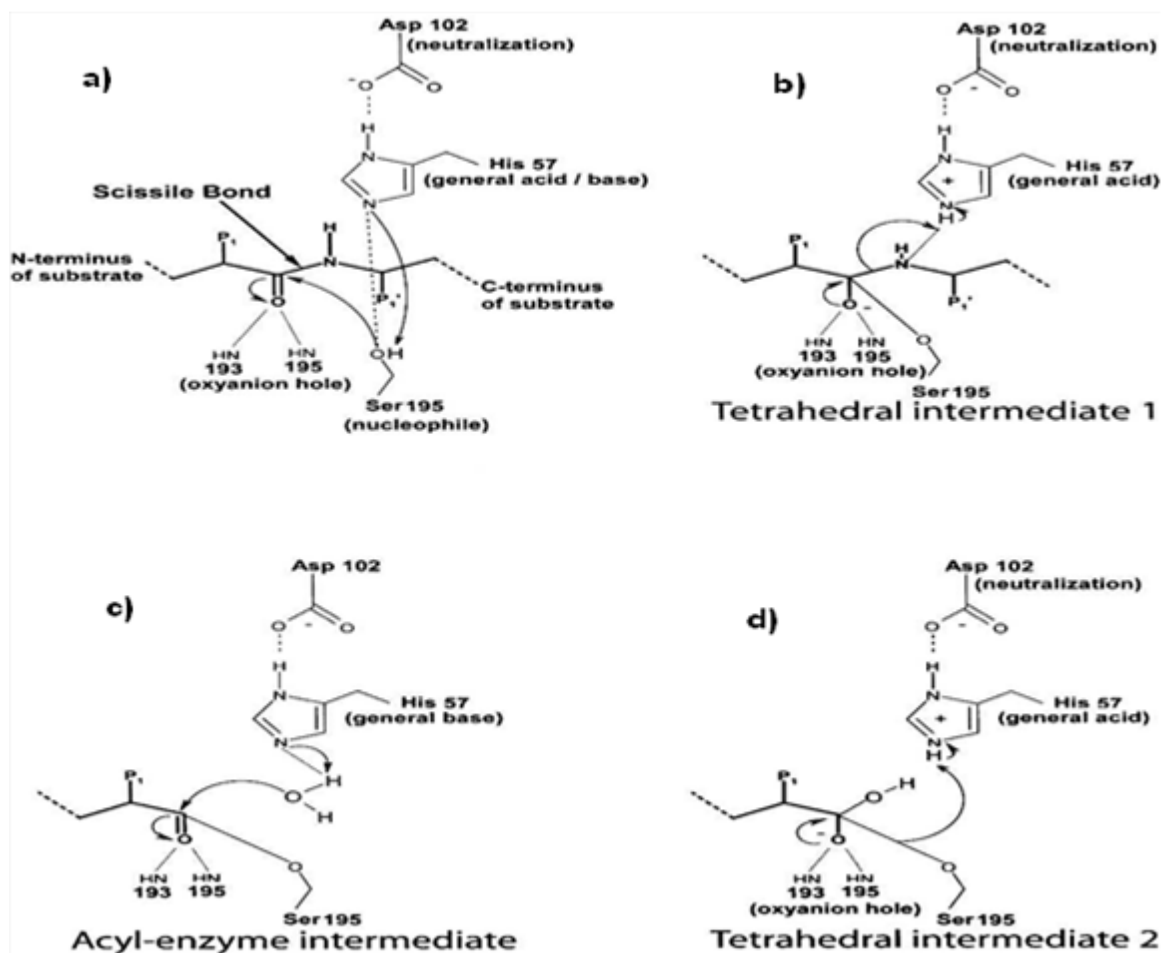


Figure 2.2 Schematic representation of the general steps employed in the classical Ser/His/Asp (the catalytic triad) serine protease catalytic mechanism: **a)** Michaelis complex, **b)** tetrahedral intermediate 1, **c)** acyl-enzyme intermediate, and **d)** tetrahedral intermediate 2. Reproduced from Ekici *et al.*^[58]

Chymotrypsin shows broad specificity, cleaving peptide bonds on the C-terminal side to hydrophobic residues such as phenylalanine, tyrosine, tryptophan, and leucine, and with secondary hydrolysis occurring at the C-terminal side to methionine, isoleucine, serine, threonine, valine, histidine, glycine, and alanine.^[58,84-88,97] Like all proteases, chymotrypsin binds peptides and proteins using substrate recognition sites which include binding pockets for the side chains of the peptide substrate.

2.1.4 Aspartic proteases

Aspartic proteases are also well-studied enzymes with solved three-dimensional structures, and are known to be a group of enzymes that consist of two lobes separated by a cleft containing the catalytic site made up of a pair of aspartic acid residues that function together permitting a water molecule to attack the peptide bond. Members of this class consist of the mammalian enzymes pepsin, gastricsin, chymosin, cathepsin D, cathepsin E and renin, as well as numerous microbial and plant enzymes. They form a class of digestive enzymes and are also known for their involvement in disease states such as Alzheimer's, and cancer, and the regulation of blood pressure.^[99-103] Furthermore, it is well known that most aspartic proteinases are inhibited by the microbial peptide pepstatin.^[100]

2.1.4.1 Pepsin (EC 3.4.23.1) as a model enzyme

Pepsin EC 3.4.23.1, an aspartic endopeptidase, is the major digestive protease in the gastric juice of vertebrates and has also been widely investigated since its crystallization was first reported in 1929 by Northrop.^[102] It consists of 327 amino acid residues which make up the N-terminal, central and C-terminal domains (from the PDB entry 1PSN). The N- and C-terminal domains consist of orthogonally packed β -sheets and α -helices whereas the central domain has a 6-stranded anti-parallel β -sheet that serves as the backbone of the enzymes' active site; it contains Asp32 and Asp215 and a water molecule located between these residues (Figure 2.3).^[103]

Aspartic proteases have various reported mechanisms, but the most accepted one is a general acid-base mechanism which involves the coordination of a water molecule between two highly conserved aspartic acid residues, Asp32 and Asp215.^[99-105]

In such a system, one of the aspartic acids acts as a nucleophile and induces hydrolysis between the P1 and P1' (nomenclature according to Schechter and Berger)^[52] residues of the substrate (Figure 2.4).

Pepsin has been extensively characterized and is known to hydrolyze peptide bonds that connect bulky hydrophobic/aromatic residues, such as Phe-Trp, Phe-Tyr and Phe-Phe and can accommodate seven residues in its active site.^[106-108]

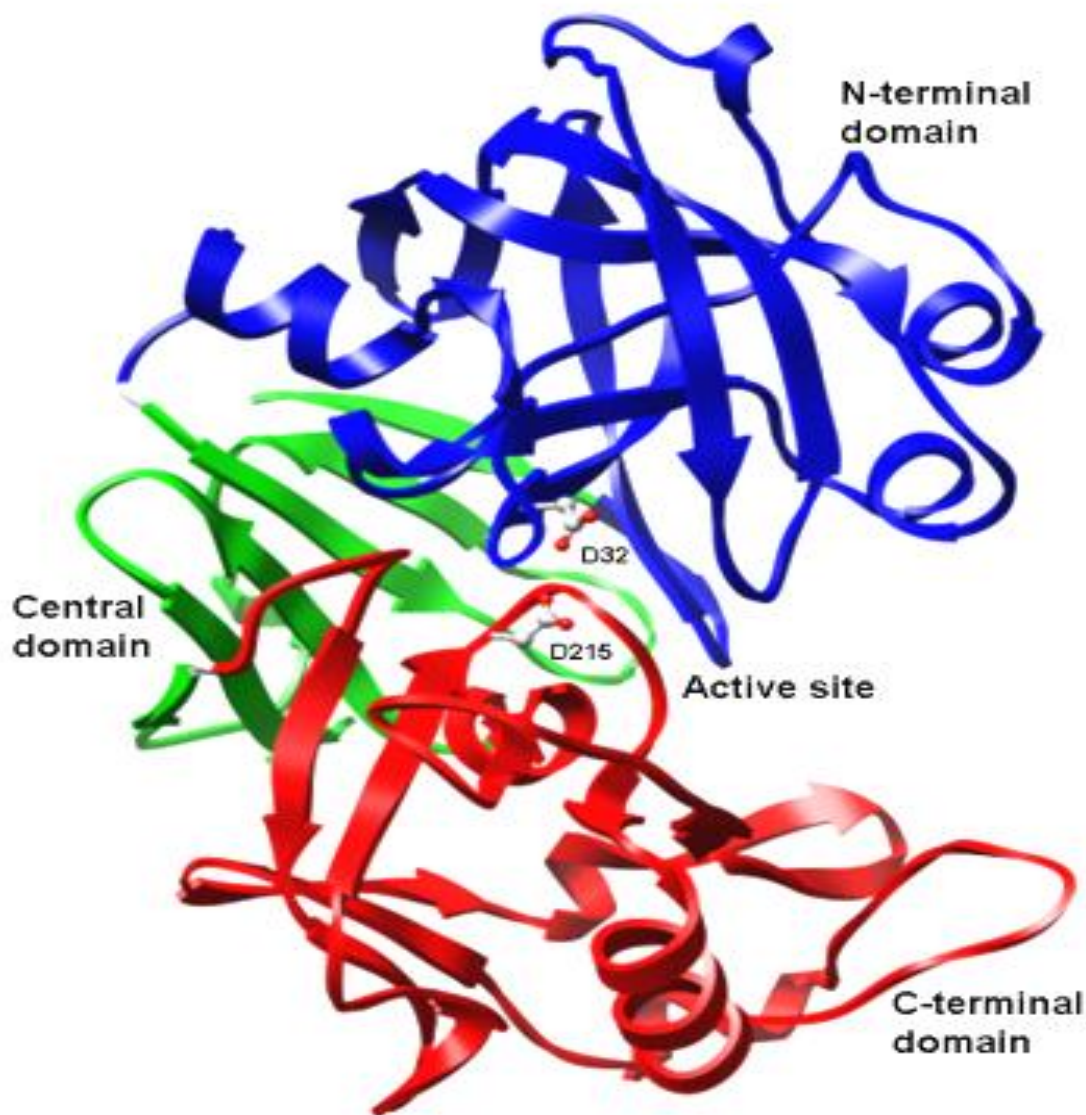


Figure 2.3 A ribbon diagram of human pepsin showing the N-terminal (blue), central (green) and C-terminal (red) domains with labelled active site aspartates (D32 and D215) PDB entry 1PSN.^[103]

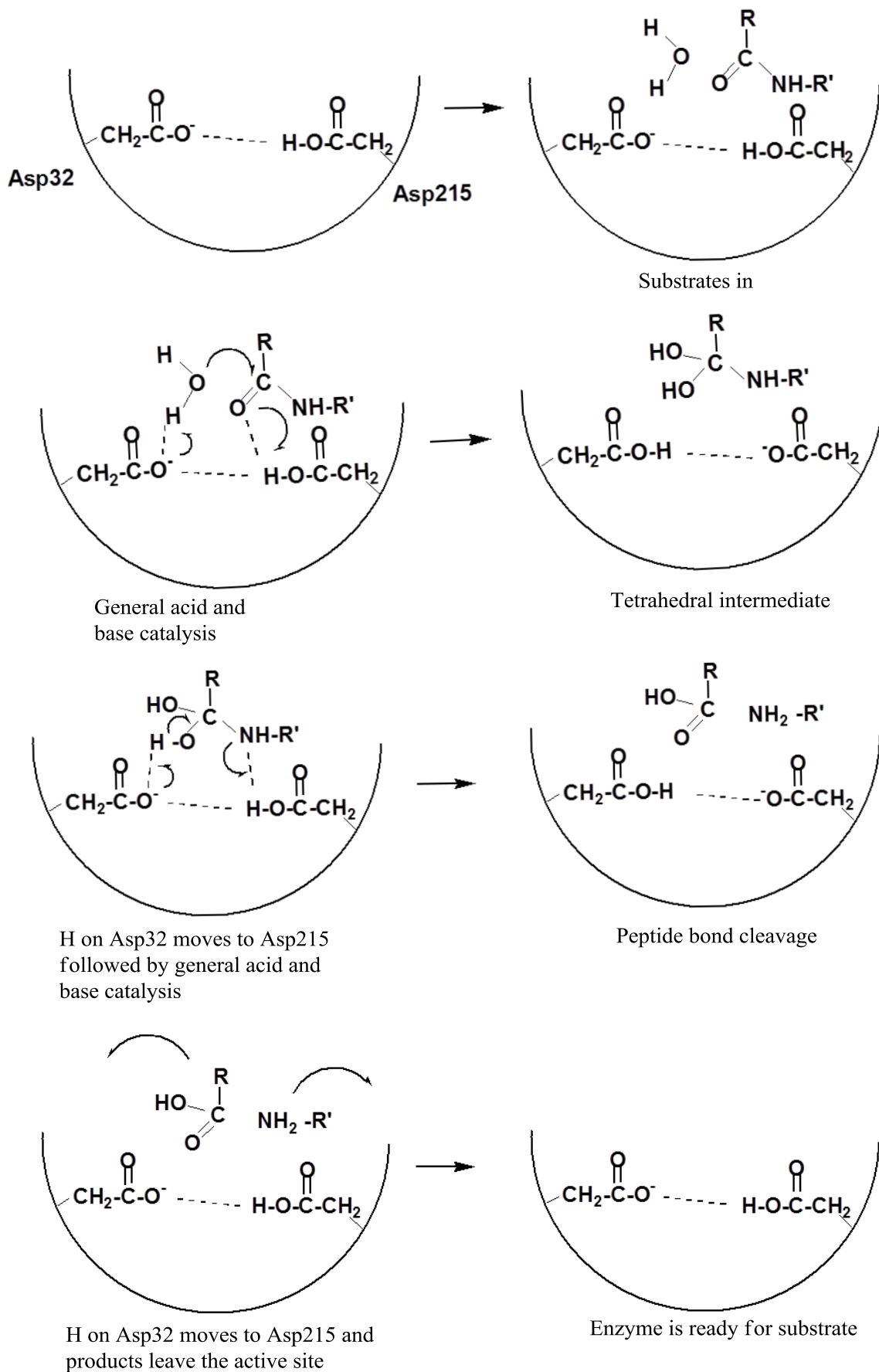


Figure 2.4 The general acid-base catalytic mechanism of aspartic proteases. Proposed pathway for the catalysis by aspartic proteases.

Nomenclature of proteases

According to the nomenclature of Schechter and Berger, the active site of proteases can be divided into subsites (S) and each subsite is capable of accommodating a single amino acid residue of the peptide substrate. The subsites are located on both sides of the catalytic site; the N-terminal side (nonprime, S1, S2, S3, S4, S_n) and the C-terminal side (prime, S1', S2', S3', S4', S_n'). The corresponding amino acid residues of the substrate (peptide) from the N- and C-terminal sides that functionally interact with the enzyme's subsites are correspondingly designated as P1, P2, P3, P4, P_n and P1', P2', P3', P4', P_n', respectively (Figure 2.5).^[52] The primary specificity describes the protease preference for the amino acids on either side of the amide bond (scissile bond) P1 and P1'. Proteases specifically hydrolyze proteins (substrates) either from the N- or C-terminus (aminopeptidases and carboxypeptidases, respectively) and/or in the middle of the sequence (endopeptidases).

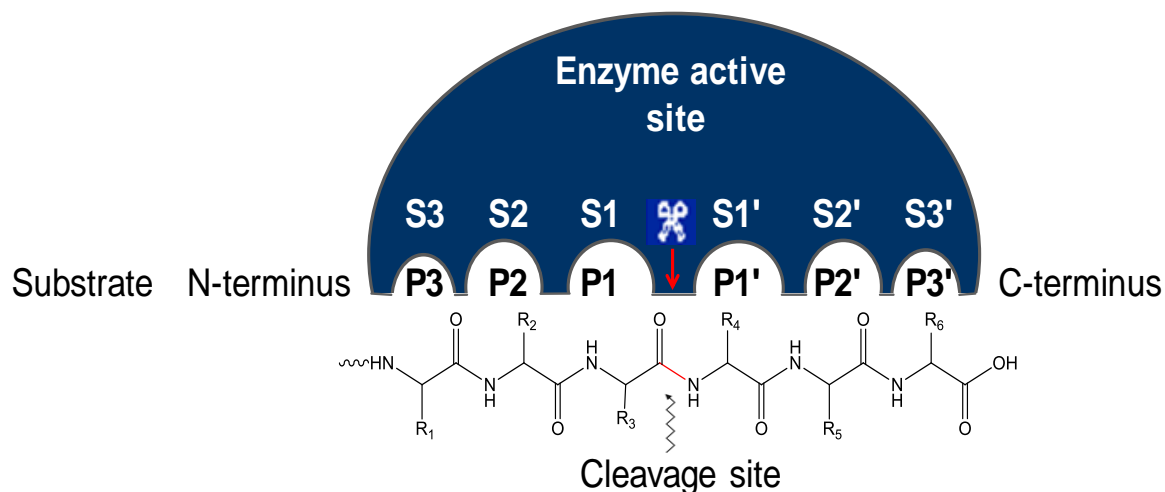
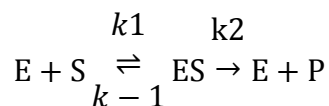


Figure 2.5 Schematic representation of substrate binding to a proteolytic enzyme, with six binding sites. Positions P3 to P3' in the substrate are counted from the bond between P1 and P1', where the cleavage occurs. The nomenclature of the active site of proteases was proposed by Schechter and Berger in 1967^[52].

2.2 Enzyme kinetics

The study of enzyme behavior under various experimental conditions yields crucial information which can be used to determine substrate affinities, its role in metabolism, specific activity, and inhibition properties. The determination of Michaelis Menten kinetic parameters such as the Michaelis constant (K_m), maximum velocity (V_{max}), and inhibition constant (K_i) is critical for the characterization, quantitative understanding and prediction of protease behavior.^[109,110] Even though different enzymes catalyze different substrates, they have a general mechanism of action. In the simplest terms, the enzyme (E) binds a substrate molecule (S) to form an initial enzyme-substrate complex (Michaelis complex, ES). The intermediate complex then further reacts with water and releases the product (P) with the regeneration of the enzyme (scheme 2.1). The rate of product formation or substrate degradation can then be monitored using different analytical methods and a plot of the velocity (v) against [S] (Michaelis-Menten plot, Figure 2.6a) used to determine the kinetic parameters.^[111,112]



Scheme 2.1 Simplified kinetic model of the hydrolysis of peptides and proteins.^[111,112]

From the Michaelis-Menten equation, the overall rate of hydrolysis (v) varies with substrate concentration [S] under steady-state conditions.

$$v = \frac{V_{max} \cdot [S]}{[S] + K_m} \tag{Equation 2.1}$$

Where V_{max} is the maximum velocity at which the rate is independent of the substrate concentration [S] and K_m (Michaelis constant) is the concentration that corresponds to $1/2V_{max}$. The value of the K_m is a measure of the affinity of an enzyme for a substrate; a low K_m indicates high affinity. Additionally, K_m depends on temperature, the nature of the substrate, pH, ionic strength, and other reaction conditions. It must be noted that other methods exist for obtaining these kinetic parameters: the Lineweaver-Burk plot (Figure 2.6b), the Hanes-Woolf, and the Eadie-Hofstee for an enzyme-catalyzed reaction obeying Michaelis-Menten kinetics.

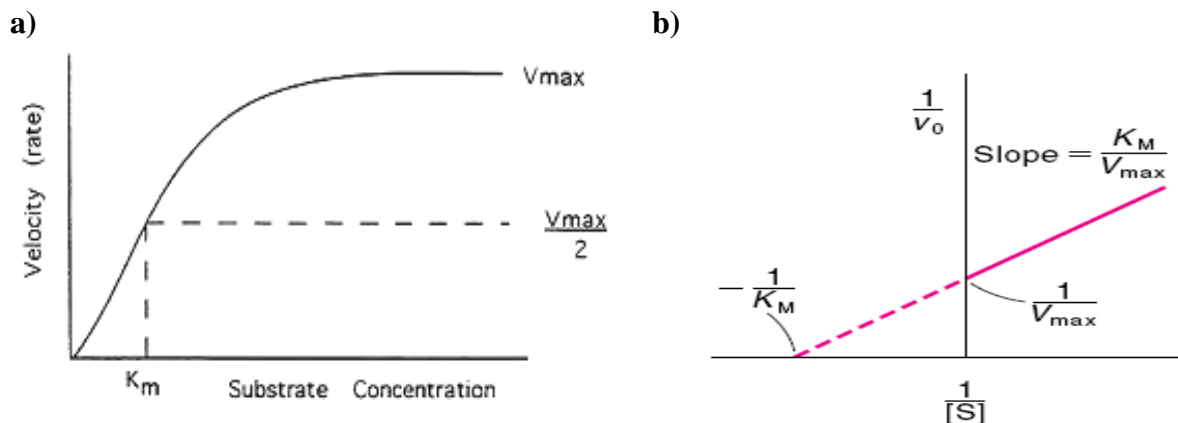
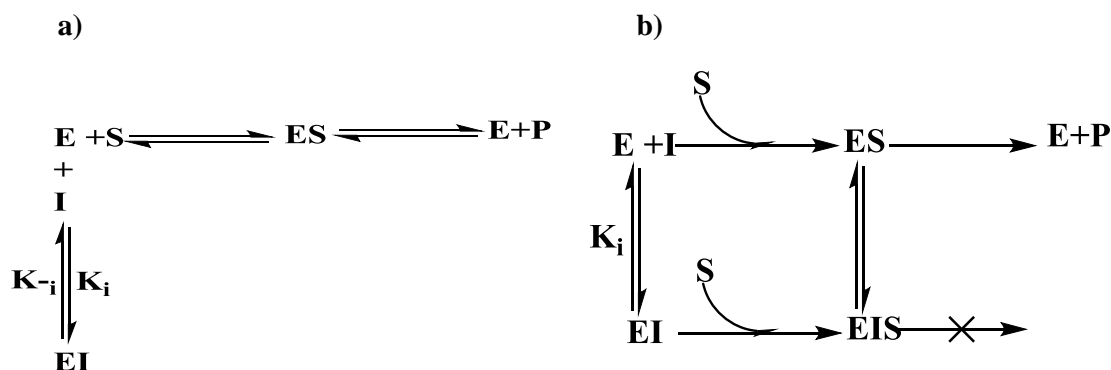


Figure 2.6 a) Michaelis-Menten Kinetics: A plot of the reaction velocity (V_0) as a function of substrate concentration $[S]$ for an enzyme that obeys Michaelis-Menten kinetics showing the maximum velocity (V_{max}) and the Michaelis constant (K_m). b) Lineweaver-Burk or double-reciprocal plot of enzyme kinetic data, showing the kinetic parameters can be acquired.^[111-113]

In enzyme kinetics, a molecule can bind to an enzyme and increase or decrease the rate of the enzyme-catalyzed activity. In the case of a decrease activity, that molecule is referred to as an inhibitor. Inhibitors are very useful in that they can be effective as drugs, poisons, pesticides and herbicides, and in metabolic control.

Enzyme inhibition can be either reversible or irreversible; reversible competition can be competitive (Figure 2.7a) or noncompetitive (Figure 2.7b). Whereas in noncompetitive inhibition, the inhibitor and substrate can bind simultaneously to an enzyme molecule at different binding sites, in competitive inhibition, which is the most common form of reversible competition, the substrate competes with the inhibitor for the substrate-binding site. In the latter, no products are formed (scheme 2.2) and the inhibition constant can be calculated as shown in equation 2.2.^[113]



Scheme 2.2 General kinetic model for: a) competitive inhibition and b) noncompetitive inhibition.^[113]

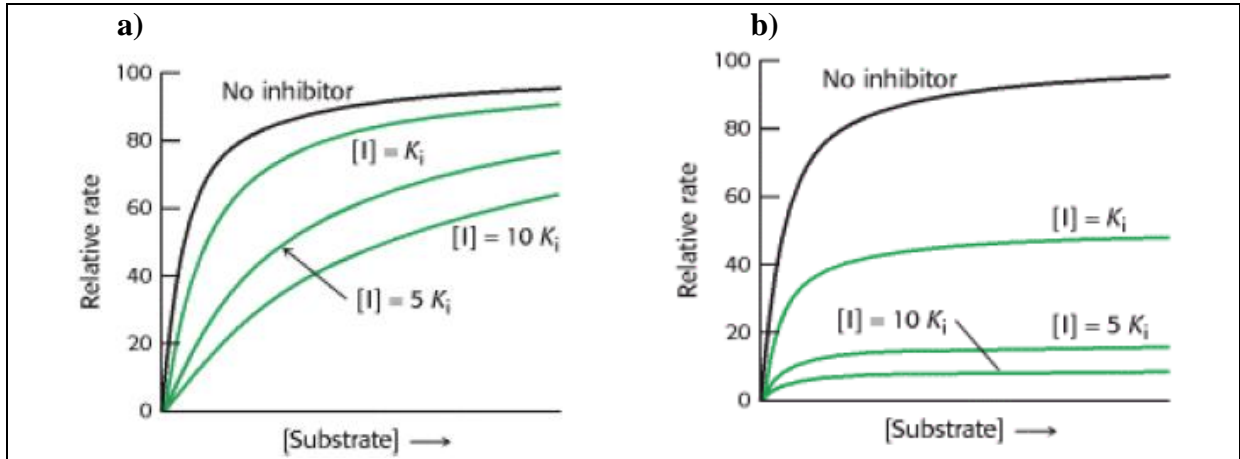


Figure 2.7 a) Kinetics of a competitive inhibitor. As the concentration of a competitive inhibitor increases, higher concentrations of substrate are required to attain a particular reaction velocity. b) Kinetics of a noncompetitive Inhibitor. The reaction pathway shows that the inhibitor binds both to free enzyme and to enzyme complex.^[113]

$$K_i = \frac{[E] \cdot [I]}{[EI]} \quad \text{Equation 2.2}$$

Where $[I]$ is the concentration of inhibitor and K_i is the dissociation constant for the enzyme-inhibitor complex $[EI]$. The Michaelis-Menten rate equation of competitive inhibition is then given by:

$$v = \frac{v_{max}[S]}{K_m(1 + \frac{[I]}{K_i}) + [S]} \quad \text{Equation 2.3}$$

2.3 Plasma

Human blood is made up of 44% red blood cells, 1% white blood cells and 55% plasma. Plasma contains 91% water, 2% salts and 7% proteins, the latter consisting of more than 120 different proteins, including human serum albumin (HSA), immunoglobulin G (IgG), fibrinogen (factor I), alpha-2-macroglobulin (α_2M), alpha-1-antitrypsin (A1AT), transferrin (siderophilin), lipoproteins and numerous proteolytic enzymes, such as esterases and peptidases.^[114,115] Table 2.2 is a list of some known plasma proteases and their cleavage specificities as present in the SwissProt database.^[116-118]

Table 2.2 Specificity of known plasma proteases^[117]

| EC number | Protease | Specificity |
|-----------|----------------------|--|
| 3.4.11.2 | Aminopeptidase N (M) | Broad, Removes N- terminal amino acids |
| 3.4.17.2 | Carboxypeptidase (B) | Removes C-terminal R, K |
| 3.4.17.3 | Carboxypeptidase N | Removes C-terminal K |
| 3.4.21.7 | Plasmin | R/X (R/S) and K/X (K/S) |
| 3.4.17.20 | Thrombin (Factor II) | R/G and K/G |
| 3.4.21.B1 | Factor VII | R/I |
| 3.4.21.27 | Factor IX | R/I |
| 3.4.21.6 | Factor X | R/I and R/T |
| 3.4.21.27 | Factor XI | R/A and R/V |
| 3.4.21.38 | Factor XII | R/I |
| 3.4.21.41 | Complement C1r | R/I and K/I |
| 3.4.21.42 | Complement C1s | K/K, R/A, and R/K |
| 3.4.21.43 | Complement C2 | R/X |
| 3.4.21.47 | Complement Factor B | R/X |
| 3.4.21.46 | Complement Factor D | R/K |
| 3.4.21.45 | Complement Factor I | R/S |
| 3.4.21.34 | Kallikrein | K/X (K/R) and R/X (R/S) |
| 3.4.21.37 | Leukocyte Elastases | A/X, F/X, L/X, M/X, and P/X, Y/X |

Note: Specificity is indicated using the single letter codes for the amino acids; X indicates any amino acid. Cleavage specificity is reported from the SwissProt entry for each protein (<http://us.expasy.org>).^[118] Adapted and slightly modified from Koomen *et al.*^[117]

2.3.1 Protease stability in blood plasma

A simple approach to investigate peptide or protein stability towards systemic metabolism is to incubate the peptide or protein at 37 °C at pH 7.4 in serum, plasma or diluted plasma, or specifically immobilized plasma proteins.^[115,116,119-122] Aliquots are withdrawn at specific time intervals in order to determine a stability profile.

By applying different analytical methods (chapter 4), the protease stability profile can be used to establish the impact of modifications in comparison to unmodified peptides or proteins.^[30,110-122]

Such studies can offer explanations about why certain compounds are unexpectedly rapidly cleared, and provide valuable information for the rational design of more effective drugs.

As discussed above, one of the greatest limitations to peptide therapeutics is a short plasma half-life (the time required by the blood plasma to eliminate half the administered dose of a drug). This is as a result of rapid renal clearance (because of the hydrophilic nature and relatively small size of most peptides), and systemic degradation by peptidases and proteases (enzymes found in the blood, liver and kidneys).^[115] Additionally a drug's efficiency is affected by the degree to which it binds to plasma proteins, as this can influence the drug's biological half-life in the body.

Nonetheless, numerous strategies have been employed to improve the plasma half-life of peptide and protein drugs, and the following sections describe some of these.

2.3.2 Chemical approaches used to enhance proteolytic stability and biological activity of peptides and proteins

Several reviews of chemical strategies employed to increase the plasma half-life of peptides have been published, and peptide therapeutic examples obtained by means of such approaches exist. The modifications include chemical groups typical of post-translational modifications in cells or noncanonical amino acids (nonnatural or nonproteinogenic amino acids).^[115,116] Whereas such chemical alterations are aimed at improving proteolytic stability, destabilization can also occur.

In one strategy, the number of amino acids within a peptide sequence is reduced while the amino acids essential for receptor binding are left intact. A typical example was shown by Harris and coworkers, in which the plasma half-life of octreotide, a drug which is used in the treatment of gastrointestinal tumors, was increased from a few minutes to 1.5 hours by shortening the overall amino acid sequence of somatostatin from 14 to 8 and replacing L-tryptophan by D-tryptophan.^[115,116,123]

Cyclization of peptide sequences has also been successful. This can decrease the conformational flexibility of linear peptides, reduce hydrogen-bonding, enhance membrane permeability and even impart resistance to endo- and exopeptidases.

Cyclization can be accomplished by exploiting the side chains or the termini of the peptide sequence (head to tail, N-backbone to N-backbone, end to N-backbone, end to side chain,

side chain to N-backbone, side chain to side chain), or by introducing disulfide (disulfide-bond cyclization scan), lanthionine, dicarba, hydrazine or lactam bridges (Figure 2.8).^[124,125]

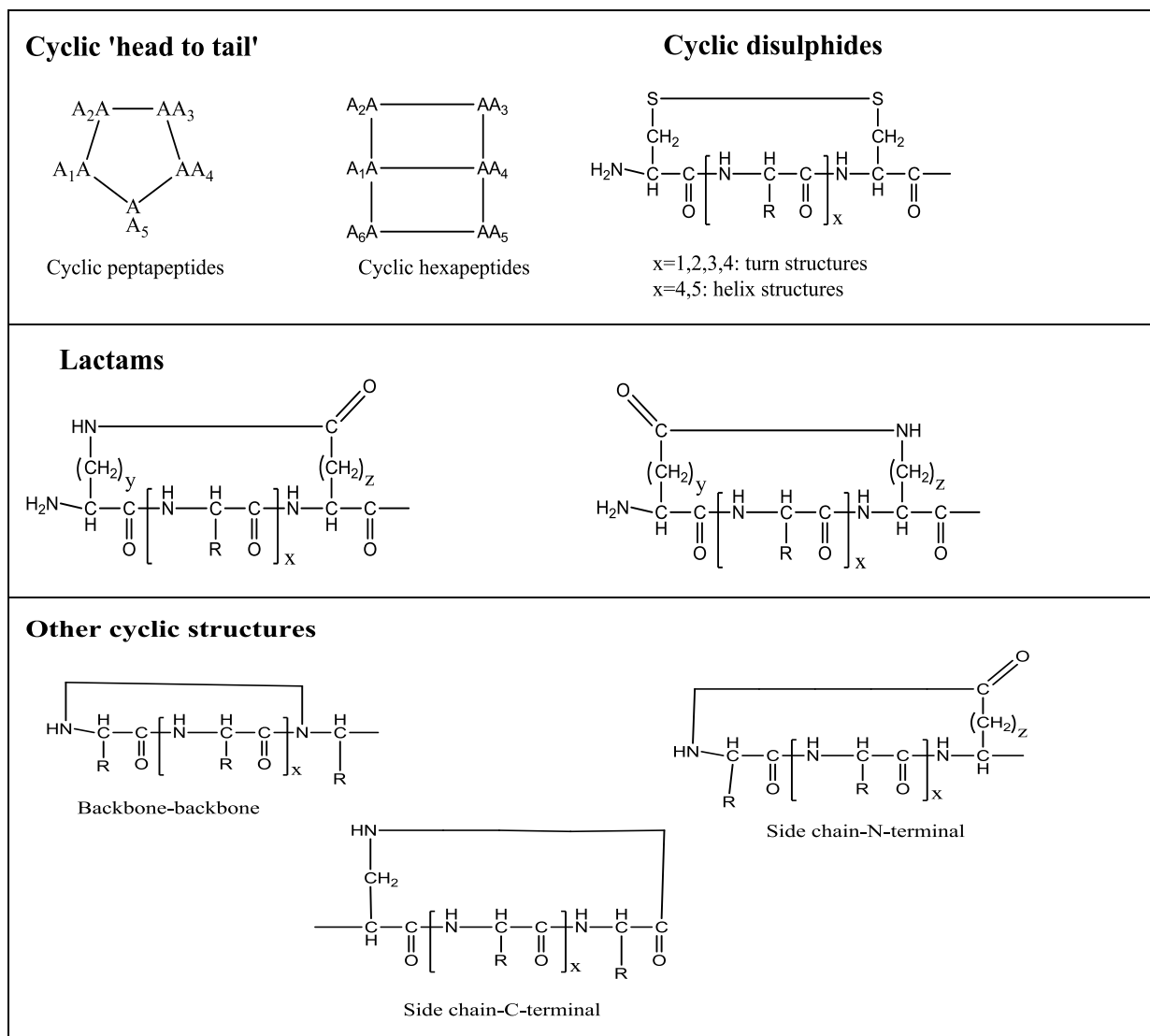


Figure 2.8 Possible approaches of peptides cyclization. Redrawn from Hruby V.J.^[125]

Furthermore, obstruction of the N- or C-terminal ends by N-acylation, N-pyroglutamate, N-terminal esterification (phosphoester), C-amidation, the addition of carbohydrate chains (glycosylation: glucose, xylose, hexose) or the conjugation with polyethylene glycol (PEGylation) can lead to increased plasma stability.^[20,115,116,126,127]

Glycosylation of amino acids represents one of the most promising advances in peptide modification as most of its significant parameters (e.g. glycosylation degree, glycan size and glycan structural composition) can be controlled.

The use of polar amino acids such as serine, asparagine, and threonine in posttranslational modification has been reported and shown to overcome most of the hindrances encountered in the use of peptides as pharmaceutical agents.^[128-130]

Attachment of PEG to amino acids like cysteine, glutamic acid, arginine and lysine within a peptide sequence imparts the peptide with special properties that make it highly water soluble, highly mobile in solution and not significantly immunogenic. This method increases the molecular weight and alters the structure of the peptide, which can prevent protease degradation and may lead to the production of peptide inhibitors with high molecular binding affinity and increased bioavailability.^[20,115,116,131,132] The improved proteolytic enhancement is typically attributed to steric hindrance.

In addition to the above mentioned modifications, the properties of a peptide can be altered by the substitution of a natural amino acid residue by a nonproteinogenic or unnatural amino acid: D-configuration, N-methyl- α -amino acids, nonproteinogenic constrained amino acids, or backbone extended building blocks.^[115]

2.3.3 Nonproteinogenic amino acids and unnatural amino acids in peptide modification

Natural or chemically designed and synthesized amino acids, which are not genetically encoded, are considered as nonproteinogenic amino acids. In nature there are 20 proteinogenic amino acids that make up about 4% of all known naturally occurring amino acids (taking into account numerous metabolites, etc.).^[133] Several nonproteinogenic amino acids play vital roles in peptide and drug discovery research and their biological activity has been established.^[134] However, most of these nonproteinogenic amino acids are used as building blocks for small bioactive peptide scaffolds and very few are utilized as intermediates in primary metabolic pathways (e.g., homoserine and ornithine). The incorporation of one or more noncanonical amino acid residues into natural peptides offers an attractive approach to confer a desired property that is not accessible using exclusively the repertoire of the 20 canonical amino acids.^[10-14,133]

2.3.4 Types of nonproteinogenic amino acids

Nonproteinogenic amino acids have attracted the interest of many chemists over the past years, and although the diversity of structural modifications is theoretically unlimited, comparatively few have been synthesized due to cost considerations. Most of the reported amino acid modifications have led to modified natural or model peptides and proteins with favorable protein-protein interactions and degradation (by endopeptidases and exopeptidases) profiles.^[13,20,115,116,131,132,135-140] Some of the methods by which amino acids may be modified include the following examples.

2.3.4.1 Inversion of configuration (D-amino acids)

Numerous investigations on the replacement of L-amino acids with D-amino acids in peptides have shown the great potential of D-peptides through improved binding properties, dramatically increased serum half-lives and a pronounced resistance to proteolytic degradation. This improved proteolytic stability is due to the chiral specificity of the enzyme.^[20,132,139]

2.3.4.2 Alkylation

Another form of modification can be carried out through the addition of one or more methylene units ($-\text{CH}_2-$)_n in the backbone (β , γ , δ amino acids) or side chain (norleucine, norvaline).^[115,141] The former type of modification offers the molecule the capability to adopt well-defined secondary or tertiary conformations. In view of the fact that proteases usually do not recognize β - and γ -amino acids, proteolytic stability can be achieved by substituting these for the native residues, increasing bioavailability and plasma half-life.^[13,142]

2.3.4.3 Fluorination

Among all the chemical modification methods, fluorination represents one of the most promising approaches as it has been shown in many examples that the incorporation of fluorine into biomolecules increases pharmacokinetics, bioavailability, and biological activity.

It can also serve as a probe (^{19}F NMR or radioactive ^{18}F) to investigate enzyme mechanisms, structure, dynamics, and interactions between proteins, peptides, lipids, and nucleic acids.^[17,143-152]

In past decades, fluorine had been extensively used in bioorganic, organic, inorganic, and medicinal chemistry, and in materials science, but had attracted relatively little interest in the fields of peptide design and protein engineering. More recently, fluorine in biological systems has gained attention, although the rational design of fluorinated proteins remains challenging.^[9-12, 14-30,143-161]

Since fluorine has a van der Waals radius (1.35 Å) comparable to that of hydrogen (1.2 Å), the replacement of a hydrogen atom with a fluorine atom within a molecule is typically not structurally perturbative, even though the C-F bond is significantly longer (~1.4 Å) than the C-H bond (~1.0 Å).^[24,149] Due to its exceptional properties (small size, very low polarizability, and the strongest inductive effect of all elements), it has been incorporated into natural amino acids creating libraries of fluorinated nonnatural or nonproteinogenic amino acids.^[24] Fluorinated amino acids have hence become a powerful tool to alter the biophysical and chemical properties of peptides and proteins such as hydrophobicity, acidity/basicity, reactivity and conformation. Although several studies had previously shown that the incorporation of fluorinated amino acids into proteins and peptides significantly enhances proteolytic stability,^[9,18,150,151] recent studies have shown less generalizable results. Thus the impact of fluorination on peptides and proteins is a complex phenomenon that depends on the size and polarity of the fluorinated building blocks and the immediate environment of the substitution.^[11,21-30,156-160] For this reason, there is a need to systematically investigate the impact of fluoroalkylated amino acids on peptide substrates for proteases.

2.3.5 Types of fluorinated amino acids used in peptide and protein modification

Over the past years, numerous fluorinated amino acid analogues have been described, synthesized and studied. In general, the chemical synthesis of these fluorinated building blocks depends on the position as well as the extent of fluorine substitution. However, most reported studies in recent years include fluorinated analogues of aliphatic or aromatic hydrophobic residues, as well as methionines and prolines, many of which are currently commercially available.^[24,159,160] Fluorinated amino acids are very often incorporated into natural or model peptides to study their structural effects.

A recent review of the types of side-chain fluorinated α -L-amino acids that have been incorporated into peptides and proteins was published within the period of this thesis, in which these amino acids were grouped based on their side chains: aliphatic/methionine, aromatic, charged, polar, and proline analogues.^[24]

The aliphatic fluorinated amino acids consist of substitution of one or two alkyl (CH₃) groups with fluorine (CF_x) in the side chain of L-aliphatic amino acids such as (Ala, Val, Ile and Leu). This therefore creates further stereocenters that present the opportunity to study the effects of stereochemistry on protein structures (Figure 2.9). Among these aliphatic fluorinated analogues, the most frequently used in peptide and protein modification are the analogues of leucine, isoleucine and valine due to their relatively high synthetic feasibility and stability.^[24]

Side chain-modified and C ^{α,α} -dialkylated fluorinated amino acids in model peptides (coiled coils) have also been extensively studied and characterized based on sterics, hydrophobicity, lipophilicity, polarity, degradation profile and protease-catalyzed peptide synthesis (see also section 2.4.6). A fundamentally separate class of building blocks is represented by fluorinated derivatives of aminobutyric acid (Abu), also referred to as ethylglycine. Studies involving its fluorinated analogues 4-monofluoroethylglycine (MfeGly), 4,4-difluoroethylglycine (DfeGly), 4,4,4-trifluoroethylglycine (TfeGly), and 4,4-difluoropropylglycine (DfpGly), have shown that varying the content of fluorine in amino acids, one atom at a time, permits fine tuning of side chain volume and polarity.^[156,157,161]

Although hydrogen and fluorine are often discussed to be almost isosteric, the CF₃ group has approximately twice the van der Waals volume of a CH₃ group and the steric effect of the CF₃ group has been shown to be closer to that of an isopropyl group,^[162] a sec-butyl, or a cyclohexyl group.^[163] The size and shape of an amino acid's side chain determine its ability to engage in packing interactions with other side chains. As the hydrophobic effect (the tendency of nonpolar solutes to avoid interactions with polar solvent molecules) is one of the key driving forces for protein folding in an aqueous environment^[164], it is always necessary to determine the experimental hydrophobicity of a given fluorinated building block. Samsonov *et al.*^[165] measured and compared the size and hydrophobicity of nonfluorinated amino acids with their fluorinated analogues using HPLC-based methods.

THEORY

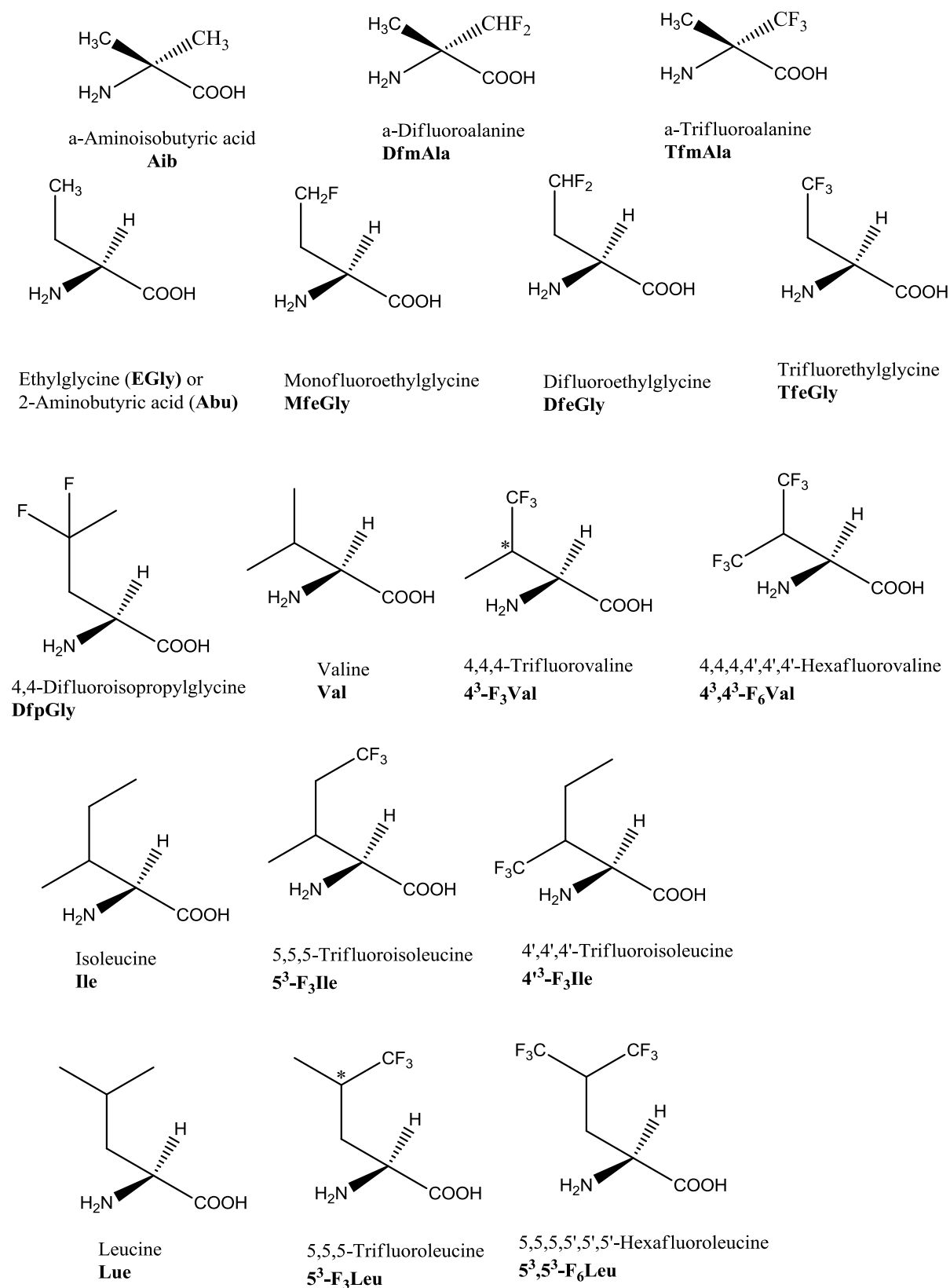


Figure 2.9 Fluorinated analogues of hydrophobic amino acids that have been incorporated into peptides and proteins. Reproduced with slight modification with permission from Salwiczek *et al.*^[24] Copyright © Royal Society of Chemistry).

In this RP-HPLC-based approach, the Fmoc-protected form of α -aminobutyric acid (Abu) and its derivatives were analyzed. The results showed that the retention time of aliphatic amino acids increases non-linearly with increasing side chain volume, and this can be explained by a decreasing polarizing effect with increasing chain length.^[165,166] However, the retention times of the partially fluorinated analogues of Abu (MfeGly, DfeGly, TfeGly, and DfpGly) do not fit into the correlation shown for their pure hydrocarbon derivatives. Thus, hydrophobicity increases more rapidly with increasing fluorine content than with size.

TfeGly was found to have similar properties (size and hydrophobicity) to valine.^[165,166] These results confirm that partial aliphatic fluorination decreases hydrophobicity, whereas perfluorination results in an increase in hydrophobicity.^[166] The rise in hydrophobicity of highly fluorinated aliphatic hydrocarbons could be attributed to the extremely low polarizability and the high electronegativity brought by the introduction of fluorine.

Fluorinated methionine analogues are obtained from the chemical substitution of the hydrogen in the S-methyl group which in turn varies the size and shape of the methyl group. In this manner, it reduces the electron density at the sulfur nucleus thereby enhancing the overall hydrophobicity of the side chain.^[24,167]

Fluorination of aromatic acids can be realized at aryl hydrogens, (Phe, Tyr, Trp), C ^{β} (Tyr), or the indole ring (Trp). It has been shown that a single hydrogen substitution with fluorine on the aromatic ring of phenylalanine leads to a rearrangement of the electrostatic potential and increases the hydrophobicity of the side chain.^[24,168] Nevertheless, the substitution of all aryl hydrogens of phenylalanine results in remarkable increase in size (molecular volumes of C₆H₆ and C₆F₅H are 106 Å³ and 141 Å³ respectively), which may destabilize proteins for steric reasons.^[169] Interactions between nonfluorinated and fluorinated phenyl side chains are favorable, due to their inverse polarity.

Single fluorination of the indole ring in Trp at the 4, 5, or 6 position leads to inverted polarities which lead to increased charge separation. Their hydrophobicities were found to be solvent dependent: at pH 7.05 in phosphate buffer 4-FTrp < 5-FTrp < 6-FTrp,^[24,170] whereas an order of 4-FTrp < 6-FTrp < 5-FTrp^[24,171] was observed in water. These conflicting results could be linked with the conditions under which the partitioning experiments of Trp were carried out and thus point out the fact that hydrophobicity of amino acids should be evaluated under conditions that are relevant to folding and activity studies especially when the side chains incorporate ionisable functional groups.

On the contrary, fluorination of tyrosine produces hydrophilic fluorinated analogues and this is due to the polarization of the hydroxyl group that becomes more acidic and a better hydrogen bond donor.^[24]

2.3.6 Fluoroalkyl amino acids and protease stability of fluorinated peptides and proteins

All modifications of amino acids and peptides aim to improve pharmacokinetics and metabolic properties of peptides and proteins. One inspiration to introduce fluorinated amino acids into peptides or proteins is the potential enhancement in proteolytic resistance. The assumption is that the nonproteinogenic amino acids are apparently not recognized by enzymes and thus prevent proteolysis. Basically, the effect or impact of fluorine substitution on peptides and protein properties has been shown to depend strongly on the position as well as the fluorine content within a certain amino acid or the peptide chain.^[21-24,30] These concepts and hypothesis have been proven by globally or site specifically introduction of the fluorinated amino acids into natural or model peptides and proteins.

Since the fluorinated analogues used in this study are exclusively analogues of fluoroalkyl amino acids, it should be noted that other fluorinated amino acids incorporated into peptides and proteins provide similar hydrolytic effects. The following section summarizes some critical examples in which fluoroalkyl amino acids were introduced into peptides or proteins to study the impact of fluorination on proteolytic stability.

Kochsch *et al.* have studied the influence of fluorination on the proteolytic stability of peptides using series of model peptides containing α -trifluoromethyl-substituted (α Tfm) amino acids in different positions, P3-P2' (nomenclature according to Schechter and Berger^[52]) relative to the principal cleavage site of α -chymotrypsin.^[21,22] They found out that, peptides substituted in the P1 position exhibited absolute proteolytic stability whereas, peptides substituted at the P2 and P2' positions showed considerable proteolytic stability compared with the unsubstituted model peptide analogues (α -aminoisobutyric acid, Aib). Thus, proteolytic stability of the fluorinated peptides was more of position dependent manner. Besides, comparison with peptides containing Aib offers good prospect to distinguish between electronic and steric effects.^[21,22]

The proteolytic stability of α -Tfm-substituted peptides was found to be conformation dependent. In this respect, the incorporation of the (*S,R,S*)-diastereomer of α Tfm in the P1' position (*Z*-Phe- (α Tfm)Ala-Ala-NH₂) showed rapid hydrolysis while the (*S,S,S*)-diastereomer showed an extraordinary proteolytic stability similar to that of the Aib model peptides.

They interpreted these findings using molecular modeling and concluded that in the case of the (*S,R,S*)-diastereomer the steric constraints exhibited by the CF₃ group can be outweighed by an advantageous interaction of the fluorine atoms with the serine side chain of the enzyme, while this interaction is absent in the (*S,S,S*)-diastereomer, leading to its stability.^[21,22] These results impressively show that even one trifluoromethyl functionality can direct enzyme-substrate interactions in a way that is not possible for the fluorine-free analogues. Such effects could have important implications in drug design strategies.

As proof of concept, fluorinated amino acids have been incorporated into several biologically active peptides and proteins. A typical illustration is the introduction of the Tfm moiety into thyrotropin releasing hormone (TRH), a central stimulator of thyroid stimulating hormone (TSH), secreted by anterior pituitary cells.^[22,172]

The substitution of pyroglutamic acid (*p*Glu) by (α Tfm)*p*Glu at the P1 position of TRH: *p*Glu-His-Pro-NH₂, Figure 2.10a^[22,173] and its hydrolysis by pyroglutamyl aminopeptidase II which selectively cleaves the *p*Glu-His bond^[174] were investigated by measuring the effectiveness of inhibition of *p*Glu[³H]TRH proteolysis.^[22,175]

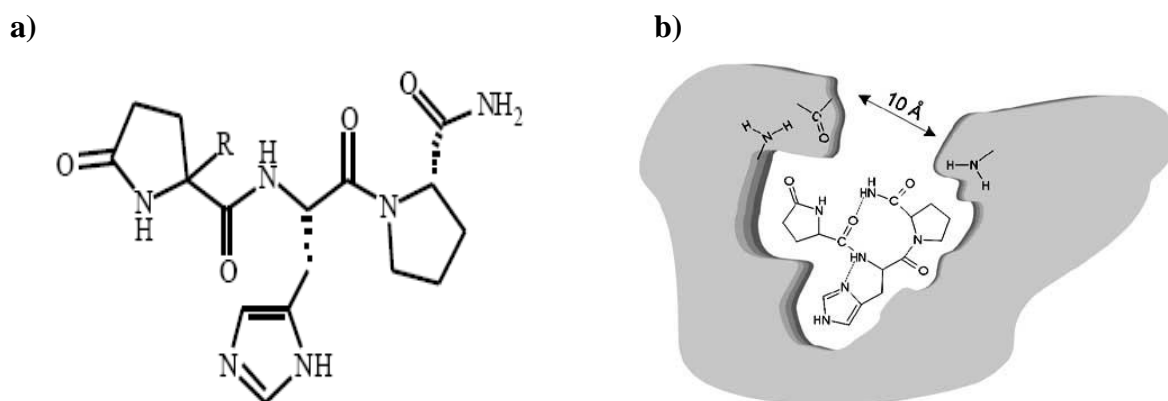


Figure 2.10 a) Structure of TRH; R = H: native peptide, R = Tfm: [(α Tfm)*p*Glu1]-TRH. b) Model of the interaction between the TRH molecule and the receptor.^[22]

The substituted P1 position α Tfm-TRH peptide showed very high resistance to proteolysis, but a 2-3 orders of magnitude decrease in binding affinity to receptor was observed compared to the native compound.

Using NMR and molecular modeling the authors explained that the existence of a hydrogen bond between the *p*Glu carboxy function and the amino moiety of Pro could result in a hairpin turn which is required for an optimal interaction with the receptor as shown in Figure 2.10b.^[22,176] However, the polarization effect of the Tfm group seems to disturb the formation of that hydrogen bond. Combined with the steric constraints exhibited by the Tfm substituent, the polarization effect obviously prevents the formation of the essential hairpin turn.

In another study, Meng *et al.* selectively incorporated hexafluoroleucine (HfL) into strategic sites (residues at P1, P1', and/or P2' positions) of the therapeutic peptide glucagon-like peptide-1(GLP-1[7-36]) with the sequence:

NH₂-HAEGTFTSDVSSYLEGQAAKEFIAWLVKGR-CONH₂.^[18,24] Single replacement of Ala8, Glu9, and Gly10 with hexafluoroleucine conferred resistance against its regulatory protease, dipeptidyl peptidase IV (DPP IV, EC 3.4.14.5) which generally cleaves the peptide between Ala8 and Glu9. Double substitution at positions 8 and 9 with HfL led to complete resistance to enzymatic hydrolysis over 24 hours.^[18] These results are of significance because of the fact that GLP-1 holds great promise as a treatment for type 2 diabetes, yet the native peptide has a half life of less than 2 minutes.

Furthermore, analogues that contain substitutions at sites vital for receptor binding (Phe28, Ile29 and Leu32) were produced. All fluorinated variants exhibited reduced affinity towards the receptor. Replacement of Phe28 and Ile29 with alanine in GLP-1 induces a dramatic loss of binding affinity to GLP-1R.

More recently, Gottler *et al.*^[12,24] globally replaced the Leu and Ile residues of pexiganan (H₂N-GIGKFLKKAKKFGKAFVKILKKCOOH), a synthetic analogue of magainin-2, with ⁵₃,⁵₃-F₆Leu (HfL). The peptide retained its antimicrobial activity while remaining haemolytically inactive. Furthermore, the fluorinated analogue showed improved stability towards trypsin as well as chymotrypsin digestion in the presence of a membrane environment. In the absence of a membrane, however, the peptide was as rapidly degraded as the wild type. Thus, the stabilizing effect was attributed to an increased tendency of the peptide to self-assemble within the lipid bilayer due to fluorination.

Meng and Kumar^[24,25] have also investigated the effect of fluorination on two host defense antimicrobial peptides (AMPs), buforin-2 (H₂N-TRSSRAGLQFPVGRVHRLLRK-COOH) and magainin-2 (H₂N-GIGKFLHAAKKFAKAFVAEIMNS-CONH₂). The replacement of Leu, Ile and Val (as well as Ala in one case) at the nonpolar peptide-membrane interface with hexafluoroleucine in both peptides yielded several variants containing different levels of ⁵₃,⁵₃-F₆Leu. Out of the six fluorinated variants used in this study, only one variant shows a decrease in bactericidal activity (highly fluorinated magainin variant) while all of the other five variants show a significantly enhanced (or similar) bactericidal activity. The decrease in bactericidal activity for the globally fluorinated magainin variant was attributed to its obviously enhanced self-assembly in aqueous solution which apparently hinders its initial interaction with the membrane. Contrary to the findings described by Gottler *et al.*^[12,24] above, these fluorinated analogues show extreme resistance, increased, or similar protease stability, even in the absence of a membrane, and have altered cleavage patterns.^[24,25]

Interestingly, Voloshchuk *et al.*^[26] globally substituted 10 Phe residues of histone acetyltransferase (HAT) tGN5 by applying SPI with three monofluorinated phenylalanines and found a loss in secondary structure as well as a decrease in thermal stability for all three variants by circular dichroism (CD) experiments. In addition, they also demonstrated that the fluorinated mutants were all degraded by chymotrypsin compared to the wild type. Thus, incorporation of monofluorinated phenylalanine led to reduced proteolytic stability.

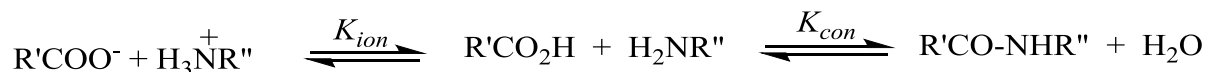
In summary, there is no general rule regarding how the incorporation of fluorinated amino acids can impact proteolytic stability, there are numerous examples in which this leads to either an increase or a decrease; thus, systematic investigation of every system is always required.

2.3.7 Protease catalyzed peptide synthesis with fluorinated amino acids

The use of basic chemical principles to manipulate the equilibrium, the concentration of products, and the kinetic parameters of the reaction results in the successful application of the catalytic properties of proteases to peptide synthesis. Generally, enzymatic peptide bond formation is based on the reversal of the hydrolytic action of proteases considered by van't Hoff in 1898.^[177]

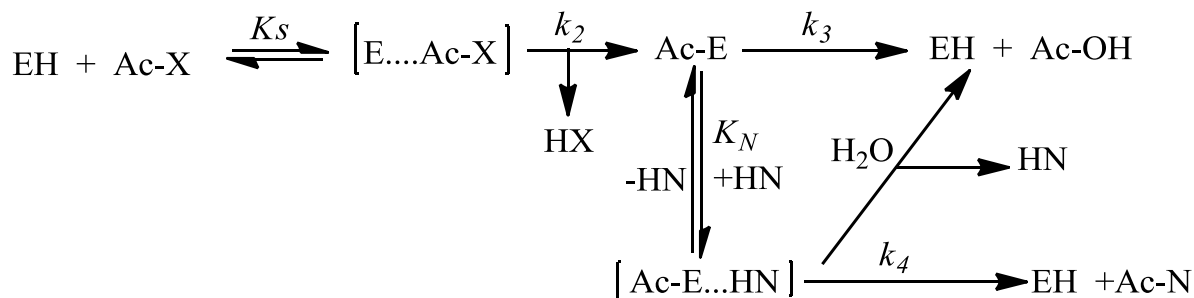
It has therefore been a well established principle in the use of proteases in peptide bond formation. Enzymatic peptide bond formation can either be thermodynamically or kinetically controlled.^[135,178]

The thermodynamically or equilibrium-controlled approach represents the direct reversal of the catalytic cleavage of peptides by proteases, which rely on the manipulation of the reaction conditions to shift the equilibrium in the direction of the peptide product to increase the yield of the coupling reaction (Scheme 2.3).^[135,178-180] The change in equilibrium can be achieved through the addition of organic co-solvents and the use of aqueous-organic biphasic systems. This approach applies the use of acyl donors with free carboxylate functions and presents the possibility of applying all proteases independently of their individual mechanism as potential catalysts. The underlying principle behind it is based on the thermodynamic barrier to the reverse of hydrolysis that is mostly determined by the energy required for the transfer of a proton from the reacting group of the nucleophile to that of the negatively charged carboxylate moiety of the acyl donor.^[135,178-180]



Scheme 2.3 General reaction scheme of thermodynamically controlled enzymatic peptide synthesis, where K_{ion} is the equilibrium constant of ionization and K_{con} is the equilibrium constant of conversion.^[135,178-180]

The kinetically controlled strategy is limited to serine or cysteine proteases which act as a transferase catalyzing the acyl transfer from a substrate ester to an N^α -unprotected amino acid or peptide derivative forming a new peptide bond.^[135,178-180] In contrast to the thermodynamically controlled strategy, the kinetically controlled approach typically proceeds faster and is easier to optimize resulting in higher product yields. The basic principle of this approach relies on the formation of an ester, an amide or a nitrile from the activated acyl donor and the binding of this to the enzyme to form a tetrahedral enzyme-substrate complex [E...Ac-X] which collapses to form the covalent acyl-enzyme intermediate [Ac-E] (Scheme 2.4). This intermediate can be nucleophilically attacked by water or a nucleophile (HN), which can be an amine, an alcohol or a thiol that will compete with water for the deacylation reaction (Scheme 2.4). The progress of the synthesis reaction depends on the kinetics of the nucleophilic reactions, hence the term “kinetically controlled”, and depends on temperature, pH, substrates concentrations and enzyme to substrate ratio.^[135,178-180]



Scheme 2.4 Schematic representation of the kinetically controlled enzymatic peptide synthesis, EH is the free enzyme; Ac-X is the acyl donor substrate; [E...Ac-X] is the Michaelis-Menten acyl-enzyme complex; HX is the released group; Ac-E is the acyl-enzyme intermediate, HN is the acceptor substrate (nucleophile), Ac-N is the product of synthesis (peptide) and Ac-OH is the product of hydrolysis of the acyl donor.^[135,178-180]

The applications of enzyme-catalyzed peptide bond formation include direct fragment condensation, substrate mimetics, and reactions in frozen aqueous systems, and have been extensively studied. The enzymatic methodology has several advantages compared to chemical methods, as it does not lead to racemization, is highly stereo- and regioselective, minimal side chain protection is required, non-toxic solvents are used, and there is a possibility to recycle the reagents used for synthesis. Also, the application of substrate mimetics allows the use of nonproteinogenic amino acids as substrates.^[22] However, protease-catalyzed peptide synthesis is limited by the specificity of enzymes (i.e., it is important to choose a protease with a different substrate specificity for a given synthesis reaction, to reduce the hydrolysis rate).^[22,181,182] Therefore, the combination of enzymatic peptide bond formation with synthetic methods for the site-specific incorporation of non-natural amino acids into peptides and proteins is most promising.

Consequently, Thust and Koksche,^[22,183] by means of a substrate mimetic approach (Figure 2.11),^[186,187] synthesized a library of peptides and site specifically introduced sterically demanding α -fluoroalkyl as well as α -methyl amino acids into the P1 position using trypsin or α -chymotrypsin. They coupled various C ^{α} -fluoroalkyl amino acids to a variety of nucleophiles of different length and sequence by means of trypsin; α -chymotrypsin only catalyzes acyl transfer reactions of Ala-derived acyl donors. The differences in synthetic efficiencies of α Dfm-substituted acyl donors compared to α Tfm as well as α -methyl derivatives could be attributed to the influence of the polarity of the fluoroalkyl substituent on enzyme-substrate interactions within the active site of the protease.^[22,183,186,187]

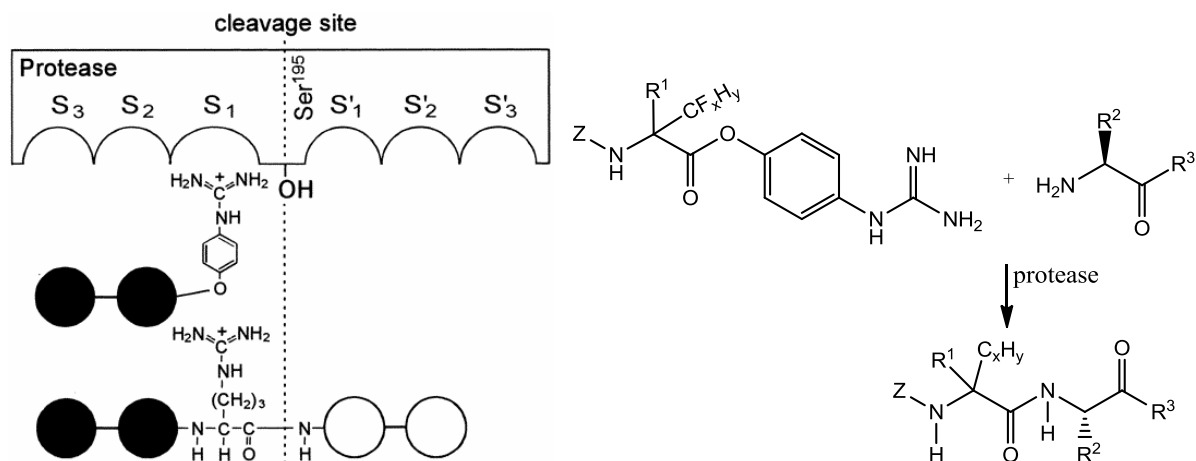


Figure 2.11 Schematic representation of the binding of a substrate mimetic (OGp ester) to the active site of trypsin and peptide synthesis using substrate mimetics of $C^{\alpha,\alpha}$ -dialkylated amino acids^[22,186,187]

2.3.8 Use of fluorinated amino acids in enzyme/protease inhibitors

From the above examples, fluorine containing peptides and proteins can possess enzymatic inhibitory potential against different kinds of enzymes (serine-, aspartyl-, and metallo proteases). Table 2.3 shows a list of some fluorinated amino acids with inhibitory potential.^[184] More recently, Geurink *et al.* reported the effect of F₅Phe incorporation in a tripeptide epoxyketone proteasome.^[28,24] Proteasomes consist of three proteolytically active sites (β 1, β 2, and β 5) with diverse substrate specificities.

The caspase-like β 1 subunit cleaves after acidic residues, the trypsin-like β 2 subunit after basic residues, and the chymotrypsin-like β 5 subunit cleaves after bulky, hydrophobic residues.^[185] They found out that the inhibitory potency is position dependent, with substitutions at the P2 and P3 sites leading to a remarkable decrease in potency, whereas substitution at P2 position shows higher potency, generating a highly specific inhibitor for the chymotrypsin-like β 5 subunit (Figure 2.12).^[28]

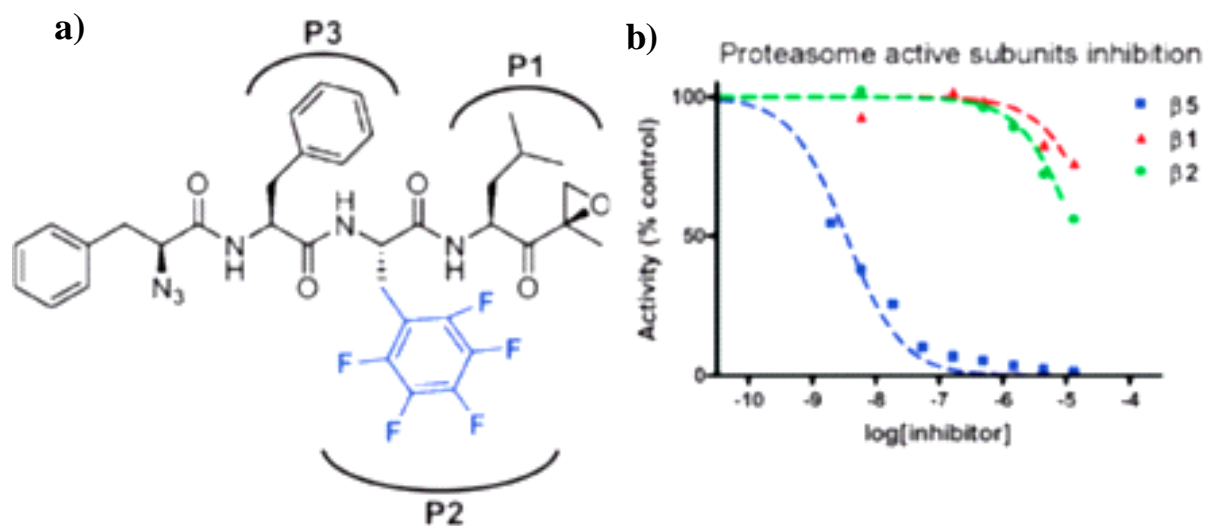
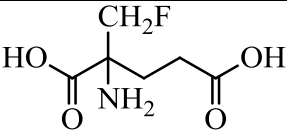
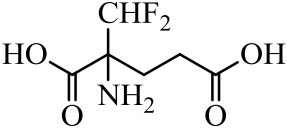
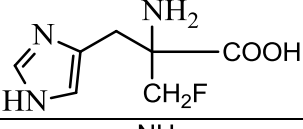
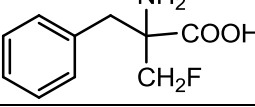
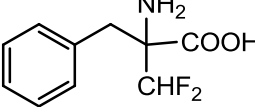
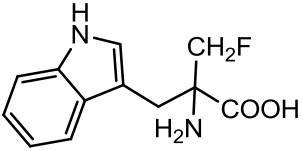
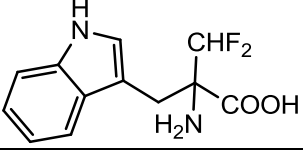
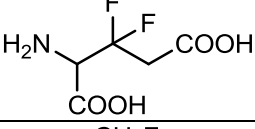
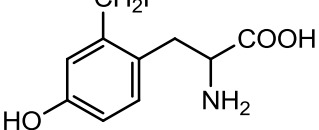
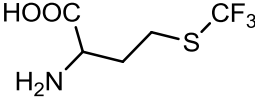
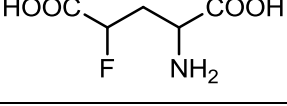


Figure 2.12 **a)** Structure of peptide epoxyketone proteasome inhibitor. Indicated are enzyme pockets (P1, P2, P3). **b)** Subunit activity post inhibition with proteasome inhibitor (adapted with from Guerink *et al.*^[28]). (Copyright 2011, American Chemical Society).

THEORY

Table 2.3 Some fluorinated amino acids with enzyme inhibitory activities (according to J. T. Welch *et al*)^[184,186]

| Fluorinated Amino acid | Structure | Activity |
|---|---|--|
| α -(fluoromethyl)glutamic acid |  | inhibitors of glutamate decarboxylase |
| α -(difluoromethyl)glutamic acid |  | |
| α -(fluoromethyl)histidine |  | inhibitors of histidine decarboxylase |
| α -(fluoromethyl)phenylalanine |  | reaction with pyridoxalphosphate |
| α -(difluoromethyl)phenylalanine |  | |
| α -(fluoromethyl)tryptophan |  | inhibitors of amino acid decarboxylase (AADC) |
| α -(difluoromethyl)tryptophan |  | |
| β -difluoroglutamic acid |  | inhibitor of polyglutamylation of folic acid |
| <i>o</i> -(fluoromethyl)tyrosine |  | inhibitor of tyrosine hydroxylase |
| trifluoromethionine |  | inhibitor of S-adenosylmethionine demethylation |
| γ -fluoroglutamic acid |  | inhibitor of polyglutamatesynthetase and glutamatemutase |

3. Aim and motivation

Improved bioavailability is vital for the successful application of fluorinated peptide-based pharmaceuticals. Because the incorporation of fluorine into peptides and proteins has effects that remain difficult to predict, it is essential that systematic investigations of the proteolytic stability of such potential therapeutics be conducted. The aim of this thesis was twofold: 1) to determine the impact of fluoroalkyl substitution on protease resistance by using several peptide substrates containing Abu, DfeGly or TfeGly at the P2, P1' or P2' positions by means of a HPLC based assay using α -chymotrypsin, pepsin, elastase, proteinase K and whole human blood plasma, and 2) to use the insights gained from such a survey to develop fluorinated peptide-based entry inhibitors against HIV.

4. Applied analytical methodologies

To investigate the effect of fluorination on the proteolytic stability of peptides, sensitive and efficient analysis of the cleavage products are required. The application of HPLC equipped with a fluorescence detector offers a unique, highly quantitative characterization of the analytes. The different analytical techniques used in this thesis are described below.

4.1 High Performance Liquid Chromatography (HPLC)

Liquid chromatography (LC) is a common technique used for the separation of components that is based on the injection of a small volume of liquid sample into a tube packed with porous particles (stationary phase), where individual components of the sample are transported along the packed tube (column) by a liquid moved by gravity. The separation of the components is based on chemical and/or physical interactions between the molecules and the packing particles.

Within the past 4 decades, HPLC has become a powerful technique used for the separation and analysis of biological and pharmaceutical compounds. The HPLC instrument consists of a reservoir for solvents (mobile phase), a high pressure pump, sample inlet device, column, detector and a recorder (Figure 4.1a). HPLC is based on the same principle as LC, but is faster, more efficient, more sensitive, and easier to operate. By the use of sensitive detectors, analysis of many trace components in complex systems can be carried out with HPLC. It also allows the use of very much smaller particle size (3 - 10 μm) for the column packing material which gives a much greater surface area for interactions between the stationary phase and the analyte, yielding much better separation of the components of the mixture (Figure 4.1b).

Presently, there are several techniques or separation modes use to analyze biomolecules. Different detection devices are now combined with HPLC for effective qualitative and quantitative data analysis. These include UV-visible absorption, fluorescence, refractive index, nuclear magnetic resonance (NMR) spectroscopy, mass spectrometry (MS), pulsed electrochemical detection (PED), and more sophisticated types such as laser-induced fluorescence (LIF).^[188-191] These detection devices are highly automated and extremely sensitive, which makes it easier to detect the compounds eluting from the HPLC column.

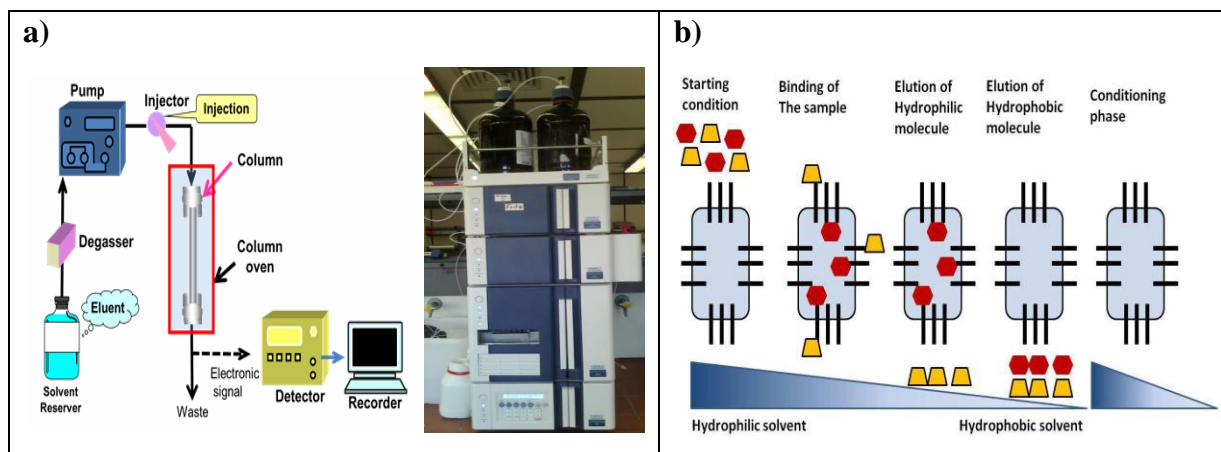


Figure 4.1 a) Basic Components of HPLC System. b) Schematic representation of reversed-phase HPLC principle.

There are two modes of HPLC, normal phase (NP) and reversed phase (RP), and their choice depends on the relative polarity of the analyte. NP, though commonly used in organic synthesis, is less frequently used for biomolecules and it depends on the analytes' ability to engage in polar interactions (such as hydrogen-bonding or dipole-dipole types of interactions) with the stationary phase and non-polar solvent (hexane or tetrahydrofuran). In contrast, RP uses a non-polar stationary phase and a polar solvent. The column used in NP-HPLC is packed with porous silica particles and has an internal diameter in the range of 1.0 - 4.6 mm and a length of 15 to 250 mm. By the use of a polar column, all polar components within an injected mixture will elute later because they stick to the polar silica while the non-polar compounds elute faster.

RP-HPLC uses similar column sizes as in NP-HPLC, the main difference being that the silica is modified to be non-polar by attaching long hydrocarbon chains to its surface, typically alkyl chains C18, C8, and C4, cyanopropyl silyl, or phenyl rings. The attachment of the hydrocarbons prevents attraction between the polar molecules and the silica thereby allowing rapid flow of polar molecules within the mobile phase. Thus, the separation of components depends on the differential adsorption of each solute according to its affinity for the immobilized stationary phase (Figures 4.1b and 4.2).^[192]

Another type of column less frequently used is the monolithic silica rod column, which consists of a single, rigid or semi-rigid, porous rod and was first introduced in 1991 by Nakanishi and Soga.^[193] This approach offers fast analysis by bypassing the limitations imposed by through-pore pressure, which allow higher flow rates than particulate columns at reasonable column backpressures.

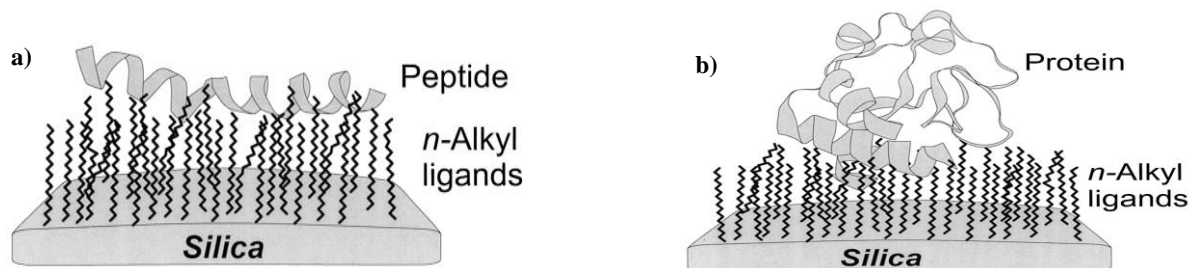


Figure 4.2 Schematic representation of the binding of **a)** a peptide and **b)** a protein, to an RP-HPLC silica-based sorbent. The peptide or protein interacts with the immobilized hydrophobic ligands through the hydrophobic chromatographic contact region (reproduced from Aguilar, M.I.)^[192]

Most RP-HPLC phases interact with analytes via weak van der Waals or dispersive interactions, which are due to an overlap of the outer electron clouds between the analyte and the bonded phase. Common RP-HPLC eluents include polar solvents such as water, acetonitrile, methanol, and 2-propanol. These solvents are either used as mixtures or as pure solvents mixed under instrument control with or without a gradient.

Reversed-phase chromatography has found both analytical and preparative applications in the preparation and characterization of biomolecules. Molecules that have some degree of hydrophobic character, such as proteins, peptides and nucleic acids, can be separated with excellent recovery and resolution.^[194]

Generally, reversed phase-separation experiments are performed in a stepwise manner. The first step is sample preparation in which the solute is dissolved in an initial mobile phase. Sample preparation is an essential part of HPLC analysis, intended to provide a reproducible and homogenous solution that is suitable for injection onto the column. Appropriate sample preparation ensures that the aliquot is free of solids, will not damage the column, and is compatible with the intended HPLC method; that is, the sample solvent will dissolve in the mobile phase without affecting sample retention or resolution.^[195] The choice of column depends on the nature of the compounds to be separated. For example, intact proteins can be separated on wide-pore silica bonded with short alkyl chains, (BioBasic 4 column). The short alkyl chains limit the denaturation or irreversible binding that can occur with longer alkyl chains.^[195]

Generally, longer columns provide better separation due to higher column efficiency, and, as the particle size decreases, the surface area available for coating increases. Columns with 5- μm particle size are usually optimal in terms of efficiency, reproducibility, and reliability.^[195]

In the second step, the analyte is loaded onto the column manually by injecting it or by the use of vials in an autosampler.^[195-197]

The third step involves the development of a method to run the separation. In this step, the sample can be separated by an isocratic (constant-composition during the entire run) approach, or by varying solvent strength and type according to a gradient. Gradients can be simple (linear gradient) or complex (start, hold, and ramp). Solvents such as methanol and acetonitrile can be mixed with water or used as pure solvents and mixed under instrumental conditions. By varying the amount (% solvent B) of the organic solvent (acetonitrile or methanol) in water (solvent A) containing the same concentration (0.01 to 0.2) of a suitable ionic modifier over time, a gradient is created and this offers a different partitioning effect. Different components in the mixture will then elute over a wide percentage of organic modifier. For peptide and protein purification and analysis, gradient elution is preferred and TFA is usually used as an ionic modifier that controls the pH and ionization state or acts as an ion-pairing reagent since pH and the state of the analyte play an important role in achieving good chromatographic separation.^[198] Gradient elution can be used for small molecule separations, if the compounds differ greatly in hydrophobicity. The gradient influences the resolution, and can be modified in the following ways: flow rate (depends on column ID), delay time (time spent at initial % organic), starting % organic, ending % organic, hold time (time spent at final % organic), rate of change (% increase in organic over time), gradient shape (linear, concave, convex), re-equilibration time (volume needed to reestablish initial conditions).

As they elute, the different components are detected using appropriate techniques for optimum sensitivity. As mentioned above, a large number of LC detectors have been developed over the past thirty years based on a variety of different sensing principles. The dominantly used detectors in LC analysis include UV (fixed or variable wavelength), electrical conductivity, fluorescence, and refractive index detectors, or mass spectrometers. The choice of detector depends on the sample and the purpose of the analysis.^[199]

4.1.1 UV detection

Many analytes absorb light in the ultraviolet or visible regions. The UV detector employs a deuterium discharge lamp (D2 lamp) as a light source and detects compounds by their absorbance of light over a range of wavelengths, from 190 to 380 nm.

Components that absorb at longer wavelengths can also be detected by the use of a UV-VIS detector, which employs an additional tungsten lamp (W lamp).^[200]

There are three types of UV absorbance detectors. These include fixed-wavelength, variable-wavelength, and diode-array detectors (DAD). The fixed-wavelength type uses a mercury vapor lamp, which emits light at 253.7 nm, and can be used to detect compounds containing carbonyl groups, multiple double bonds, or aromatic rings. The variable-wavelength detector uses a deuterium lamp that produces a broad spectrum of wavelengths and is more sensitive due to a photomultiplier tube or amplification circuitry. The DAD or photodiode array detector (PAD) can measure absorption at different wavelength which allows for the monitoring over a wide range of wavelengths simultaneously. The diode array detector records UV/Visible absorption spectra in real time while compounds are eluting from a column.

In the detection process, an ultraviolet light beam is directed through a flow cell and a sensor measures the light passing through the cell. If a compound elutes from the column that absorbs this light energy, it will change the amount of light energy falling on the sensor. The resulting change in this electrical signal is amplified and directed to a recorder or data system as shown in Figure 4.3. This response is amplified and plotted against time to give a chromatogram (Figure 4.5). A UV spectrum is sometimes also obtained which may aid in the identification of a compound or series of compounds. The detection of components by the detector is displayed on a chart or computer screen (chromatogram).^[200]

In RP-HPLC, detection of peptides and proteins are generally carried out between 210 and 220 nm, which is particular for the amide bond, or at 280 nm, which is specific for the aromatic amino acids tryptophan, phenylalanine and tyrosine that absorb ultraviolet light in the range of 250 to 290 nm. These spectra can be used to identify peaks specifically on the basis of spectral characteristics and for the assessment of peak purity.^[201-203] In addition, second derivative spectroscopy can provide information on the conformational integrity of proteins following elution.^[204]

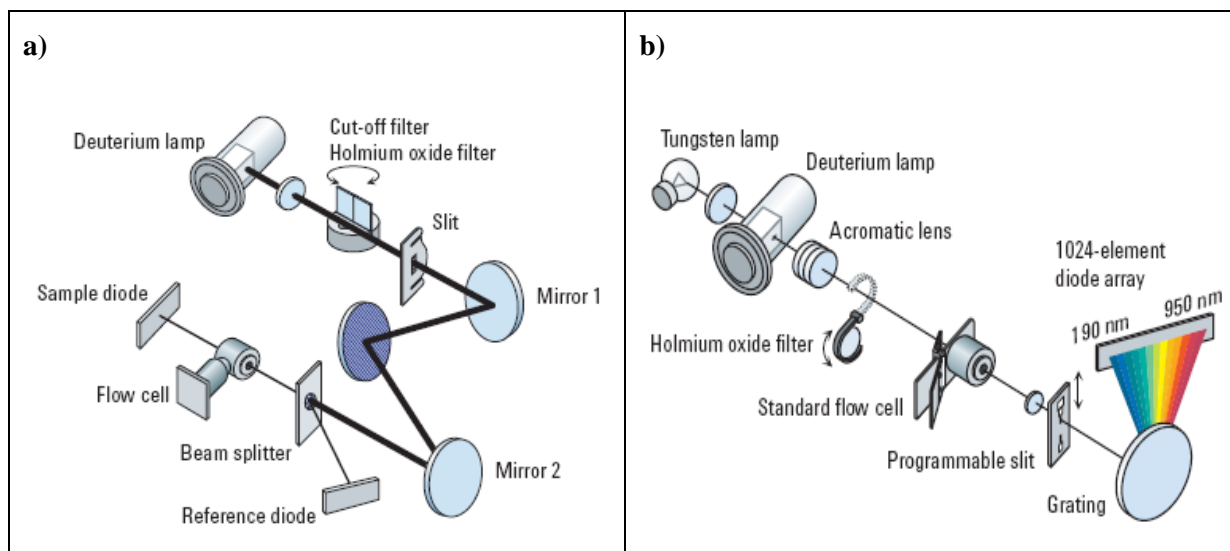


Figure 4.3 Diagrammatic illustration of UV detector optical system: **a)** Variable Wavelength Detector (monochromator) and **b)** Diode array detector (polychromator).

4.1.2 Fluorescence detection

Fluorescence detectors are the most sensitive detectors in liquid chromatography, offering an advantage over UV detectors due to higher selectivity that allows the quantification and identification of compounds and impurities in complex mixtures at extremely low concentrations. Even though fluorescence detectors are very specific and selective, their use is somewhat limited because the number of naturally fluorophoric compounds that can be analyzed by fluorescence detection only account for about 10 percent of organic molecules. These fluorophore characteristics enable the molecules to absorb and emit light over a range of wavelengths.^[205]

The general principle is based on the excitation of molecules from their ground state to their excited state by the absorption of light (provided by a Xenon flash lamp). The absorbed energy is then emitted at longer wavelengths subsequent to nonradiative relaxation and the molecule returns to the ground state; this process is known as fluorescence.^[206] The emission wavelength is then monitored by a detector which is set at a right angle to the UV light source used to excite the analyte (Figure 4.4). The result of this fluorescence scan can be viewed in a three-dimensional plot showing excitation wavelength, emission wavelength and fluorescence intensity.^[207]

Fluorescence of molecules can be measured as a function of their concentration at appropriate excitation and emission wavelengths for qualitative and quantitative analyses.^[205]

Analytes that are present at trace levels are commonly derivatized by attaching a fluorescent marker.^[208]

Both excitation and emission fluorescence spectra help to characterize individual compounds. While excitation spectra are identical to UV/Visible absorption spectra, emission spectra can give additional information.

Proteins and peptides sometimes contain aromatic amino acids that are also fluorophores. Phenylalanine, tyrosine, and tryptophan are the only naturally fluorescent amino acids among the 20 canonical amino acids, with tryptophan being highly fluorescent and phenylalanine the least. Their excitation wavelengths are 260 nm, 274 nm, and 280 nm and emission wavelengths 295 nm, 324 nm, and 348 nm, respectively.^[205,209-211]

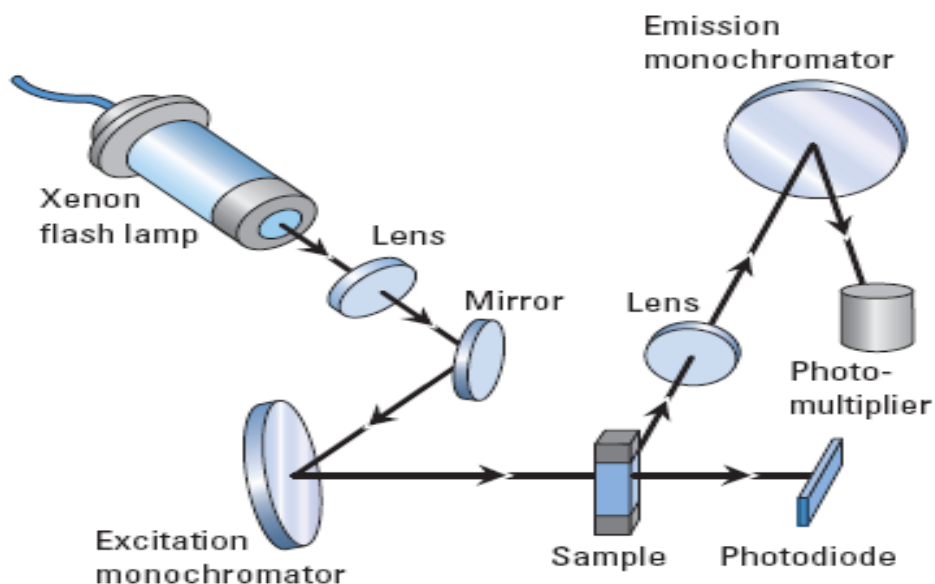


Figure 4.4 Illustration of the optical design of the Agilent 1100 Series fluorescence detector.

4.1.3 Coupling liquid chromatography to a mass spectrometer (LC/MS)

Mass spectrometers are used to generate mass spectral data that can provide important information on the molecular weight, structure, identity, quantity, and purity of a sample.^[212]

Coupling this instrument to an HPLC system provides much more information and leads to the specific characterization of compounds. The coupling of MS to RP-HPLC (LC/MS) is the most common form of LC/MS and offers reliable separation of a wide range of organic compounds, from small-molecule drug metabolites to peptides and proteins. It provides information on both molecular weight and structural peak confirmation.

Of late, LC/MS has become a crucial technique used to study the kinetics of proteolytic reactions and for the screening of proteolytic activities.^[213]

A mass spectrometer consists of 3 major parts: an ionization source, a mass analyzer, and a detector. It works by ionizing molecules (ionization source) and then sorting (mass analyzer) and identifying the ions according to their mass-to-charge (m/z) ratios (detector). Diverse types of ion sources are commonly used for LC/MS including; electron ionization (EI), chemical ionization (CI), fast atom bombardment (FAB), electrospray ionization (ESI), and matrix-assisted laser desorption/ionization (MALDI). Electrospray ionization and MALDI are mostly used for analyzing large biomolecules such as proteins, peptides, and oligonucleotides.^[214,215] The basic principle of LC/MS follows the liquid chromatographic procedures described above and a MS detector senses a compound eluting from the HPLC column, ionizes it and then measures its mass and/or fragments the molecule into smaller pieces that are unique to the compound. Depending on the nature of the analyte, the ion source could be operated in positive (addition of a proton ($M+H^+$)) or negative (the loss of a proton ($M-H^-$)) modes. With the presence of salts, adduction of cations (e.g. $M+NH_4^+$, $M+Na^+$, $M+K^+$) and anions (e.g. $M+formate^-$, $M+acetate^-$) can occur. Higher mass analytes, such as proteins and peptides with various charge functionalities can exhibit multiple charges that result in cationized ions such as $[M+nH]^{n+}$.^[214-217]

After the detection of the components using one of the modern analytical detectors listed above, the final step in the HPLC measurement is the interpretation of the output from the detector. The set of peaks which represents the available individual chemical (analytes) within the sample mixture appears at different times (retention times) depending on the chemical properties of the chromatographic medium (Figure 4.5). The assignment of peaks can be authenticated using standards from calibration curves, UV or mass spectrometers. Thus, peaks can be used as a means to measure the quantitative (amount) and qualitative (purity and components) aspects of the sample. The area under the peak is proportional to the amount of a particular component which has passed through the detector, and this area can be integrated automatically by the software on the computer linked to the instrument.^[192]

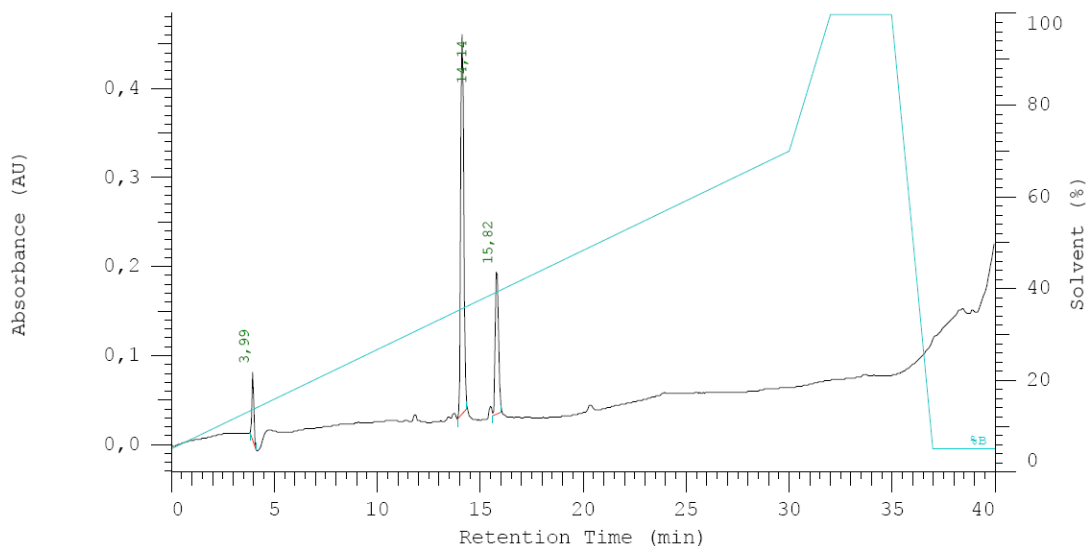


Figure 4.5 Example of an HPLC chromatogram of a peptide showing all the available components and the gradient scheme used.

4.2 Molecular modelling (molecular dynamics)

Computational approaches have gained wide use in the drug design process. In general, computational tools can be utilized for the generation, manipulation, or visualization of three-dimensional models of small molecules, peptides, or proteins. Computer-aided investigation of molecular complexes can provide a different perspective for the interpretation of experimental data in the field of molecular recognition. Molecular docking is frequently used to predict the most probable binding orientation (pose) of a ligand within a defined environment, such as a protein binding site, and in turn predict the affinity and activity of the ligand.^[218-220] Such software allows molecular data to be obtained, including geometries (bond lengths, bond angles, torsion angles), energies (heats of formation, activation energy, etc.), and properties (volumes, surface areas, diffusion, viscosity, etc.).^[220,221] Docking algorithms share the strategy to geometrically fit a ligand into a binding site that is mostly assumed to be rigid. However, the algorithms and search strategies differ significantly from one method to another. Ultimately, the resulting docking poses can be prioritized manually or by using a scoring function.^[222]

5. Results and Discussion

5.1 Design of model peptides for proteolytic stability studies

Several model peptide substrates with different non-canonical amino acids in the P2, P1' or P2' position (nomenclature according to Schechter & Berger, 1967)^[52] were designed and synthesized with the aim of investigating their impact on proteolytic stability. A standard positive control peptide (FA peptide): Abz-Lys-Ala-Ala-Phe-Ala-Ala-Ala-Lys as illustrated in Figure 5.1 was designed with a central phenylalanine residue in the P1 position as the substrate specificity of both chymotrypsin and pepsin mainly relies on large hydrophobic residues, such as Phe, Trp and Tyr at the P1 position.^[84-88]

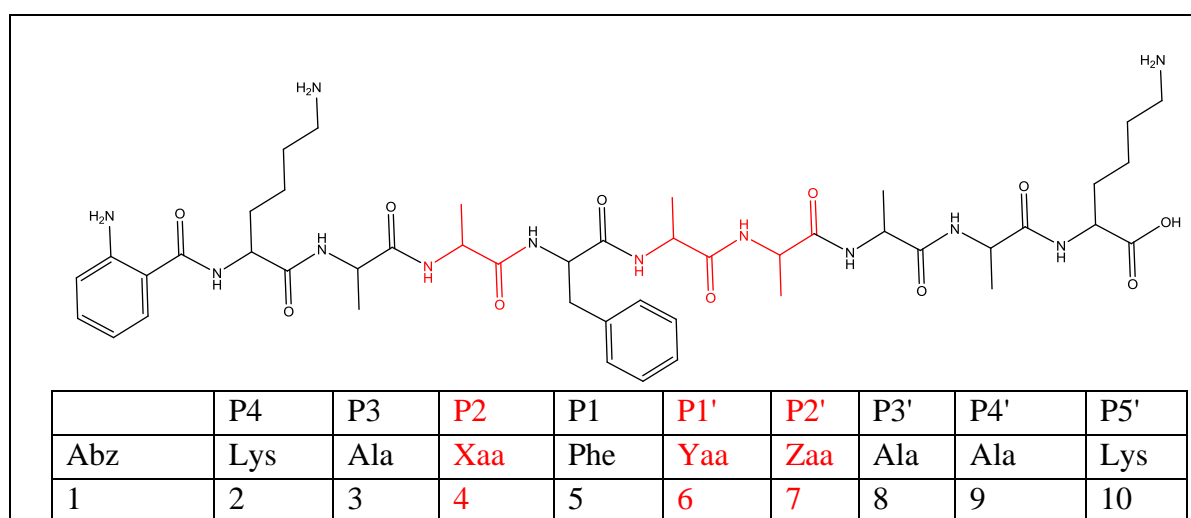


Figure 5.1 Control peptide sequence designed for protease stability study involving chymotrypsin, pepsin, proteinase K, elastase and human blood plasma. X-, Y-, and Zaa, marked in red, are positions containing alanine in the control peptide or nonproteinogenic amino acids in the other variants.

Alanine in the P1' position was replaced by either lysine or phenylalanine to optimize the substrate characteristics for chymotrypsin, pepsin, and other proteases. As the substrate binds to the enzyme's active site in an extended conformation,^[100] alanines in positions P3, P3' and P4' act as spacers. Lysines were attached to the ends of the sequence to enhance solubility, and *o*-aminobenzoic acid (Abz) was used as a photometric label. Alanines in the P2, P1' and P2' positions were singly replaced with the nonproteinogenic amino acids; aminobutyric acid (1, Abu), difluoroethylglycine (2, DfeGly) and trifluoroethylglycine (3, TfeGly) (Figure 5.2) to yield the different peptide analogues shown in Table 5.1.

The fluorinated amino acids differ in their degree of fluorination and hence are expected to place different steric demands on the enzyme's binding pocket. Additionally, such fluoroalkyl

side chains have been shown to polarize neighboring C-H bonds with sometimes appreciable effects on intermolecular noncovalent interactions.^[11,23]

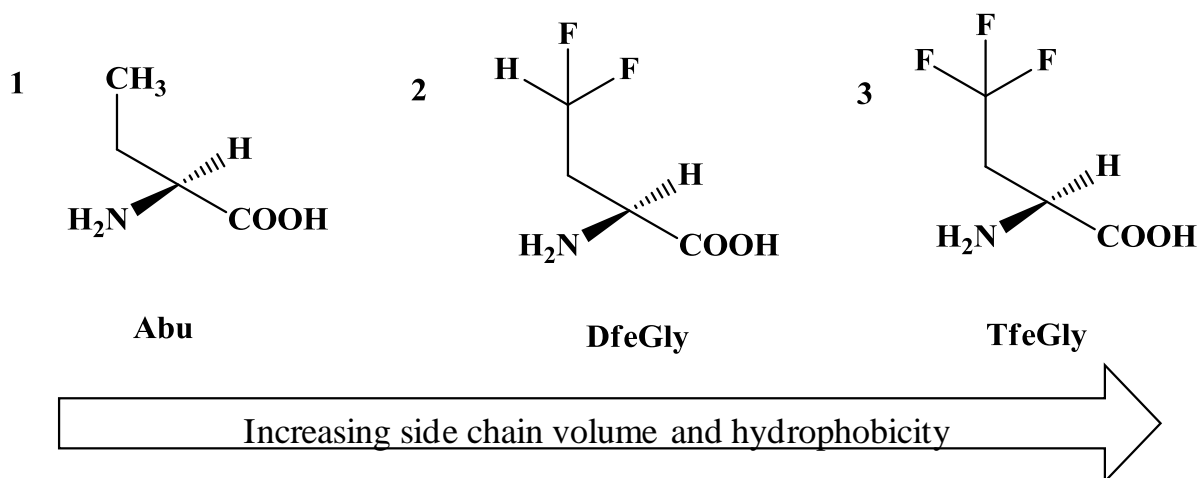


Figure 5.2 Structures of ethylglycine and fluorinated amino acids used in this study. 1. (*S*)-ethylglycine or aminobutyric acid (Abu), 2. (*S*)-4,4-difluoroethylglycine (DfeGly) and 3. (*S*)-4,4,4-trifluoroethylglycine (TfeGly). Adapted from Jäckel et. al.^[156]

Aminobutyric acid (Abu) was included in this study to distinguish between effects relating to fluorine and those relating to the hydrocarbon chain itself. This strategy led to the synthesis of the three series FA, FF, and FK, each containing numerous variants carrying nonproteinogenic residues in positions that are significant for substrate recognition by the protease. These peptides are named according to the residue present at the P1 and P1' positions, and the identifier for the particular unnatural building block. It is important to note that the P1 position was not mutated because the control peptide was designed such that the substrate specificities of several proteases are represented, and also the presence of phenylalanine ensures that the incorporation of the nonproteinogenic amino acids will not generate a new cleavage site.

RESULTS AND DISCUSSION

Table 5.1 List of studied peptides with cleavage occurring between P1 and P1'. The names of the control peptides were assigned according to the amino acid residues occupying the P1 and P1' positions. Marked in grey are the reduced FA peptide sequences used for the molecular modeling study.

| Peptide Names | | P4 | P3 | P2 | P1 | P1' | P2' | P3' | P4' | P5' |
|---------------------------|------|-----|-----|---------------|-----|---------------|---------------|-----|-----|-----|
| FA | Abz- | Lys | Ala | Ala | Phe | Ala | Ala | Ala | Ala | Lys |
| P2-TfeGlyFA | Abz- | Lys | Ala | TfeGly | Phe | Ala | Ala | Ala | Ala | Lys |
| P2-DfeGlyFA | Abz- | Lys | Ala | DfeGly | Phe | Ala | Ala | Ala | Ala | Lys |
| P2-AbuFA | Abz | Lys | Ala | Abu | Phe | Ala | Ala | Ala | Ala | Lys |
| P1'-TfeGlyFA ¹ | Abz- | Lys | Ala | Ala | Phe | TfeGly | Ala | Ala | Ala | Lys |
| P1'-DfeGlyFA | Abz- | Lys | Ala | Ala | Phe | DfeGly | Ala | Ala | Ala | Lys |
| P1'-AbuFA | | | | | | Abu | | | | |
| P2'-TfeGlyFA | Abz- | Lys | Ala | Ala | Phe | Ala | TfeGly | Ala | Ala | Lys |
| P2'-DfeGlyFA | Abz- | Lys | Ala | Ala | Phe | Ala | DfeGly | Ala | Ala | Lys |
| P2'-AbuFA | Abz- | Lys | Ala | Ala | Phe | Ala | Abu | Ala | Ala | Lys |
| FK | Abz- | Lys | Ala | Ala | Phe | Lys | Ala | Ala | Ala | Lys |
| P2-TfeGlyFK | Abz- | Lys | Ala | TfeGly | Phe | Lys | Ala | Ala | Ala | Lys |
| P2-DfeGlyFK | Abz- | Lys | Ala | DfeGly | Phe | Lys | Ala | Ala | Ala | Lys |
| P2'-TfeGlyFK | Abz- | Lys | Ala | Ala | Phe | Lys | TfeGly | Ala | Ala | Lys |
| P2'-DfeGlyFK | Abz- | Lys | Ala | Ala | Phe | Lys | DfeGly | Ala | Ala | Lys |
| P2'-AbuFK | Abz- | Lys | Ala | Ala | Phe | Lys | Abu | Ala | Ala | Lys |
| FF | Abz- | Lys | Ala | Ala | Phe | Phe | Ala | Ala | Ala | Lys |
| P2-TfeGlyFF | Abz- | Lys | Ala | TfeGly | Phe | Phe | Ala | Ala | Ala | Lys |
| P2-DfeGlyFF | Abz- | Lys | Ala | DfeGly | Phe | Phe | Ala | Ala | Ala | Lys |
| P2'-TfeGlyFF | Abz- | Lys | Ala | Ala | Phe | Phe | TfeGly | Ala | Ala | Lys |
| P2'-DfeGlyFF | Abz- | Lys | Ala | Ala | Phe | Phe | DfeGly | Ala | Ala | Lys |
| P2'-AbuFF | Abz- | Lys | Ala | Ala | Phe | Phe | Abu | Ala | Ala | Lys |

5.2 Enzymatic assay and protease stability of peptides^{II}

5.2.1 Stability Measurements

The ability of the peptides to interact with serine proteases (α -chymotrypsin, elastase, proteinase K) and aspartic protease (pepsin) were determined by an analytical RP-HPLC assay coupled with fluorescence detection and characterization by ESI. The use of HPLC (fluorescence) to analyze cleavage products is a well-established method which offers fast, highly sensitive and reproducible quantitative monitoring of proteolytic activity.^[192,223-225]

¹ For simplicity, the P1'-FA variants are named so even though they technically lack the alanine at the P1' position.

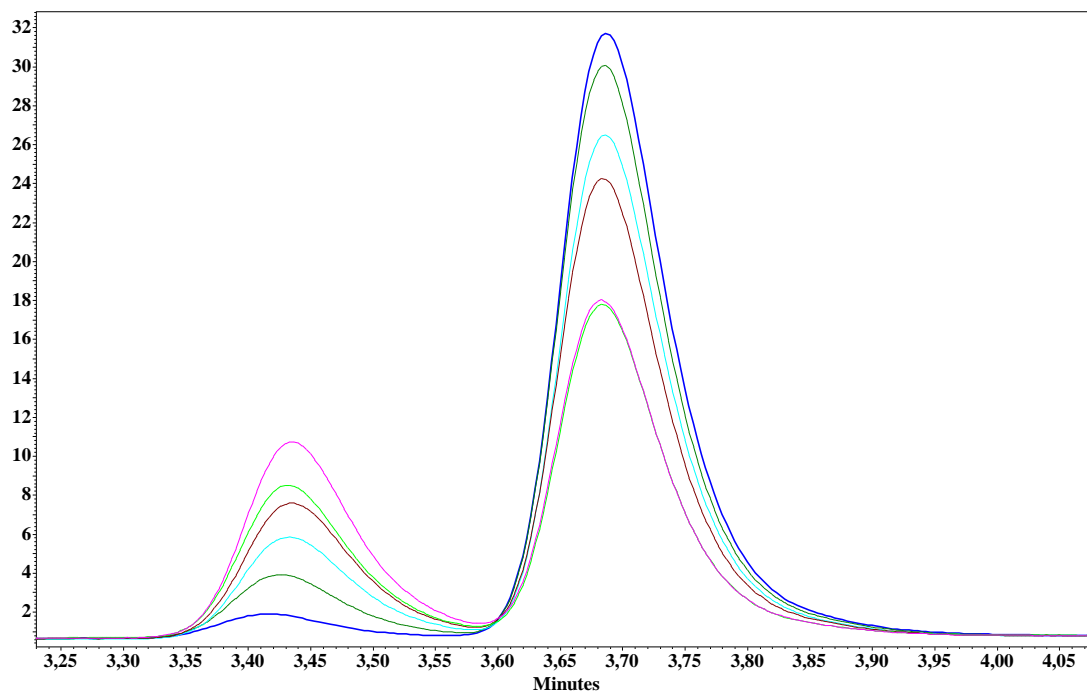
^{II}Part of these results has been published in Amino Acids. Co-Authors; Jérémie Mortier, Gerhard Wolber, Beate Kokschi. This does not include results from the FK and FF variants.

RESULTS AND DISCUSSION

The peptides were incubated with each enzyme at different conditions as described in the experimental section (9.4.1).

Aliquots were withdrawn at different time intervals from each enzyme digestion mixture, quenched with the appropriate solution and run on an analytical RP-HPLC equipped with a fluorescence detector (see Figure 5.3 for representative chromatogram).

a)



b)

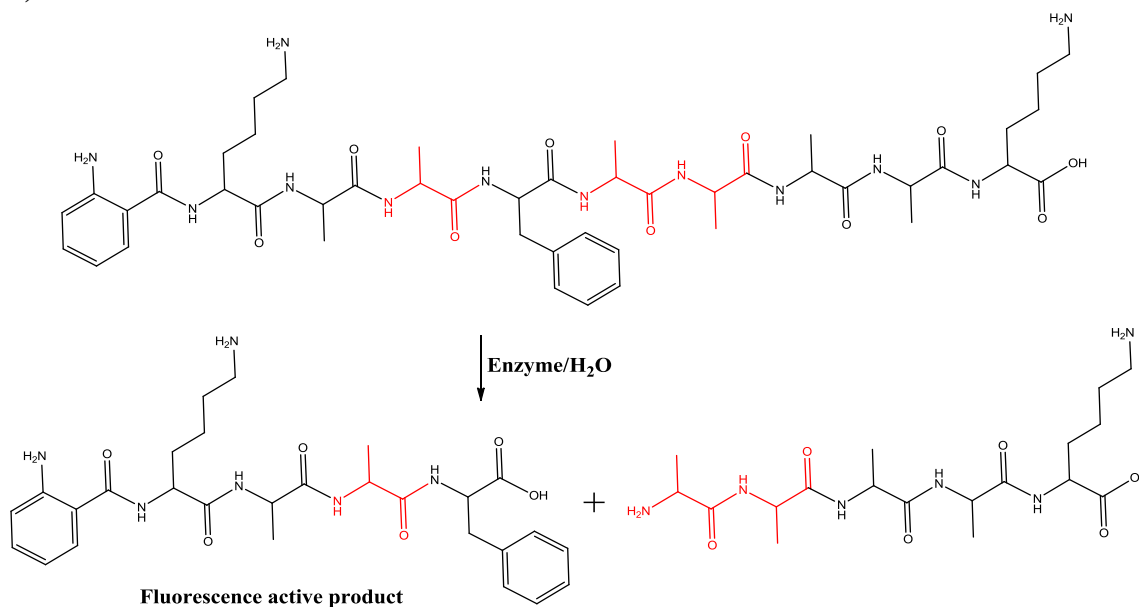


Figure 5.3 a) Fluorescence HPLC chromatograms showing increasing or decreasing peak heights of product (Abz-KAAF) and educt (Abz-KAAFAAAAK) at different reaction times, respectively. b) Schematic representation of the degradation of the control peptide.

The systematic degradation of all peptides by the different enzymes over a period of 120 minutes was then analyzed.

Quantification and characterization of the nondegraded substrates and the products formed were carried out using the chromatography software (EZChrom Elite Version 3.1.7). The percentage integration of HPLC peak area of the educts and the N-terminal fragments (products) were determined and used as the basis for understanding the effect of fluorination on the enzymes' activity.

5.2.2 Molecular modeling of FA variants with α -chymotrypsin and pepsin

To gain insight into the interaction between the peptide ligand and the enzyme binding site, the three FA peptide series were further investigated by molecular modeling. Each peptide/protease combination was subjected to molecular docking using GOLD.^[226,227] This software implements a genetic algorithm to represent the rotational, translational and torsion angles of a molecule to explore the conformational space of a ligand within an enzyme binding site. Such an approach remains challenging with peptide structures that have multiple rotatable bonds. To decrease the number of atoms and bonds for the calculation, each sequence was built from the P2 to the P2' unit, and both the carboxy-terminus and the amino-terminus were methylated (Me). Thus, the substrates were constructed according to the following short sequence: MeHN-P2-P1-P1'-P2'-Me (sequences also shown in grey part of Table 5.1). For these 10 peptide variants, docking conformations were generated within the α -chymotrypsin and pepsin enzymatic cavities. The best poses were achieved when the P1 phenylalanine side chain was oriented towards the hydrophobic S1 pocket of the enzyme and the backbone of the peptide was stabilized, in agreement with previously published studies,^[86,88,103,228] as summarized in Table 5.2.

These results show excellent complementarity between the residues from P2 to P2' of the ligand and their corresponding protein subsites S2 to S2'. Moreover, the side chain of Ser195 is always ideally oriented between the P1 and P1' positions which is in accord with the key role of this residue in the enzymatic mechanism of α -chymotrypsin. These conformations were therefore considered to be a solid basis to support structural arguments regarding the ligand-enzyme interactions studied here, and their influence on proteolytic stability.

Table 5.2 Common intermolecular interactions for all valid docking poses into the α -chymotrypsin (Chymo) and pepsin binding sites^[86,88]

| INTERACTION | LIGAND | | PROTEIN | | |
|-------------|---------|-------------------|---------|---|---------------|
| | residue | atoms | enzyme | residues | atoms |
| H-bond | P2 | backbone NH | Chymo | Ser214 | backbone CO |
| H-bond | P1 | backbone CO | Chymo | Gly193, Ser195 | backbone NH's |
| Hydrophobic | P1 | Phe aromatic ring | Chymo | Met192, Cys191-Cys220^{III} , Val213 | side chains |
| H-bond | P2' | backbone NH | Chymo | Phe41 | backbone CO |
| H-bond | P2 | backbone CO | Pepsin | Thr77 | backbone NH |
| H-bond | P1 | backbone NH | Pepsin | Gly217 | backbone CO |
| Hydrophobic | P1 | Phe aromatic ring | Pepsin | Ile120, Phe117, Val30 | side chains |
| H-bond | P1 | backbone CO | Pepsin | Gly76 | backbone NH |
| H-bond | P2' | backbone NH | Pepsin | Gly34 | backbone CO |

5.2.3 Hydrolysis of peptides by α -chymotrypsin (EC 3.4.21.1)

Alpha-chymotrypsin, a well-studied serine endoprotease was used to screen the effect of fluorination on proteolytic stability of the peptides. As mentioned in section 2.1.3.1, α -chymotrypsin preferentially catalyzes the hydrolysis of peptide bonds at the carbonyl end of Trp, Tyr, Phe and Leu in P1 position (high specificity), and, to a lesser extent, Ile, Met, Ser, Thr, Val, His, Gly and Ala.^[84-88,97]

The peptides were subjected to degradation by chymotrypsin and the stepwise hydrolysis was monitored with an analytical HPLC equipped with a fluorescence detector at an excitation wavelength of 320 nm and an emission wavelength of 420 nm.

The results of the hydrolysis experiments and details of the molecular modeling studies (for the reduced FA variants) are presented in the next section and grouped according to the position of the nonproteinogenic amino acid modification.

5.2.3.1 P2 variants

P2FA variants

The S2 subsite of α -chymotrypsin forms a shallow hydrophobic groove and generally prefers to accommodate hydrophobic residues.^[86,229] The data obtained from the proteolysis assay suggested that P2-TfeGlyFA is well accommodated by the active α -chymotrypsin and clearly demonstrate that this peptide is the most rapidly degraded of all studied P2 variants

^{III} Cys 191 and Cys220 are connected by a disulfide bridge.

(88% of the initial concentration hydrolyzed after 2 h versus 36% for FA and 73% for P2-AbuFA) as shown in Figure 5.4a. Molecular docking shows that the residue in the P2 position is likely to face the Ile99 side chain of the S2 pocket (Figure 5.4b)^{IV}, creating an environment that is well suited to accommodate the trifluoroalkyl side chain. Interestingly, the presence of a difluoromethyl group in the P2 position significantly reduces the rate of hydrolysis, 30% of the initial concentration of P2-DfeGlyFA hydrolyzed after 2 h, compared to its natural analogue. This observation might be due to the polarized γ C-H methine moiety of the difluoromethyl group.^[11,23] To summarize the protease stability results for the FA series in which the P2 position was substituted, the following trend was observed: P2-DfeGlyFA>FA>>P2-AbuFA>P2-TfeGlyFA (Figure 5.4a).^V

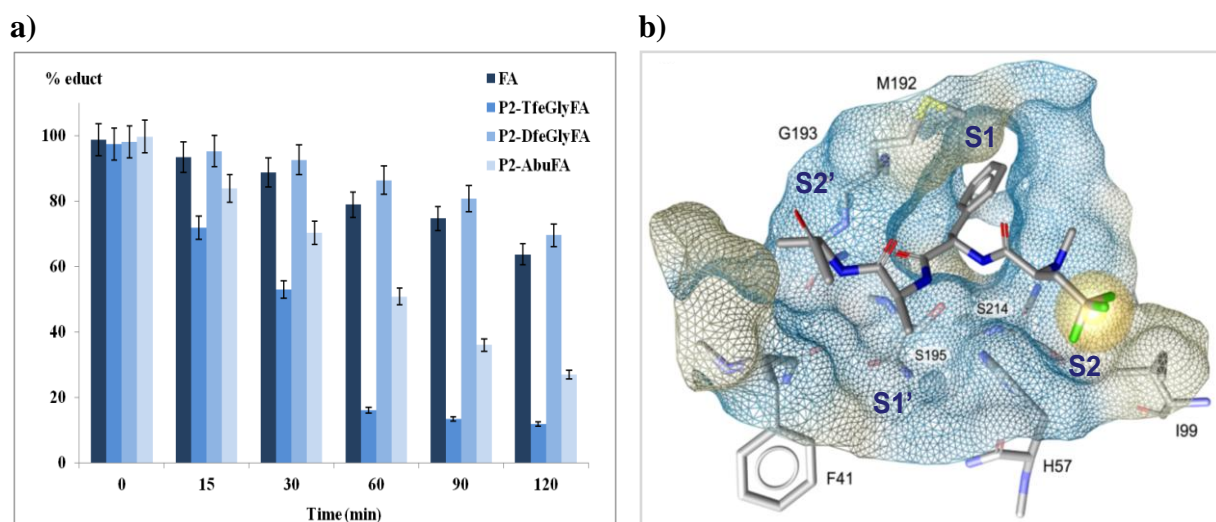


Figure 5.4 a) Time course of changes in the area of the HPLC peaks representing the fluorescent fragments present after hydrolysis of the P2FA by α -chymotrypsin (10 mM phosphate buffer, pH 7.4) at 30 °C and b) suggested binding poses for P2-TfeGlyFA bound to α -chymotrypsin. The color code of the surface of the cavity is yellow for lipophilic regions and blue for hydrophilic regions. Highlighted hydrophobic moieties are depicted as yellow spheres.^[244]

Michaelis Menten kinetics

The incorporation of fluorinated amino acids into peptide substrates presents conformational changes and different interactions within the enzyme's active site.^[21,22] Therefore, the systematic investigation of the kinetics of these peptides, and the characterization of how varying the substrate concentration changes the velocity of the reaction in the presence of a constant enzyme concentration, is critical.^[109,110]

^{IV} The molecular modeling was only carried out for the most degraded peptides.

^V In all proteolytic stability "X>Y>>Z" type relationships are showing from most stable to the least stable.

The determination of both K_m and V_{max} can provide information on the enzyme's affinity for a substrate, its role in metabolism, its activity and inhibition properties.^[111,112]

Because of the very rapid rate of degradation observed in the P2-trifluoroalkyl peptide in the presence of α -chymotrypsin, the P2-TfeGlyFA peptide and FA as a control were selected for determination of the Michaelis-Menten kinetic parameters. To examine these properties, the peptides FA and P2-TfeGlyFA were subjected to enzymatic degradation. The amount of product (Abz-KAAF or Abz-KATfeGlyF, respectively) formed at different times was measured by analytical RP-HPLC equipped with a fluorescence detector at an excitation wavelength of 320 nm and an emission wavelength of 420 nm. A standard calibration curve was generated using stock solutions of pure Abz-KAAF and P2-TfeGlyFA peptides ranging from 6 μ M to 3 mM, where the area of peak integration was plotted as a function of concentration (Figure 5.5a and b). The resulting linear regression, calculated using equations 5.1 and 5.2, yields the values used to determine the concentration of product formed in each reaction (Figure 5.5c and d).

$$y = ax + b \tag{Equation 5.1}$$

Where a = slope and b = intercept and x can be written as

$$X = \frac{\text{Peak area (y)} - \text{intercept (b)}}{\text{slope (a)}} \tag{Equation 5.2}$$

The parameters K_m and V_{max} were obtained by using different common methods including the Lineweaver-Burk, Hanes-Woolf, and the Eadie-Hofstee plots. The first is produced by plotting the reciprocal of reaction velocity (obtained from the Michaelis Menten curve, Figure 5.6) against the reciprocal of substrate concentration. The second is obtained by plotting the ratio of initial substrate concentration [S] to reaction velocity v against substrate concentration.

The third is a plot of reaction velocity against the ratio between reaction velocity and substrate concentration (Table 5.3).

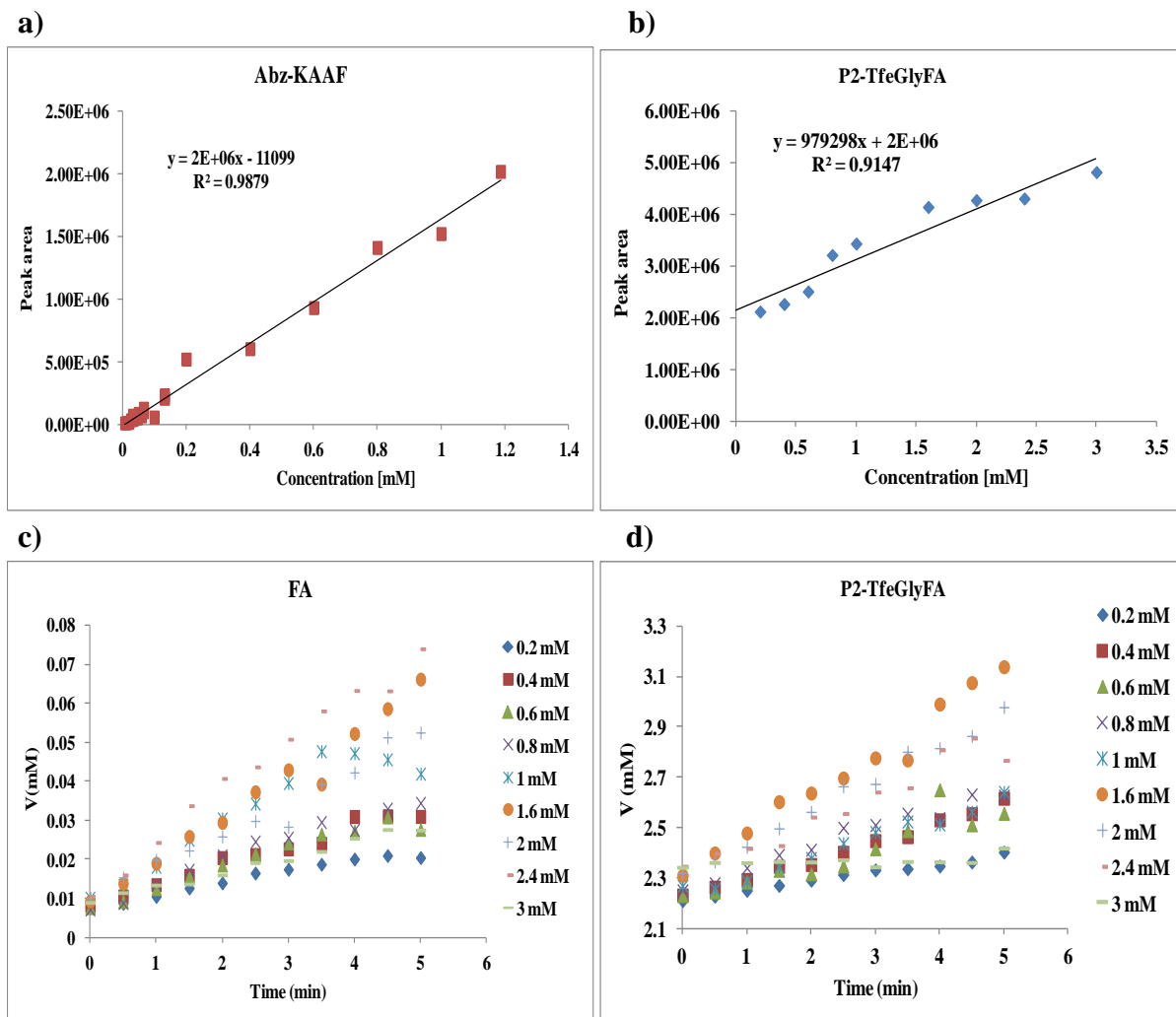


Figure 5.5 Calibration curves: HPLC peak integration versus different concentrations of **a)** Abz-KAAF (red) and **b)** P2-TfeGlyFA (blue) peptides for the conversion of peak area to reaction velocity. The stepwise increase in product formation at different reaction times with various peptide concentrations is used to determine the initial velocities of **c)** FA and **d)** P2-TfeGlyFA peptides.

The observed K_m of P2-TfeGlyFA for α -chymotrypsin is reproducibly lower than that of FA and the rate of degradation (reaction velocity, V_{max}) of P2-TfeGlyFA is significantly faster than that of FA (Table 5.3 and Figure 5.6). The lower K_m value of P2-TfeGlyF contributes to its more efficient hydrolysis, as K_m is a measure of the affinity of the enzyme (in this case α -chymotrypsin) for its substrate; the lower the K_m value, the higher the affinity of the enzyme for the substrate.^[109-112]

This finding is consistent with the molecular docking studies, which show that the residue in the P2 position is likely to face the Ile99 side chain of the S2 pocket, an environment that seems well-suited to accommodate the trifluoromethylated variant.

RESULTS AND DISCUSSION

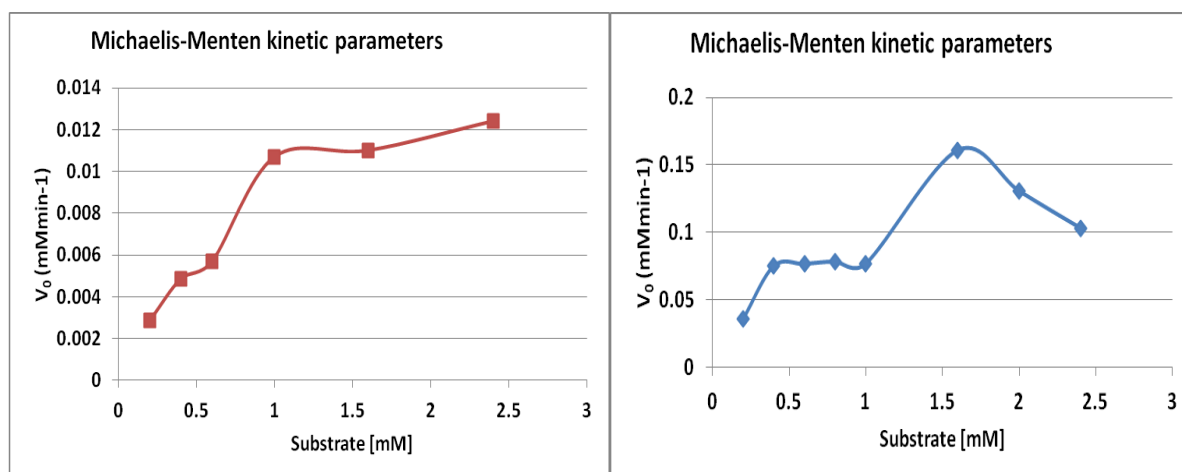


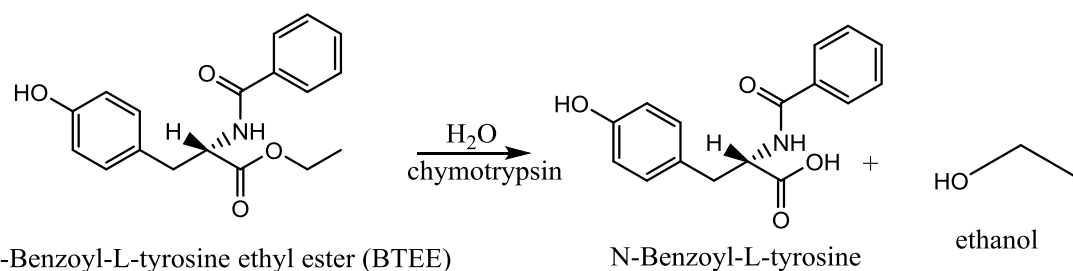
Figure 5.6 Plot of reaction rate (V_o) against substrate concentration $[S]$ showing the Michaelis Menten curve for FA (red) and P2-TfeGlyFA peptides (blue)

Table 5.3 Calculation of Michaelis Menten parameters of both peptides with different methods from initial velocities and substrate concentrations

| FA peptide | Equation | Plot | K_m (mM) | V_{max} (mM/min) |
|----------------------------|--|-----------------------|------------|--------------------|
| Lineweaver-Burk | $\frac{1}{V} = \frac{K_m + [S]}{V_{max}[S]} = \frac{K_m}{V_{max}} \frac{1}{[S]} + \frac{1}{V_{max}}$ | $1/v$ against $1/[S]$ | 0.8020 | 0.0142 |
| Hanes-Woolf | $\frac{[S]}{v} = \frac{1}{V_{max}} [S] + \frac{K_m}{V_{max}}$ | $[S]/v$ against $[S]$ | 0.9373 | 0.0154 |
| Eadie-Hofstee | $v = -K_m \frac{v}{[S]} + V_{max}$ | v against $v/[S]$ | 0.6247 | 0.0131 |
| P2-TfeGlyFA peptide | | | | |
| Lineweaver-Burk | $\frac{1}{V} = \frac{K_m + [S]}{V_{max}[S]} = \frac{K_m}{V_{max}} \frac{1}{[S]} + \frac{1}{V_{max}}$ | $1/v$ against $1/[S]$ | 0.6544 | 0.1590 |
| Hanes-Woolf | $\frac{[S]}{v} = \frac{1}{V_{max}} [S] + \frac{K_m}{V_{max}}$ | $[S]/v$ against $[S]$ | 0.5476 | 0.1478 |
| Eadie-Hofstee | $v = -K_m \frac{v}{[S]} + V_{max}$ | v against $v/[S]$ | 0.5108 | 0.1516 |

Inhibition assay

Because we observed a nontypical saturation profile, further experiments were conducted to determine whether the FA peptide behaves as an inhibitor at higher concentrations. An inhibition assay was carried out using N-benzoyl-L-tyrosine ethyl ester (BTEE) and the control peptide (FA); BTEE is a standard α -chymotrypsin substrate, which enables the reaction velocity to be determined by measuring an increase in absorbance at 256 nm resulting from the hydrolysis of the benzoyl-L-tyrosine ethyl ester (Scheme 5.1).^[230]



Scheme 5.1 The degradation of N-benzoyl-L-tyrosine ethyl ester (BTEE) by α -chymotrypsin

BTEE was subjected to enzymatic degradation and absorbance was measured at 260 nm using a UV spectrophotometer. A standard curve was generated using BTEE at a concentration range from 10.7 μM to 0.642 mM. Absorbance was plotted against time (Figure 5.7a) and the calculated slopes ($\Delta A_{260}/\text{min}$) from the initial linear portion of the curve were used to determine the concentration of product formed per minute in each reaction.

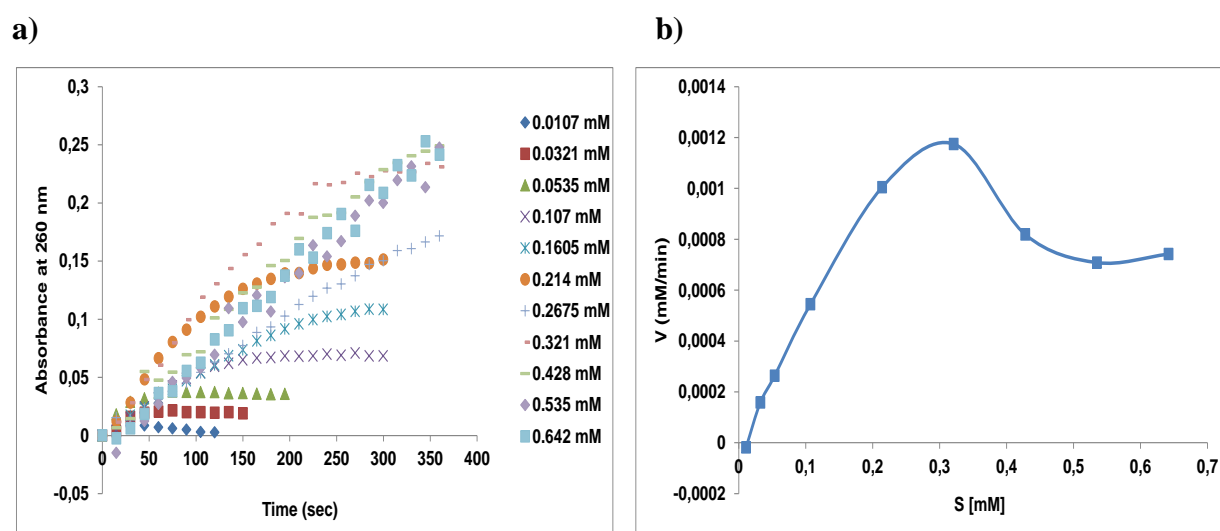


Figure 5.7 a) Measured UV absorbance at 260 nm as a function of time for BTEE at different initial sample concentrations and b) Michaelis-Menten curve for BTEE.

At lower substrate concentrations, UV absorbance of product formation increases proportionally with time whereas at higher concentrations the UV absorbance of product formation decreases over time (Figure 5.7a). This may be attributed to the higher concentrations of organic solvent that accompany greater substrate volumes (25% - 30%) v/v, making the reaction medium less favorable for the enzyme.

The determined K_m (Table 5.4) of BTEE, in good agreement with the literature, is much lower than that calculated for the P2 variant peptides, contributing to the much higher hydrolysis rate of BTEE compared to the substrates studied here. These data indicate that BTEE binds

RESULTS AND DISCUSSION

more strongly to α -chymotrypsin and demonstrates α -chymotrypsin's known preference for tyrosine at P1 position over phenylalanine.

Table 5.4 Calculation of Michaelis Menten parameters of BTEE with different methods

| BTEE | K_m (mM) | V_{max} (mM/min) |
|------------------------|------------------------------|--------------------------------------|
| Lineweaver-Burk | 0.2774 | 0.0015 |
| Hanes-Woolf | 0.0662 | 0.0009 |
| Eadie-Hofstee | 0.0730 | 0.0009 |

To determine competitive inhibition, BTEE and the FA peptide were subjected to enzymatic hydrolysis by chymotrypsin. Aliquots from the reaction mixture were analyzed by RP-HPLC monitored at 256 nm. In the presence of the FA peptide, BTEE is degraded within the first 10 minutes of reaction while less than 30% of the FA peptide is hydrolyzed after 20 minutes. Thus, the presence of the peptide has no effect on BTEE hydrolysis and the peptide does not behave as an inhibitor. Additional experiments were conducted to determine whether the product of FA peptide hydrolysis, Abz-KAAF, could inhibit degradation. FA peptide was incubated with this enzyme for 40 hours to ensure complete digestion prior to the addition of BTEE. BTEE hydrolysis was not inhibited by the presence of the product (Figure 5.8a and b). The results of the inhibition experiments show that the presence of neither the FA peptide nor its hydrolysis product affects the hydrolysis of BTEE by chymotrypsin. This suggests that these species are not enzyme inhibitors at this concentration (3 mM), which would have been one possible explanation for the outcomes of the steady-state kinetic experiments.

The other explanation would be that the presence of organic solvents (DMSO and methanol) creates unfavorable conditions for optimal enzyme activity, and that more time would be required for further hydrolysis.

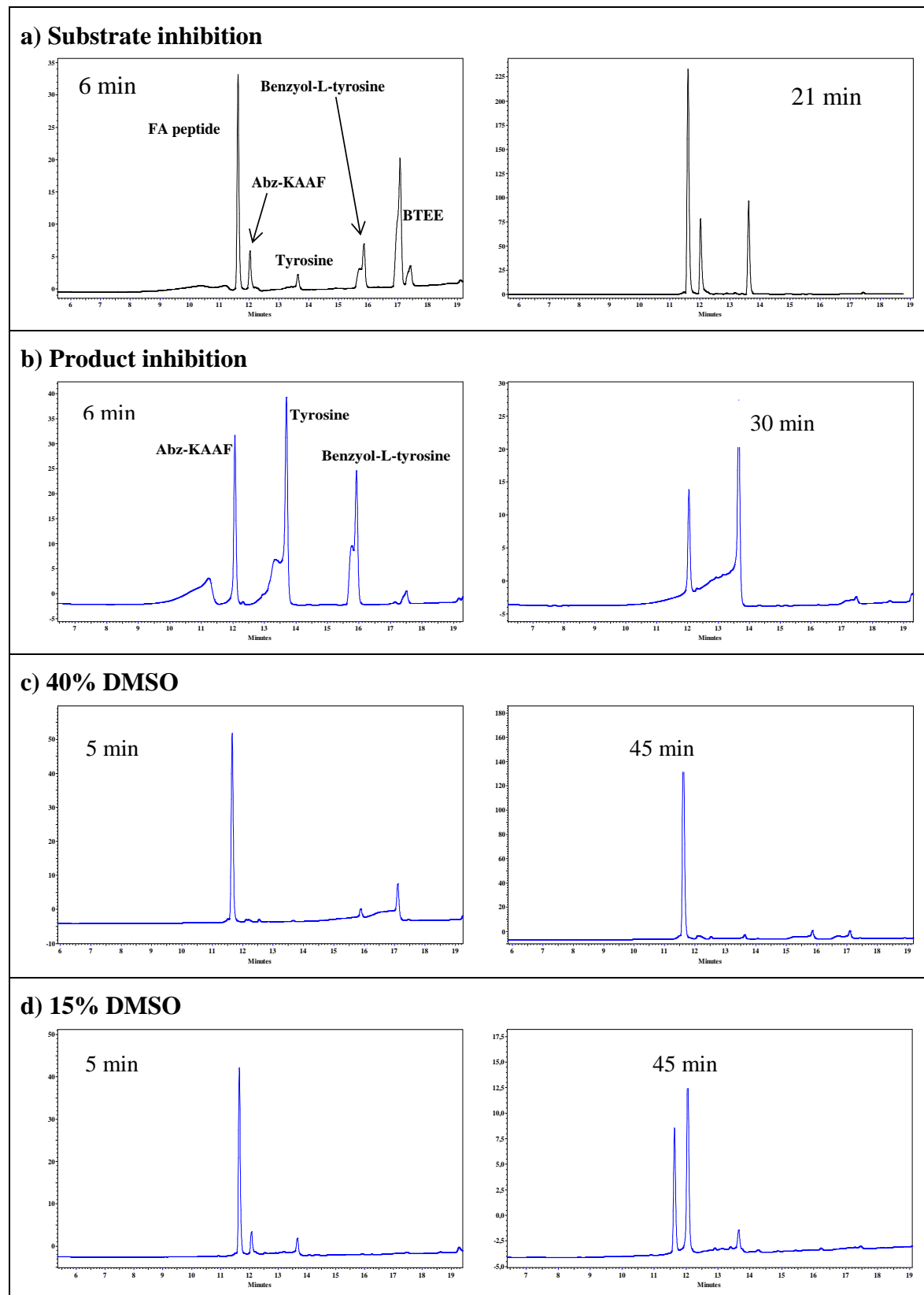


Figure 5.8 HPLC chromatograms of **a)** substrate inhibition and **b)** product inhibition, comparison of the digestion products of FA peptide and BTEE with chymotrypsin at different reaction conditions after 5 and 45 minutes **c)** with 40% DMSO and **d)** with 15% DMSO.

To test this hypothesis, a 1:1 and 3:1 mixture of BTEE and FA peptide in buffer containing DMSO (final concentration 40%) were subjected to chymotrypsin hydrolysis (Table 9.3 in Chapter 9; the same conditions were used as previously reported in Asante *et al.* 2013).^[30] HPLC analysis showed that only half of the BTEE is hydrolyzed within 45 minutes, and none of the FA peptide ((Figure 5.8c). This could be explained as the BTEE is dissolved in 1:1 Methanol and water, the presence of DMSO makes the reaction medium more organic; the reactions with higher organic solvent content were less highly buffered which could lead to a pH effect. However, in the previously reported method,^[30] there was no methanol present and the extra DMSO did not interfere with the hydrolysis since the reaction mixture was made up of 60% buffer. In a second setup with 15% DMSO (final concentration), BTEE was degraded within 5-15 minutes and more than 50% of FA peptide was degraded within 45 minutes as expected (Figure 5.8d).

P2FK variants

α -Chymotrypsin hydrolysis of this series of peptides also revealed that the fluorinated peptides were susceptible to degradation^{VI}. The stability trend was as follows: FK>P2-TfeGlyFK \geq P2-DfeGlyFK (Figure 5.9). As the S2 subsite of α -chymotrypsin forms a shallow hydrophobic groove bounded by His57, Trp215, and Leu99, and generally prefers to accommodate hydrophobic residues,^[86,229] it is not surprising that the fluorinated variants of this peptide are rapidly hydrolyzed. The di- and trifluoroethylglycine groups are larger and more hydrophobic than alanine,^[11,23] and would be assumed to better fill space within the S2 subsite of chymotrypsin leading to a better binding and more efficient hydrolysis.

Even though the S1' subsite of α -chymotrypsin generally accommodates basic residues with long side chains, due to electrostatic interaction with aspartates 35 and 64,^[86,231,232] the FK peptide used as positive control for this set of peptides was not degraded.

^{VI} It should be noted that the Abu variant of this peptide series was not included in this investigation

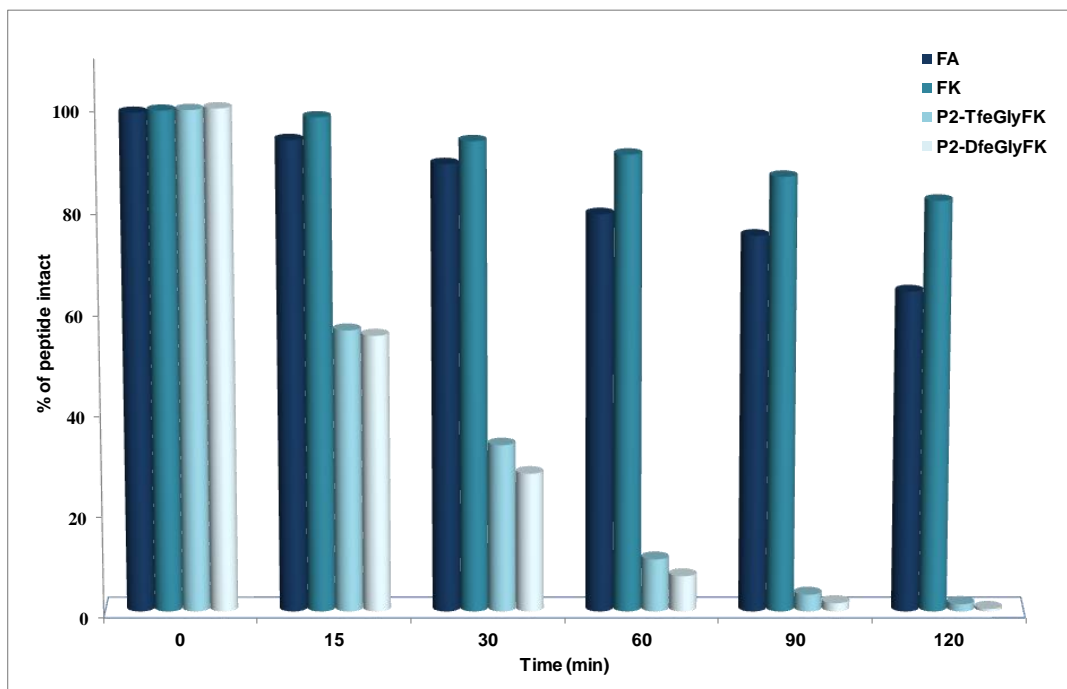


Figure 5.9 Time course of changes in the area of the HPLC peaks representing the fluorescent fragments present after hydrolysis of the P2FK peptides by α -chymotrypsin (10 mM phosphate buffer, pH 7.4) at 30 °C.

5.2.3.2 P1' variants

The S1' subsite of α -chymotrypsin generally accommodates basic residues with long side chains, due to electrostatic interaction with aspartates 35 and 64.^[86,231,232] The P1'FA peptides designed for this study have amino acids with shorter side chains in the P1' position, and molecular modeling shows that the geometric constraints are such that Asp35 and Asp64 cannot be reached when TfeGly, DfeGly and Abu^[233] are bound to this subsite. Consistent with previous crystal structures^[86], our docking poses highlight that residues His57 and Phe41 are brought into proximity by the disulfide bridge Cys42-58 and delineate the edge of the S1' cavity. The enzyme experiments show that the incorporation of Abu disfavors the hydrolysis of the substrate compared to alanine. On the other hand, the two peptides carrying the fluorinated amino acids are well accommodated and faster degraded compared to both the Abu variant and the parent FA sequence. This could be due to the fluorine-induced polarity of the side chains.^[11,23,156,157] Specifically, the slightly higher affinity of DfeGly for the S1' subsite may be explained by its ability to create a hydrogen bond (H-bond) between the difluoromethyl group of the substrate (H-bond donor) and the Cys42-58 disulfide bridge (H-bond acceptor).

Due to the presence of two electron-attracting fluorine atoms on the same carbon, the hydrogen of the S1' DfeGly unit is a potential H-bond donor,^[235] and can interact with the

sulfur of the Cys (Figure 5.10b).^[236] Even though this H-bond is expected to be weak, this might explain the difference between the affinities of P1'-DfeGlyFA and P1'-TfeGlyFA towards α -chymotrypsin. The replacement of this hydrogen by a third fluorine atom in the P1'-TfeGlyFA variant apparently decreases the efficiency of its hydrolysis by α -chymotrypsin such that the measured trend in peptide stability at the P1' position is as follows: P1'-AbuFA>FA>P1'-TfeGlyFA>P1'-DfeGlyFA (Figure 5.10a).

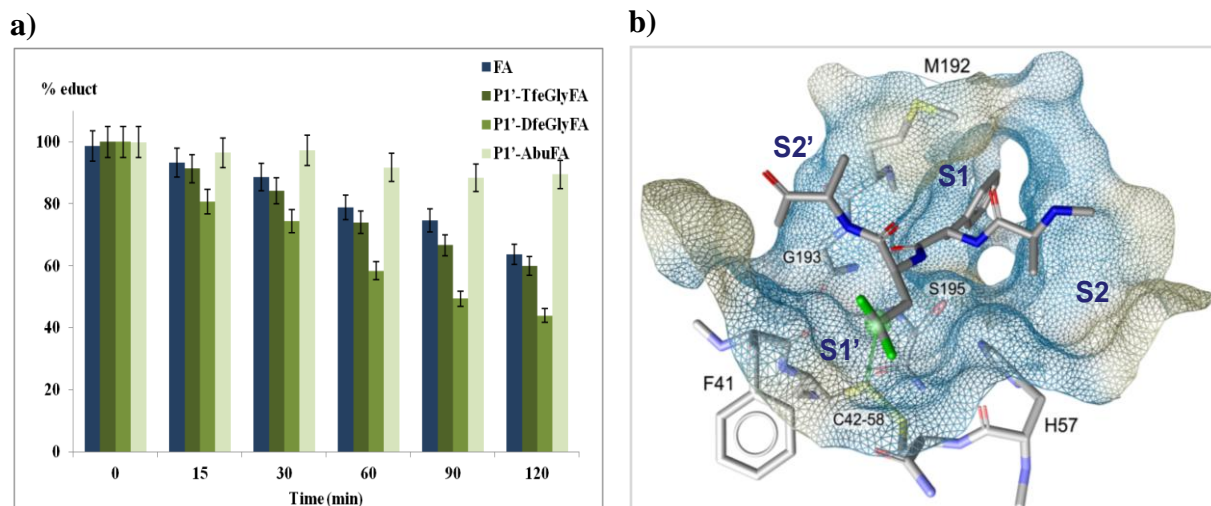


Figure 5.10 **a)** Time course of changes in the area of the HPLC peaks representing the fluorescent fragments present after hydrolysis of the P1'FA peptides by α -chymotrypsin (10 mM phosphate buffer, pH 7.4 at 30 °C). **b)** Suggested binding poses for the P1'-DfeGlyFA bound to α -chymotrypsin. The color code of the surface of the cavity is yellow for lipophilic regions and blue for hydrophilic regions. The potential C-H...S-C hydrogen bond is shown as a green arrow.^[244]

5.2.3.3 P2' variants

P2'FA peptides

The S2' subsite of α -chymotrypsin prefers hydrophobic residues.^[86,234] Phe39 and Thr151 are the main residues that impart hydrophobic character to the S2' pocket. It was therefore assumed that substrates with hydrophobic residues in the P2' position would display better packing, as illustrated for P2'-TfeGlyFA in Figure 5.11b, and in turn more rapid hydrolysis.

Accordingly, the observed proteolytic stability decreased along with the hydrophilicity^[11,23] of the P2' residue: FA>P2'-AbuFA>P2'-DfeGlyFA>P2'-TfeGlyFA (Figure 5.11a).

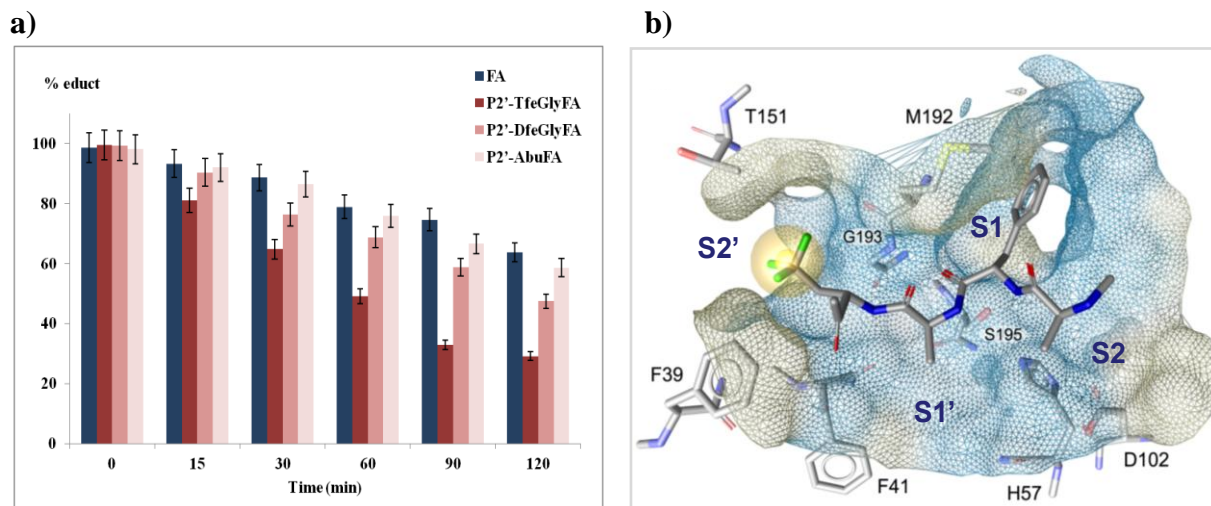


Figure 5.11 **a)** Time course of changes in the area of the HPLC peaks representing the fluorescent fragments present after hydrolysis of the P2'FA peptides by α -chymotrypsin (10 mM phosphate buffer, pH 7.4) at 30 °C. **b)** Suggested binding poses for the P2'-TfeGlyFA bound to α -chymotrypsin. The color code of the surface of the cavity is yellow for lipophilic regions and blue for hydrophilic regions. The important hydrophobic moieties are depicted as yellow spheres.^[244]

P2'FK variants

The use of the peptide variants with Lys in the P1' position and the nonproteinogenic amino acids at P2' position (P2'FK series), gave proteolytic stability of the following, ranging from most stable to the least: FK>P2'-DfeGlyFK>P2'-AbuFK>P2'-TfeGlyFK (Figure 5.12).

The fluorinated variants of these peptides show a dramatic increase in stability compared to P2 fluorinated variants. Whereas the fluorinated P2FK peptides are almost entirely degraded after 120 minutes, their P2'FK fluorinated variants show ~ 50-75% of the substrate still present.

Thus, the effect or magnitude of the effect of the fluorinated amino acids is again shown to be position dependent.^[11,22,24,26,173] Comparing the nonfluorinated and fluorinated analogues of the FK peptides, a general trend cannot be drawn but the proteolytic behavior could be explained on the basis of a model in which the most hydrophobic side chain (TfeGly) is best accommodated by the S2' subsite and leads to fastest degradation.

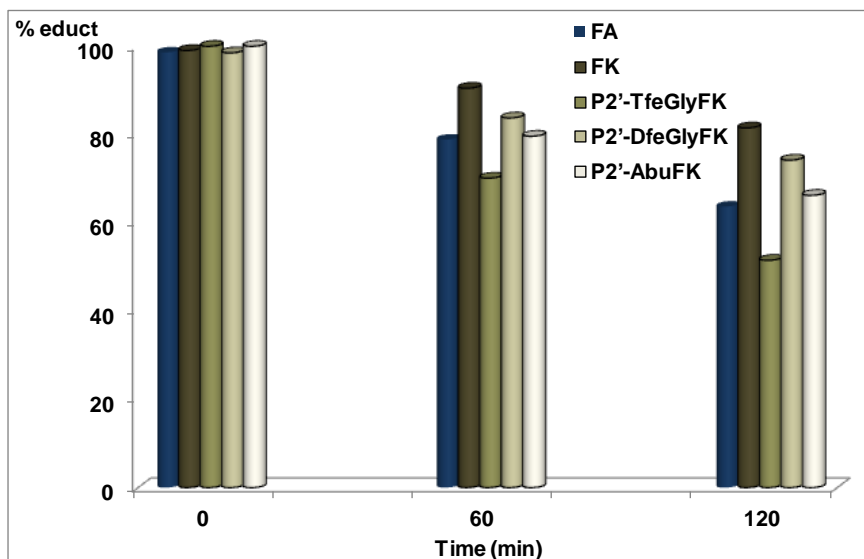


Figure 5.12 Time course of changes in the % area of the HPLC peaks representing the fluorescent fragments present after hydrolysis of the P2'FK variants by α -chymotrypsin (10 mM phosphate buffer, pH 7.4) at 30 °C.

It has been reported that fluorination of Lys causes destabilization of the positive charge in the side chain (protonated ammonium) due to the strong electronic effect of fluorine.^[237] As such, the introduction of fluorinated amino acids in the vicinity of Lys could have an interaction/effect (presumably due to the unique fluorine contacts within the binding pocket) on the enzymatic hydrolysis which then explains the stability of the FK peptide. Inserting the fluorinated amino acids further away (P2 position), breaks this interaction which then results in the faster hydrolysis of the fluorinated P2FK variants.

Table 5.5 shows the calculated and measured masses of the cleavage products from the hydrolysis of the different peptide variants by α -chymotrypsin.

RESULTS AND DISCUSSION

Table 5.5 Identification of proteolyzed fragments, by means of ESI-MS and LC-MS after 120 minutes, generated by α -chymotrypsin; cleavage site indicated in red

| Name of peptide | Full sequences and fragments | MW calculated (Da) [M+1] ¹⁺ | MW observed (Da) [M+1] ¹⁺ |
|-----------------|------------------------------|--|--------------------------------------|
| FA | Abz-KAA F AAAK | 967.4993 | 967.5255 |
| | Abz-KAAF | 555.2559 | 555.2924 |
| | AAAK | 431.2617 | 431.2610 |
| P2DfeGlyFA | Abz-KADfeGly F AAAK | 1017.4622 | 1017.5342 |
| | Abz-KADfeGlyF | 605.2188 | 605.2910 |
| | AAAK | 431.2617 | 431.2630 |
| P2TfeGlyFA | Abz-KATfeGly F AAAK | 1035.4622 | 1035.5251 |
| | Abz-KATfeGlyF | 623.2188 | 623.2812 |
| | AAAK | 431.2617 | 431.2625 |
| P2'-DfeGlyFA | Abz-KAA F ADfeGlyAAK | 1017.4622 | 1017.4622 |
| | Abz-KAAF | 555.2559 | 555.2999 |
| | ADfeGlyAAK | 481.2246 | 481.2641 |
| P2'FA-Abu | Abz-KAA F (Abu)AAK | 981.4622 | 981.5522 |
| | Abz-KAAF | 555.2559 | 555.2933 |
| | A(Abu)AAK | 445.2246 | 445.2775 |
| | Abz-KAAFA | 626.2930 | 626.3315 |
| | (Abu)AAK | 374.1875 | 374.2424 |
| FK | Abz-KAA F KAAAK | 1024.5572 | 1024.5929 |
| | Abz-KAAF | 555.2559 | 555.2953 |
| | KAAAK | 488.3196 | 488.3219 |
| P2'-TfeGlyFK | Abz-KAA F KTfeGlyAAK | 1092.5201 | 1092.5814 |
| | Abz-KAAF | 555.2559 | 555.2920 |
| | KTfeGlyAAK | 556.2825 | 556.3039 |
| P2'-DfeGlyFK | Abz-KAA F KDfeGlyAAK | 1074.5201 | 1074.5945 |
| | Abz-KAAF | 555.2559 | 555.2953 |
| | KDfeGlyAAK | 538.2825 | 538.2925 |
| P2'FK-Abu | Abz-KAA F K(Abu)AAK | 1038.5201 | 1038.6101 |
| | Abz-KAAF | 555.2559 | 555.2947 |
| | K(Abu)AAK | 502.2825 | 502.3357 |

5.2.4 Hydrolysis of peptides by pepsin (EC 3.4.23.1)

Pepsin, an aspartic endopeptidase, is a major digestive protease in the gastric juice of vertebrates. It is optimally active at acidic pH, can catalyze the hydrolysis of a broad variety of synthetic peptides, and has a preference for substrates that contain hydrophobic residues on both sides of the scissile bond.^[106-108] As already mentioned in section 2.1.4.1, the enzyme uses an acid-base mechanism that involves the coordination of a water molecule between two highly conserved aspartic acid residues, Asp32 and Asp215.^[99,104-108]

The FA and FF variants described above were subjected to pepsin degradation and the proteolytic products were characterized and analyzed by HPLC, MS and molecular modeling. Within the active site of this protease, the water molecule stabilized between Asp32 and Asp215 plays a key role in the hydrolysis mechanism.^[99,238] Therefore, this water molecule was manually merged into the 3D structure of pepsin before performing the docking study. When a peptide conformation fulfilled the interaction requirements reported in Table 5.2, then the water molecule was positioned directly under the amide bond between positions P1 and P1'. Similarly, positions P2 to P2' of this peptide were well accommodated by their corresponding enzyme subsites S2 to S2'. Therefore, such a conformation was considered to be highly plausible and was subjected to more detailed structural investigation.

5.2.4.1 P2 variants

P2FA peptides

Residues lining the walls of the S2 subsite of pepsin consist of: Thr218, Thr222, Glu287, Met289, Gly76, and Thr77 which create a hydrophobic environment for the S2 pocket.^[103]

Peptides modified at the P2 position are generally degraded more rapidly than the FA control peptide, indicating a better geometric fit (Figure 5.13a). P2-DfeGlyFA is the fastest hydrolyzed of all substrates, with only 19% of the initial amount of full-length peptide remaining in solution after 2 h of reaction time. Interestingly, analysis of the docking results shows that the DfeGly side chain is in the vicinity of the Met289 side chain within the S2 pocket (Figure 5.13b). It has been shown that the S2 pocket can exhibit multiple conformations and that could account for different specificities.^[103] It must of course be noted that the side chain of methionine is flexible and should be considered as such in the context of a potential interaction with a ligand.

The observed distance between the sulfur of Met289 and the DfeGly γ -carbon is in the range of 4.5 Å, which could indicate the existence of a weak hydrogen bond, as depicted in Figure 5.13b. Behaviors of this kind have been reported in the literature, that is, in separate cases, methionine acting as H-bond acceptor and a difluoromethyl group of a small molecule acting as H-bond donor.^[235,236] Since this polarized, electron-deprived hydrogen is absent in the structure of P2-TfeGlyFA, the trifluorinated variant could still be accommodated but not equally enthalpically stabilized within the enzyme cavity. Finally, the P2-AbuFA variant was also very well accommodated within the hydrophobic S2 subpocket. The extent of proteolytic stability observed is as follows: FA>P2-TfeGlyFA>P2-DfeGlyFA=P2-AbuFA (Figure 5.13a).

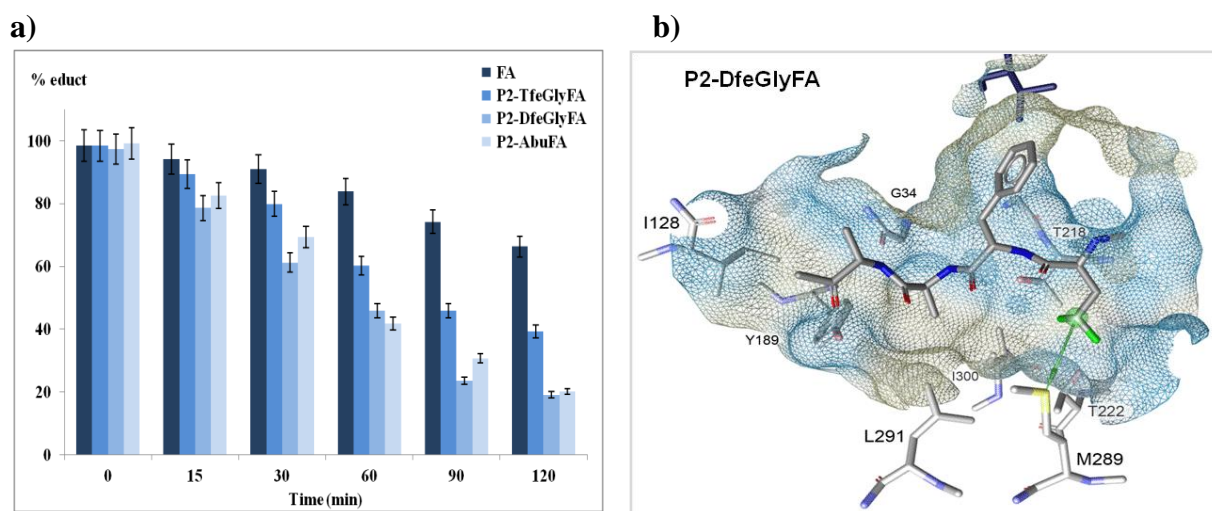


Figure 5.13 a) Time course of changes in the area of the HPLC peaks representing the fluorescent fragments present after hydrolysis of the P2FA peptides by pepsin (10 mM acetate buffer, pH 4.0) at 30 °C. b) Suggested binding poses for P2-DfeGlyFA bound to pepsin. The color code of the surface of the cavity is yellow for lipophilic regions and blue for hydrophilic regions. The potential hydrogen bond is depicted as a green arrow.^[244]

FF peptides

Hydrolysis of the P2FF variants by pepsin clearly demonstrates pepsin's preference for hydrophobic aromatic residues at the P1 and P1' positions (Figure 5.14a). Replacing the alanine in P2 position with DfeGly or TfeGly confers a 30-60 fold increase in stability toward pepsin hydrolysis. This improvement in stability can be a result of the repulsion between the fluorinated amino acids and the residues of the enzyme's subpocket and also due to the size of the fluorinated analogues compared to alanine in the control peptides.

Even though the incorporation of fluorine increases the peptide's proteolytic stability, further studies were not carried out with this set of peptides because additional cleavage sites were

observed. That is, cleavage between P1 and P1' (major product) and then P1' and P2' (minor product) and that stability could not be judged from the two products (Figure 5.14b and Table 5.6). It is important to note here that the substrate and not the product is being quantified (Figure 5.14a).

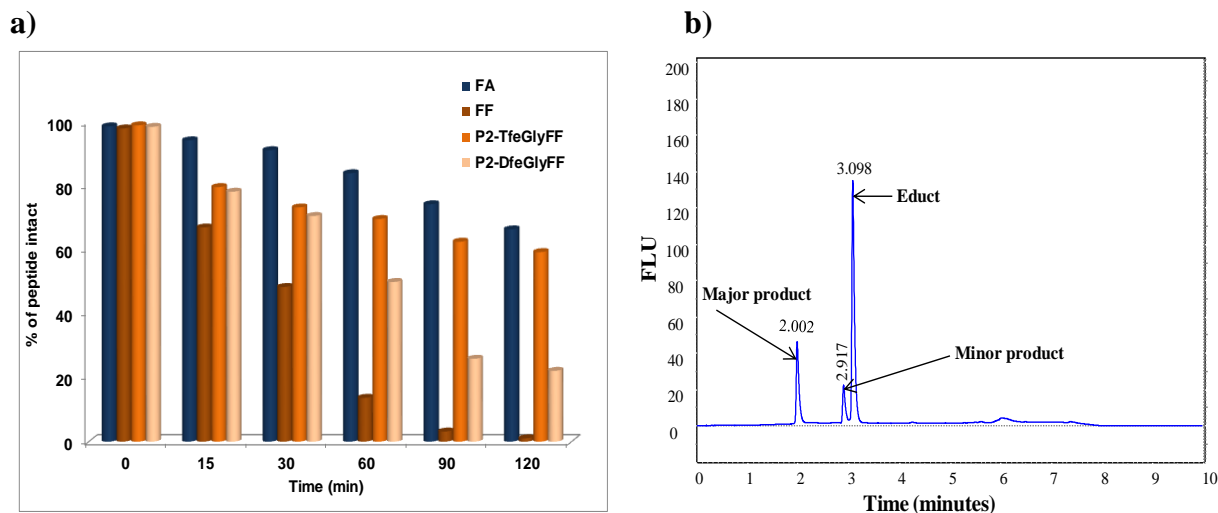


Figure 5.14 a) Time course of changes in the area of the HPLC peaks representing the educts present after hydrolysis of P2FF peptides with pepsin at 30 °C in 10 mM acetate buffer, pH 4.0 b) Fluorescence HPLC chromatogram showing the educt and the cleaved products formed during the hydrolysis of the P2'-TfeGlyFF peptide with pepsin indicating the presence of a second product.

5.2.4.2 P1'FA peptides

As mentioned above, pepsin hydrolyzes peptides that have hydrophobic residues in the P1' position.^[238,239] This specificity is due to the nature of the S1' subsite constituents, namely Ile213, Ile300, Leu291 and Thr218. Among all peptides evaluated, the P1'-AbuFA variant is degraded very rapidly by pepsin (26% of the initial concentration remaining after 2 h). Peptides containing fluorine in the P1' positions are hydrolyzed faster than FA but slower than P1'-AbuFA by pepsin.

The DfeGly variant displays a rate of reaction similar to that of Abu, with 28% of full-length substrate remaining after 2 h. The trifluoroalkyl variant is not as well degraded as Abu or DfeGly, thus in this case proteolytic stability phenomenologically corresponds to the steric bulk of the side chain of the nonproteinogenic amino acid:

FA>P1'-TfeGlyFA>>P1'-DfeGlyFA≥P1'-AbuFA (Figure 5.15).

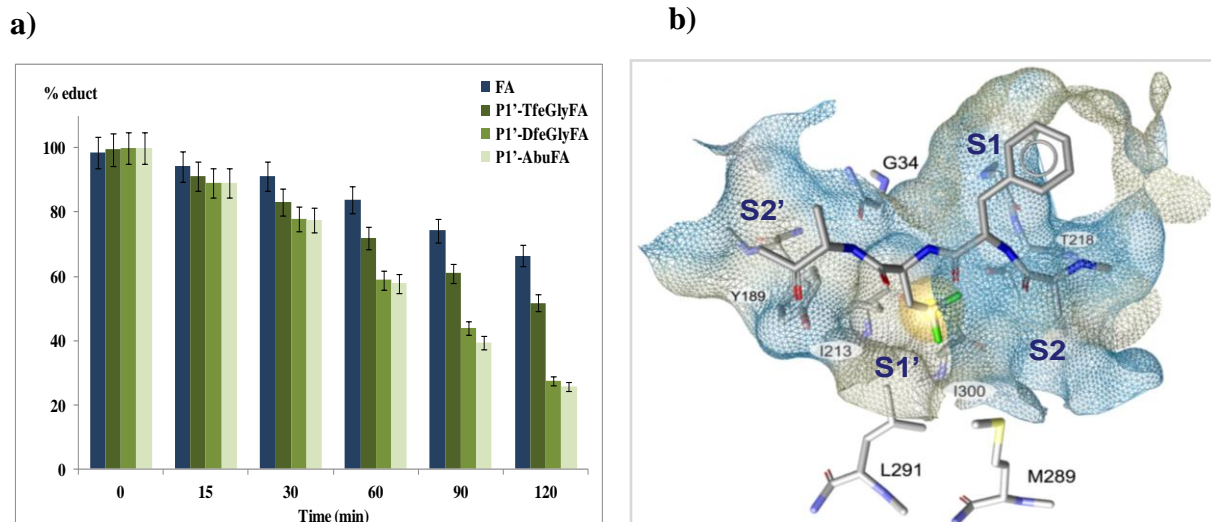


Figure 5.15 a) Time course of changes in the area of the HPLC peaks representing the fluorescent fragments present after hydrolysis of the P1'FA peptides by pepsin (10 mM acetate buffer, pH 4.0) at 30 °C. b) Suggested binding poses for P1'-DfeGlyFA bound to pepsin. The color code of the surface of the cavity is yellow for lipophilic regions and blue for hydrophilic regions. Hydrophobic pocket depicted as yellow sphere.^[244]

5.2.4.3 P2' variants

P2'FA peptides

The S2' subsite of pepsin preferentially binds hydrophobic amino acids.^[240-243] Accordingly, the substrate conformations highlighted by the molecular modeling study demonstrate that the P2' residue interacts with the hydrophobic environment of the S2' enzyme subsite. In these docking poses, the amino acids of the enzyme involved in interactions with the P2' amino acid of the substrate are Ile128, Ile73, Ser35, and Tyr75. The experimental data indicate that the introduction of fluorinated amino acids into the P2' position of the peptide sequence remarkably improves its proteolytic stability, providing evidence that TfeGly and DfeGly are geometrically not well accommodated within the lipophilic S2' subpocket. This result can be correlated with the increase in size of the fluorinated variants.

In agreement with this interpretation, the peptide variant P2'-AbuFA, smaller than the fluorinated variants, is rapidly hydrolyzed (61.5% degraded after 120 minutes). Furthermore, Abu, more hydrophobic than alanine, may engage in optimal interactions with the hydrophobic S2' subsite of pepsin as shown in Figure 5.16b.^[165]

Resistance towards proteolysis is thus greater in the case of the fluorinated variants, and can be summarized as follows: P2'-TfeGlyFA>P2'-DfeGlyFA>FA>P2'-AbuFA (Figure 5.16a).

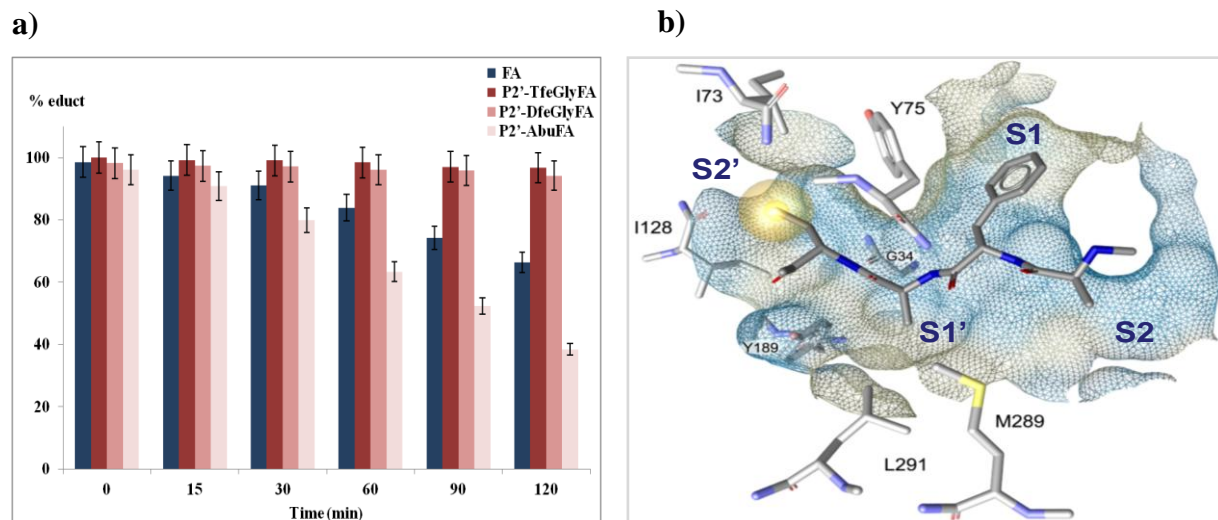


Figure 5.16 a) Time course of changes in the area of the HPLC peaks representing the fluorescent fragments present after hydrolysis of the P2'FA peptides by pepsin (10 mM acetate buffer, pH 4.0) at 30 °C. b) Suggested binding poses for the P2'-AbuFA bound to pepsin. The color code of the surface of the cavity is yellow for lipophilic regions and blue for hydrophilic regions. Hydrophobic pocket depicted as yellow sphere.^[244]

P2'FF variants

The P2'FF variants show a stability pattern similar to that of the P2FF variants, with the fluorinated variants leading to a dramatic increase in proteolytic resistance (FA>P2'-TfeGlyFF>P2'-DfeGlyFF>>P2'-AbuFF> FF (Figure 5.17)). The observed increase in stability (12-22 folds) suggests that the fluorinated amino acids interact significantly differently with the S2' subsite than do alanine or Abu. Phenomenologically, the proteolytic stability of these variants increases with the size and hydrophobicity of the nonproteinogenic amino acids.

RESULTS AND DISCUSSION

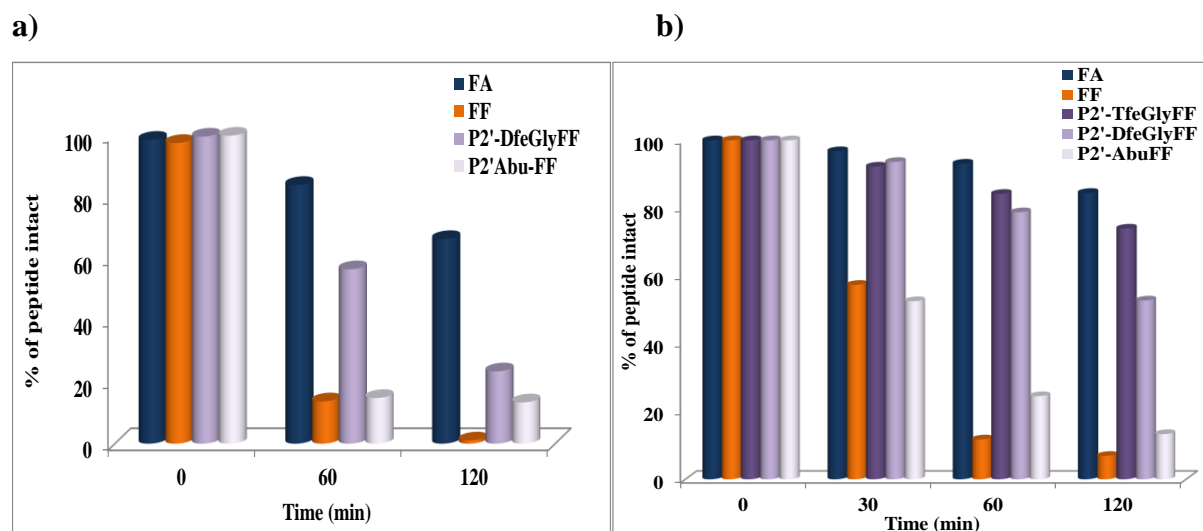


Figure 5.17 Percentage of educts remaining at different times in the reaction of P2'-FF peptides at 30 °C in 10 mM acetate buffer, pH 4.0, using different pepsin concentrations a) 0.5 mg/mL b) 0.29 mg/mL buffer.

Table 5.6 Identification of proteolyzed fragments of FF peptides variants in ESI-MS and LC-MS after 120 minutes

| Name of peptides | Fragments | MW cal. (Da) | MW obs. (Da) |
|------------------|--------------------|--------------|--------------|
| FF | Abz-KAAFFAAK | 1043.5306 | 1043.5696 |
| | Abz-KAAF | 555.2559 | 555.2953 |
| | FAAAK | 507.2930 | 507.2862 |
| | Abz-KAAFF | 702.3243 | 702.3605 |
| | AAAK | 410.1875 | 410.2212 |
| P2'-TfeGlyFF | Abz-KATfeGlyFFAAK | 1111.4935 | 1111.5572 |
| | Abz-KATfeGlyF | 623.2188 | 623.2769 |
| | FAAAK | 507.2930 | 507.2911 |
| | Abz-KATfeGlyFF | 770.2872 | 770.3505 |
| | AAAK | 360.2246 | 360.2252 |
| P2'-DfeGlyFF | Abz-KADfeGlyFFAAK | 1093.4935 | 1093.5646 |
| | Abz-KADfeGlyF | 605.2188 | 605.2866 |
| | FAAAK | 507.2930 | 507.2959 |
| | Abz-KADfeGlyFF | 752.2872 | 752.3972 |
| | AAAK | 360.2246 | 360.2249 |
| P2'-TfeGlyFF | Abz-KAAFFTfeGlyAAK | 1111.4935 | 1111.5634 |
| | Abz-KAAF | 555.2559 | 555.2953 |
| | FTfeGlyAAK | 575.2559 | 557.2893 |
| | Abz-KAAFF | 702.3243 | 702.3605 |
| | TfeGlyAAK | 428.1875 | 428.2163 |
| P2'-DfeGlyFF | Abz-KAAFFDfeGlyAAK | 1093.4935 | 1093.5705 |
| | Abz-KAAF | 555.2559 | 555.2953 |
| | FDfeGlyAAK | 557.2559 | 557.2893 |
| | Abz-KAAFF | 702.3243 | 702.3605 |
| | DfeGlyAAK | 410.1875 | 410.2212 |

5.2.5 Reaction of the peptides with proteinase K (EC 3.4.21.64)

The peptides were designed such that the substrate specificities of several proteases are represented. Based on this fact, proteinase K, a non-specific serine endopeptidase produced by the fungus *Tritirachium album* Limber, was also investigated in this study. As a serine protease, the catalytic mechanism is based on the catalytic triad of Asp39, His69 and Ser224. Proteinase K consists of 279 amino acids and has preference for aromatic, aliphatic or hydrophobic amino acids in position P1; Ala in position P2 enhances the cleavage efficiency.^[84] In order not to lose focus in this study, only a selected number of peptides were investigated in the context of this enzyme.

Hydrolysis was monitored in an assay similar to the one described for pepsin and α -chymotrypsin above with detailed experimental conditions described in chapter 9, section 9.4.1. The time course of HPLC fluorescence peak area representing the amount of peptide remaining at different reaction times was estimated and is presented in Figure 5.18. From the graph, the control peptide FA was almost entirely degraded after 120 minutes whereas the nonproteinogenic P2- and P2'-FA variants are highly stable (Figure 5.18a and b). However, the replacement of alanine with the nonproteinogenic amino acids in the FK variants led to a decrease in proteolytic stability compared to the FK control peptide (Figure 5.18a and c). This effect could be due to the longer side chain of the lysine residue in the S1' pocket of the enzyme. In contrast, incorporation of the nonproteinogenic analogues into the P2 and P2' positions of the FF variants led to a remarkable increase in proteolytic stability (Figure 5.18a and d). The variation in proteolytic stability occurring with the introduction of Abu and its fluorinated analogues, depending on the primary sequence and position of substitution, undoubtedly demonstrates the effect of nonnatural amino acids on the enzyme's activity. With the preference for aliphatic and aromatic amino acids in position P1, and Ala in P2 position enhancing cleavage by proteinase K,^[84] it is not surprising that all peptides with these alanines replaced demonstrate improved proteolytic stability, with the exception of the fluorinated FK variants, which actually show a decrease in stability. The preference for Ala in P2 is due to the possibility for the methyl group to participate in van der Waals interactions with S2.^[245]

RESULTS AND DISCUSSION

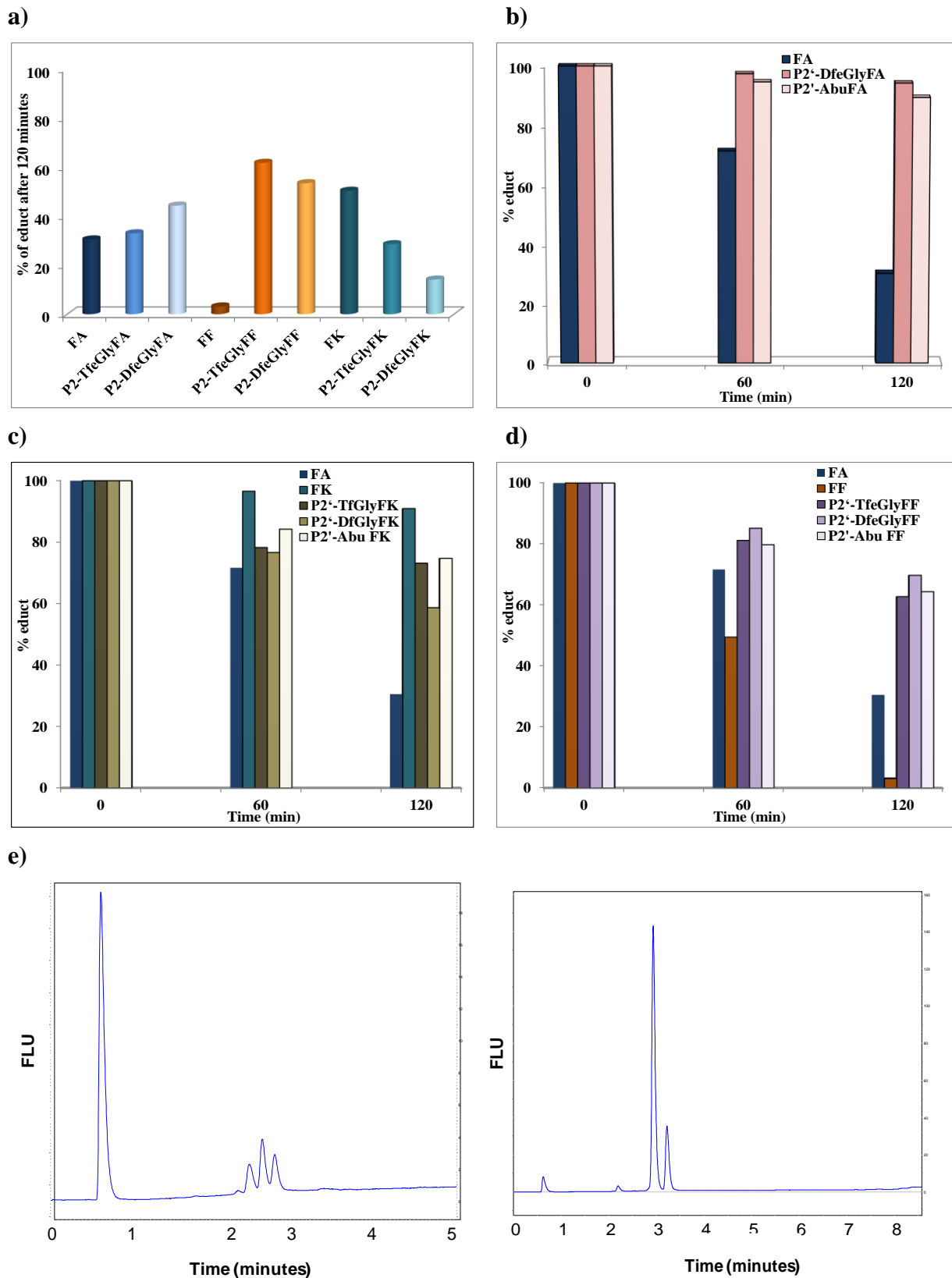


Figure 5.18 Hydrolysis of the peptide variants, with substitution at a)=P2 position, b), c), d)= P2' positions by proteinase K at 37 °C in 50 mM Tris-HCl/10 mM CaCl₂ buffer, pH 7.5. e) HPLC chromatogram showing the educt and the cleaved product in the hydrolysis of peptides by proteinase K enzyme.

RESULTS AND DISCUSSION

Due to the broad substrate specificity of proteinase K for aliphatic and aromatic amino acids, the presence of a number of alanines presents multiple cleavage site possibilities other than P1 and P1'. These heterogeneous cleavage sites were observed in all variants, even the nonproteinogenic variants. Table 5.7 shows the masses of generally observed cleaved products from the reaction.

Table 5.7 Observed and calculated masses of cleaved products from the reaction of all control peptides with proteinase K enzyme

| Name | Fragment | MW calculated (Da) | MW observed (Da) |
|------|-----------------------------------|--------------------|------------------|
| FA | Abz-KAAF ³ AAAK | 967.4993 | 967.5399 |
| | Abz-KAAF ³ AAA | 768.3673 | 768.4071 |
| | Abz-KAAF ³ AA | 697.3301 | 697.3697 |
| | Abz-KAAF ³ A | 626.2930 | 626.3331 |
| | F ³ AAAK | 578.3301 | 578.3325 |
| | Abz-KAA | 408.1875 | 408.9470 |
| | AAAK | 360.2246 | 360.2265 |
| | AAK | 289.1875 | 289.1877 |
| | AK | 218.1504 | 218.1509 |
| FK | Abz-KAAF ³ KAAK | 1024.5572 | 1024.5996 |
| | Abz-KAAF ³ KAA | 825.4251 | 825.4661 |
| | Abz-KAAF ³ KA | 754.3880 | 754.4244 |
| | Abz-KAA | 408.1875 | 408.2247 |
| | F ³ KAAK | 635.3880 | 635.3903 |
| | AAK | 289.1875 | 289.1886 |
| | AK | 218.1504 | 218.1504 |
| FF | Abz-KAAFF ³ AAK | 1043.5306 | 1043.5723 |
| | Abz-KAAFF ³ AA | 844.3986 | 844.4393 |
| | Abz-KAAFF ³ A | 773.3614 | 773.4020 |
| | Abz-KAA | 408.1875 | 408.2264 |
| | F ³ F ³ AAK | 654.3614 | 654.3643 |
| | AAK | 289.1875 | 289.1894 |
| | AK | 218.1504 | 218.1511 |

A comparable cleavage pattern was observed in the hydrolysis of the peptides with elastase; however, these data will be discussed under the plasma hydrolysis studies due to the related actions of the plasma proteases.

5.2.6 Comparing all control peptides with studied enzymes

The stabilities of the control peptides in the presence of all the isolated enzymes used in this study are summarized below. Comparing the hydrolysis of the peptides by the various isolated enzymes, the stability can be expressed as $FK > FA > FF$, in most cases (Figure 5.19a). While, about 18% of the FF peptide is degraded by chymotrypsin, with proteolytic cleavage occurring between P1' and P2' (Figure 5.19b), only 4% of this peptide is degraded in the presence of elastase (Figure 5.19a). In contrast to this, little or no proteolysis of the FK peptide occurs in the presence of elastase and pepsin; only about 10% degradation occurs with proteinase K (Table 5.8). The FK peptide shows slight resistance to pepsin, elastase and proteinase K although it has phenylalanine at the P1 position; the presence of the lysine at the P1' position prevents cleavage due to similar reasons given above. In all cases, the FA peptide seems to be a good substrate for all the proteases.

The Abu variants of these peptide series seem to be well accommodated by pepsin, chymotrypsin, proteinase K and elastase (from least stable to the most stable) (Figure 5.19c). The P2'-Abu variants are the least degraded by elastase and proteinase K whereas the only P1'Abu variant is highly stable towards chymotrypsin. It should be noted that P2 (FF and FK) Abu variants were not included in this study and also the P2'-AbuFF were not subjected to degradation by chymotrypsin.

Table 5.8. Percent of educt still present after 120 minutes of reaction with the control peptides by the various isolated enzymes

| Name of peptide | Chymotrypsin | Pepsin pH 4.0 | Proteinase K | Elastase |
|------------------|--------------|---------------|--------------|----------|
| FF | 82.376 | 1.039 | 3.132 | 96.213 |
| FA | 63.696 | 66.358 | 30.48 | 78.79967 |
| FK | 81.501 | 100 | 90.93267 | 93.534 |
| P2-AbuFA | 26.992 | 20.157 | | |
| P1'-AbuFA | 89.453 | 25.692 | | |
| P2'-AbuFA | 58.671 | 38.407 | 89.511 | 97.482 |
| P2'-AbuFF | | 13.384 | 64.396 | 97.189 |
| P2'-AbuFK | 66.228 | | 74.733 | 77.361 |

RESULTS AND DISCUSSION

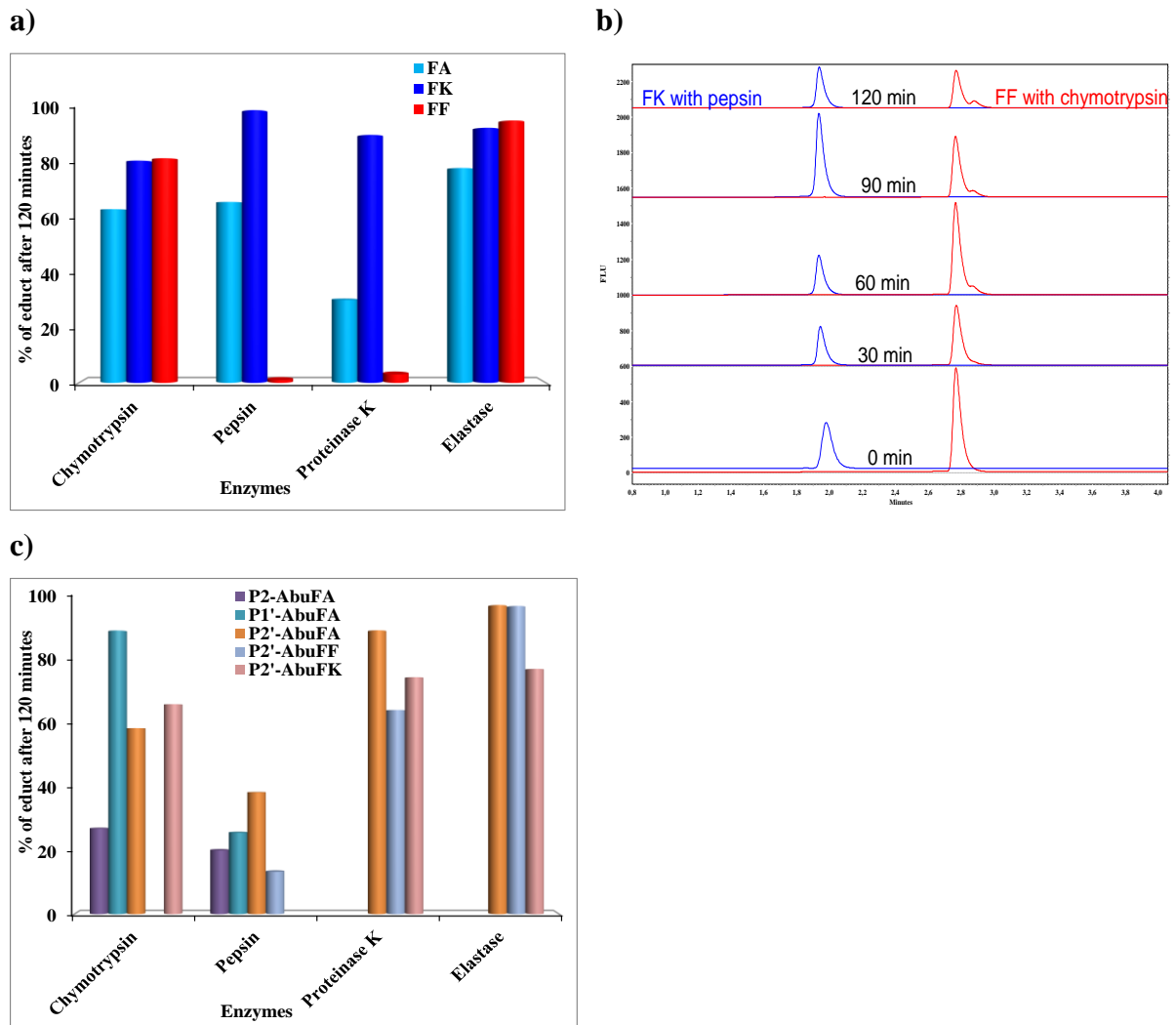


Figure 5.19 a) and c) Mean percent of substrate (educt) still present after 120 minutes of reaction of the control peptides and Abu variants with the different enzymes. b) Fluorescent HPLC chromatograms showing the time course of hydrolysis of the FK and FF peptides with pepsin and chymotrypsin.

5.3 Plasma studies

Over the past decade, investigations into the proteolytic resistance of unnatural peptides have typically employed isolated enzymes, fetal bovine serum, or human serum. The proteolytic stability of small molecules and peptides in plasma is a key factor that strongly influences the in vivo efficacy of a test compound. Upon entering the blood stream, drug molecules are exposed to a host of enzymes present in the plasma: proteinases, aminopeptidases, dipeptidylaminopeptidases, dipeptidylcarboxypeptidases and esterases.^[246] The protease-mediated degradation of proteins and peptides presents a significant hurdle to their development as pharmaceuticals, and numerous approaches have been employed to increase their plasma half-life. This includes the incorporation of fluorine, which has been shown to improve the pharmacokinetic aspects of therapeutic agents, i.e., by increasing their hydrophobicity and metabolic stability, typically leading to improved bioactivity and bioavailability.^[19,247]

Therefore, this part of this thesis aimed at investigating the effect of side chain fluorination on model peptides in the presence of human blood plasma.

5.3.1 Plasma assay

To measure the influence of fluorine on the stability of peptides towards proteolysis, a series of peptides was designed and synthesized based on a ten amino acids sequence including *o*-aminobenzoic acid (Abz) as a fluorescent label: Abz-Lys-Ala-Ala-Phe-Ala-Ala-Ala-Lys (Figure 5.1). The processing of the peptides by human plasma proteases was investigated through the use of analytical RP-HPLC equipped with a fluorescence detector and LC-MS, leading to the identification of the responsible proteases.

The plasma stability measurements were carried out through incubation of the peptides with either immobilized human plasma proteins or whole human plasma in solution. ESI-MS and LC/MS were used to identify and characterize the possible cleaved peptide fragments.

5.3.2 Incubation of substrate with immobilized plasma proteases

In order to minimize interference from the biological matrix (salts and proteins), enzymes can be covalently immobilized on chromatographic resins through the free amino groups.

The immobilization of plasma proteins coupled with mass spectrometry is a well established method which enables the screening of unknown protease substrates. It is important to note

that not all enzymes present in the plasma are equally reactive to the matrix, and that their orientation upon immobilization may not allow for optimal activity.^[120] By covalently immobilizing the proteins and incubating individual immobilized proteins from the library, enzymatic activities can be detected with reaction-specific probes. Aliquots taken from the reaction mixture at certain time points can be analyzed with HPLC and LC-MS.

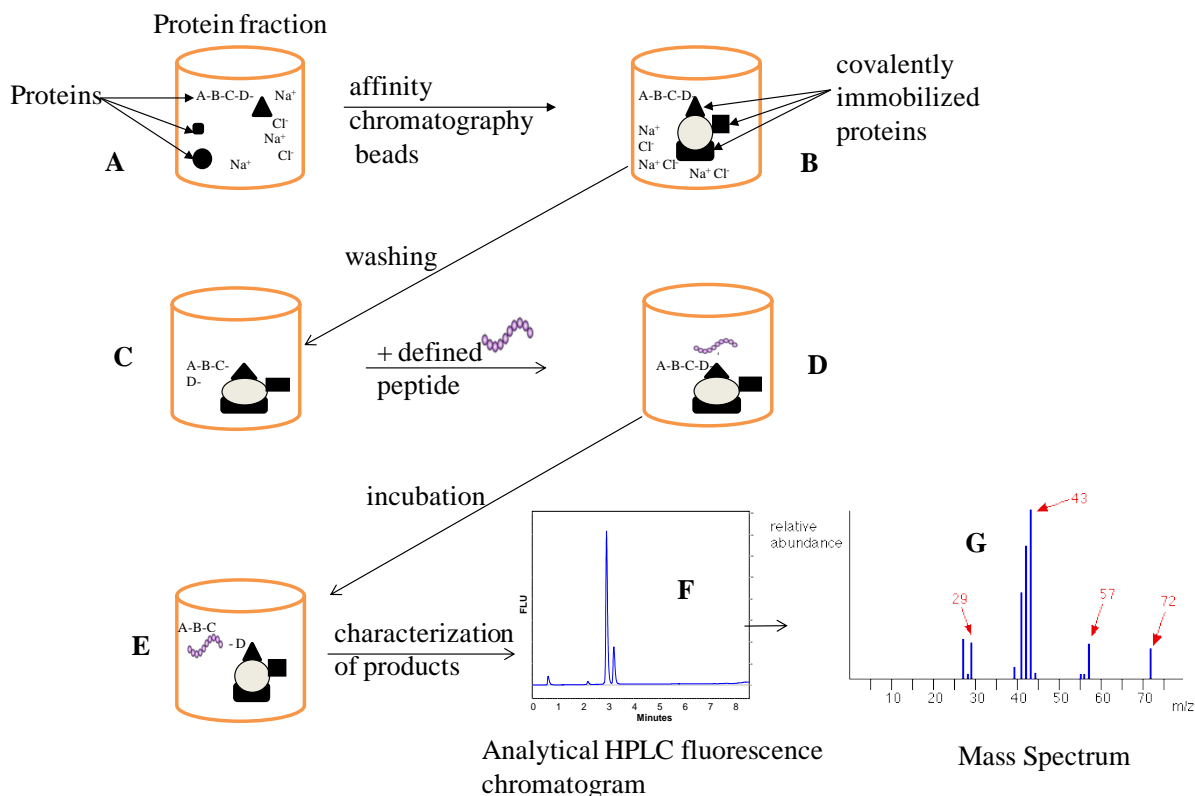


Figure 5.20 Slight modification of the principle of the Mass Spectrometry-Assisted Protease Substrate Screening (MAPS) system. Proteins from any protein fraction (plasma) (A) are covalently immobilized onto cyanogen bromide-activated Sepharose beads (A → B). The immobilized proteins (B) are washed several times with pure water and buffer to remove any molecules (B → C), which are not immobilized. A defined amount of peptide (**in the original method protease was added**) is added to the mixture of the immobilized proteins and buffer (C → D). After defined incubation times (E), an aliquot of the reaction mixture is quenched by ACN containing 0.1% TFA and analyzed by analytical RP-HPLC (F) and the reaction products are identified by mass spectrometry (G). Reproduced with permission from Schlüter et al.^[120] (Copyright 2007, American Chemical Society).

In this case, a range of plasma volumes were combined with 6 MB cyanogen bromide-activated Sepharose beads for covalent immobilization; this should lead to variable loading of the plasma proteins. A constant peptide concentration was used and incubation was carried out at 37 °C over a specific period and the released products were obtained by quenching aliquots at defined times.

The amount of substrate (full-length peptides) remaining and product formed (fragment cleaved) at a particular time were analyzed with analytical RP-HPLC equipped with a

fluorescence detector and identified by ESI-MS and LC-MS. Figure 5.20 summarizes the immobilization procedure as established by Schlüter and co-workers.^[120] To compare the effect of plasma protein loading, different volumes of plasma (50 μL , 10 μL , 5 μL) were used in the immobilization on the 6 MB Cyanogen bromide activated sepharose beads.

In all cases, the control (FA) was more stable than the fluorinated variants. The amount of peptide remaining after 120 minutes of incubation with 50 μL immobilized plasma proteins decreased in the order: FA>P2'-TfeGlyFK>FK>P2'-DfeGlyFK and FA>P2'-TfeGlyFF>P2'-DfeGlyFF>P2'-DfeGlyFA>FF (Figure 5.21). Upon reducing the amount of plasma proteins immobilized, a comparable stability trend was observed for all the peptide variants studied. Thus the rate of hydrolysis of the peptide analogues by immobilized human blood plasma proteins depended mainly on the amount of plasma used and the number of fluorine atoms present in the side chain (Figure 5.21).

RESULTS AND DISCUSSION

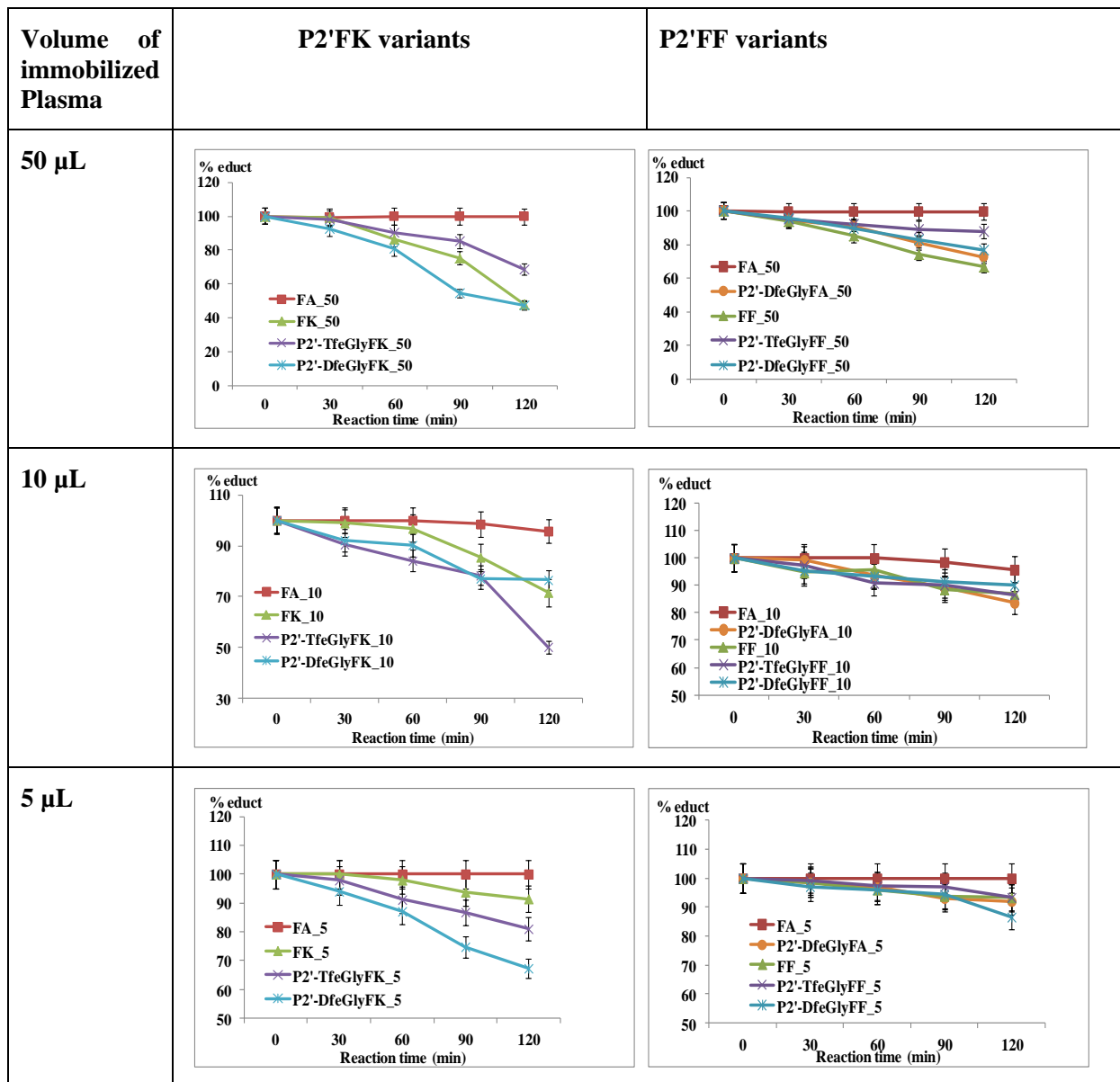


Figure 5.21 Percent of educts (P2'FK peptides and P2'FF peptides) remaining at different incubation times in different volumes of immobilized plasma proteins.

For reasons mentioned above, the peptide analyte will only be degraded by immobilized enzymes that retain activity and that recognize it as a substrate. Interestingly, the fluorescence HPLC chromatograms showed only one cleaved product for all the different peptide variants (Figure 5.22a); this was identified by mass spectrometry to be the degradation product of an exopeptidase (carboxypeptidase) that cleaves only the C-terminal amino acid residue (lysine), in this case corresponding with the P4' position (Table 5.9). Among the numerous plasma proteins that could theoretically be immobilized (Table 2.2 in chapter 2, section 2.4), only the carboxypeptidase N could hydrolyze these peptides.^[117,248]

RESULTS AND DISCUSSION

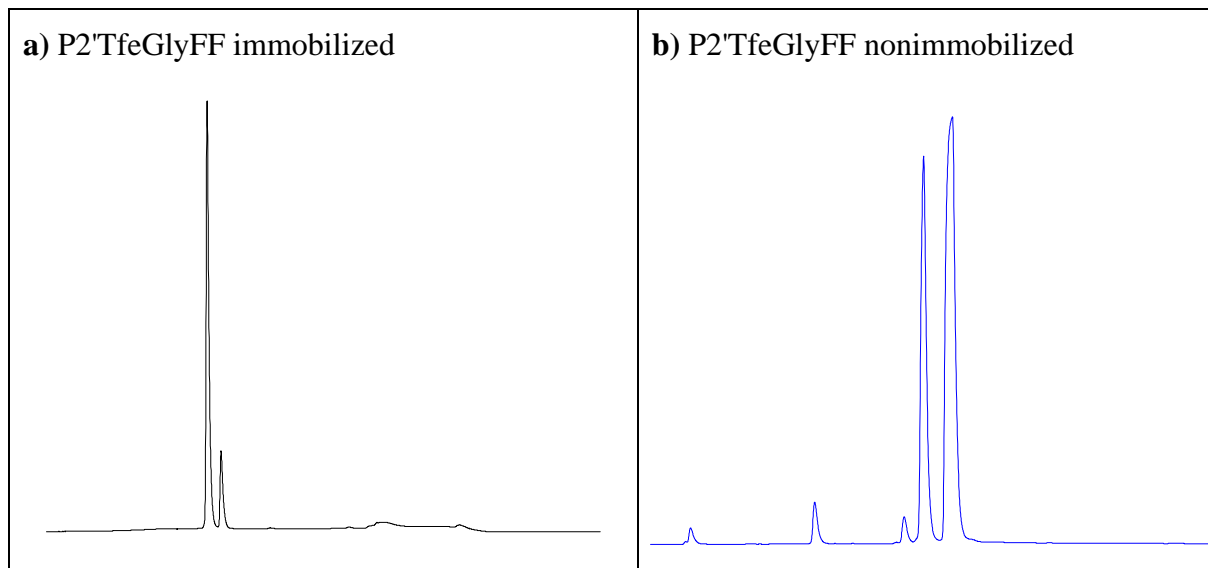


Figure 5.22 HPLC chromatograms of the degradation products of P2'TfeGlyFF peptide using 50 μ L **a)** immobilized and **b)** nonimmobilized plasma proteins after 120 minutes of reaction.

Table 5.9 Immobilized plasma proteins: characterization of cleaved products of peptides obtained by mass spectrometry.

| Peptides | Fragments | MW calculated [M+1] ¹⁺ | MW observed [M+1] ¹⁺ |
|---------------------|-----------------------------|--------------------------------------|------------------------------------|
| FA | Abz-KAAF ¹ AAAK | 967.4993 | 967.5364 |
| | Abz-KAAF ¹ AAAA | 839.4044 | 839.4362 |
| FF | Abz-KAAFF ¹ AAAK | 1043.5306 | 1043.6929 |
| | Abz-KAAFF ¹ AAA | 915.4357 | 915.4696 |
| P2'-TfeGlyFF | Abz-KAAFFTfeGlyAAK | 1111.4935 | 1111,5517 |
| | Abz-KAAFFTfeGlyAA | 983.3986 | 983.4591 |
| P2'-DfeGlyFF | Abz-KAAFFDfeGlyAAK | 1093.4935 | 1093.5601 |
| | Abz-KAAFFDfeGlyAA | 965.3986 | 965.4652 |
| P2'-DfeGlyFA | Abz-KAAFADfeGlyAAK | 1017.4622 | 1017.5306 |
| | Abz-KAAFADfeGlyAA | 889.3673 | 889.4340 |
| FK | Abz-KAAF ¹ KAAAK | 1024.5572 | 1024.5996 |
| | Abz-KAAF ¹ KAAA | 896.4622 | 896.4944 |
| P2'-TfeGlyFK | Abz-KAAFKTfeGlyAAK | 1092.5201 | 1092.5875 |
| | Abz-KAAFKTfeGlyAA | 964.4251 | 964.4801 |
| P2'-DfeGlyFK | Abz-KAAFKDfeGlyAAK | 1074.5201 | 1074.6152 |
| | Abz-KAAFKDfeGlyAA | 946.4251 | 946.4995 |

5.3.3 Nonimmobilized plasma reactions

Experiments were also conducted to determine the product spectrum from whole human blood plasma that had not been immobilized on a chromatographic resin. In this procedure, the peptides were incubated in various volumes (50, 15 and 5 μL) of human blood plasma for a period of two hours. Aliquots were taken at regular time intervals, quenched and analyzed by RP-HPLC equipped with a fluorescence detector. In contrast to the results from the immobilized plasma assay, the peptides were cleaved at various positions producing different peaks at different retention times (Figure 5.22b).

The amount of peptides remaining after 120 minutes of incubation with 50 μL plasma proteins decreased in the order: P2-DfeGlyFA>P2-TfeGlyFA \geq FA; P2-TfeGlyFF>FF>P2-DfeGlyFF \geq FA; and FK>FA>P2-TfeGlyFK \geq P2-DfeGlyFK (Figure 5.23a).

Whereas incorporation of the fluorinated amino acids in the P2 position of the FF and FA peptides reduced the rate of proteolysis, it had the opposite effect in the FK series. Nevertheless, the amino acid at the P1' position appears to play a key role in the hydrolysis of the control peptides, thus Phe (FF)>Lys (FK)>Ala (FA), and it seems to be an important determinant of the specificity.

Similarly, substitutions of the FF and FK variants at P2' position exhibited rates of proteolysis in the order: FF>P2'-TfeGlyFF>P2'-DfeGlyFF=P2'-AbuFF, and FK>P2'-TfeGlyFK=P2'-DfeGlyFK=P2'-AbuFK (Figure 5.23b).

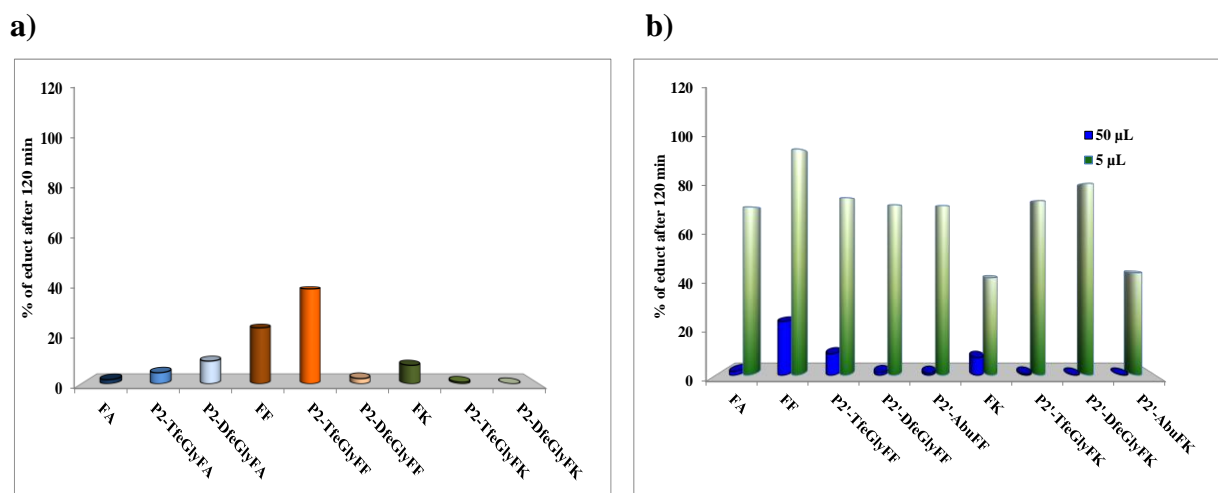


Figure 5.23 Percent of peptides remaining after 120 minutes of incubation with 50 μL human blood plasma at 37°C, **a)** P2FK and P2FF variants. **b)** Comparing the educts remaining after 120 minutes of incubation in different volumes of human blood plasma (50 μL [blue] and 5 μL [green]).

Thus, all FF and FK analogues containing a nonproteinogenic amino acid demonstrated a decrease in stability in the presence of 50 μL of plasma, with FK being the least stable series. The fluorinated FK variants in all positions showed lower stability than the control FK peptide. This behavior is discussed in detail in the FA section below (5.4.1).

A drug's half life in blood plasma has been shown to be an important pharmacokinetic parameter; additionally, a drug's efficacy can be affected by the degree to which it binds to plasma proteins. Therefore, the impact of fluorination on the half life of these peptides is worth studying as a means to improve bioavailability.

Since more than 50% of the control peptide (FA) was degraded by 50 μL of plasma within the first few minutes of the reaction, the volume of the plasma was varied to obtain an optimal condition. With 1:1 peptide/plasma (v/v), the half life of the FA peptide could be determined after 24 hours; adjusting the peptide/plasma ratio to 1/3 (v/v), the half life of the FA peptide was improved to about 40 minutes. In effect, the fluorine content within these peptides does not have a significant impact but the stability depends on position, sequence and plasma protease concentration. Subjecting the FA peptide to plasma degradation at this adjusted plasma concentration led to the hydrolysis of more than 60% of the initial amount after 120 min (Figure 5.24).

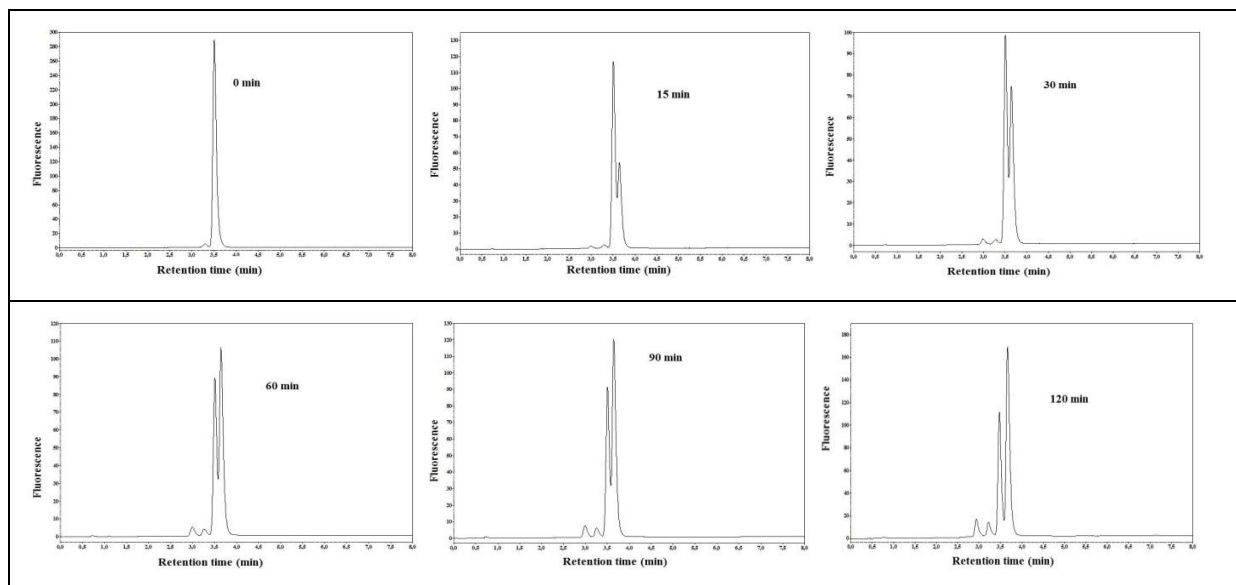


Figure 5.24 HPLC chromatograms illustrating the systematic digestion of the control peptide over a period of 120 minutes with 15 μL plasma in PBS at 37 $^{\circ}\text{C}$. Reproduced with permission from Asante V. et al.^[30] Copyright © 2013, Elsevier.

Surprisingly, in almost all cases, the degradation of the nonproteinogenic FA peptides is faster compared to the native control. Among all the investigated sequences, the P1'-TfeGlyFA is the only variant that displays improved stability towards proteolysis (Figure 5.25).

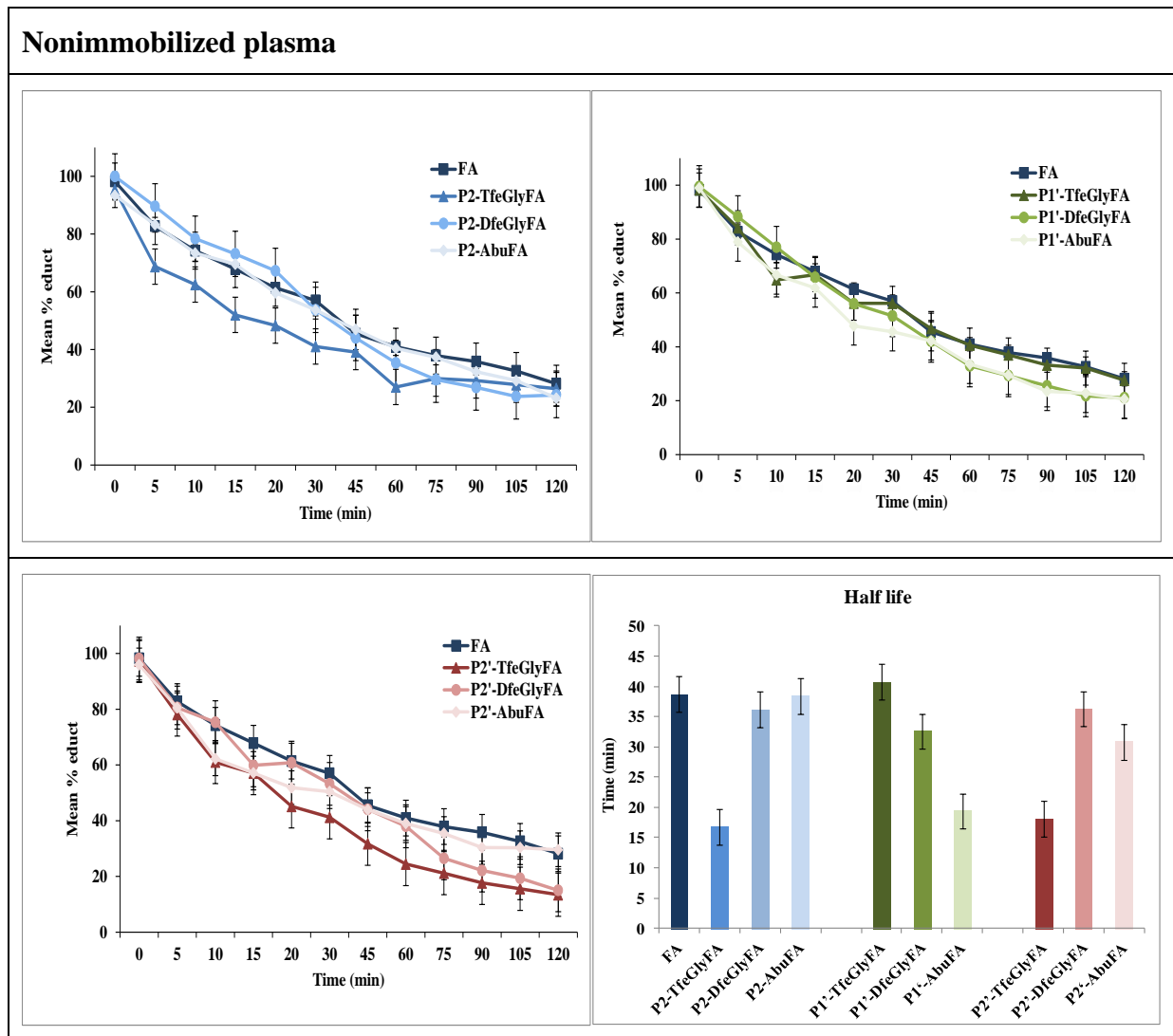


Figure 5.25 Percentage of educts of FA peptide variants remaining at different reaction times with 15 μ L human blood plasma in PBS at 37 $^{\circ}$ C over 120 minutes, and the time required for the degradation of 50% of the initial peptide amount when incubated with human plasma at 37 $^{\circ}$ C in PBS (half life). Reproduced with permission from Asante V. et al.^[30] Copyright \copyright 2013, Elsevier.^{VII}

The impact of fluorine is strictly position dependent since the P2'-TfeGlyFA variant was the fastest degraded among all the FA peptides. In the P2' FA series, the P2'-AbuFA was the most stable peptide, followed by P2'-DfeGlyFA and P2'-TfeGlyFA.

^{VII} The results presented in section 5.3 have been published in: Asante V. et al^[30]. Since this part was published exclusive of the isolated enzymes studies, the peptides were named according to the position of substitution using numbers (P2=4, P1'=6 and P2'=7) as shown in Figure 5.1.

For the peptides substituted at the P2 position, the fluorination of ethylglycine accelerates hydrolysis and the P2-AbuFA variant is more stable with a plasma half life equal to the native control (FA) peptide.

Thus, depending on the position within the peptide substrate, fluorination can either induce faster degradation (P2-variants) or improved stability towards proteolysis (P1'-variants).

To identify the main plasma proteinases involved in the degradation of the studied peptides, the same experiments were undertaken with a peptide/plasma ratio of 1/10 (v/v) (like the FK and FF variants above) and separation of the cleavage products was carried out by HPLC. After 60 min of digestion, some of the peptide substrates had almost completely disappeared and one key metabolic product **m1** was observed in the HPLC chromatogram (Figure 5.26a). Prolonged incubation caused the hydrolysis of **m1** and three new metabolic products were detected by chromatography. They are reported in Figure 5.26 as **m2**, **m3** and **m4**.

Analysis of the metabolites by mass spectrometry enabled identification of the cleaved products, and these data are reported in Table 5.10. First, the measured mass of the metabolite **m1** corresponds to the truncated peptide missing the carboxy-terminal lysine: Abz-KAAFAAAA which holds true for all peptide variants using both methods (solution and immobilization).

This selective hydrolysis of a basic amino acid in the C-terminal end is characteristic of the carboxypeptidase N.^[117,248]

The concentration of the other three metabolites increased in intensity proportionally with the decrease in the concentration of **m1**. These metabolites were the result of secondary hydrolysis of **m1** occurring between the residues 7Ala-8Ala resulting in **m2**, 5Phe-6Ala resulting in **m3**, and 4Ala-5Phe resulting in **m4**.

Since elastase specifically cleaves after small hydrophobic side chains such as glycine, valine, leucine, isoleucine, and especially alanine,^[249,250] the presence of such secondary hydrolysis of the peptides in the plasma reaction could therefore be a result of the action of human leukocyte elastase (EC 3.4.21.37).

The plasma study shows that the substitution of Ala with nonproteinogenic amino acids at positions P2, P1' and P2' still leads to the cleavage of the peptide variants by elastase, which demonstrates elastase's broad specificity. To verify this hypothesis and determine the influence of fluorination on peptide stability towards elastase (EC 3.4.21.36), an assay with the isolated proteinase using the same peptide library was carried out.

RESULTS AND DISCUSSION

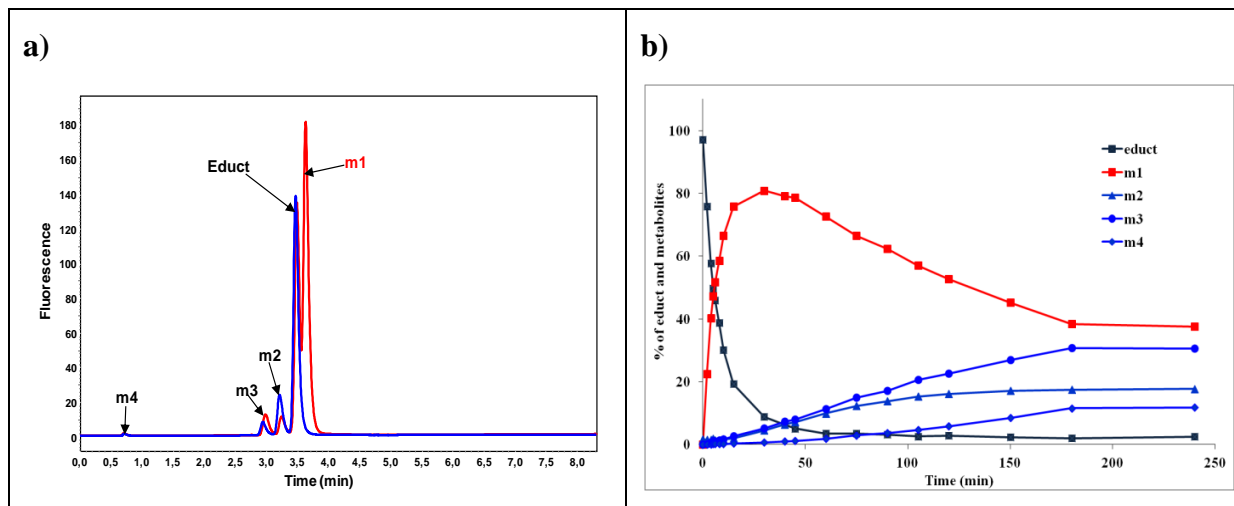


Figure 5.26 a) Comparison of the HPLC chromatograms of the control peptide digested by 50 μL plasma (red) and elastase (blue) after 120 minutes of reaction time. b) Percentage of educt and products formed from the reaction of the control peptide in 50 μL human blood plasma at different reaction times over 240 minutes at 37 °C in PBS. Reproduced with permission from Asante V. et al.^[30] Copyright © 2013, Elsevier.

Table 5.10 Sequences and corresponding calculated (cal.) and observed (obs.) masses of cleaved products with responsible protease in the human blood plasma. Reproduced from Asante V. et al.^[30] Copyright © 2013, Elsevier

| Name | Sequence | Mass calculated (m/z) | Mass observed (m/z) | Protease |
|-----------------|----------------------------|-----------------------|---------------------|--------------------|
| control peptide | Abz-KAAF ³ AAAK | 967.4993 | 967.5364 | |
| m1 | Abz-KAAF ³ AAA | 839.4044 | 839.4362 | Carboxypeptidase N |
| m2 | Abz-KAAF ³ AA | 697.3301 | 697.3672 | Elastase |
| m3 | Abz-KAAF ³ A | 555.2559 | 555.2940 | |
| m4 | Abz-KAA | 408.1875 | 408.2251 | |

5.4 Proteolytic stability of peptides towards elastase (EC 3.4.21.36)

5.4.1 FA Analogues

Elastase, a serine protease with a molecular weight of approximately 25.9 kDa, digests a wide variety of protein substrates, with a preferred specificity for bonds involving uncharged, non-aromatic amino acids (e.g., Ala, Val, Leu, Ile, Gly, Ser): its natural substrates include proteins like elastin.^[250,251]

In this study, the enzymatic digestion of peptide variants by elastase was determined by an analytical RP-HPLC assay and the products were characterized by ESI mass spectrometry and LC/MS. The investigation of the time-dependent hydrolysis of the peptides carrying non-proteinogenic amino acids in position P2 or P1' showed tendencies similar to degradation by plasma. On the one hand, the DfeGly variants in both cases were more rapidly degraded with up to 35-40% of the initial substrate hydrolyzed after 120 min (Figure 5.27). On the other hand, a significantly increased stability was observed for the two TfeGly variants. The initial concentration of P1'-TfeGlyFA remained unchanged even after two hours of incubation. This stability towards elastase correlates with the excellent stability of P1'-TfeGly in plasma compared to its hydrocarbon parent (P1'-AbuFA) or the natural control peptide (FA). Here, substitution by a TfeGly residue can be a promising strategy for improving peptide stability and, thus, bioavailability. Nevertheless, the stability for the third peptide series (modified at the P2' position) shows opposite behavior compared to the other two series. Here, the TfeGly analogue is much more rapidly digested by elastase, and is the least stable peptide of all studied variants. Elastase is well known to preferentially cleave at small hydrophobic amino acids like valine, so substituting alanine in the P2' position with TfeGly, which was shown by Samsonov *et al* et al.^[165] to have comparable size and hydrophobicity to valine, could be assumed to contribute to the faster degradation by elastase.

In contrast, P2'-DfeGlyFA and P2'-AbuFA exhibit outstanding stabilities compared to the FA peptide, confirming the observed trend in stability for these peptide variants in plasma. These findings clearly indicate that fluorination has a significant influence on the proteolytic stability of peptides.

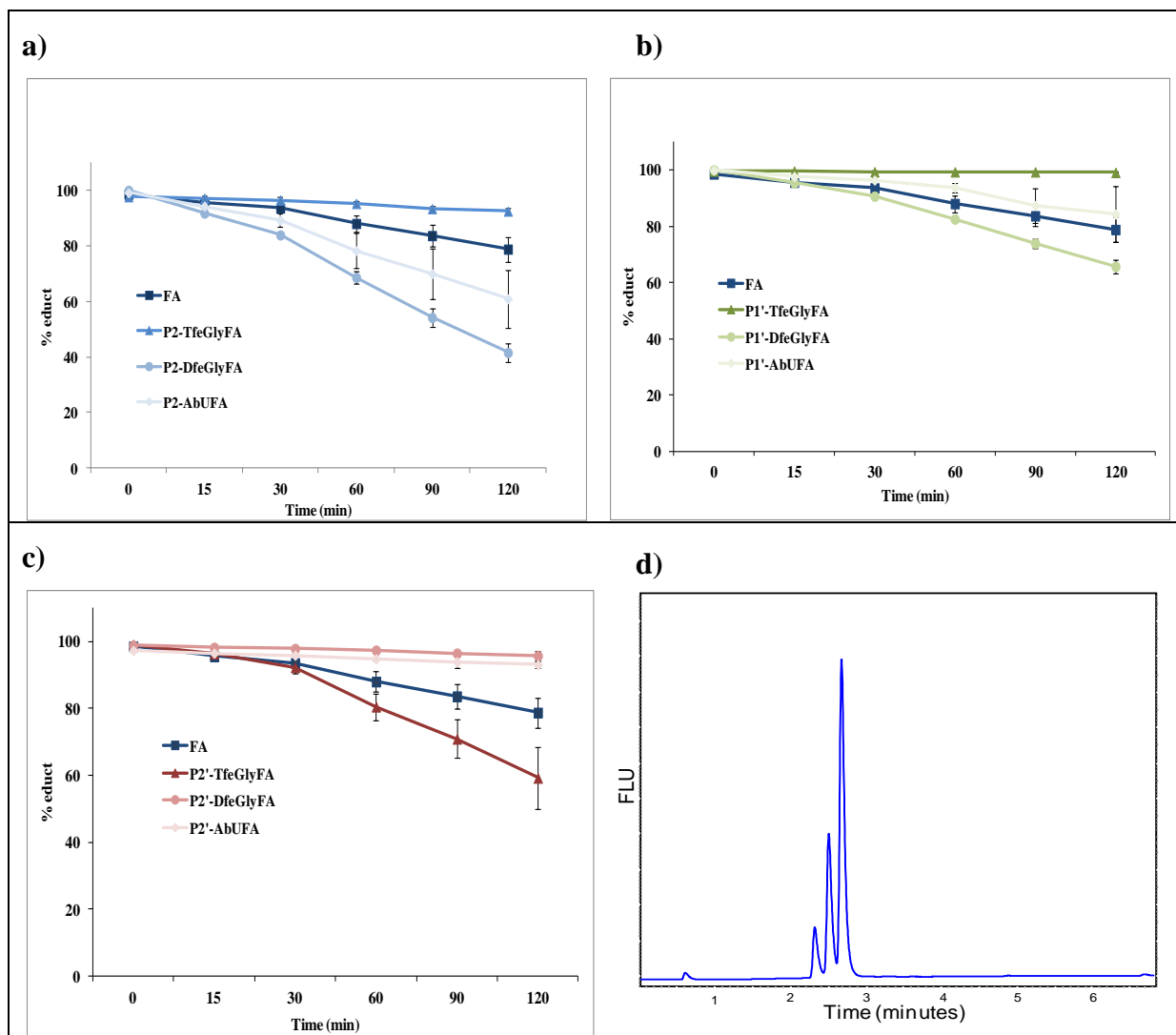


Figure 5.27 Time course of changes in the area of the HPLC peaks representing the educts (FA variants, **a**=P2, **b**=P1', **c**=P2' variants) present after hydrolysis by elastase at 37 °C in 100 mM Tris-HCl buffer, pH 8.0. **d**) Fluorescence HPLC chromatogram of FA peptide hydrolysis after 120 minutes.^[30] Reproduced with permission from Asante V. et al.^[30] Copyright © 2013, Elsevier.

5.4.2 Hydrolysis of the FK and FF peptide analogues

The control FK and FF peptides were more stable toward elastase proteolysis whereas the P2'-fluorinated variants were efficiently degraded. Comparing the stabilities of the nonproteinogenic amino acid containing variants: P2'-AbuFK>P2'-TfeGlyFK>P2'-DfeGlyFK; P2'-AbuFF>P2'-TfeGlyFF>P2'-DfeGlyFF (Figure 5.28). Comparing the fluorinated variants, the TfeGly substitution seems to stabilize the peptide, whereas the DfeGly destabilizes the peptides.

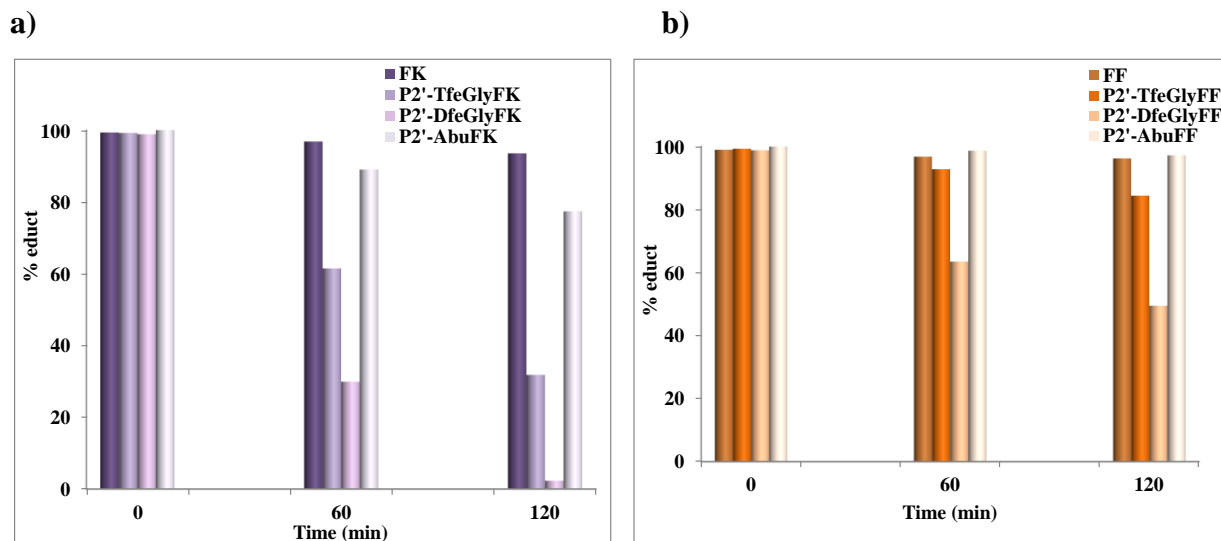


Figure 5.28 Time course of changes in the area of the HPLC peaks representing the educts (P2'-FK and P2'-FF peptides) present after hydrolysis by elastase at 37 °C in 100 mM Tris-HCl buffer, pH 8.43.

According to Renaud *et al.*,^[251] who studied the subsite specificities of both porcine pancreatic elastase and human leucocyte elastase with trifluoroacetylated inhibitors (CF₃CO peptides), the highest binding affinity is observed when Lys occupies the S1' subsite. They explained that this may be due to a favorable van der Waals interaction of the δ -CH₂ group of Lys with the $-\gamma$ -CH₃ group of Val 99. In this case, the FK peptides which carry Lys instead of Ala in this position are more likely to have a higher affinity for elastase which could probably lead to faster hydrolysis. Replacing this Lys with an aromatic amino acid in the FF variants and Ala in the FA variants thus reduces hydrolysis. As the S2' subsite in porcine pancreatic elastase has been shown to have a marked specificity for Ala, and can only accommodate bulkier residues with difficulty, substitution of the alanine with the nonproteinogenic amino acids in this position leads to the destabilization of the peptides perhaps for steric reasons. In view of this explanation, it is not surprising that all the fluorinated P1'-Lys containing peptides show decreased stability towards elastase and plasma.

6. Potential Application: Efforts toward protease stable and high affinity fluorinated HIV entry inhibitors

The human immunodeficiency virus (HIV) pandemic is one of the greatest health crises the world faces today. Over the last three decades, there have been several attempts to produce antiretroviral (ARV) drugs that target different stages of the virus life cycle. Most currently used anti-HIV drugs target either the HIV-1 reverse transcriptase, protease, or integrase (Figures 6.1 and 6.2).^[252-256] Neither curative nor preventive treatment against HIV-1 is available, even though combined anti-viral treatments can dramatically decrease the viral load. Due to either the toxicity of these molecules or virus mutation leading to resistance, interest in alternative therapeutic approaches is rising. New targets are being explored, such as the proteins involved in the process of fusion of the virus with the host cell.^[254-256] The development of agents that block viral entry would protect human cells from infection by all HIV-1 strains, including those with mutations that confer resistance to current therapies.^[257]

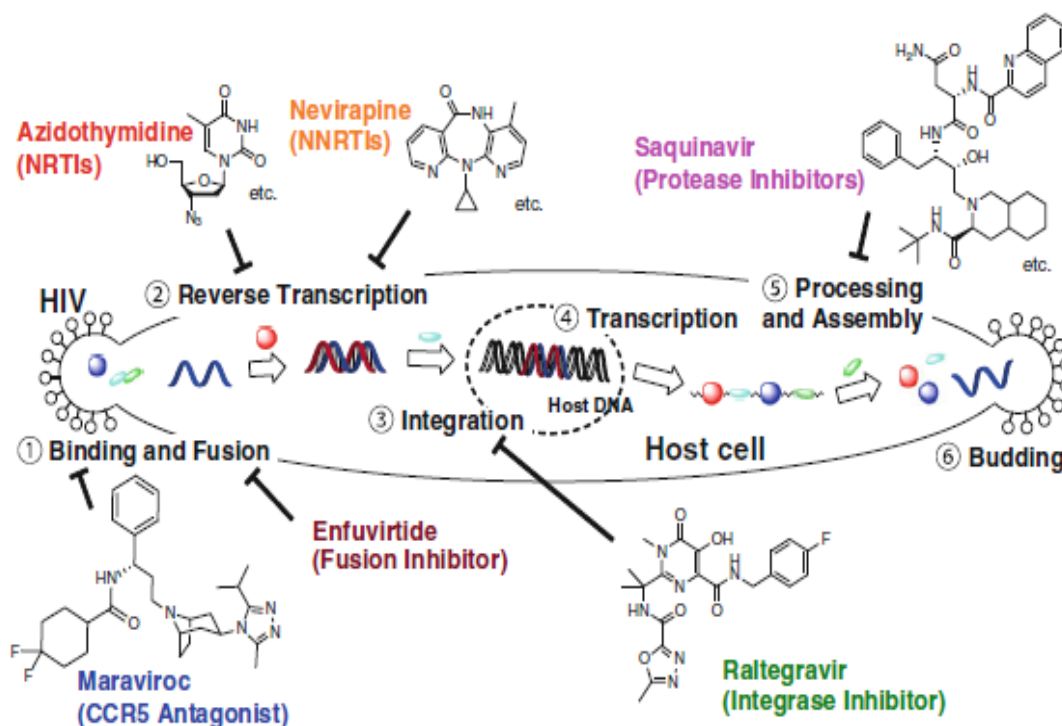


Figure 6.1 Structure of approved anti-HIV-1 agents and the target process in HIV-1 life cycle. Reproduced from Mizuhara^[256]

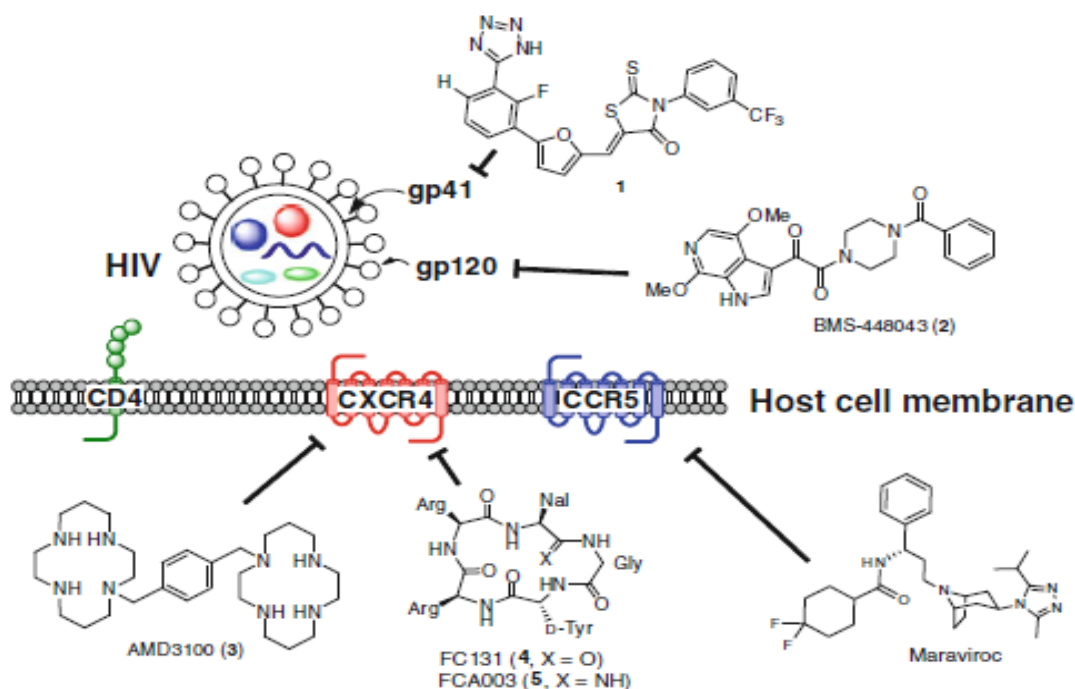
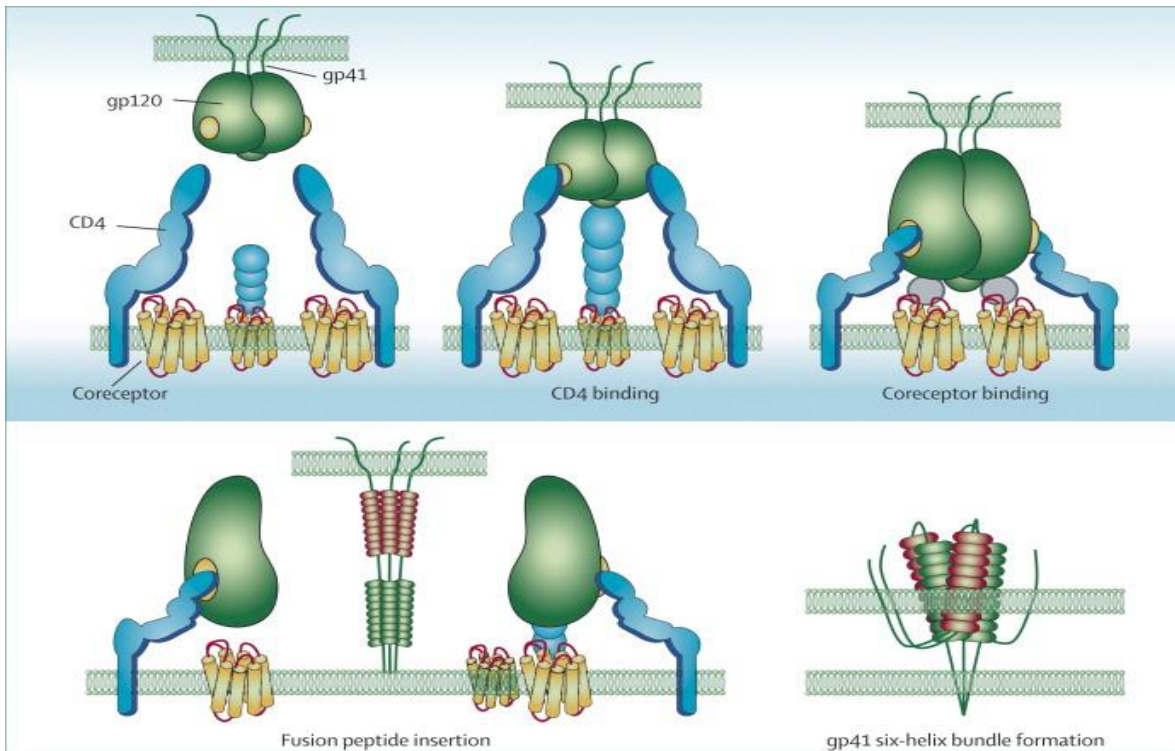


Figure 6.2 Structures of anti-HIV-1 agents targeting HIV-1 entry process. Reproduced from Mizuhara^[256]

The HIV-1 fusion mechanism is a well-known process which has been shown to involve the envelope glycoproteins gp120 and gp41.^[258] Cellular receptor and co-receptor recognition by gp120 induces conformational changes in gp41. The N-terminal heptad repeat (NHR) and C-terminal heptad repeat (CHR) of the gp41 ectodomain form a six-helix bundle that makes up the core of a trimer of hairpins. This brings the viral and cellular membranes into the close proximity necessary for fusion, resulting in the subsequent delivery of the viral genome into the host cell (Figure 6.3a).^[259-261] Interfering with this fusion process thus prevents infection (Figure 6.3b).

Owing to its relatively conserved sequence, compounds targeted to gp41 may be broadly effective and be less likely to induce drug-resistant HIV-1 isolates. Several peptide analogues that have inhibitory activity in the context of HIV-1 infection and HIV-1-mediated cell-cell fusion have already been reported, and some have been approved for use.^[256,260-271] These entry inhibitors or fusion inhibitors (FI) that block HIV from fusing with a cell's membrane and prevent the infection of CD4 cells include Maraviroc, inhibitor of the interaction between the chemokine receptor CCR5 and HIV-1 gp120,^[268] and enfuvirtide (also referred to as Fuzeon or T-20), which binds to the transmembrane domain and prevents fusion with the host cell.^[269]

a)



b)

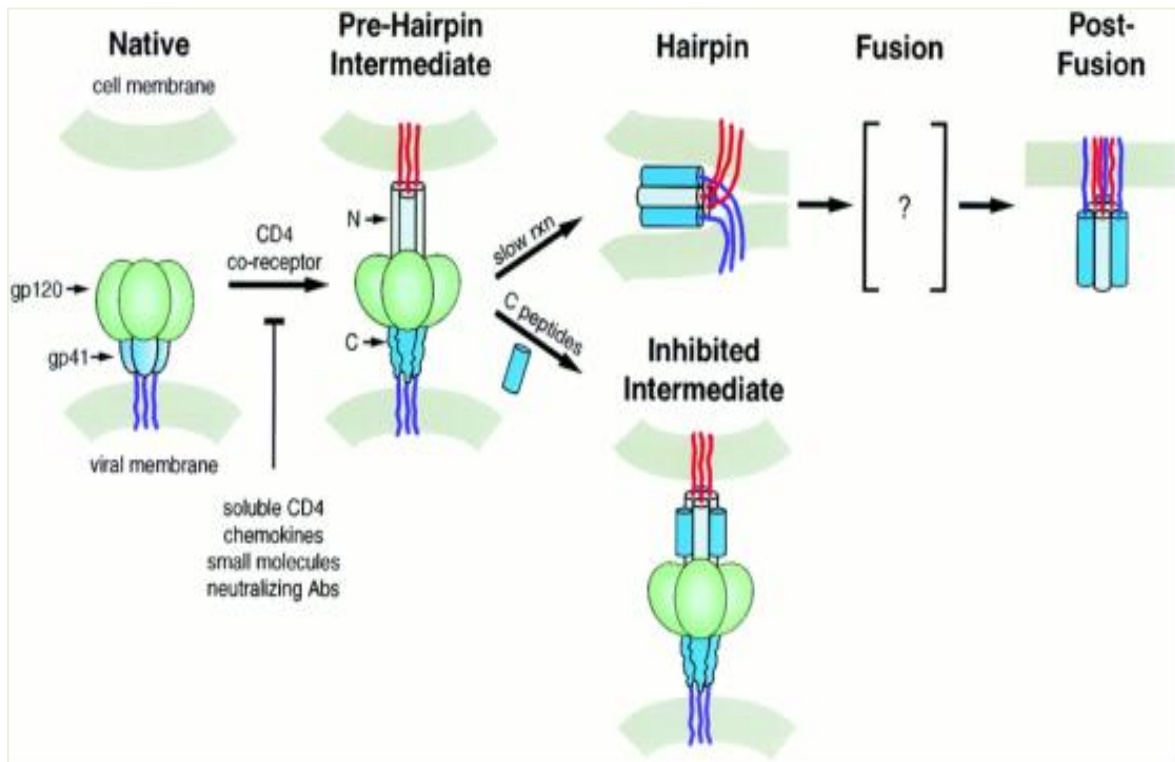


Figure 6.3 a) A model of HIV-1 membrane fusion and b) its potential inhibition; showing gp120, the prehairpin intermediate of gp41 its associated NHR and CHR peptides, and the six-helix-bundle. Reproduced from Esté and Teleni^[260], Chan and Kim^[261].

The major drawbacks of these analogues are their fast proteolytic degradation, lack of pocket-binding domain, resistance and oral bioavailability.^[262,270,271] Diverse approaches have been applied to HIV-1 peptide inhibitors to extend their plasma half-life, potent antiviral activity against a broad spectrum of HIV-1 strains, water solubility, and specificity,^[272-280] but there is still a great demand for improved entry inhibitors.

Within the framework of this thesis, one aim was to identify a peptide-based substance with high binding affinity to the parts of the gp41 region that mediate fusion between the viral membrane and the host cell and improved protease stability. Site-specific fluoroalkylation of CHR-peptide analogues is the approach we envisioned. In a recent study from our group^[281], newly generated shorter CHR-peptide analogues (Table 6.1) which contain the highly conserved Trp-Trp-Ile motif show affinity for the T21 (NHR) peptide, and may therefore efficiently compete with the native CHR-domain to prevent bundle formation. Within these CHR-peptide analogues, the systematic replacement of aliphatic residues critical for the six helix bundle formation of the gp41^[282-284] with their fluorinated counterparts DfeGly, 5³-F³Ile, and 5³,5^{3'}-F⁶Leu (Figure 6.4) is expected to yield new CHR-peptide analogues that efficiently bind NHR peptides.

Due to the fact that certain studies have shown that substituting fluoroalkyl-amino acids for their hydrocarbon analogues can have a stabilizing effect on the secondary structure of peptides as well as their protease stability,^[12,18,30,151-154,281,301] it may be expected that new C-peptide analogues having shorter sequences compared to other analogues will have improved characteristics.

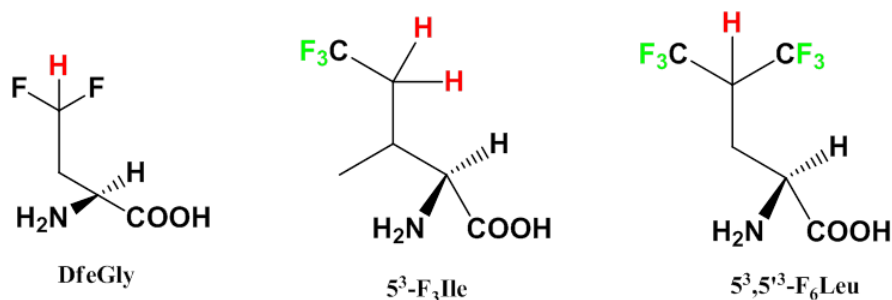


Figure 6.4 Structures of fluorinated amino acids showing the polarized hydrogen atoms highlighted in red.

Currently, the available methods (for example, plaque-based assays and immunostaining) for the identification and quantification of particular virus particles are time consuming and often expensive, creating the demand for sensitive and accurate viral biosensors with rapid detection systems.

Surface plasmon resonance (SPR) is a surface sensitive optical technique that can be used to study thin (organic) layers on noble metal films. The basic principle of biosensor experiments is to immobilize one analyte on a surface (either a ligand or a binding protein) and monitor its interaction with a second analyte in buffer solution flowing over the surface. The SPR spectrometer then measures changes in the refractive index at the metal surface upon interaction between the two analytes, yielding important information about the association kinetics in the form of a graph called the sensorgram. In the second stage of the experiment, pure buffer is flowed over the surface to enable determination of the dissociation kinetics. Compared with traditional methods of analysis, SPR offers rapid and highly-sensitive determination of binding kinetics, and uses small amounts of sample: furthermore, no labelling is required. Since SPR biosensors monitor complex formation in the presence of free analyte, it is also possible to characterize low-affinity or transient interactions.^[285-287]

SPR has been used extensively in HIV-1 peptide-therapeutic research. Recent applications rely on modification methods such as (N-acetylation, N-methylation and PEGylation) of lysine residues at different positions,^[288] use of bifunctional molecules,^[289] biotin-modified peptides, antibodies, thiol-selective functionalized^[255,290-292] and D-peptides.^[293] Different lengths of PEG monomers have been attached site specifically to the NHR peptides and the effects of PEG position and chain length on the kinetics and proteolytic degradation of HIV-1 membrane fusion inhibition have been studied.^[294,295] Almost all of these methods rely on modified immobilized N36 peptides that are monomeric but must oligomerize with the C-peptide partner to form the stable six-helix bundle (Figure 6.5a).^[293,296,297] With the application of different strategies to obtain multivalency (flexible PEG fragments^[298], disulfide linkages^[278], three-armed cysteine scaffold,^[299] etc.) of the CHR and NHR peptides of the gp41, researchers have observed better binding and improved IC50s. This lead us to ask the question whether SPR-based analysis could be improved by developing a multivalent format based on trimeric N36 immobilization.^[300] We therefore propose to provide trimeric N36 via a trivalent ethylene glycol linker on the SPR gold surface (Figure 6.5b).

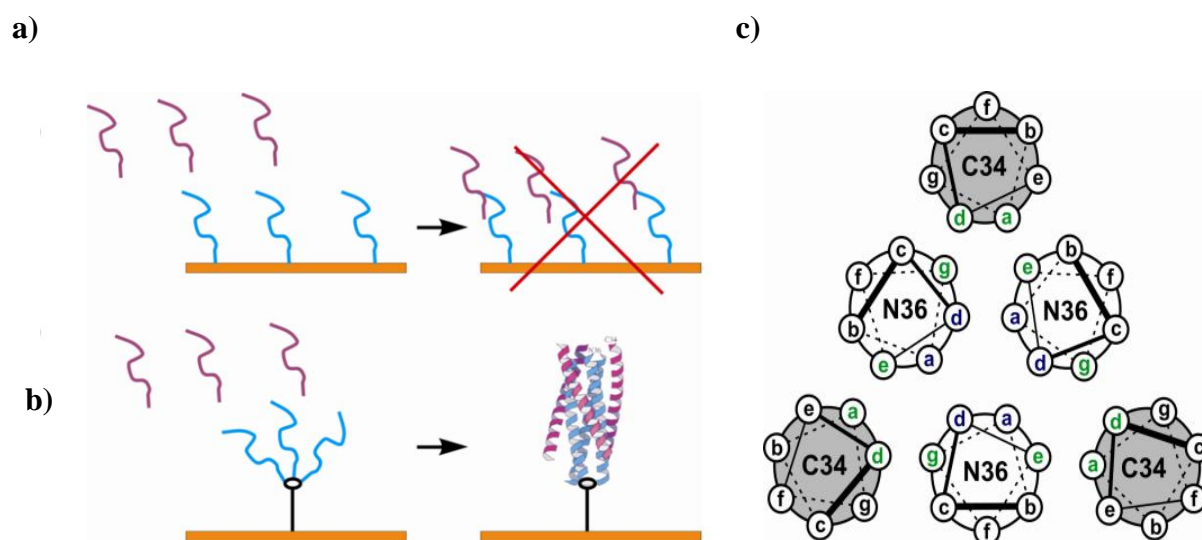


Figure 6.5 a) Conventional, monomeric mode of N36 immobilization. b) Intended, trimeric mode of N36 immobilization. N36 in blue and C34 in violet c) Helical-wheel-diagram of the active fusion hexamers

Our proposed design of the N (polyethylene trimeric N36) and C (shorter and fluorinated sequence) peptides (Table 6.1) for the SPR studies, described herein, presents a powerful strategy to provide crucial information on the molecular interaction of the peptidic inhibitor with its ligand to achieve high-affinity binding of entry-inhibitor candidates with increased bioavailability and protease stability.

Table 6.1 Names and sequences of gp41 NHR, CHR and newly proposed shorter CHR peptides showing the position of substitution (highlighted in green) with the fluorinated amino acids listed in Figure 6.4.

| Name | Sequences |
|------|---|
| N36 | SGIVQQQNLLRAIEAQQHLLQLTVWGIKQLQARIL |
| C34 | 628 661 WMEWDREINNYTSLIHSLIEESQNQQEKNEQELL |
| C33 | 620 652 EQIWNNMTWMEWDREINNYTSLIHSLIEESQNQ |
| C31 | 620 650 EQIWNNMTWMEWDREINNYTSLIHSLIEESQ |

PEG can be functionalized (Hetero or bifunctional: SH, COOH, NH₂ etc.) by substituting one or both terminal hydroxyl groups with suitable initiator and/or termination reagents. The resulting mono or hetero-functionalized molecule can be used as a capping ligand, a substrate for synthesis of bioconjugates, or a linking agent between multiple gold nanoparticles (AuNPs).^[302] There are several steps required to fully synthesize branched chain (trivalent linker) polypeptides.

In an attempt to synthesize this trivalent linker, a functionalized PEG and a compound with the required branching, in this case a trivalent compound, tris(hydroxymethyl)aminomethane (Tris), were used as building blocks (Figure 6.6).

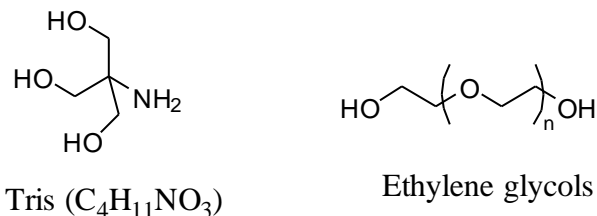
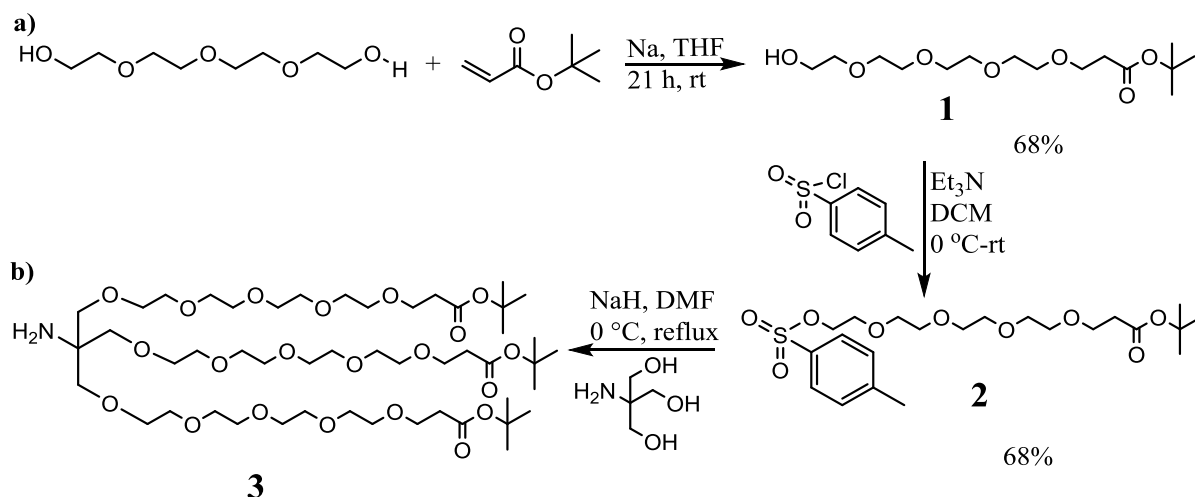


Figure 6.6 Building blocks required for the synthesis of the trivalent linker

In a variation of a literature procedure, tetraethylene glycol was converted to a carboxyl functionality which enables the coupling of the N-terminal amino group of the N36 peptide to the linker through nucleophilic esterification as shown in Schemes 6.1 and 6.2.



Scheme 6.1 Reaction of tetraethylene glycol with *tert*-butyl acrylate, tosylation of PEG ester and coupling of tosylated PEG ester to Tris.

The Michael addition step was achieved through the treatment of tetraethylene glycol (HO-PEG₄-OH) with *tert*-butyl acrylate in the presence of Na metal under argon in tetrahydrofuran (THF) solution. After a stepwise work up and purification, *tert*-butyl 1-hydroxy-3,6,9,12-tetraoxapentadecan-15-oate **1** was obtained in 68% pure yield (Scheme 6.1A).^[303-309]

The second step involves the conversion of the free OH group at the other terminus into a good leaving group to enhance nucleophilic substitutions with Tris.

Tosylate is well known to be a very good leaving group, and its PEG derivatives undergo nucleophilic substitutions at much higher rates.

POTENTIAL APPLICATION

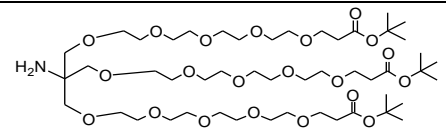
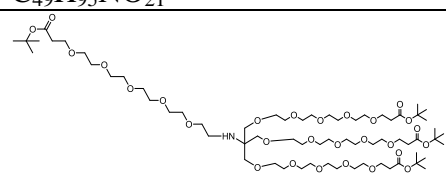
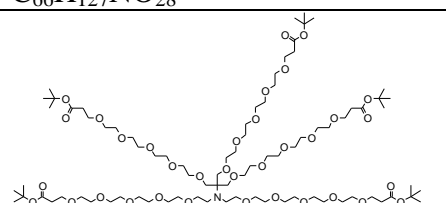
The *tert*-butyl 1-(tosyloxy)-3,6,9,12-tetraoxapentadecan-15-oate **{2}** was obtained by reacting compound **{1}** with *p*-toluenesulfonyl chloride in the presence of triethylamine (necessary to remove HCl byproduct). The subsequent separation of the crude product yielded 68% monotosylated PEG ester **{2}**^[303-309] which was analyzed and characterized by mass spectrometry (Table 6.2) and NMR.

Table 6.2 Measured masses of 4,7,10,13-Tetraoxapentadecanoic acid, 15-[[[4-methylphenyl)sulfonyl]oxy]-, 1,1-dimethylethyl ester **{2}**.

| Compounds | m/z calculated | m/z observed |
|---|----------------|--------------|
| C ₂₂ H ₃₆ O ₉ SNa | 499.2 | 499.1955 |
| C ₂₂ H ₃₆ O ₉ SNH ₄ | 494.21 | 494.2403 |
| C ₂₂ H ₃₆ O ₉ SK | 515.21 | 515.1718 |

In the third step, Tris (nucleophile) was deprotonated with an excess of NaH under anhydrous conditions and the nucleophilic substitution of the tosylated PEG ester {compound **2**} with Tris was carried out to give compound **{3}** in good crude yields. Due to the formation of heterogeneous mixtures, separation of the desired product could not be achieved. The mass to charge ratio and the NMR spectra indicate the formation of the following products as shown in Table 6.3 below.

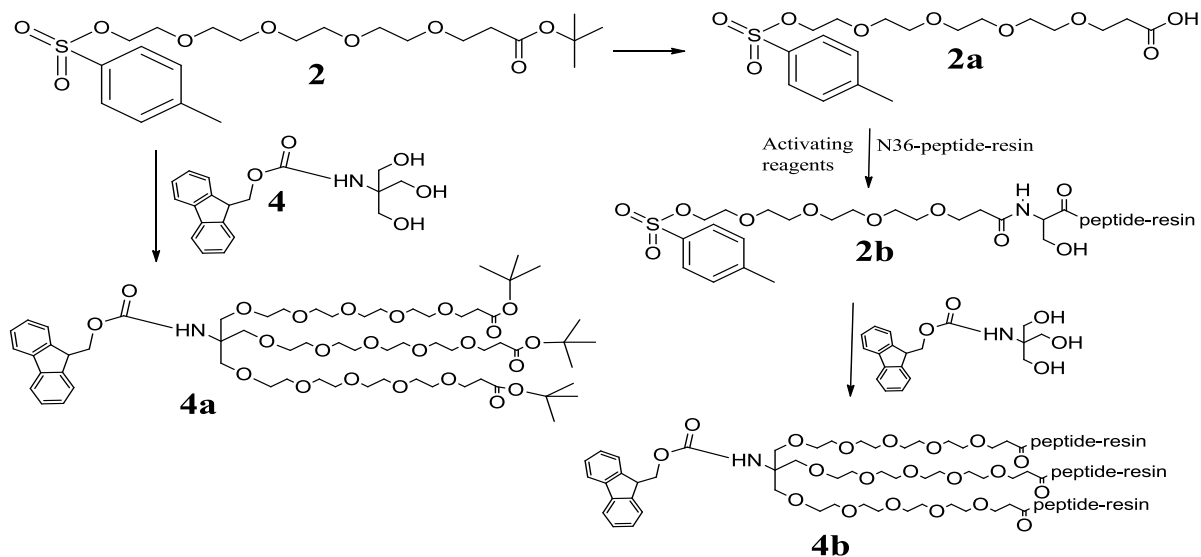
Table 6.3 Possible products from reaction with their calculated mass to charge ratios (**Major peaks**)

| Possible products | m/z calculated | m/z calculated | m/z observed |
|--|-------------------------|---------------------|---------------------|
| | [M+1] ¹⁺ | [M+2] ²⁺ | [M+2] ²⁺ |
|  C ₄₉ H ₉₅ NO ₂₁ | 1033.64 ^{VIII} | 517.82 | 516.34 |
|  C ₆₆ H ₁₂₇ NO ₂₈ | 1381.85 ^{VIII} | 691.93 | 692.45 |
|  C ₈₃ H ₁₅₉ NO ₃₅ | 1732.08 ^{VIII} | 867.04 | 868.56 |

^{VIII}In these cases, no corresponding mass was observed

POTENTIAL APPLICATION

An alternative path to limit the formation of undesired side products is to couple compound **2** to N-protected Tris (Fmoc-Tris) or convert the PEG ester to the corresponding acid and then couple this to the peptide on the resin as shown in Scheme 6.2. Subsequent synthetic steps are detailed in the outlook.



Scheme 6.2 Alternative path to the synthesis of trimer linker

7. Conclusion

A comprehensive and systematic characterization of proteolytic stability provides important information that could be used to aid in the design of effective fluorine-modified peptides with enhanced bioavailability, intended to serve as pharmaceutical agents. The impact of fluorine substitution on the properties of peptides and proteins has been shown to depend strongly on the position as well as on the extent of fluorine substitution within a certain amino acid or within the peptide chain. It was therefore the aim of this thesis to systematically elucidate the impact of fluoroalkyl substitution on the protease resistance of model peptides towards digestive enzymes and proteases of the human blood plasma with the goal towards enhancement of bioavailability.

The use of model peptides allows for a systematic comparison of the substitution effects with respect to the kind of amino acid as well as its position relative to the enzymatic cleavage site. To investigate the effect of side chain fluorination on proteolytic stability, a library of model peptides was synthesized in which Abu, DfeGly, and TfeGly were incorporated at different positions and subjected to enzymatic degradation using the serine proteases α -chymotrypsin, proteinase K, and elastase, the aspartic protease pepsin, or human blood plasma. All cleavage products were resolved by HPLC equipped with a fluorescence detector, an efficient and reproducible means of analyzing hydrolysis products, and identified by ESI/MS and LC/MS. The results are summarized in the following paragraphs.

The experimental analysis demonstrates that the incorporation of unnatural building blocks bearing fluoroalkyl side chains into a substrate can significantly affect its proteolytic stability in various ways. In the case of α -chymotrypsin and pepsin it was observed that the fluorinated variants are generally well processed, in certain cases even more rapidly than the natural control peptide. This observation indicates that these substrates are geometrically well accommodated within the enzyme subsites S2 to S2'. Molecular modeling was used to identify potential noncovalent interactions between the enzymes and their substrates, in order to rationalize the experimentally determined proteolytic stabilities.

In three particular cases the observed rate of hydrolysis is significantly reduced upon incorporating fluorinated residues into the peptide sequence. First, strong enhancements in stability are observed when fluorinated amino acids occupy either the P2' position of the FA peptide or the P2 or P2' positions of the FF peptide, in the context of proteolysis by pepsin.

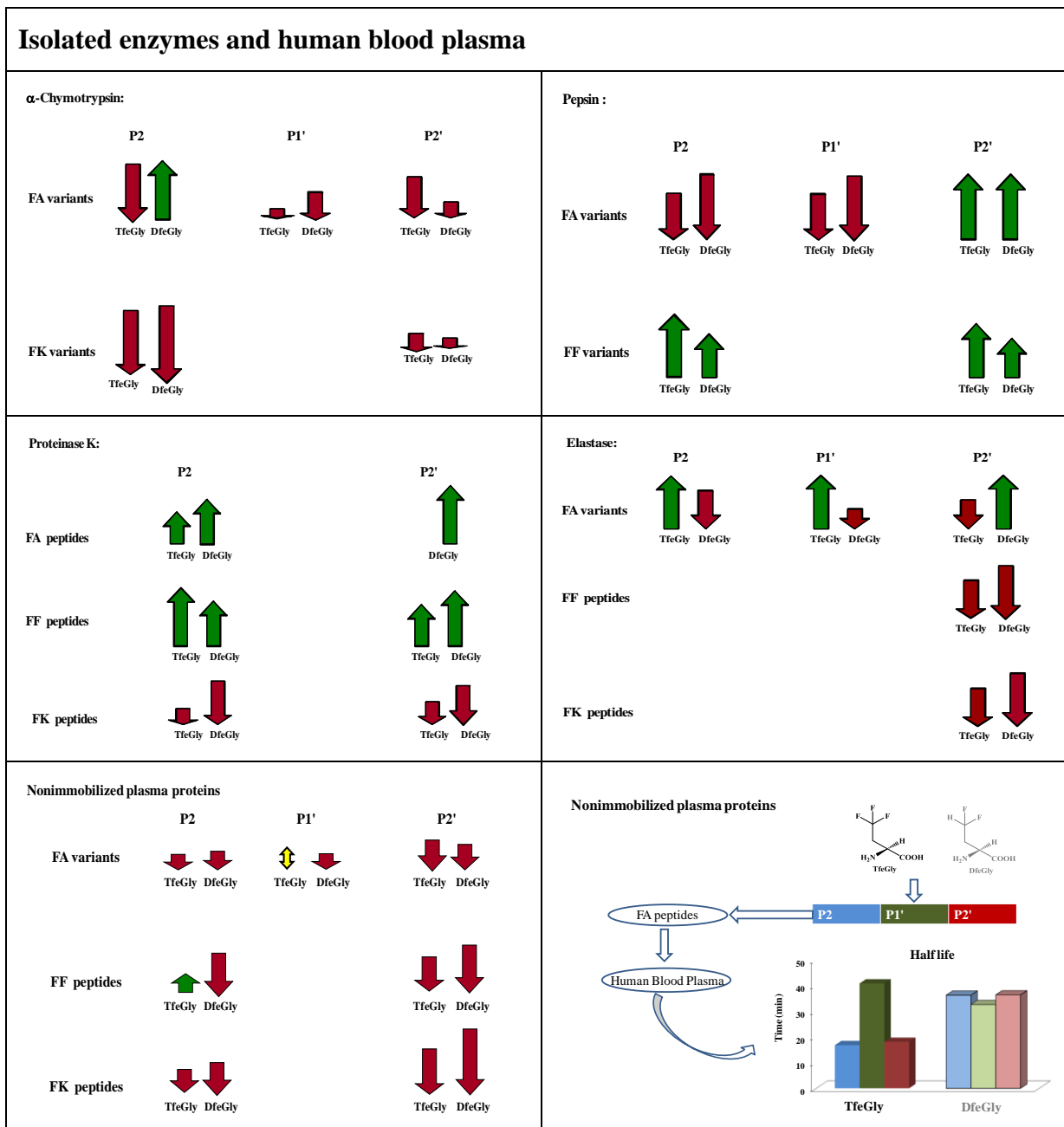
CONCLUSION AND OUTLOOK

This is likely due to the larger solvent-accessible surface area of both TfeGly and DfeGly compared to Ala and Abu. Second, in the context of digestion with α -chymotrypsin, improved proteolytic stability is observed when DfeGly is present in position P2. This can be attributed to the fluorine-induced polarity of the side chain, which appears to disfavor the accommodation of the P2-DfeGlyFA variant within the S2 subsite of the protease.

Furthermore, in the case of proteinase K, incorporation of TfeGly and DfeGly in the P2 and P2' positions of the FA and FF variants dramatically enhance proteolytic resistance; in contrast, all forms of fluorinated FK variants at these positions lead to a reduction in stability. Because proteinase K has a preference for aliphatic and aromatic amino acids in position P1, and Ala in position P2 enhances cleavage, it is not surprising that all peptides with this alanine replaced demonstrated improved stability. The proteolytic stability pattern of fluorinated amino acids used in all peptide series with the isolated enzymes are summarized in the diagram below.

Screening these peptides against human blood plasma shows different outcomes. Cleavage products are dependent upon the method used for the reaction. Immobilization of plasma proteins gave only one major cleavage product, which was identified to be the result of the action of carboxypeptidase N. However, in solution (nonimmobilized), this reaction gave 4-6 distinct cleavage products depending on the peptide sequence. Analysis of the analytes reveals common products with similar properties (retention time on fluorescence HPLC and molecular mass), indicating the action of leukocyte elastase. The stability of the non-fluorinated peptides was dependent upon the amount of plasma proteins present, while the fluorinated peptides did not have any discernible stability pattern.

- the introduction of TfeGly at the P2 position of the FF variant provides resistance against proteolysis, DfeGly destabilizes the peptide
- all fluorinated P2FK variants show a significant decrease in stability
- the introduction of di- or trifluoroethylglycine at different positions in the FA variants imparts the peptides with a plasma half life comparable to that of the control peptide, especially with TfeGly in the P1' position



Diagrammatic representation of the impact of fluorination on the proteolytic stability of model peptides used in this thesis, in all cases as compared to the control peptide. The green “up arrow” indicates greater resistance to proteolysis; the red “down arrow” indicates more rapid hydrolysis, and; the yellow “up and down arrow shows similar proteolytic degradation.

The incubation of the peptides with elastase leads to cleavage products similar to those obtained from the action of proteinase K or the nonimmobilized plasma. TfeGly in two cases shows resistance (P2 and P1’ position), whereas DfeGly only shows resistance at the P2’ position. All FF and FK variants bearing the fluorinated amino acids at the P2’ position show decreased stability.

CONCLUSION AND OUTLOOK

These investigations demonstrate that the use of fluorine as a tool for protein engineering does not automatically improve the stability of peptides towards proteases, as one may expect based on the bioorthogonality of this element. This result is even more important in the field of medicinal chemistry, as this tendency cannot be reconciled with the generally improved metabolic stabilities observed for small drug molecules containing fluorine atoms. Hence, the impact of side chain fluorination on the proteolytic stability of peptides is a complex phenomenon that depends upon the position of the substitution relative to the cleavage site, the type of enzyme, and the chemical nature and fluorination state of the side chain because all of these parameters dictate the precise nature of the noncovalent interactions that the substrate and enzyme will engage in. For this reason, the improved resistance to hydrolysis observed in isolated cases, listed above and shown in diagram above, is a valuable observation that has the potential to make an impact on the design of more bioavailable peptides or peptidomimetics. It should be noted that although the information gained from this thesis is of value for the application of fluorine in the design of proteolytically stable peptide drugs, it is likely that similar systematic investigations will always be required to further elucidate the effect of fluorine, because there is still no general rule for predicting its impact.

8. Outlook

In this thesis, the impact of TfeGly and DfeGly in the context of proteolytic stability of model peptides was envisaged. As described above in the conclusion, these two fluorinated analogues of Abu appear to show different behavior with the herein studied proteases. Interestingly, in some cases, namely TfeGly and DfeGly at the P2' position with pepsin, DfeGly at P2 position with chymotrypsin, TfeGly and DfeGly at the P2 and P2' positions with proteinase K and TfeGly at P2, P1' and DfeGly P2' positions with elastase, fluorination leads to dramatic improvements in resistance to degradation. Future experiments involving this particular set of substrates should include:

- MfeGly, the singly fluorinated member of the series used in these studies
- fluorinated analogues of valine, leucine, isoleucine, phenylalanine
- the introduction of paired/double fluorinated amino acids into these series of peptides; to probe their fluorous effects (fluorine-fluorine interaction)
- even though the FA control peptide seems to be a good substrate (among all the control peptides) for all the studied enzymes, small modification of this model sequence could also be envisaged, thus, the introduction of leucine or arginine or glutamate to occupy the P1 position in a new set of model substrates; this will allow testing the peptide's stability against a number of proteases that accept hydrophobic aliphatic or charged residues at their S1 subsite; pronase (EC3.4.24.4), subtilisin Carlsberg (EC 3.4.21.62), trypsin (EC 3.4.21.4) and thermolysin (EC 3.4.24.27)
- as all peptides were degraded by the proteases of the blood plasma due to the presence of the lysine, it could be helpful to design further model peptides with the exclusion of charged amino acids and reduction in sequence length to achieve proteolytic stability towards human blood plasma

Although these model substrates have enabled us to systematically investigate the impact of fluorination on protease stability, future directions should focus on more biologically relevant peptides, such as HIV-1 peptide-based entry inhibitors. In our lab, newly generated shorter CHR-peptide analogues which contain the highly conserved Trp-Trp-Ile motif show affinity for the T21 (NHR) peptide, and may therefore efficiently compete with the native CHR-domain to prevent bundle formation. Within these CHR-peptide analogues, the systematic replacement of aliphatic residues critical for the six helix bundle formation of the gp41 with

their fluorinated counterparts is expected to yield new CHR-peptide analogues that efficiently bind NHR peptides, and these may also be expected to display improved protease stability.

In order to characterize the effectiveness of such fluorinated HIV-1 entry inhibitors, many diverse analytical methods will be required. Among these, SPR has proven highly useful, but there are aspects of this approach that remain problematic. Typically, monomeric N36 peptides are immobilized on the gold surface, a regime which may not be optimal considering that three such monomers must complex with three CHR peptides to form a stable six-helix bundle. The application of multivalency is an outstanding procedure since multivalent interactions play a vital role in many biological recognition events and are also thought to provide more effective binding. To demonstrate the effect of multivalency, we propose the immobilization of trimeric N36 via a trivalent ethylene glycol linker on the SPR gold surface (see Figure 8.1).

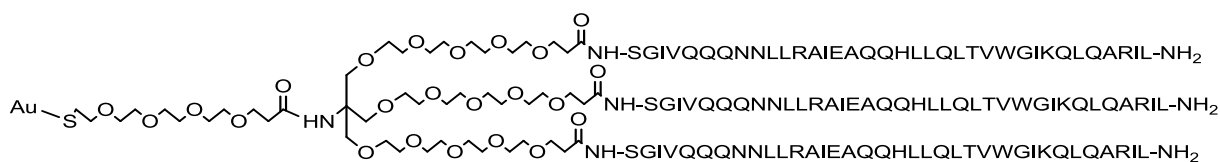


Figure 8.1 Propose trimeric linker of N36 attached to the gold plate through a trivalent ethylene glycol linker

The systematic synthesis of this linker was envisaged and the first few steps were successfully carried out. The products were obtained in good yields and the continuation of this synthetic route, aiming at the full trimeric linker, could be carried out using the following outlined approaches (Figure 8.2).

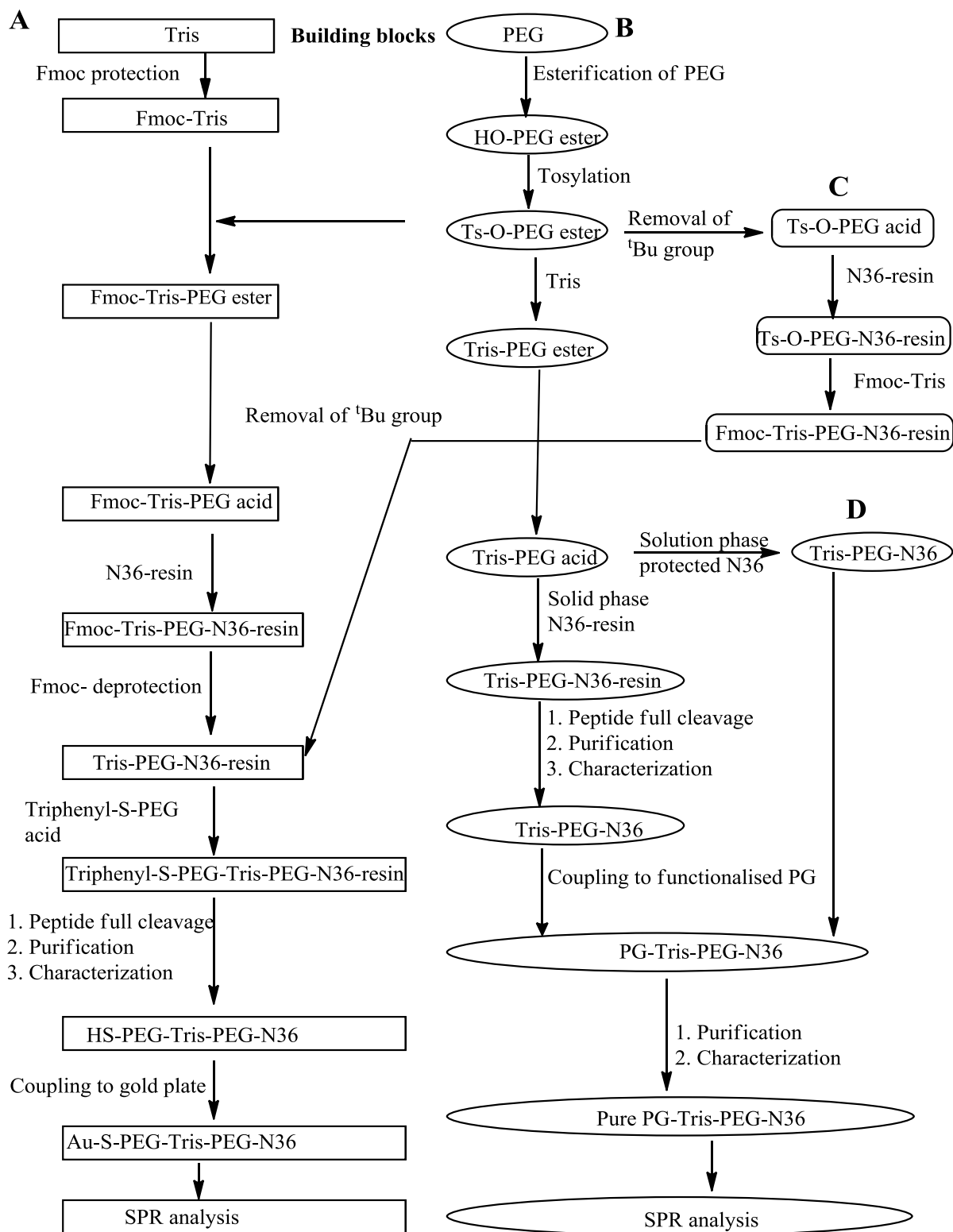


Figure 8.2 Flow chart summarizing the possible routes to the synthesis of the trimeric linker.

Route D seems feasible but problems with the purification of side chain protected peptides are to be encountered. Solid phase-peptide synthesis has always been a good strategy to improve peptide synthesis, therefore the approaches A, B and C look more promising.

9. Experimental part

9.1 General methods

All commercially obtained solvents and reagents were of synthetic grade and were used as supplied. DMF, piperidine (99%, extra pure) and DIPEA (VWR or Acros Organics) for peptide synthesis were of pure analytical grade. Water used for High Performance Liquid Chromatography (HPLC) and to prepare buffers was purified on a Millipore device. Acetonitrile (HPLC grade) used for analytical and preparative HPLC, was purchased from VWR or Acros Organics. Trifluoroacetic acid (TFA) for HPLC (Uvasol® grade) and DBU (synthesis grade) were obtained from Merck.

Resins for peptide synthesis were purchased from NovaBiochem. Fully protected amino acids and coupling reagents were obtained from Iris Biotech, NovaBiochem, Fa. Gehardt, Sigma Aldrich, Opregen, or VWR and applied without further purification.

Solvents used for synthesis of the fluorinated amino acids were dried with the solvent purification system MB-SPS 800 from M. Braun, or freshly distilled in accordance with standard laboratory methods. Peptide coupling reagents were obtained from Acros (DIPEA), NovaBioChem / MultiSynTech (HOBt, HBTU, TBTU, TCTU), Sigma (DIC), and Perspective Biosystems (HATU, HOAt).

Disodium hydrogen phosphate and sodium dihydrogen phosphate were purchased from Merck (Darmstadt, Deutschland). Tris(hydroxymethyl)aminomethane was purchased from Acros Organics (Geel, Belgium).

The substrate N-Benzoyl-L-tyrosine ethyl ester and the enzymes α -chymotrypsin from bovin pancreas, pepsin, proteinase K, and elastase were purchased from Sigma-Aldrich Chemie GmbH Steinheim, Germany. Human blood plasma was donated by Prof. Dr. Hartmut Schlüter, Universitätsklinikum Hamburg-Eppendorf. Cyanogen bromide-activated sepharose 6 MB beads for affinity coupling were purchased from GE Healthcare.

Room temperature (RT) indicates 23-25°C.

^1H and ^{19}F NMR spectra were recorded at room temperature using a Bruker AC 250 and JEOL ECX 400. ^1H NMR and ^{13}C NMR: chemical shift (δ) is given relative to TMS and referenced to the solvent signal. ^{19}F NMR: chemical shift (δ) is given relative to CFCl_3 (external reference). Data are reported in the following order: a) multiplicity (s = singlet, d = doublet, t = triplet, q = quartet, m = multiplet, br = broad), b) coupling constant, c) number of nuclei, and d) assignment. Coupling constants (J) are reported in Hertz (Hz).

9.2 Synthesis of fluorinated amino acids

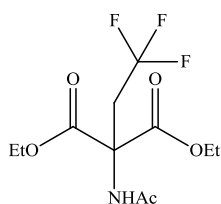
9.2.1 Synthesis of (S)-2-amino-4,4,4-trifluoroethylglycine (TfeGly)

9.2.1.1 Synthesis of diethyl 2-acetamido-2-(2,2,2-trifluoroethyl) malonate (**3a**)

This addition step was accomplished by following the reaction procedure described by Tsushima *et al.*^[310] Malonic ester (1 eq., 8.7 g, 40.05 mmol) and potassium tert-butoxide (1.0 eq., 4.5 g, 40.10 mmol) were dissolved in 60 mL anhydrous THF, heated to 60 °C and left to reflux for 2 h. The mixture was cooled to room temperature and trifluoromethyl 2,2,2-trifluoroethanesulfonate (1.1 eq., 6.5 mL, 44.0 mmol) was added by cannula. This mixture was refluxed for 2 days.

The reaction was cooled to room temperature and the solvent was removed in vacuo. The reaction was quenched with 1M HCl (50 mL) and extracted with ethyl acetate (4 x 50 mL). The combined organic phases were washed 2 times with 20 mL water, dried over magnesium sulfate, and condensed in vacuo. The crude product was purified by column chromatography on silica gel using a mixture of hexane and ethyl acetate (3:1) as eluent. The pure product (white needle-like crystals (**3a**)) was obtained from the recrystallization of the yellow solid with diethyl ether and hexane. **Yield:** 4.5 g (19.67 mmol, 38%).

The obtained spectra agree with the literature.

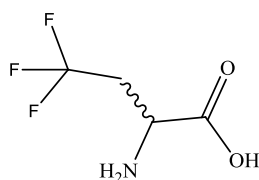


¹H NMR (400 MHz, 298 K, CDCl₃): δ [ppm] = 6.91 (s, 1H, NH), 4.28 (q, *J*_{HH} = 7.2 Hz, 4H, 2 x CH₂), 3.35 (q, *J*_{HH} = 10.5 Hz, 2H, CH₂CF₃), 2.04 (s, 3H, COCH₃), 1.27 (t, *J*_{HH} = 7.1 Hz, 6H, 2 x CH₃).

¹⁹F NMR (376 MHz, 298 K, CDCl₃): δ [ppm] = -62.00 (t, 1*J*_{HF} = 5.3 Hz, 3F, CF₃).

9.2.1.2 Synthesis of 2-amino-4,4,4-trifluoroethylglycine (**3b**)

The white crystals of **3a** (4.5 g, 15.05 mmol) were dissolved in concentrated HCl (15 mL) and refluxed overnight. The reaction mixture was concentrated in vacuo and the brown residue lyophilized to yield 3.75 g of the crude product **3b**. The obtained spectra agree with the literature.

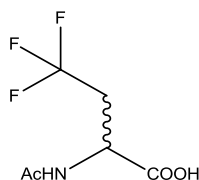


$^1\text{H NMR}$ (400 MHz, 298 K, D_2O): δ [ppm] = 4.28 (dd, $J_{\text{HH}} = 8.1, 4.0$ Hz, 1H, CH), 2.89-3.13 (m, 2H, CH_2).

$^{19}\text{F NMR}$ (376 MHz, 298 K, D_2O): δ [ppm] = -62.06 (t, $1J_{\text{HF}} = 10.2$ Hz, 3F, CF_3).

9.2.1.3 Synthesis of 2-acetamido-4,4,4-trifluoroethylglycine (3c)

For the separation of the racemic amino acids **3b**, the method described by Chiu *et al.* was used.^[311] In this method, **3b** (1.0 eq., 3.75 g, 23.89 mmol) was dissolved in water (50 mL Millipore) and the pH adjusted to 9 with 2 M NaOH. The reaction mixture was cooled to 0 °C in an ice bath. Acetic anhydride (1.0 eq., 2.5 mL, 26.19 mmol) was added dropwise, and the pH was adjusted to 8-9 using 2 M NaOH, monitored by a WTW pH 526 pH-meter and an InLab® microelectrode (Mettler Toledo). The reaction mixture was stirred for 30 min at 0 °C, warmed to room temperature, and stirred for another 2 h. The reaction was acidified with conc. HCl to pH 2 and extracted 5 times with ethyl acetate (50 mL). The combined organic layers were dried over sodium sulfate and the solvent removed. The crude product **3c** was obtained as a white solid (2.56 g). The obtained spectra agree with the literature.^[311]



$^1\text{H NMR}$ (400 MHz, 298 K, D_2O): δ [ppm] = 4.70 (dd, $J_{\text{HH}} = 9.5, 3.8$ Hz, 1H, CH), 2.69-2.92 (m, 2H, CH_2), 2.01 (s, 3H, OCH_3).

$^{19}\text{F NMR}$ (376 MHz, 298 K, D_2O): δ [ppm] = -64.30 (t, $1J_{\text{HF}} = 10.2$ Hz, 3F, CF_3).

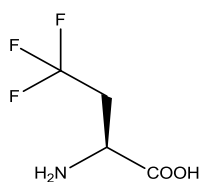
9.2.1.4 Synthesis of (S)-2-amino-4,4,4-trifluoroethylglycine (3d)

The N-acetylated amino acid **3c** (1.0 eq., 2.5 g, 12.86 mmol) was dissolved in water (Millipore) to give a concentration of 50 mM. The pH was adjusted to 11 with 1 N NaOH and readjusted to 7 with 10% AcOH to produce a buffer system. Acylase I (0.10 g, grade II, 553 units/mg) was dissolved in 5 mL of water and added to the amino acid solution, after which the pH was checked again and readjusted to 7 using either 0.1% AcOH or 0.01 N NaOH, as necessary. The mixture was gently stirred at 36 °C for a few hours and then at room temperature overnight.

EXPERIMENTAL PART

To quench the reaction, the pH was lowered to 4 with 10% AcOH. The mixture was then loaded onto an ion-exchange resin (Dowex 50W X8; 100-200 mesh).

The resin was washed with Millipore water until the pH of the eluting solution was neutral (the acylated D-enantiomer is washed away). Then the free (deacylated) L-amino acid was eluted from the resin with 1 N NH₃. All fractions containing amino acid (positive Ninhydrin reaction) were combined, and the product (**3d**) lyophilized to give a white fluffy solid. **Yield:** 0.25 g (1.59 mmol, ~12%).



¹H NMR (400 MHz, 298 K, D₂O): δ [ppm] = 3.57 (dd, *J*_{HH} = 8.1, 4.4 Hz, 1H, CH), 2.42-2.66 (m, 2H, CH₂).

¹⁹F NMR (376 MHz, 298 K, D₂O): δ [ppm] = -63.33 (t, *J*_{HF} = 10.2 Hz, 3F, CF₃).

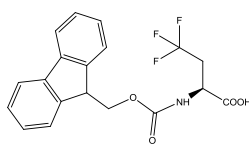
9.2.1.5 Synthesis of (S)-2-(((9H-fluoren-9-yl)methoxy)carbonylamino)-4,4,4-trifluoroethylglycine (**3e**)

Similar to the method of Chiu *et al.*^[311] the L-amino acid **3d** (1.0 eq., 0.25 g, 1.59 mmol) was dissolved in 10% Na₂CO₃ (3 mL) and cooled to 0 °C with an ice bath. Dioxane (1mL) was added dropwise via cannula to the suspension and stirred for 15 min at 0 °C. Fmoc succinimide (1.1 eq., 0.59 g, 1.75 mmol), dissolved in peroxide-free dioxane, was added dropwise over 15 min. The mixture was stirred for 3 h at 0 °C and at room temperature overnight.

The reaction was quenched with 50 mL water and extracted once with 50 mL diethyl ether. The aqueous solution was cooled in an ice bath and carefully acidified with conc. HCl to pH 2. The suspension was allowed to precipitate and then extracted with DCM (4 x 50 mL). The combined organic phases were washed with water, dried over sodium sulfate and concentrated *in vacuo*.

The crude product was purified using preparative HPLC (Knauer; see section 9.3.6) with a Phenomenex ® Luna C8 10 μm (250 mm x 21.2 mm) reversed-phase column. HPLC runs were performed with a flow rate of 20 mL/min applying a linear eluent gradient of H₂O (solvent A) and ACN (solvent B) containing 0.1% TFA (30% to 100% solvent B over 30 min), with UV-detection ($\lambda_{\text{abs}} = 280$ nm). The fractions containing the pure Fmoc-protected amino acid were combined and ACN was removed *in vacuo*.

The pure product (**3e**) was obtained as a white solid after lyophilization and identified by ESI-ToF MS. **Yield:** 0.43 g (1.13 mmol, 71%).



¹H NMR (400 MHz, 298 K, CDCl₃): δ [ppm] = 7.77 (d, *J*_{HH} = 7.5 Hz, 2H, Ar (Fmoc)), 7.58 (d, *J*_{HH} = 7.4 Hz, 2H, Ar (Fmoc)), 7.42 (t, *J*_{HH} = 7.4 Hz, 2H, Ar (Fmoc)), 7.38 (t, *J*_{HH} = 7.4, 1.0 Hz, 2H, Ar (Fmoc)), 5.53 (d, *J*_{HH} = 9.4 Hz, 1H, NH), 4.64 (dd, *J*_{HH} = 8.1, 4.4 Hz, 1H, CH), 4.42-4.25 (m, 2H, COOCH₂ (Fmoc)), 4.23 (t, *J*_{HH} = 6.1 Hz, 1H, COOCH₂CH (Fmoc)), 2.85-2.72 (m, 2H, CH₂CF₃).

¹³C NMR (126 MHz, CDCl₃) δ [ppm] = 168.75 (s, COOH), 151.67 (s, COOCH₂), 142.54 (s, Ar-C), 141.42 (s, Ar-C), 128.33 (s, Ar-C), 127.91 (q, *1J*_{CF} = 276.2 Hz, CF₃), 127.56 (s, Ar-C), 125.33 (s, Ar-C), 120.29 (s, Ar-C), 73.06 (s, COOCH₂CH), 57.37 (s, HO₂CCH), 46.46 (s, CHCOOH), 25.56 (q, *2J*_{CF} = 28.2 Hz, CH₂CF₃).

¹⁹F NMR (376 MHz, 298 K, CDCl₃): δ [ppm] = -62.92 (t, *1J*_{HF} = 10.2 Hz, 3 F, CF₃).

HRMS (ESI): found *m/z*: 378.1091, calculated [C₁₉H₁₅F₃NO₄]=378.0959

9.2.2 Synthesis of (*S*)-2-amino-4,4-difluoroethylglycine (DfeGly)

The fluorinated amino acid (*S*)-2-amino-4,4-difluorobutanoic acid (**DfeGly**, (**2**)) was synthesized according to Winkler *et al.*^[312] and kindly provided as the Fmoc-protected derivative by Dr. Cosimo D. Cadicamo.

9.3 Solid-Phase Peptide Synthesis (SPPS)

All peptides were synthesized from the C-terminal to the N-terminal end on a solid support, applying an Fmoc/*tert*-butyl protecting group strategy. The general principle of SPPS is repeated cycles of amino acid coupling and deprotection. The peptide chain is built on a small solid yet porous polymer carrier (a resin in bead form). The coupling of the first amino acid to an appropriate linker is necessary to guarantee specific cleavage of the peptide from the resin after synthesis is complete. In Fmoc SPPS it is important to block the functional groups of the amino acid side chains to prevent side reactions during coupling. Conventionally, most amino acids have a *t*-Bu side chain protecting group as this is base stable and TFA labile. The cycle of coupling and deprotection then continues until the designated sequence is

accomplished. Cleavage of the side chain protecting groups and peptide can be accomplished simultaneously by using strongly acidic conditions such as TFA.^[313]

The following protected derivatives of standard canonical amino acids were used for the synthesis of all peptides: Fmoc-Lys(Boc)-OH (lysine), Fmoc-L-Ala-OH (alanine) and Fmoc-Phe-OH (phenylalanine). The peptides FA, FK, and FF, and their fluorinated variants, were synthesized by standard Fmoc chemistry on preloaded Fmoc-Lys(Boc)-Wang-resin (0.7 mmol/g, 0.05 mmol scale) using either an automated Multi-Syntech Syro XP peptide synthesizer (MultiSynTech GmbH, Witten, Germany) or manual couplings in 10 mL polypropylene reactors.

9.3.1 Automated peptide synthesis

The peptides described in this work were to some extent synthesized in an automated fashion. Prior to the first coupling cycle, swelling of the resins was performed in 2.5 mL DMF for 15 minutes. Each reaction cycle begins with Fmoc-deprotection by treatment of the resin with 2% piperidine and 2% DBU (4x5 min) in DMF. The coupling reaction was performed in 2.4 mL DMF, either with or without the addition of NaClO₄ (0.8 mM), containing 4 equivalents of the α -amino-Fmoc-protected and fully side chain-protected amino acid. The chaotropic salt NaClO₄ was added to the dissolved amino acid to avoid on-resin aggregation during peptide synthesis. The C-terminal activation was achieved through 4 eq. TBTU / HOBt and 8 eq. DIPEA and coupling proceeded for 30 min with agitation at defined intervals. After washing the resin with 2.5 mL DMF for 1 min, the amino acid coupling reaction was repeated once. Prior to Fmoc-deprotection of the next coupling cycle, the resin was washed 3 times with 2.5 mL DMF for 1 min. The peptide chain elongation process ended with an Fmoc-deprotection step. Table 9.1 summarizes the standard protocol used with the automated Multi-Syntech Syro XP peptide synthesizer.

EXPERIMENTAL PART

Table 9.1 Sample of coupling protocol in Fmoc SPPS

| Process | | Reagent | Time (min) |
|---------------------------------------|-------------------|---|------------|
| Beginning of double coupling | Swelling | 2.5 mL DMF | 2 x 15 |
| | Fmoc-deprotection | 2% piperidine, 2% DBU in DMF | 4 x 5 |
| | Washing | 2.5 mL DMF | 6 x 1 |
| Double coupling of amino acids | Coupling | 4eq. Fmoc-amino acid-OH 4eq. HOBt in 0.8 mL DMF 4eq. TBTU in 1.2 mL DMF 8eq. DIPEA in 0.4 mL NMP | 30 |
| | Washing | 2.5 mL DMF | 1 x 1 |
| | Coupling | 4eq. Fmoc-amino acid-OH 4eq. HOBt in 0.8 mL DMF 4eq. TBTU in 1.2 mL DMF 8eq. DIPEA in 0.4 mL NMP | 30 |
| | Washing | 2.5 mL DMF | 3 x 1 |
| | Fmoc-deprotection | 2% piperidine, 2% DBU in DMF | 4 x 5 |
| | Washing | 2.5 mL DMF | 6 x 1 |

9.3.2 Manual peptide synthesis

In other cases, the peptides described in this work were manually synthesized using a preloaded Fmoc-Lys-(Boc)-Wang resin (0.7 mmol/g, 0.05 mmol scale) via standard Fmoc strategy. The *N*-Fmoc-protected and fully side chain-protected natural amino acids (4eq) were manually coupled 2 x 2 h using HOBt (4eq) and DIC (4eq) activation, whereas the Fmoc-protected fluorinated amino acids were coupled using 2 eq. of the amino acid; two couplings were carried out, first with HOBt / DIC for 4 h and second with HOAt / DIC overnight. The use of HOAt has been shown to enhance coupling yields, shorten coupling times, and reduce racemization. The resin was then washed with DMF (6 x 3ml). Fmoc deprotection was carried out by treatment of the resin with 2% piperidine and 2% DBU in DMF. All peptides were finally *N*-terminally labeled with para-aminobenzoic acid (Abz) to enable photometric detection.

9.3.3 Capping of free α -amino groups

The blocking of the nonreacted free amino groups with acetic anhydride was carried out with a freshly prepared solution of Ac₂O (10% (v/v)) and DIPEA (10% (v/v)) in DMF (3 mL). The reaction was shaken for 3 x 10 min (fresh each time), after which the resin was washed with 5 mL DMF (3 x 1 min) and 5 mL DCM (3 x 1 min).

9.3.4 Cleavage of peptide from resin

All the peptides were cleaved from the resin with a 2 mL solution (cocktail) of triisopropylsilane (TIS):TFA:H₂O (5%:95%:10 μ L). The resin was shaken for 3 h and filtered into a 100 mL flask. The resin was then washed with 1 mL TFA and DCM (3 x 1 mL). The combined mixture was concentrated under a gentle stream of argon and the peptides were precipitated by the addition of 50 mL chilled diethyl ether. The mixture was centrifuged down at 4,400 rpm for 5 minutes and the supernatant removed. The precipitated crude peptide was washed several times with 15 mL ice-cold diethyl ether. The dried crude peptide was then purified by means of preparative RP-HPLC.

9.3.5 Analytical HPLC

Determination of the purity of the synthesized peptides was carried out by reversed-phase analytical HPLC. This was performed on either of two systems: **a)** a computer-controlled high-pressure-gradient Elite LaChrom-HPLC-system (VWR-Hitachi) with two pumps L-2130, a diode array detector L-2455, a fluorescence detector L-2485, an autosampler L-2200 with 100 μ L sample loop, and a solvent degasser L-7612; **b)** a computer-controlled LaChrom-HPLC (Merck-Hitachi), consisting of L-7000 interface, two HPLC L-7100 pumps, an L-7450 diode array continuous flow detector, an L-7200 autosampler with 100 μ L sample loop, a solvent degasser L-7612, a high-pressure gradient mixer, a Rheodyne injection valve 7725i, and a 20 μ L sample loop.

The following reversed-phase columns were used: Phenomenex® Luna C8 (2) 10 micron (250 mm x 4.6 mm), Capcell C18 5 micron (250 mm x 4.6 mm), Phenomenex® Luna C8 (2) 5 micron (250 mm x 4.6 mm) and Merck's Chromolith® C8 endcapped 2 micron (100 mm x 4.6 mm). HPLC runs were performed with a flow rate between 1-5 mL/min applying linear gradients with solutions A and B, where A is 100% H₂O with 0.1% TFA (v/v) and B is 100% ACN with 0.1% TFA (v/v). The applied gradient for the analysis of the peptides was as follows: 5% to 45% B, over 30 min at a flow rate of 1 mL/min, or over 12 min at a flow rate of 3-5 mL/min. UV and fluorescence detection was at $\lambda_{\text{abs}} = 320$ nm and $\lambda_{\text{abs}} = 420$ nm, respectively, for all Abz-labeled peptides. Data were quantified and characterized by means of the chromatographic software (EZChrom Elite Version 3.1.7).

9.3.6 Preparative HPLC

The crude peptides were purified by reverse-phase HPLC on a Smartline system (Knauer GmbH, D-14163 Berlin) equipped with a Smartline manager 5000 interface with solvent degasser, two Smartline pumps 1000, a variable UV detector 2500, injection valve, high-pressure gradient mixer and a 5 mL sample loop. Separation was carried out on a Phenomenex[®] Luna C8 (2) column (10 µm particle size, 300 Å pore size and 250 mm x 21.2 mm inner diameter). The dry peptides were dissolved in 5-10 mL of a 1:1 mixture of solvents A and B, where solvent A is 100% water with 0.1% TFA (v/v) and solvent B is 100% acetonitrile with 0.1% TFA (v/v) and filtered prior to injection into the HPLC. A maximum of 20 mg crude peptide was purified per each run with a linear gradient of 95% A to 50% B over 30 minutes at a flow rate of 20 mL/min. UV-detection was at $\lambda_{\text{abs}} = 320 \text{ nm}$.

Pooled pure fractions containing the peptide were collected and ACN and TFA were removed on a rotary evaporator, affording a suspension of the solid in water. This solution was finally lyophilized (freeze dried) to yield the pure peptides.

The purity of the peptides was determined through analytical HPLC, and the quality by means of mass spectrometry. All peptides were > 96% pure.

9.3.7 Mass spectrometry analysis

Quality Control: Characterization of the synthesized peptides was conducted by means of an Agilent 6210 ESI-ToF LC-MS spectrometer (Agilent Technologies Inc., Santa Clara, CA, USA) with manual sample injection by syringe pump (Harvard Apparatus 11 Plus) at a flow rate of 0.2 mL/min. The molecular masses and sequences of the synthesized peptides are summarized in Table 9.2.

Proteolytic Assay: Characterization of the products of proteolytic cleavage were carried out on the Agilent 6210 ESI-ToF LC-MS spectrometer consisting of an Agilent 1100 HPLC system with an additional DAD (diode array detector) and an ESI-MSD TOF by Agilent Technologies. LC-MS was carried out using a linear gradient of 5% B to 70% B over 30 minutes at a flow rate of 0.5 mL/min. Mass spectra were acquired using electrospray ionization in positive ion mode. Data were analyzed with Agilent MassHunter and quantified by Agilent qualitative analysis software.

EXPERIMENTAL PART

Table 9.2 Names, molecular masses and sequences of the synthesized peptides

| Name | Sequence | Molecular mass | Molecular mass |
|---------------------------------|--------------------|----------------|----------------|
| | | (g/mol) Calc. | (g/mol) Obs. |
| | | $[M+1]^{1+}$ | $[M+1]^{1+}$ |
| P2-TfeGlyFA^{IX} | Abz-KATfeGlyFAAAAK | 1035.4622 | 1035.5259 |
| P2-DfeGlyFA^{IX} | Abz-KADfeGlyFAAAAK | 1017.4622 | 1017.5252 |
| P2-AbuFA | Abz-KA(Abu)FAAAAK | 981.4622 | 981.5416 |
| P1'-TfeGlyFA | Abz-KAAFTfeGlyAAAK | 1035.4622 | 1035.5168 |
| P1'-DfeGlyFA | Abz-KAAFDfeGlyAAAK | 1017.4622 | 1017.5296 |
| P1'-AbuFA | Abz-KAAF(Abu)AAAK | 981.4622 | 981.5487 |
| P2'-TfeGlyFA | Abz-KAAFATfeGlyAAK | 1035.4622 | 1035.5200 |
| P2'-DfeGlyFA | Abz-KAAFADfeGlyAAK | 1017.4622 | 1017.5487 |
| P2'-AbuFA | Abz-KAFA(Abu)AAK | 981.4622 | 981.5546 |
| FK | Abz-KAAFKAAAK | 1024.5572 | 1024.5996 |
| P2-TfeGlyFK^{IX} | Abz-KATfeGlyFKAAAK | 1092.5201 | 1092.5875 |
| P2-DfeGlyFK^{IX} | Abz-KADfeGlyFKAAAK | 1074.5201 | 1074.5957 |
| P2'-TfeGlyFK | Abz-KAAFKTfeGlyAAK | 1092.5201 | 1092.5875 |
| P2'-DfeGlyFK | Abz-KAAFKDfeGlyAAK | 1074.5201 | 1074.5957 |
| P2'-AbuFK | Abz-KAAFK(Abu)AAK | 1038.5201 | 1038.6101 |
| FF | Abz-KAAFFAAAK | 1043.5306 | 1043.5617 |
| P2-TfeGlyFF^{IX} | Abz-KATfeGlyFFAAAK | 1111.4935 | 1111.5465 |
| P2-DfeGlyFF^{IX} | Abz-KADfeGlyFFAAAK | 1093.4935 | 1093.5623 |
| P2'-TfeGlyFF | Abz-KAAFFTfeGlyAAK | 1111.4935 | 1111.5634 |
| P2'-DfeGlyFF | Abz-KAAFFDfeGlyAAK | 1093.4935 | 1093.5705 |
| P2'-AbuFF | Abz-KAAFF(Abu)AAK | 1057.4935 | 1057.5861 |
| | Abz-KAAF | 555. | 555.2908 |

^{IX} These peptides were synthesized by Susanne Huhmann during her bachelor thesis under my supervision, 2011

9.4 Protease stability of peptides

9.4.1 Isolated enzyme assay

The proteolytic stability of peptides toward α -chymotrypsin from bovine pancreas, (80.0 U/MG), pepsin from porcine gastric mucosa (≥ 250 U/MG), proteinase K from *Tritirachium album* (≥ 30 U/MG) and elastase from porcine pancreas (≥ 4 U/MG) were determined by an analytical RP-HPLC assay.

Stock solutions (1 mg/mL) for each enzyme were prepared in the appropriate buffer, followed by subsequent dilution to the needed enzyme concentration. The concentration of enzyme was optimized so that the hydrolysis of the control peptide was about 40% at the end of 120 min as shown in Table 9.3. Since peptide/protein based drugs have been shown to exhibit less than 1% oral bioavailability; improving this pharmacokinetic parameter to at least 30-50% would be of great significance.^[314,315]

Table 9.3 Conditions applied to various isolated enzymes

| Enzyme | Buffers used | Enzyme Concentration (mg/mL) | Final Concentration in reaction mixture (mg/mL) | Enzyme in mixture | pH | Temp. °C | Quenching solution |
|--------------|---|------------------------------|---|-------------------|--------------|----------|--------------------------|
| Chymotrypsin | 10 mM Phosphate | 0.1 | 0.01 | | 7.4 | 30 | 100% ACN + 0.1% TFA |
| Pepsin | 10 mM Acetate | 0.29 and 0.5 | 0.029 and 0.05 | | 4.0 | 30 | 2 % NH ₃ (aq) |
| Elastase | 100 mM Tris-HCl | 0.01 | 0.001 | | 8.0 and 8.43 | 37 | 100% ACN + 0.1% TFA |
| Proteinase K | 50 mM Tris-Cl/ 10 mM CaCl ₂ | 0.04 | 0.004 | | 7.5 | 37 | 100% ACN + 0.1% TFA |

Stock solutions of the peptides (0.002 mmol) were prepared by dissolving the required amount of peptide in DMSO (100 μ L). The peptides were incubated with each enzyme in a test set up of 5 μ L peptide (20 μ mol/ml DMSO), 15 μ L DMSO, 25 μ L of the different buffers and 5 μ L enzyme (X mg/mL buffer) (50 μ L total volume) using variable conditions as shown in Table 9.3 over a period of 2 h. Aliquots of 5 μ L were removed at different reaction times (0, 5, 15, 30, 60, 90, 120 min) and quenched with 95 μ L of the appropriate solution.

EXPERIMENTAL PART

Then 5 μL aliquots of the terminated digestion mixture were mixed with 95 μL of a 1:1 mixture of HPLC solvents A and B containing 0.1% TFA v/v, or 100% solvent A in the case of pepsin. Finally, 10 μL of this diluted sample was injected into the HPLC column.

A Capcell C18 5 micron (250 mm x 4.6 mm) and Merck's Chromolith[®] C8 endcapped 2 micron (100 mm x 4.6 mm) analytical columns were used for the separation and quantification of digested products.

A linear gradient from 5-45% of eluent B was applied over 12 minutes with a 3 mL/min flow rate. The amount of products formed and educt remaining at different times were recorded using UV and fluorescence detection at an excitation wavelength (λ_{EX}) of 320 nm and an emission wavelength (λ_{EM}) of 420 nm.

In all runs, the percentage of substrates remaining at the individual time points relative to the initial sample (0 minute) and the N-terminal fragments were integrated and used to determine the speed of the reaction. Each fragment cleaved from the full length peptide was identified by ESI/TOF and LC/MS so that the cleavage patterns could be established and compared.

A diagrammatic representation of this procedure is shown in Figure 9.1.

All experiments were done at least in triplicate. The same procedure was used for all isolated enzymes (Table 9.3).

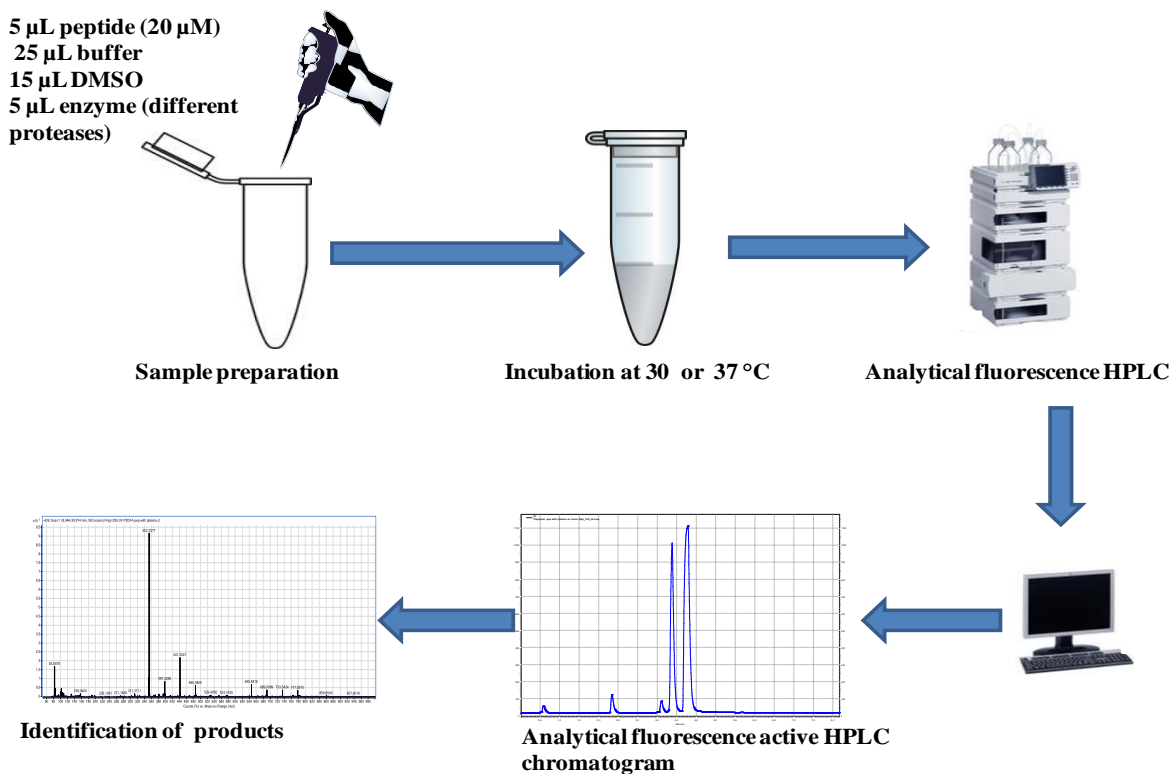


Figure 9.1 Summary of the stability measurement

9.4.1 Determination of Michaelis Menten kinetics using HPLC

The kinetic studies of the control peptide FA and the fluorinated peptide P2-TfeGlyFA (the most hydrolyzed by chymotrypsin in the isolated enzyme study) were conducted by subjecting different concentrations (0.2 mM to 3 mM) of the peptides to enzymatic degradation within a 5 min time range. Aliquots of 5 μ L were taken after every 30 sec and quenched with 95 μ L 100% ACN containing 0.1% TFA v/v. The amount of products (Abz-KAAF and Abz-KATfeGlyF) formed at different times were measured on analytical RP-HPLC as described in section 9.3.5. To determine the concentration of product formed in each reaction and the kinetic parameters, a standard curve was generated using stock solutions of pure Abz-KAAF and P2-TfeGlyFA peptides in the range of 6 μ M to 3 mM.

9.4.2 Inhibition assay

N-Benzoyl-L-tyrosine ethyl ester (BTEE) stock solution of final concentration 1.07 mM was prepared by dissolving 6.706 mg BTEE in 20 mL of 1:1 MeOH/H₂O. In different sets of experiments (Table 9.4), FA peptide (20 μ mol/mL DMSO) and BTEE (1.07 mM) in 0:08 M Tris containing 0.1 M CaCl₂ or 10 mM phosphate buffers (pH 7.4 - 8) were subjected to enzymatic degradation (enzyme concentration; 0.1 mg/mL). Aliquots of 5 μ L was quenched with 95 μ L ACN containing 0.1% TFA and analyzed by analytical HPLC at 256 nm using a linear CH₃CN/H₂O gradient. The effect of product formation and substrate on hydrolysis was monitored and recorded.

A calibration curve was generated using stock solutions of BTEE in the range of 10.7 μ M to 0.642 mM. The measurement of an increase in absorbance at 260 nm resulting from the hydrolysis of benzoyl-L-tyrosine ethyl ester was recorded through the use of a UV spectrometer (Eppendorf BioPhotometer plus). A graph of absorbance as a function of concentration was then plotted. The calculated slopes ($\Delta A_{260}/\text{min}$) from the initial linear portion of the curve were used to determine the concentration of product formed in each reaction.

Also, to examine the effect of the product (step 5 of Table 9.4), 5 μ L of the FA peptide was incubated at 30 °C with chymotrypsin (0.1 mg/mL) for 40 hours to ensure complete digestion of the peptide. BTEE (100 μ L) was added to this mixture and then monitored by analytical HPLC.

EXPERIMENTAL PART

Further experiments were also conducted to test the effect of DMSO on the hydrolysis reactions. In a 1:1 and 3:1 mixture of BTEE and FA peptide, buffer, and DMSO in a total reaction volume of 50 μL (step 3 and 4 of Table 9.4) were subjected to chymotrypsin hydrolysis.

Table 9.4 Different sets of experiments for inhibition studies

| Assay | Tris/phosphate buffer (μL) | Peptide (μL) | BTEE (μL) | Enzyme (μL) | Extra DMSO (μL) | Total volume (μL) | % DMSO in reaction mixture | % organic solvent |
|----------------------|---|---------------------------|------------------------|--------------------------|------------------------------|--------------------------------|----------------------------|-------------------|
| 1 | 395 | 0 | 100 | 5 | 0 | 500 | 0 | 10 |
| 2 | 30 | 7.5 | 7.5 | 5 | 0 | 50 | 15 | 15 |
| 3 | 17.5 | 7.5 | 7.5 | 5 | 12.5 | 50 | 40 | 47.5 |
| 4 | 15 | 7.5 | 22.5 | 5 | 0 | 50 | 15 | 37.5 |
| 5 product inhibition | 490 | 5 | 100 | 5 | 0 | 600 | 1 | NA |
| 6 | 380 | 15 | 100 | 5 | 0 | 500 | 3 | NA |

9.5 Plasma studies

9.5.1 Plasma preparation

Human blood plasma was kindly provided by Prof. Dr. Hartmut Schlüter and was prepared as follows: peripheral blood (10 mL) from healthy volunteers was obtained by catheterization of the cubital vein and was collected in tubes containing K2-EDTA (7.2 mg). The study was approved by the local ethical committee. The blood sample was centrifuged at 2100 G for 10 minutes at 4 °C for isolation of plasma. After centrifugation, the supernatant (plasma) was collected and the cell containing fraction (mainly red blood cells) was discarded.

9.5.2 Immobilization of plasma proteins onto CNBr-activated Sepharosebeads®

The method of immobilization was performed in a similar manner as reported by Schlüter et al.^[120] and was kindly provided by Maria Trusch of AG Prof. Dr. Hartmut Schlüter, Universitätsklinikum Hamburg-Eppendorf.

9.5.2.1 Preparation of the gel

Accordingly, 25 mg of Cyanogen bromide activated sepharose 6 MB beads (GE Healthcare) were suspended in 500 μL of 1 mM HCl solution in an eppendorf tube.

HCl was used to preserve the active groups on the beads since these active groups hydrolyze at high pH. The beads were allowed to swell for 30 min on an overhead rotating shaker and were washed 3 times each with water (Millipore) and the protein coupling buffer (100 mM NaHCO_3 , 500 mM NaCl, pH 8.3) to equilibrate the Sepharosebeads®.

9.5.2.2 Immobilization of plasma proteins

The plasma proteins were immobilized on the Sepharosebeads® according to the method established by Schlüter *et al* 2007^[120]. In this procedure, 40 μL of the prepared beads was filled into a 0.5 mL low bind eppendorf tube and the coupling buffer was removed. A mixture of 50 μL plasma and 200 μL coupling buffer were mixed with the swollen Sepharosebeads® and incubated on a rotating shaker at room temperature for 2 h. Afterwards, the beads were washed three times each with Millipore water and blocking buffer (100 mM NaHCO_3 , 500 mM NaCl, 1 M Glycine, pH 8.3). The addition of 1 M glycine to the blocking buffer was necessary to avoid background activity in the control. A final volume of 250 μL of blocking buffer was left on the beads and incubated on a shaker at room temperature for 2h, then at 4°C over night to saturate the free binding sites of the Sepharosebeads®. Subsequently the blocking buffer was removed by washing repeatedly with Millipore water. A control for all incubation experiments was carried out with the Sepharosebeads® without immobilized plasma proteins. Different volumes of plasma proteins (5 μL and 10 μL) were immobilized through the same approach and then used in the proteolysis of the peptides.

9.5.2.3 Incubation of the peptides with the immobilized proteins

Before the incubation, the Sepharosebeads® were washed 3 times with the incubating buffer (PBS pH 7.4). The different volumes of immobilized plasma proteins (5 μL , 10 μL , 50 μL) on the Sepharosebeads® were incubated with the different substrates (peptides) in a test set up of 5 μL peptide solution (20 $\mu\text{mol/mL}$ DMSO), 15 μL DMSO, 25 μL and buffer (pH 7.4). Incubation was carried out at 37 °C on a rotating shaker over a period of 2 h. Aliquots of 5 μL were taken at different reaction times (0, 30, 60, 90, and 120) minutes and quenched with

95 μ L of HPLC solvent B (100% ACN + 0.1% TFA v/v). The quenched solution (10 μ L) was mixed with 90 μ L of HPLC solvent A (100% H₂O + 0.1% TFA v/v) and run on an analytical RP-HPLC system equipped with a fluorescence detector. The HPLC samples were then treated in the same procedure as described in section 9.4.1 for the isolated enzymes.

9.5.3 Nonimmobilization of plasma proteins experiments

The hydrolysis of the peptides by the immobilized plasma proteins showed the activity of only one plasma protease (carboxypeptidases N) and therefore, the need for further clarification or the presence of other proteases in the plasma was important. Another set of experiments was conducted without immobilizing the plasma proteins on to the resin. In these experiments, different volumes of plasma (5 μ L, 15 μ L, 50 μ L) were incubated with the peptides in a similar set up at 37°C as described in section 9.5.2.3. The reaction mixture was shaken at 300 rpm in a thermomixer over a period of 2h. Aliquots of 5 μ L from each reaction mixture were removed at different reaction times (0, 5, 10, 15, 20, 30, 45, 60, 75, 90, 105, 120 minutes) and quenched with 100% ACN/0.1% TFA. The quenched samples were centrifuged at 6,000 rpm for 2 minutes and the supernatants were analyzed. All samples were either stored frozen or immediately run on analytical HPLC as described above.

Each fragment cleaved from the full-length peptide was identified by ESI/TOF and LC/MS. All experiments were done at least in triplicate.

9.6 Molecular modeling

The peptide ligands were built in an extended conformation using MOE (Molecular Operating Environment 2011) provided by the Chemical Computing Group (<http://www.chemcomp.com>). The Protein Data Bank (PDB)^[316] entry code 4CHA^[317] was selected as the starting structure for α -chymotrypsin. The protein was prepared for docking with the LigX module (default parameters) as implemented in MOE with a particular emphasis on the enzymatic cavity and the protonation state of the catalytic triad. Docking studies were carried out using the software GOLD 5.1^[226,227] using a 100% search efficiency parameter. The active site was determined by selecting all residues within 10 Å around the hydroxyl group of Ser214. A stepwise increasing number of constraints was set until a conformation in agreement with the literature was obtained. Three constraints were required

to orient the peptides in a conformation in agreement with the literature;^[86,103,228] a distance range from 2 Å to 5 Å between (i) the backbone CO of Ser214 (protein) and backbone NH of Phe at position P1 (ligand), (ii) the backbone NH of Gly193 (protein) and the backbone CO of Phe at position P1 (ligand), (iii) the backbone CO of Phe41 (protein) and the backbone NH of the P2' position (ligand).

The PDB entry 1PSA^[318] was selected as the starting structure for pepsin. The enzyme was prepared for docking with MOE and the water molecule involved in the hydrolysis mechanism but absent from the crystal structure was manually added between the two carboxylic acids Asp32 and Asp215. Docking studies were also carried out using GOLD 5.1 with a 100% search efficiency parameter and activated toggle + spin options for the water molecule. The active site was determined by selecting all residues within 6 Å around the ligand, pepstatin A, co-crystallized within the pepsin binding cleft. With pepsin, only one constraint was sufficient to generate a peptide orientation in agreement with the literature: a distance range from 1 Å to 3 Å between the backbone CO of Gly34 (protein) and the backbone NH in position P2 (ligand). After docking, all valid poses were minimized using the MMFF94 force field as implemented in LigandScout version 3.1.^[319-321] LigandScout was also used for visualization and analysis of all docking results.

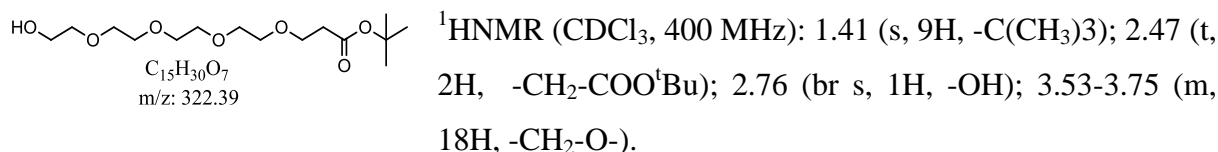
9.7 Synthesis of trivalent linker

9.7.1 Synthesis of tert-butyl 1-hydroxy-3,6,9,12-tetraoxapentadecan-15-oate {1}^[303-309]

To 100 mL anhydrous THF, 0.04 g of sodium metal (1.7 mmol) and 25 mL (36.12 g, 186 mmol) of tetraethylene glycol were added under argon condition with stirring. After complete dissolution of the Na, 9.6 mL (8.476 g, 66 mmol) tert butyl acrylate was added to the mixture and the reaction was stirred overnight at room temperature. The mixture was then quenched with 1.6 mL 1 M aqueous HCl.

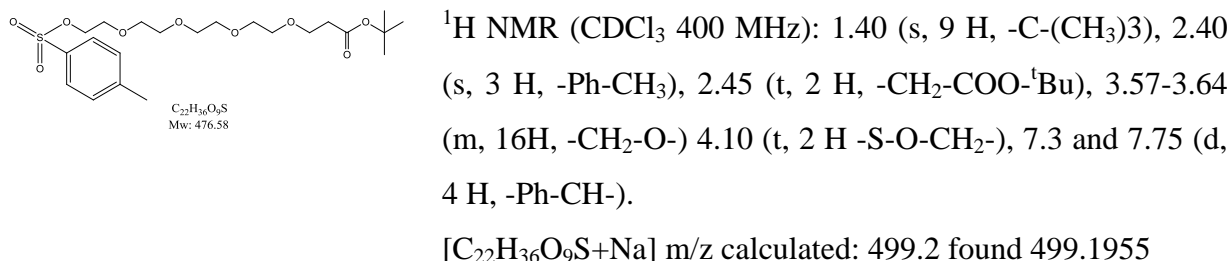
EXPERIMENTAL PART

The solvent was removed by evaporation and the residue was suspended in 70 mL saturated NaCl solution and extracted three times with 50 mL portions of ethyl acetate. The combined organic phases were washed with water and dried over Na₂SO₄. The solvent was removed and the resulting oil was dried under reduced pressure to give the crude product. Purification by column chromatography (2% methanol: 98% DCM) yielded a pure product of 13.9 g (68%) in different fractions.



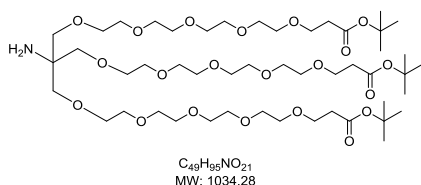
9.7.2 Synthesis of *tert*-butyl 1-(tosyloxy)-3,6,9,12-tetraoxapentadecan-15-oate **{2}**^[303-309]

p-Toluenesulfonyl chloride (4.56 g, 24 mmol) in 80 mL of methylene chloride (DCM) was added dropwise to a mixture of (4.51 g, 14 mmol) of *tert*-butyl tetraethylene glycol ester (*tert*-butyl-hydroxy-3,6,9,12-tetraoxapenta decan-15-oate) **{1}** and 3.5 mL (2.35 g, 23.2 mmol) of triethylamine (Et₃N) was added over 1 hour at 0 °C. The mixture was then stirred overnight at room temperature. The white triethylamine hydrochloride precipitate was filtered off and washed with cold 50 mL DCM. The DCM was removed under reduced pressure to leave a yellow-brown oil, which was purified by flash chromatography on silica using 95% hexane and 5% ethyl acetate to remove unreacted tosyl chloride, followed by 100% ethyl acetate to elute the product. The solvents were evaporated to give 4.54 g (68%) of viscous colorless oil as the pure product **{2}**.



9.7.3 Coupling of *tert*-butyl 1-(tosyloxy)-3,6,9,12-tetraoxapentadecan-15-oate to Tris

Tris(hydroxymethyl)aminomethane (Tris), 58 mg (0.478 mmol, 1 eq) was dissolved in 3 mL anhydrous THF under argon condition. 60.45 mg (2.519 mmol, 5 eq) of 60% NaH was dissolved in 3 mL anhydrous THF under argon condition and added in small portions to the Tris solution at 0 °C under argon for 30 minutes. The reaction was then allowed to reflux for one hour and then cooled to 0 °C. To this mixture, 603 mg (1.265 mmol, 2.6 eq) *tert*-butyl 1-(tosyloxy)-3,6,9,12-tetraoxapentadecan-15-oate **{2}**, dissolved in 2 mL THF, was added drop-wise through a dropping funnel over 30 minutes. The reaction mixture was then allowed to reflux overnight. The mixture was then cooled to 0 °C, neutralized with saturated ammonium chloride, and extracted with DCM to separate the aqueous phase from the organic phase. The remaining white solid was washed several times with DCM and the combined organic layer was dried over Na₂SO₄ and concentrated to yield the crude product as a light yellow oil (416 mg, **{3}**). Purification of the crude product was not possible due to the similar polarity of the side products.



di-*tert*-butyl 18-amino-18-(19,19-dimethyl-17-oxo-2,5,8,11,14,18-hexaoxaicosyl)-4,7,10,13,16,20,23,26,29,32-decaoxapentatriacontane-1,35-dioate

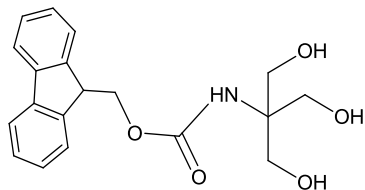
9.7.4 Synthesis of N-Fmoc-tris(hydroxymethyl)aminomethane

Tris (305 mg, 2.5mmol) was dissolved in 10% NaHCO₃ (6.7 mL). The reaction flask was placed in an ice bath and Dioxane (5 mL) was added. The mixture was stirred for a few minutes in the ice bath and Fmoc-succinimide (335.7 mg, 1.038 mmol, 1.1 eq), dissolved in 5 mL peroxide-free dioxane, was slowly added over a 15 minute period. After 3h, the ice bath was removed and the reaction mixture was stirred at room temperature overnight. The mixture was diluted with water and extracted two times with 50 mL diethyl ether.

The aqueous solution was placed in an ice bath and acidified with conc. HCl solution. The acidified mixture was allowed to precipitate at 4 °C and then extracted 3 times with DCM (50 mL). The combined organic phase was washed once with water, dried over Na₂SO₄ and

EXPERIMENTAL PART

the solvent removed under reduced pressure to give 69 mg of a white solid as the crude product.



(9*H*-fluoren-9-yl)methyl (1,3-dihydroxy-2-(hydroxymethyl)propan-2-yl)carbamate

C₁₉H₂₁NO₅

Mw: 343.37

¹H NMR (400 MHz, CDCl₃) : 3.18 (bs, 3H, OH); 3.69 (bs, 6H, (CH₂O)₃); 4.22 (t, 1H, CH) ; 4.45 (d, 2H, CH₂); 5.73 (bs, 1H, NH) ; 7.26-7.45 (m, 4H, arom), 7.57-7.61 (m, 2H, arom) ; 7.76-7.79 (m, 2H, arom)

10. References

1. Coughlin, S.R. Thrombin signalling and protease-activated receptors. *Nature* **2000**, 407: 258-264.
2. Yang, Y., Hong, H., Zhang, Y., Cai, W. Molecular imaging of proteases in cancer. *Cancer Growth and Metastasis*. **2009**, 2: 13-27.
3. Saeki, K., Ozaki, K., Kobayashi, T., Ito, S. Enzymatic properties, genes, and crystal structures. *Journal of Biosci. Bioeng.* **2007**, 103: 501-508.
4. Craik, C.S., Page, M.J., Madison, E.L. Proteases as therapeutics. *Biochem. J.* **2011**, 435: 1-16. doi:10.1042/BJ20100965
5. McGregor, D.P. Discovering and improving novel peptide therapeutics. *Curr. Opin. Pharmacol.* **2008**, 8: 616-619.
6. Saladin, P.M., Zhang, B.D., Reichert, J.M. Current trends in the clinical development of peptide therapeutics. *IDrugs* **2009**, 12: 779-784.
7. Łęgoska, A., Dębowski, D., Lesner, A., Wysocka, M., Rolka, K. Introduction of non-natural amino acid residues into the substrate-specific P1 position of trypsin inhibitor SFTI-1 yields potent chymotrypsin and cathepsin G inhibitors. *Bioorg. Med. Chem.* **2009**, 17: 3302-3307
8. Sani, M., Sinisi, R., Viani, F. PeptidylFluoro-Ketones as proteolytic enzyme inhibitors. *Curr. Top. in Med. Chem.* **2006**, 6: 1545-1566
9. March, T.L., Johnston, M.R., Duggan, P.J., Gardiner, J. Synthesis, structure, and biological applications of α -fluorinated β -amino acids and derivatives. *Chem Biodiversity* **2012**, 9: 2410-2441. doi: 10.1002/cbdv.201200307
10. Dougherty, D.A. Unnatural amino acids as probes of protein structure and function. *Curr. Opin. Chem. Biol.* **2000**, 4: 645-652.
11. Salwiczek, M., Samsonov, S., Vagt, T., Baldauf, C., Nyakatura, E., Fleige, E., Numata, J., Cölfen, H., Pisabarro, M.T., Kokschi, B. Position dependent effects of fluorinated amino acids on hydrophobic core formation of a coiled coil heterodimer. *Chem. Eur. J.* **2009**, 15: 7628-7636.
12. Gottler, L.M., Lee, H.Y., Shelburne, C.E., Ramamoorthy, A., Marsh, E.N.G. Modulating the biological activity of an antimicrobial peptide using fluorous amino acids. *Chembiochem.* **2008**, 9: 370-373.
13. Frackenhohl, J., Arvidsson, P.I., Schreiber, J.V., Seebach, D. The outstanding biological stability of β - and γ -peptides toward proteolytic enzymes: An in vitro investigation with fifteen peptidases. *ChemBioChem.* **2001**, 2: 445-455.
14. Kokschi, B., Sewald, N., Burger, K., Jakubke, H-D. Peptide modification by incorporation of α -trifluoromethyl substituted amino acids. *Amino Acids.* **1996**, 11: 425-434.
15. Isanbor, C., O'Hagan, D. Fluorine in medicinal chemistry: a review of anticancer agent. *J Fluorine Chem.* **2006**, 127: 303-319.
16. Filler, R., Saha, R. Fluorine in medicinal chemistry: a century of progress and a 60-years retrospective of selected highlights. *Future Med. Chem.* **2009**, 1: 777-791.

REFERENCES

17. Muller, K., Faeh, C., Diederich, F. Fluorine in pharmaceuticals: looking beyond intuition. *Science*. **2007**, 317: 1881-1886.
18. Meng, H., Krishnaji, S.T., Beinborn, M., Kumar, K. Influence of selective fluorination on the biological activity and proteolytic stability of glucagon-like peptide-1. *J Med Chem* **2008**, 51: 7303-7307. doi: 10.1021/jm8008579
19. Böhm, H.J., Banner, D., Bendels, S., Kansy, M. Fluorine in medicinal chemistry. *ChemBioChem*. **2004**, 5: 637-643.
20. Sato, A.K., Viswanathan, M., Kent, R.B., Wood, C.R. Therapeutic peptides: technological advances driving peptides into development. *Curr. Opin. Biotechnol.* **2006**, 17: 638-642.
21. Kokschi, B., Sewald, N., Hofmann, H-J., Burger, K., Jakubke, H-D. Proteolytically stable peptides by incorporation of alpha-Tfm amino acids. *J Peptide Sci.* **1997**, 3: 157-167.
22. Smits, R., Kokschi, B. How C α -fluoroalkyl amino acids and peptides interact with enzymes: Studies concerning the influence on proteolytic stability, enzymatic resolution and peptide coupling. *Curr. Top. Med. Chem.* **2006**, 16: 1483-1498.
23. Salwiczek, M., Vagt, T., Kokschi, B. Artificial model systems designed to investigate fluorinated amino acids in native protein environments. In Ojima, I. (Ed.) *Fluorine in bioorganic and medicinal chem.* **2009**, 391-409.
24. Salwiczek, M., Nyakatura, E.K., Gerling, U.I.M., Ye, S., Kokschi, B. Fluorinated amino acids: Compatibility with native protein structures and effects on protein-protein interactions. *Chem. Soc. Rev.* **2012**, 41: 2135-2171. doi:10.1039/C1CS15241F
25. Meng, H., Kumar, K. Antimicrobial activity and protease stability of peptides containing fluorinated amino acids. *J. Am. Chem. Soc.* **2007**, 129: 15615-15622.
26. Voloshchuk, N., Zhu, A.Y., Snyder, D., Montclare, J.K. Positional effects of monofluorinated phenylalanines on histone acetyltransferase stability and activity. *Bioorg Med. Chem. Lett.* **2009**, 19: 5449-5451.
27. Budisa, N., Wenger, W., Wiltschi, B. Residue-specific global fluorination of *Candida antarctica* lipase B in *Pichiapastoris*. *Mol. Bio. Syst.* **2010**, 6: 1630-1639.
28. Geurink, P.P., Liu, N., Spaans, M.P., Downey, S.L., van den Nieuwendijk, A.M.C.H., van der Marel, G.A., Kisselev, A.F., Florea, B.I., Overkleeft, H.S. Incorporation of fluorinated phenylalanine generates highly specific inhibitor of proteasome's chymotrypsin-like sites. *J. Med. Chem.* **2010**, 53: 2319-2323.
29. Baker, P.J., Montclare, J.K. Enhanced refoldability and thermoactivity of fluorinated phosphotriesterase. *ChemBioChem.* **2011**, 12: 1845-18481. doi: 10.1002/cbic.201100221
30. Asante, V., Mortier, J., Schlüter, H., Kokschi, B. Impact of fluorination on proteolytic stability of peptides in human blood plasma. *Bioorg. Med. Chem.* **2013**, 21: 3542-3546. doi: 10.1016/j.bmc.2013.03.051
31. Barrett, A.J., Rawlings, N.D., Woessner, J.F. *Handbook of proteolytic enzymes.* Academic press, San Diego, CA. **1998**.
32. Northrop, J.H., Kunitz, M., Herriott, R.M. *Crystalline enzymes* (Columbia Univ. press, New York). **1938**.

REFERENCES

33. Puente, X.S. Sanchez, L.M., Overall, C.M., Lopez-Otin, C. Human and mouse proteases: a comparative genomic approach, *Nat. Rev. Genet.* **2003**, 4: 544-548.
34. Poorman, R.A., Tomasselli, A.G., Heinrikson, R.L., Kezdy, F.J. A cumulative specificity model for proteases from human immunodeficiency virus types 1 and 2, inferred from statistical analysis of an extended substrate database, *J. Biol. Chem.* **1991**, 266: 14554-14561.
35. Chou, K.C. Jones, D. Heinrikson, R.L. Prediction of the tertiary structure and substrate binding site of caspase-8, *FEBS Lett.* **1997**, 419: 49-54.
36. Chou, J.J., Matsuo, H., Duan, H., Wagner, G. Solution structure of the RAIDD CARD and model for CARD/CARD interaction in caspase-2 and caspase-9 recruitment. *Cell* **1998**, 94: 171-180.
37. Qin, H., Srinvasula, S.M., Wu, G., Fernandes-Alnemri, T. Alnemri, E.S., Shi, Y. Structural basis of procaspase-9 recruitment by the apoptotic protease activating factor 1, *Nature* **1999**, 399: 549-557.
38. Chou, J.J., Li, H., Salvessen, G.S., Yuan, J., Wagner, G. Solution structure of BID, an intracellular amplifier of apoptotic signaling, *Cell* **1999**, 96: 615-624.
39. Watt, W., Koeplinger, K.A., Mildner, A.M., Heinrikson, R.L., Tomasselli, A.G., Watenpaugh, K.D. The atomic resolution structure of human caspase-8, a key activator of apoptosis, *Structure.* **1999**, 7: 1135-1143.
40. Chou, K.C., Tomasselli, A.G., Heinrikson, R.L. Prediction of the tertiary structure of a caspase-9/inhibitor complex. *FEBS Lett.* **2000**, 470: 249-256.
41. Chou, K.C. Review: structural bioinformatics and its impact to biomedical science. *Curr. Med. Chem.* **2004**, 11: 2105-2134.
42. Bordusa, F. Proteases in organic synthesis. *Chem. Rev.* **2002**, 102: 4817-4867.
43. Neurath, H. The diversity of proteolytic enzymes. In: "Proteolytic enzymes a practical approach", Beynon R.J, Bond J.S (Eds.), IRL press, Oxford, U.K. **1989**, pp. 1-12.
44. Feliú, J.A., De Mas, C., López-Santín, J. Studies on papain action in the synthesis of Gly-Phe in two-liquid-phase media. *Enzyme and Microbial Technology.* **1995**, 17: 882-887.
45. Neurath, H. Proteolytic enzymes, past and future. *Proc. Natl. Acad. Sci.* **1999**, 96: 10962-10963.
46. López-Otín, C., Bond, J.S. Proteases: Multifunctional enzymes in life and disease Minireviews: *J. Biol. Chem.* **2008**, 283: 30433-30437. doi: 10.1074/jbc.R800035200
47. <http://merops.sanger.ac.uk>
48. Rawlings, N.D., Morton, F.R., Kok, C.Y., Kong, J., Barrett, A. J. MEROPS: The peptidase database. *Nucleic Acids Res* **2008**, 36: 320-325.
49. Rawlings, N.D., Barrett, A.J. Evolutionary families of peptidases. *Biochem. J.* **1993**, 290: 205-218.
50. Rawlings, N.D, Barrett, A.J. Families of cysteine peptidases. *Methods Enzymol.* **1994**, 244: 461-486.
51. Wlodawer, A. Proteasome: a complex protease with a new fold and a distinct mechanism. *Structure* **1995**, 3: 417-420.

REFERENCES

52. Schechter, I., Berger, A. On the size of the active site in proteases. *Biochem. Biophys. Res. Com.* **1967**, 27: 157-162.
53. Berg, J.M., Tymoczko, J.L., Stryer, L. *Biochemistry*. 5th ed., New York: W H Freeman; **2002**. Section 8.1, enzymes are powerful and highly specific catalysts.
54. Goldberg, A.L., Rock, K.R. Proteolysis, proteasomes and antigen presentation. *Nature* **1992**, 357: 375-379.
55. Brannigan, J.A., Dodson, G., Duggleby, H.J., Moody, P.C., Smith, J.L., Tomchick, D.R., Murzin, A.G. "A protein catalytic framework with an N-terminal nucleophile is capable of self-activation." *Nature* **1995**, 378: 416-419.
56. Cheng, H., Grishin, N.V. "DOM-fold: a structure with crossing loops found in DmpA, ornithine acetyltransferase, and molybdenum cofactor-binding domain". *Protein sci.* **2005**, 14: 1902-1910.
57. Dodson, G., Wlodawer, A. "Catalytic triads and their relatives". *Trends in Biochem. Sci.* **1998**, 23: 347-352.
58. Ekici, O.D., Paetzel, M., Dalbey, R.E. Unconventional serine proteases: variations on the catalytic Ser/His/Asp triad configuration. *Protein Sci.* **2008**, 17: 2023-37.
59. Buller, A.R., Townsend, C.A. Intrinsic evolutionary constraints on protease structure, enzyme acylation, and the identity of the catalytic triad. *Proc. Nat. Aca. Sci. USA.* **2013**, 110: 653-661.
60. Erez, E., Fass, D., Bibi, E. How intramembrane proteases bury hydrolytic reactions in the membrane. *Nature* **2009**, 459, 371-378.
61. Huxley-Jones, J., Clarke, T.K., Beck, C., Toubaris, G., Robertson, D.L., Boot-Handford, R.P. The evolution of the vertebrate metzincins; insights from *Ciona intestinalis* and *Danio rerio*. *BMC Evol. Biol.* **2007**, 7: 63. doi: 10.1186/1471-2148-7-63.
62. Gill, S.E., Parks, W.C. Metalloproteinases and their inhibitors: regulators of wound healing. *Int. J. Biochem. Cell Biol.* **2008**, 40: 1334- 1347.
63. Egeblad, M., Werb, Z. New functions for the matrix metalloproteinases in cancer progression. *Nat. Rev. Cancer.* **2002**, 2: 161-174.
64. Mott, J.D., Werb, Z. Regulation of matrix biology by matrix metalloproteinases. *Curr. Opin. Cell Biol.* **2004**, 16: 558-564.
65. Parks, W.C., Wilson, C.L., Lopez-Boado, Y.S. Matrix metalloproteinases as modulators of inflammation and innate immunity. *Nat. Rev. Immunol.* **2004**, 4: 617-629.
66. Zhang, C., Kim, S.K. Matrix metalloproteinase inhibitors (MMPi)s from marine natural products: the current situation and future prospects. *Marine Drugs*, **2009**, 7: 71-84.
67. Kheradmand, F., Werb, Z. Shedding light on sheddases: Role in growth and development. *Bioessays.* **2002**, 24: 8-12.
68. Moss, M.L., Bartsch, J.W. Therapeutic benefits from targeting of ADAM family members. *Biochemistry.* **2004**, 43: 7227-7235.
69. Seals, D.F., Courtneidge, S.A. The ADAMs family of metalloproteases: multidomain proteins with multiple functions. *Genes Dev.* **2003**, 17: 7-30.
70. Thomas, N.V., Kim, S-K. Metalloproteinase inhibitors: Status and scope from marine organisms. *Biochem. Res. Int.* **2010**, Article ID 845975, 10 pages, 2010. doi:10.1155/2010/845975

REFERENCES

71. Berg, J.M., Tymoczko, J.L., Stryer, L. *Biochemistry*. 5th ed., New York: W H Freeman; **2002**. Section 9.1, Proteases: Facilitating a difficult reaction.
72. Dubey, V.K., Pande, M., Singh, B.K., Jagannadham, M.V. Papain-like proteases: Applications of their inhibitors. *Afri. J. of Biotechnol.* **2007**, 6: 1077-1086.
73. Bromme, D., Wilson, S. Extracellular matrix degradation: Role of cysteine cathepsins in extracellular proteolysis. *Biology of extracellular matrix.* **2011**, 2: 23-51.
74. Polgár, L. Mechanisms of protease action. CRC press, Boca Raton, FL. **1989**, 87-122.
75. Borg, T.K. It's the matrix! ECM, proteases, and cancer. *Am. J. Pathol.* **2004**, 164: 1141-1142.
76. Bender, M.L., Kézdi, F.J. Mechanism of action of proteolytic enzymes. *Annu. Rev. Biochem.* **1965**, 34: 49-76.
77. Hess, G.P. Chymotrypsin-chemical properties and catalysis, in *The Enzymes*, Boyer, P.D. (ed.), **1971**, 3: 213-248, Academic press, New York.
78. Kraut, J. Serine proteases: structure and mechanism of catalysis. *Annu. Rev. Biochem.* **1977**, 46: 331-358.
79. Huber, R., Bode, W. Structural basis of the activation and action of trypsin. *Acc. Chem. Res.* **1978**, 11: 114-122.
80. James, M.N. An X-ray crystallographic approach to enzyme structure and function. *Can. J. Biochem.* **1980**, 58: 252-271.
81. Polgár, L., Halász, P. Current problems in mechanistic studies of serine and cysteine proteinases. *Biochem. J.* **1982**, 207: 1-10.
82. Polgár, L. Structure and function of serine proteases. *New Comp. Biochemistry.* **1987**, 16: 159-200.
83. Perona, J.J., Craik C.S. Structural basis of substrate specificity in the serine proteases. *Protein Sci.* **1995**, 4: 337-360.
84. Keil, B. Specificity of proteolysis. Springer-Verlag Berlin-Heidelberg-New York, **1992**, p. 335.
85. Czapinska, H., Otlewski, J. Structural and energetic determinants of the S1-site specificity in serine proteases. *Eur. J. Biochem.* **1999**, 260: 571-595.
86. Hedstrom, L. Serine protease mechanism and specificity. *Chem. Rev.* **2002**, 102: 4501-4524.
87. Polgár, L. The catalytic triad of serine peptidases, *Cell. Mol. Life Sci.* **2005**, 62: 2161-2172. doi: 10.1007/s00018-005-5160-x
88. Blow, D.M., Birktoft, J.J., Hartley, B.S. Role of a buried acid group in the mechanism of action of chymotrypsin. *Nature* **1969**, 221: 337-340.
89. Robillard, G., Shulman, R.G. High resolution nuclear magnetic resonance studies of the active site of chymotrypsin. II. Polarization of histidine 57 by substrate analogues and competitive inhibitors. *J. Mol. Biol.* **1974**, 86: 541-558.
90. Bachovchin, W.W. Confirmation of the assignment of the low-field proton resonance of serine proteases by using specifically nitrogen-15 labeled enzyme. *Proc. Natl. Acad. Sci.* **1985**, 82: 7948-7951.

REFERENCES

91. Kossiakoff, A.A., Spencer, S.A. Direct determination of the protonation states of aspartic acid-102 and histidine-57 in the tetrahedral intermediate of the serine proteases: Neutron structure of trypsin. *Biochemistry*. **1981**, 20: 6462-6474.
92. Matthews, D.A., Alden, R.A., Birktoft, J.J., Freer, T., Kraut, J. Re-examination of the charge relay system in subtilisin comparison with other serine proteases. *J. Biol. Chem.* **1977**, 252: 8875-8883.
93. Fodor, K., Harmat, V., Neutze, R., Szilagyi, L., Graf, L., Katona, G. Enzyme: substrate hydrogen bond shortening during the acylation phase of serine protease catalysis. *Biochemistry*. **2006**, 45: 2114-2121.
94. Huber, R., Kukla, D., Bode, W., Schwager, P., Bartels, K., Deisenhofer, J., Steigemann, W. Structure of the complex formed by bovine trypsin and bovine pancreatic trypsin inhibitor. II. Crystallographic refinement at 1.9 Å resolution. *J. Mol. Biol.* **1974**, 89: 73-101.
95. Matthews, B.W., Sigler, P.B., Henderson, R., Blow, D.M. Three dimensional structure of tosyl- α -chymotrypsin. *Nature* **1967**, 214: 652-656.
96. Stroud, R.M., Kay, L.M., Dickerson, R.E. The structure of bovine trypsin: Electron density maps of the inhibited enzyme at 5 Å and at 2-7 Å resolution. *J. Mol. Biol.* **1974**, 83: 185-208.
97. Blow, D.M. The structure of chymotrypsin. *The enzymes*, 3rd ed., Boyer, P. D., Ed., Academic press, New York. Vol. 3 **1971**: 185-212.
98. Derewenda, Z.S., Derewenda, U., Kobos, P.M. (His) C epsilon-H...O=C < hydrogen bond in the active sites of serine hydrolases. *J. Mol. Biol.* **1994**, 241: 83-93.
99. Suguna, K., Padlan, E.A., Smith, C.W., Carlson, W.D., Davies, D.R. Binding of a reduced peptide inhibitor to the aspartic proteinase from *Rhizopus chinensis*: implications for a mechanism of action. *Proc. Natl. Acad. Sci. USA.* **1987**, 84: 7009-13.
100. Davies, D.R. The structure and function of the aspartic proteinases. *Annu. Rev. Biophys. Chem.* **1990**, 19: 189-215.
101. Rakashanda, S., Rana, F., Rafiq, S., Masood, A., Amin, S. Role of proteases in cancer: A review. *Biotechnol. Mol. Biol. Rev.* **2012**, 7: 90-101.
102. Northrop, J.H. Crystalline pepsin. I. Isolation and tests of purity. *J Gen Physiol.* **1930**, 13: 739-766
103. Fujinaga, M., Chernaia, M.M., Tarasova, N.I., Mosimann, S.C., James, M.N.G. Crystal-structure of human pepsin and its complex with pepstatin. *Protein Sci.* **1995**, 4: 960-972.
104. Antonov, V.K., Ginodman, L.M., Kapitannikov, Y.V., Barshevskaya, T.N., Gurova, A.G., Rumsh, L.D. Mechanism of pepsin catalysis: General- base catalysis by the active site carboxylate ion. *FEBS. Lett.* **1978**, 88: 87-90.
105. Antonov, V.K., Ginodman, L.M., Rumsh, L.D., Kapitannikov, Y.V., Barshevskaja, T.N., Yavashev, L.P., Gurova, A.G., Volkova, L.I. Studies on mechanism of action of proteolytic enzymes using heavy oxygen exchange. *Eur. J. Biochem.* **1981**, 17: 195-200.
106. Fruton, J.S. The specificity and mechanism of pepsin action. *Adv. Enzymol. Relat. Areas Mol. Biol.* **1970**, 33: 401-443.

REFERENCES

107. Powers, J.C., Harley, A.D., Myers, D.V. Subsite specificity of porcine pepsin. *Adv. Exp. Med. Biol.* **1977**, 95: 141-157.
108. Sampath-Kumar, P.S., Fruton, J.S. Studies on the extended active sites of acid proteinases. *Proc. Natl. Acad. Sci. USA.* **1974**, 71: 1070-1072.
109. Michaelis, L., Menten, M.L. Die Kinetik der Invertinwirkung. *Biochemistry Zeitschrift.* **1913**, 49: 333-369.
110. Johnson, K.A., Goody, R.S. The original Michaelis constant: Translation of the 1913 Michaelis-Menten paper. *Biochemistry.* **2011**, 50: 8264-8269.
111. Cornish-Bowden, A. *Fundamentals of enzyme kinetics*, 3rd ed., Portland press Ltd: London, **2004**, p 422.
112. Bisswanger, H. *Enzyme kinetics: Principles and Methods*, 1st ed. Wiley-VCH: Weinheim, **2002**, p 301.
113. Berg, J.M., Tymoczko, J.L., Stryer, L. *Biochemistry*, 5th ed., New York: W H Freeman; **2002**: 8.4. The Michaelis-Menten model accounts for the kinetic properties of many enzymes, 8.5. Enzymes can be inhibited by specific molecules.
114. Anderson, N.L., Polanski, M., Pieper, R., Gatlin, T., Tirumalai, R.S., Conrads, T.P., Veenstra, T.D., Adkins, J.N., Pounds, J.G, Fagan, R., and Lobley, A. The human plasma proteome: A non-redundant list developed by combination of four separate sources. *Mol. Cell. Proteomics.* **2004**, 4: 311-326.
115. Werle, M., Bernkop-Schnürch, A. Strategies to improve plasma half life time of peptide and protein drugs. *Amino Acids.* **2006**, 30: 351-367. doi: 10.1007/s00726-005-0289-3
116. Vlieghe, P., Lisowski, V., Martinez, J., Khrestchatsky, M. Synthetic therapeutic peptides: science and market. *Drug Discov. Today.* **2010**, 15: 40-56.
117. Koomen, J.M., Li, D., Xiao, L., Liu, T.C., Coombes, K.R., Abbruzzese J., Kobayashi, R. Direct tandem mass spectrometry reveals limitations in protein profiling experiments for plasma biomarker discovery. *J of Proteome Res.* **2005**, 4: 972-981.
118. <http://us.expasy.org>
119. Fredholt, K., Adrian, C., Just, L., Hoj Larsen, D., Weng, S., Moss, B., Juel, F.G. Chemical and enzymatic stability as well as transport properties of a Leu-enkephalin analogue and ester prodrugs thereof. *J. Control Rel.* **2000**, 63: 261-273.
120. Schlüter, H., Jankowski, J., Rykl, J., Thiemann, J., Belgardt, S., Zidek, W., Wittmann, B., Pohl, T. Detection of protease activities with the mass-spectrometry-assisted enzyme-screening (MES) system. *Anal. Bioanal. Chem.* **2003**, 377: 1102-1107.
121. Schlüter, H., Rykl, J., Thiemann, J., Kurzawski, S., Gobom, J., Tepel, M., Zidek, W., Linscheid, M. Mass spectrometry-assisted protease substrate screening. *Anal. Chem.* **2007**, 79: 1251-1255.
122. Schlüter, H., Hildebrand, D., Gallin, C., Schulz, A., Thiemann, J., Trusch, M. Mass spectrometry for monitoring protease reactions. *Anal. Bioanal. Chem.* **2008**, 392:783-792.
123. Harris, A.G. Somatostatin and somatostatin analogues: pharmacokinetics and pharmacodynamic effects. *Gut.* **1994**, 35: 1-4.
124. Hummel, G. Reineke, U., Reimer, U. Translating peptides into small molecules. *Mol. Biosyst.* **2006**, 2: 499-508.

REFERENCES

125. Hruby, V.J. Designing peptide receptor agonists and antagonists. *Nat. Rev. Drug Discov.* **2002**, 1: 847-858.
126. Dasgupta, P., Singh, A., Mukherjee, R. N-terminal acylation of somatostatin analog with long chain fatty acids enhances its stability and anti-proliferative activity in human breast adenocarcinoma cells. *Biol. Pharm. Bull.* **2002**, 25: 29-36.
127. Lee, H., Jang, I.H., Ryu, S.H., Park, T.G. N-terminal site-specific mono- PEGylation of epidermal growth factor. *Pharm. Res.* **2003**, 20: 818-825.
128. Veronese, F.M. Peptide and protein PEGylation: a review of problems and solutions. *Biomaterials.* **2001**, 22: 405-417.
129. Solá, R.J., Griebenow, K. Effects of glycosylation on the stability of protein pharmaceuticals. *J. Pharm. Sci.* **2009**, 98: 1223-1245. doi: 10.1002/jps.21504
130. Cleland, J.L., Powell, M.F., Shire, S.J. The development of stable protein formulations: a close look at protein aggregation, deamidation, and oxidation. *Crit. Rev. Ther. Drug Carrier Syst.* **1993**, 10: 307-377.
131. Heard, K.R., Wu, W., Li, Y., Zhao, P., Woznica, I., Lai, J.H., Beinborn, M., Sanford, D.G., Dimare, M.T., Chiluwal, A.K., Peters, D.E., Whicher, D., Sudmeier, J.L., Bachovchin, W.W. A general method for making peptide therapeutics resistant to serine protease degradation: Application to dipeptidyl peptidase IV substrates. *J Med Chem.* **2013**, 56: 8339-8351.
132. Kreuzfeld, H.J., Döbler, C., Schmidt, U., Krause, H.W. Synthesis of non-proteinogenic (D)- or (L)-amino acids by asymmetric hydrogenation. *Amino Acids* **1996**, 11: 269-282.
133. Walsh, C.T., O'Brien, R.V., Khosla, C. Nonproteinogenic amino acid building blocks for nonribosomal peptide and hybrid polyketide scaffolds. *Angew. Chem. Int. Ed.* **2013**, 52: 7098-7124. doi: 10.1002/anie.201208344
134. Wagner, I., Musso, H., Neue natürliche Aminosäuren. *Angew. Chem.* **1983**, 95: 827-839: New naturally occurring amino acids. *Angew. Chem. Int. Ed. Engl.* **1983**, 22, 816-828.
135. Guzmán, F., Barberis S., Illanes A. Peptide synthesis: chemical or enzymatic. *Elect. J. Biotechnol.* **2007**, 10: 279-314.
136. Werder, M., Hauser, H., Abele, S., Seebach, D. β -peptides as inhibitors of small intestinal cholesterol and fat adsorption. *Helvetica Chimica Acta.* **1999**, 82: 1774-1783.
137. Von Moos, E., Ben, R.N. Recent advances in the synthesis of C-linked glycoconjugates. *Curr. Topics in Med. Chem.* **2005**, 5: 1351-1361.
138. Kasperkiewicz, P., Gajda, A.D., Drag, M. Current and prospective applications of non-proteinogenic amino acids in profiling of proteases substrate specificity. *Biol. Chem.* **2012**, 393: 843-851. doi: 10.1515/hsz-2012-0167
139. Jain, R., Chawrai, S. Advancements in the anti-diabetes chemotherapeutics based on amino acids, peptides, and peptidomimetics. *Mini Rev. Med. Chem.* **2005**, 5: 469-477.
140. Wang, L., Xie, J., Schultz, P.G. Expanding the genetic code. *Annu. Rev. Biophys. Biomol. Struct.* **2006**, 35: 225-249.
141. Powell, M.F., Stewart, T., Otvos Jr., L., Urge, L., Gaeta, F.C.A., Sette, A., Arrhenius, T., Thomson, D., Soda, K., Colon, S.M. Peptide stability in drug development II. Effect of

REFERENCES

- single amino acid substitution and glycosylation on peptide reactivity in human serum. *Pharm. Res.* **1993**, 10: 1268-1273.
142. Vasudev, P.G., Chatterjee, S., Shamala, N., Balaram, P. Structural chemistry of peptides containing backbone expanded amino acid residues: conformational features of beta, gamma, and hybrid peptides. *Chem. Rev.* **2011**, 111: 657-687.
143. van Niel, M.B., Collins, I., Beer, M.S., Broughton, H.B., Cheng, S.K.F., Goodacre, S.C., Heald, A., Locker, K.L., MacLeod, A.M., Morrison, D., Moyes, C.R., O'Connor, D., Pike, A., Rowley, M., Russell, M.G.N., Sohal, B., Stanton, J.A., Thomas, S., Verrier, H., Watt, A.P., Castro, J.L. Fluorination of 3-(3-(Piperidin-1-yl)propyl)indoles and 3-(3-(Piperazin-1-yl)propyl)indoles gives selective human 5-HT_{1D} receptor ligands with improved pharmacokinetic profiles. *J. Med. Chem.* **1999**, 42: 2087-2104.
144. O'Hagan, D., Schaffrath, C., Cobb, S.L., Hamilton, J.T.G., Murphy, C.D. Biosynthesis of an organofluorine molecule-a fluorinase enzyme has been discovered that catalyses carbon-fluorine bond formation. *Nature* **2002**, 416: 279-279.
145. Deng, H., O'Hagan, D., Schaffrath, C. Fluorometabolite biosynthesis and the fluorinase from *Streptomyces cattleya*. *Nat. Prod. Rep.* **2004**, 21: 773-784.
146. Dong, C., Huang, F., Deng, H., Schaffrath, C., Spencer, J.B., O'Hagan, D., Naismith, J.H. Crystal structure and mechanism of a bacterial fluorinating enzyme. *Nature* **2004**, 427: 561-565.
147. Begue, J.P., Bonnet-Delpon, D. Recent advances (1995-2005) in fluorinated pharmaceuticals based on natural products. *J. Fluorine Chem.* **2006**, 127: 992-1012.
148. Purser, S., Moore, P.R., Swallow, S., Gouverneur, V. Fluorine in medicinal chemistry. *Chem. Soc. Rev.* **2008**, 37: 320-330.
149. O'Hagan D. Understanding organofluorine chemistry. An introduction to the C-F bond. *Chem. Soc. Rev.* **2008**, 37: 308-319.
150. Yoder, N.C., Kumar, K. Fluorinated amino acids in protein design and engineering. *Chem. Soc. Rev.* **2002**, 31: 335-341.
151. Buer, B.C., de la Salud-Bea, R., Al Hashimi, H.M., Marsh, E.N.G. Engineering protein stability and specificity using fluorous amino acids: The importance of packing effects. *Biochemistry.* **2009**, 48: 10810-10817.
152. Buer, B.C., Meagher, J.L., Stuckey, J.A., Marsh, E. N. G. Structural basis for the enhanced stability of highly fluorinated proteins. *Proc. Natl. Acad. Sci. USA.* **2012**, 109: 4810-4815.
153. Lee, H.-Y., Lee, K.-H., Al-Hashimi, H.M., Marsh, E.N.G. Modulating protein structure with fluorous amino acids: increased stability and native-like structure conferred on a 4-helix bundle protein by hexafluoroleucine. *J. Am. Chem. Soc.* **2006**, 128: 337-343.
154. Lee, K.-H., Lee, H.-Y., Slutsky, M.M., Anderson, J.T., Marsh, E.N.G. Fluorous effect in proteins: de novo design and characterization of a four- α -helix bundle protein containing hexafluoroleucine. *Biochemistry.* **2004**, 43: 16277-16284.
155. Bilgiçer, B., Fichera, A., Kumar, K. A coiled coil with a fluorous core. *J. Am. Chem. Soc.* **2001**, 123: 4393-4399.

REFERENCES

156. Jäckel, C., Salwiczek, M., Kokschi, B. Fluorine in a native protein environment-how the spatial demand and polarity of fluoroalkyl groups affect protein folding. *Angew. Chem. Int. Ed.* **2006**, 45: 4198-4203. doi: 10.1002/anie.200504387
157. Jäckel, C., Seufert, W., Thust, S., Kokschi, B. Evaluation of the molecular interactions of fluorinated amino acids with native polypeptides. *ChemBioChem.* **2004**, 5: 717-720.
158. Sutherland, A., Willis, C.L. Synthesis of fluorinated amino acids. *Nat. Prod. Rep.* **2000**, 17: 621-631.
159. Qiu, X.-L., Meng, W.-D., Qing, F.-L. Synthesis of fluorinated amino acids. *Tetrahedron* **2004**, 60: 6711-6745.
160. Marsh, E.N.G., Suzuki, Y. Using ¹⁹F NMR to probe biological interactions of proteins and peptides. *ACS Chem. Biol.* **2014**, Article ASAP. doi: 10.1021/cb500111u
161. Salwiczek, M., Kokschi, B. Effects of fluorination on the folding kinetics of a heterodimeric coiled coil. *ChemBioChem.* **2009**, 10: 2867-2870.
162. Bott, G., Field, L.D., Sternhell, S. Steric effects. A study of a rationally designed system. *J. Am. Chem. Soc.* **1980**, 102: 5618-5626.
163. Nagai, T., Nishioka, G., Koyama, M., Ando, A., Miki, T., Kumadaki, I. Reactions of trifluoromethyl ketones. IX. Investigation of the steric effect of a trifluoromethyl group based on the stereochemistry of dehydration of trifluoromethyl homoallyl alcohols. *J. Fluorine Chem.* **1992**, 57: 229-237.
164. Kauzmann, W. Some factors in the interpretation of protein denaturation. *Adv. Protein Chem.* **1959**, 14: 1-63.
165. Samsonov, S.A., Salwiczek, M, Anders, G., Kokschi, B., Pisabarro, M.T. Fluorine in protein environments: A QM and MD study. *J. Phys. Chem. B.* **2009**, 113: 16400-16408.
166. Smart, B.E. Fluorine substituent effects on bioactivity. *J. Fluorine Chem.* **2001**, 109: 3-11.
167. O'Hagan, D. Rzepa, H.S. Some influences of fluorine in bioorganic chemistry. *Chem. Commun.* **1997**, 645-652. doi: 10.1039/A604140J
168. Danielson, M.A., Falke, J.J. Use of ¹⁹F NMR to probe protein structure and conformational changes. *Annu. Rev. Biophys. Biomol. Struct.* **1996**, 25: 163-195.
169. Woll, M.G., Hadley, E.B., Mecozzi, S., Gellman, S.H. Stabilizing and destabilizing effects of phenylalanine --> F5-phenylalanine mutations on the folding of a small protein *J. Am. Chem. Soc.* **2006**, 128: 15932-15933.
170. Xu, Z.J., Love, M.L., Ma, L.Y., Blum, M., Bronskill, P.M., Bernstein, J., Grey, A.A., Hofmann, T., Camerman, N., Wong, J.T. Tryptophanyl-tRNA synthetase from *Bacillus subtilis*. Characterization and role of hydrophobicity in substrate recognition. *J. Biol. Chem.*, **1989**, 264: 4304-4311.
171. Wong, C.-Y., Eftink, M.R. Incorporation of tryptophan analogues into staphylococcal nuclease; stability toward thermal and guanidine-HCl induced unfolding. *Biochemistry.* **1998**, 37: 8947-8953.
172. Ladram, A., Bulant, M., Delfour, A., Montagne, J.J., Vaudry, H., Nicolas, P. Modulation of the biological activity of thyrotropinreleasing hormone by alternate processing of pro-TRH. *Biochimie.* **1994**, 76: 320-328.

REFERENCES

173. Kokschi, B., Ullmann, D., Jakubke, H.-D. Synthesis, structure and biological activity of α -trifluoromethyl substituted thyrotropin releasing hormone. *J. Fluorine Chem.* **1996**, 80: 53-57.
174. Bauer, K., Nowak, P., Kleinkauf, H. Specificity of a serum peptidase hydrolyzing thyroliberin at pyroglutamyl-histidine bond. *Eur. J. Biochem.* **1981**, 118: 173-176.
175. Bauer, K., Carmeliet, P., Schulz, M., Baes, M., Deneg, C. Regulation and cellular localization of the membrane-bound thyrotropin-releasing hormone-degrading enzyme in primary cultures of neuronal, glial and adenohypophyseal cells. *Endocrinology.* **1990**, 127: 1224-1233.
176. Grant, G., Ling, N., Rivier, J., Vale, W. Orientation restrictions of the peptide hormone, thyrotropin-releasing factor, due to intramolecular hydrogen bonding. *Biochemistry.* **1972**, 11: 3070- 3073.
177. van't Hoff, J.H. Z. *Anorg. Allg. Chem.* **1898**, 18: 1-13.
178. Jakubke, H.-D., Kuhl, P., Könnecke, A. Basic principles of protease-catalyzed peptide bond formation. *Angew. Chem. Int. Ed. Engl.* **1985**, 24: 85-93.
179. Jakubke, H.-D. In: Udenfriend, S., Meienhofer, J. (Eds), *The Peptides: Analysis, biology.* Vol. 9. Academic press, New York, **1987**: pp 103-165.
180. Bordusa, F. Proteases in organic synthesis. *Chem. Rev.* **2002**, 102: 4817-4868.
181. Lombard, C., Saulnier, J., Wallach, J. Recent trends in protease-catalyzed peptide synthesis. *Protein and Peptide Lett.* **2005**, 12: 7, 621-629.
182. Salam, S.M.A., Kagawa, K., Matsubara, T., Kawashiro, K. Protease-catalyzed dipeptide synthesis from N-protected amino acid carbamoylmethyl esters and free amino acids in frozen aqueous solution. *Enzyme and Microbial Technol.* **2008**, 43: 537-543.
183. Thust, S., Kokschi, B. Protease-catalyzed peptide synthesis for the site-specific incorporation of α -fluoroalkyl amino acids into peptides. *J. Org. Chem.* **2003**, 68: 2290-2296. doi: 10.1021/jo020613p
184. Welch, J.T., Gyenes, A., Jung, M.J. Fluorine-containing amino acids: Synthesis and properties. Kukhar, V.P., Soloshonok, V.A. (Eds.) Wiley, Chichester. **1995**, 311-331.
185. Borissenko, L., Groll, M. 20S Proteasome and its inhibitors: crystallographic knowledge for drug development. *Chem. Rev.* **2007**, 107: 687-717.
186. Jäckel, C. PhD thesis: "Development of a screening system for the systematic evaluation of the interactions of fluoroalkyl-substituted amino acids in polypeptide environments" **2006**. Dissertation online der Freien Universität Berlin.
187. Thormann, M., Thust, S., Hofmann, H.-J., Bordusa, F. Protease-catalyzed hydrolysis of substrate mimetics (inverse substrates): A new approach reveals a new mechanism. *Biochemistry.* **1999**, 38: 6056-6062.
188. Christie, W.W. Detectors for high-performance liquid chromatography of lipids with special reference to evaporative light scattering detection. In: *Advances in lipid methodology - One.* (Oily press). **1992**, 239-271.
189. Petritis, K., Elfakir, C., Dreux, M. A comparative study of commercial liquid chromatographic detectors for the analysis of underivatized amino acids. *J. Chromatogr. A*, **2002**, 961: 9-21.

REFERENCES

190. Reed, G. D. An evaluation of electrochemical detection in reverse-phase HPLC. *J. High Resolut. Chrom. Chrom. Comm.* **1988**, 11: 675- 677.
191. Ajeetkumar Patil, Choudhari, K. S., Vijendra Prabhu, Unnikrishnan, V. K., Sujatha Bhat, Keerthilatha M. Pai, Kartha, V. B., Santhosh, C. Highly sensitive high performance liquid chromatography-laser induced fluorescence for proteomics applications. *ISRN Spectroscopy*. **2012**, Article ID 643979, 9 pages, doi: 10.5402/2012/643979
192. Aguilar, M.I. HPLC of peptides and proteins: Methods and protocols. Humana press, Totowa, New Jersey **2004**.
193. Nakanishi, K., Soga, N. Phase separation in gelling silica-organic polymer solution: systems containing poly(sodium styrenesulfonate). *J. Am. Ceram. Soc.* **1991**, 74: 2518-2530.
194. Renlund, S., Erlandsson, I., Hellman, U., Silberring, J., Wernstedt, C., Lindstrom, L., Nyberg, F. Micropurification and amino acid sequence of beta-casomorphin-8 in milk from a woman with postpartum psychosis. *Peptides*. **1993**, 14: 1125-1132.
195. Snyder, L.R., Kirkland, J.J., Glajch, J.L. Practical HPLC method development. 2nd ed., **2001**. doi: 10.1002/9781118592014
196. Sethi, P.D. HPLC: Quantitative analysis of pharmaceutical formulations. 1st ed., New Delhi, CBS publishers and distributors, **2001**.
197. Lindholm, J. Development and validation of HPLC methods for analytical and preparative purposes. *Acta Universitatis Upsaliensis. Comprehensive summaries of uppsala dissertations from the faculty of science and technology 995*, **2004**, 87 pp.
198. Nledner, W., Karsten, M., Stelner, F., Swart, R. Automating method development with an HPLC system optimized for scouting of columns, eluents and other method parameters. Pittcon presentation. **2008**.
199. Scott, P.W.R. Liquid chromatography for the analyst. New York: Marcel Dekker Inc. **1994**, 1-10.
200. http://www.hitachi-hitec.com/global/science/lc/lc_basic_7.html
201. Mant, C.T., Hodges, R.S. The effects of anionic ion-pairing reagents on peptide retention in reversed phase chromatography. (In high performance liquid chromatography of peptides and proteins: Separation, analysis and conformation). Mant, C.T., Hodges, R.S., eds. CRC, Boca Raton FL. **1991**, 327-341.
202. Welling, G.W., Van der Zee, R., Welling-Wester, S. Column liquid chromatography of integral membrane proteins. *J. Chromatogr.* **1987**, 418: 223-243.
203. Frank, J., Braat, A. Duine, J.A. Assessment of protein purity by chromatography and multiwavelength detection. *Anal. Biochem.* **1987**, 162: 65-73.
204. (a) Nyberg, F., Pernow, C., Moberg, U., Eriksson, R.B. High performance liquid chromatography and diode array detection for the identification of peptides containing aromatic amino acids in studies of endorphin-degrading activity in human cerebrospinal fluid. *J. Chromatogr.* **1986**, 359: 541-551. (b) Rozing, G.P. Diode array detection. *Meth. Enzymol.* **1996**, 270: 201-234.
205. Lakowicz, J.R. Principles of fluorescence spectroscopy. 2nd ed., Springer: New York, Kluwer Academic/Plenum Publishers. **1999**, 530-531.
206. Lakowicz, J.R. Principles of fluorescence spectroscopy. Plenum press, New York, **1983**.

REFERENCES

207. Schuster, R., Schulenberg-Schell, H., A new approach to lower limits of detection and easy spectral analysis. (Fluorescence detection in liquid chromatography). Agilent technologies. **2000**.
208. Schuster, R., Gratzfeld-Hüsgen, A. A comparison of pre- and post-column derivatization for the analysis of glyphosate. Agilent technologies application note. Environmental analysis. **1991**, 5091-3621.
209. Bin, L., Qing-gaung, D., Lin, S., Meng-shu, W., Chun, L., Yong-ge, W., Xiang-hui, Y., Ya-ming, S., Yan, C., Wei, K., Jia-cong, S., Development and validation of a reverse-phase high performance liquid chromatography method for determination of exenatide in poly(lactic-co-glycolic acid) microspheres. Chem. Res. Chinese U. **2010**, 26, 33-37.
210. Chen, Y., Barkley, M.D. Toward understanding tryptophan fluorescence in protein, Biochemistry, **1998**, 37, 9976-9982.
211. Sanchez-Machado, D.I., Chavira-Willys, B., Lopez-Cervantes, J. High-performance liquid chromatography with fluorescence detection for quantitation of tryptophan and tyrosine in a shrimp waste protein concentrate. J. Chromatogr. B. **2008**, 863: 88-93.
212. Watson, J.T., Sparkman, O.D. Introduction of mass spectrometry: Instrumentation, applications and strategies for data interpretation. (4th Ed.), John Wiley and Sons Ltd, West Sussex, England. **2007**.
213. Yates, J.R., Ruse, C.I., Nakorchevsky, A. Proteomics by mass spectrometry: approaches, advances, and applications. Annu. Rev. Biomed. Eng. **2009**, 11: 49-79.
214. Fenn, J.B., Mann, M., Meng, C.K., Wong, S.F., Whitehouse, C.M. Electrospray ionization for mass spectrometry of large biomolecules. Science. **1989**, 246, 64-71.
215. Schlüter, H., Jankowski, J., Rykl, J., Thiemann, J., Belgardt, S., Zidek, W., Wittmann, B., Pohl, T. Detection of protease activities with the mass-spectrometry-assisted enzyme-screening (MES) system. Anal. Bioanal. Chem. **2003**, 377: 1102-1107.
216. Kebarle, P. A brief overview of the present status of the mechanisms involved in electrospray mass spectrometry. J. Mass Spectrom. **2000**, 35: 804-817.
217. Ho, C.S., Lam, C.W.K., Chan, M.H.M., Cheung, R.C.K., Law, L.K., Lit, L.C.W., Ng, K.F., Suen, M.W.M., Tai, H.L. Electrospray ionisation mass spectrometry: principles and clinical applications. Clin. Biochem. Rev. **2003**, 24: 3-12.
218. Gohlke, H., Klebe, G. Approaches to the description and prediction of the binding affinity of small-molecule ligands to macromolecular receptors. Angew. Chem. Int. Ed. **2002**, 41: 2644-2676.
219. Kuntz, I.D., Blaney, J.M., Oatley, S.J., Langridge, R., Ferrin, T.E. A geometric approach to macromolecule-ligand interactions. J. Mol. Biol. **1982**, 161: 269-288.
220. Nadendla, R.R. Molecular modeling: A powerful tool for drug design and molecular docking. Resonance. **2004**, 9: 51-60.
221. Redhu, S., Jindal, A. Molecular modelling: A new scaffold for drug design. Int. J. Pharm. Pharm. Sci. **2013**, 5: Suppl 1:5-8.
222. Mortier, J., Rakers, C., Frederick, R., Wolber, G. Computational tools for in silico fragment-based drug design, Curr. Topics in Med. Chem. **2012**, 12: 1935-1943.
223. Hua, J., Huang, K-L. A reversed phase HPLC method for the analysis of nucleotides to determine 5'-PDE enzyme activity. Bull. Chem. Soc. Ethiop. **2010**, 24: 167-174.

REFERENCES

224. Shrimpton, C.N., Abbenante, G., Lew, R.A., Smith, A.I. Development and characterization of novel potent and stable inhibitors of endopeptidase EC3.4.24.15. *Biochem. J.* **2000**, 345: 351-356.
225. Ferrie, J.J., Gruskos, J.J., Goldwaser, A.L., Decker, M.E., Guarracino, D.A. A comparative protease stability study of synthetic macrocyclic peptides that mimic two endocrine hormones. *Bioorg. Med. Chem. Lett.* **2013**, 23: 989-995.
226. Jones, G., Willett, P., Glen, R.C. Molecular recognition of receptor sites using a genetic algorithm with a description of desolvation. *J. Mol. Biol.* **1995**, 245: 43-53. doi: 10.1016/S0022-2836(95)80037-9
227. G., Willett, P., Glen, R.C., Leach, A.R., Taylor, R. Development and validation of a genetic algorithm for flexible docking. *J. Mol. Biol.* **1997**, 267: 727-748. doi: 10.1006/jmbi.1996.0897
228. Fujinaga, M., Cherney, M.M., Tarasova, N.I., Bartlett, P.A., Hanson, J.E., James, M.N.G. Structural study of the complex between human pepsin and a phosphorus-containing peptidic -transition-state analog. *Acta Crystallogr. D Biol. Crystallogr.* **2000**, 56: 272-279.
229. Brady, K., Abeles, R.H. Inhibition of chymotrypsin by peptidyltrifluoromethyl: determinants of slow-binding kinetics. *Biochemistry* **1990**, 29: 7608-7617.
230. Rick, W. α -Chymotrypsin: measurements with N-benzoyl-L-tyrosine ethyl ester as substrate: In methods of enzymatic analysis, 2nd ed., Academic press Inc., New York. **1974**, pp 1009-1012.
231. Schellenberger, V., Jakubke, H.D. A spectrophotometric assay for the characterization of the S' subsite specificity of alpha-chymotrypsin. *Biochim. Biophys. Acta.* **1986**, 869: 54-60.
232. Schellenberger, V., Turck, C.W., Rutter, W.J. Role of the S' subsites in serine protease catalysis-active-site mapping of rat chymotrypsin, rat trypsin, alpha-lytic protease, and cercarial protease from *Schistosoma-Mansoni*. *Biochemistry.* **1994**, 33: 4251-4257.
233. Ye, S., Loll, B., Berger, A.A., Mülrow, U., Alings, C., Wahl, M., Koks, B. Fluorine teams up with water to restore inhibitor activity to mutant BPTI. *Chem. Sci.* **2014**, submitted.
234. Antal, J., Pál, G., Asbóth, B., Buzás, Z., Patthy, A., Gráf, L. Specificity assay of serine proteinases by reverse-phase high-performance liquid chromatography analysis of competing oligopeptide substrate library. *Anal. Biochem.* **2001**, 288: 156-167. doi:10.1006/abio.2000.4886
235. Erickson, J.A., McLoughlin, J.I. Hydrogen bond donor properties of the difluoromethyl group. *J. Org. Chem.* **1995**, 60: 1626-1631. doi: 10.1021/jo00111a021
236. Zhou, P., Tian, F., Lv, F., Shang, Z. Geometric characteristics of hydrogen bonds involving sulfur atoms in proteins. *Proteins.* **2009**, 76: 151-163. doi: 10.1002/prot.22327
237. Schlosser, M. Parametrization of Substituents: Effects of fluorine and other heteroatoms on OH, NH, and CH acidities. *Angew. Chem. Int. Ed.* **1998**, 37: 1496-1513.
238. Cornish-Bowden, A.J., Knowles, J.R. The pH-dependence of pepsin-catalysed reactions. *Biochem. J.* **1969**, 113: 353-362.

REFERENCES

239. Kageyama, T. Pepsinogens, progastricsins, and prochymosins: structure, function, evolution, and development. *Cell Mol. Life Sci.* **2002**, 59: 288-306.
240. Dunn, B.M. Structure and mechanism of the pepsin-like family of aspartic peptidases. *Chem. Rev.* **2002**, 102: 4431-4458.
241. Dunn, B.M., Jimenez, M., Parten, B.F., Valler, M.J., Rolph, C.E., Kay, J. A systematic series of synthetic chromophoric substrates for aspartic proteinases. *Biochem. J.* **1986**, 237: 899-906.
242. Dunn, B.M., Valler, M.J., Rolph, C.E., Foundling, S.I., Jimenez, M., Kay, J. The pH dependence of the hydrolysis of chromogenic substrates of the type, Lys-Pro-Xaa-Yaa-Phe-(NO₂) Phe-Arg-Leu, by selected aspartic proteinases: evidence for specific interactions in subsites S3 and S2. *Biochim. Biophys. Acta.* **1987**, 913: 122-130.
243. Dunn, B.M., Hung, S. The two sides of enzyme-substrate specificity: lessons from the aspartic proteinases. *Biochim. Biophys. Acta.* **2000**, 1477: 231-240.
244. Mortier J. Modeling and molecular dynamics simulations conducted in **2012-2013**.
245. Georgieva, D., Genov, N., Voelter, W., Betzel, C. Catalytic efficiencies of alkaline proteinases from microorganisms. *Zeitschrift fur Naturforschung. C, J. of Biosciences* **2006**, 61: 445-452.
246. <http://www.aminolab-pharma.com/in-vitro.asp>
247. Welch, J.T., Eswarakrishnan, S. Fluorine in bioorganic chemistry. John Wiley and Sons, New York, **1991**.
248. Keil, C., Maskos, K., Than, M., Hoopes, J.T., Huber, R., Tan, F., Deddish, P.A., Erdos, E.G., Skidgel, R.A., and Bode, W. Crystal structure of the human carboxypeptidase N (kininase I) catalytic domain, *J. Mol. Biol.* **2007**, 366: 504-516.
249. Naughton, M.A., Sanger, F. Purification and specificity of pancreatic elastase *Biochemical J.* **1961**, 78: 156-163.
250. Shotton, D.M. Elastase. *Methods Enzymol.* **1970**, 19: 113-140.
251. Renaud, A., Lestienne, P., Hughes, D.L. Bieth, J.G., Dimicoli, J.L. Mapping of the S' subsites of porcine pancreatic and human leucocyte elastases. *J. Biol. Chem.* **1983**, 258: 8312-8316.
252. Fauci, A.S. The AIDS epidemic-considerations for the 21st century. *N. Engl. J. Med.* **1999**, 341: 1041-1050.
253. Finzi D., Siliciano R.F. Viral dynamics in HIV-1 infection. *Cell.* **1998**, 93: 665-671.
254. Moore, J. P. and Stevenson, M. New targets for inhibitors of HIV-1 replication. *Nat. Rev. Mol. Cell. Biol.*, **2000**, 1: 40-49
255. Lu, L., Pan, C., Li, Y., Lu, H., He, W., Jiang, S. A bivalent recombination protein inactivates HIV-1 by targeting the gp41 prehairpin fusion intermediate induced by CD4 DID2 domains. *Retrovirology* **2012**, 9: 104. doi:10.1186/1742-4690-9-104
256. Mizuhara, T. Development of novel anti-HIV pyrimidobenzothiazine derivatives, Springer Theses, doi: 10.1007/978-4-431-54445-6_1, Springer Japan **2013**.
257. Jiang, S., Debnath, A.K. Development of HIV entry inhibitors targeted to the coiled-coil regions of gp41. *Biochem. Biophys. Res. Commun.* **2000**, 269: 641-646.
258. Freed, E. O. and Martin, M. A., The role of human immunodeficiency virus type-1 envelope glycoproteins in virus infection. *J. Biol. Chem.* **1995**, 270: 23883-23886.

REFERENCES

259. Chan, D. C., Fass, D., Berger, J. M. and Kim, P. S., Core structure of gp41 from the HIV envelope glycoprotein, *Cell* **1997**, 89: 263-273
260. Esté, J. A., Teleni, A. HIV entry inhibitors. *Lancet* **2007**, 370: 81-88.
261. Chan, D. C., Kim, P. S. HIV entry and its inhibition. *Cell* **1998**, 93: 681-684.
262. De Feo, C.J., Weiss, C.D. Escape from human immunodeficiency virus type 1 (HIV-1) entry inhibitors. *Viruses* **2012**, 4: 3859-3911. doi:10.3390/v4123859
263. Qiu, J., Ashkenazi, A., Liu, S., Shai, Y. Structural and functional properties of the membranotropic HIV-1 glycoprotein gp41 loop region are modulated by its intrinsic hydrophobic core. *J Biol Chem.* **2013**, 288: 29143-29150.
264. Eckert, D.M., Kim, P.S. Mechanisms of viral membrane fusion and its inhibition. *Annu Rev Biochem.* **2001**, 70: 777-810.
265. Fuzeon Product Information, <http://www.fuzeon.com>.
266. Jiang, S., Tala, S.R., Lu, H., Abo-Dya, N.E., Avan, I., Gyanda, K., Lu, L., Katritzky, A.R., Debnath, A.K. Design, synthesis, and biological activity of novel 5-((Arylfuran/1H-pyrrol-2-yl)methylene)-2-thioxo-3-(3-(trifluoromethyl)phenyl)thiazolidin-4-ones as HIV-1 fusion inhibitors targeting gp41. *J. Med. Chem.* **2011**, 54: 572-579.
267. Liu, S., Wu, S., Jiang, S. HIV entry inhibitors targeting gp41: from polypeptides to small-molecule compounds. *Curr. Pharm. Des.* **2007**, 13: 143-162.
268. Dorr, P., Westby, M., Dobbs, S., Griffin, P., Irvine, B., Macartney, M., Mori, J., Rickett, G., Smith-Burchnell, C., Napier, C., et al. Maraviroc (UK-427,857), a potent, orally bioavailable, and selective small-molecule inhibitor of chemokine receptor CCR5 with broad-spectrum anti-human immunodeficiency virus type 1 activity. *Antimicrob. Agents Chemother.* **2005**, 49: 4721-4732.
269. Lalezari, J.P., Henry, K., O'Hearn, M., Montaner, J.S., Piliero, P.J., Trottier, B., Walmsley, S., Cohen, C., Kuritzkes, D.R., Eron, J.J., Jr., et al. Enfuvirtide, an HIV-1 fusion inhibitor, for drug-resistant HIV infection in North and South America. *New Engl. J. Med.* **2003**, 348: 2175-2185.
270. Bird, G. H., Madani, N., Perry, A. F., Princiotta, A. M., Supko, J. G., He, X., Gavathiotis, E., Sodroski, J. G., Walensky, L. D. Hydrocarbon double-stapling remedies the proteolytic instability of a lengthy peptide therapeutic. *Proc. Natl. Acad. Sci. USA.* **2010**, 107: 14093-14098.
271. Lobritz, M.A., Ratcliff, A.N., Arts, E.J. HIV-1 entry, inhibitors, and resistance. *Viruses* **2010**, 2: 1069-1105.
272. Veronese, F. M. Peptide and protein PEGylation: A review of problems and solutions. *Biomaterials* **2001**, 22: 405-417.
273. Caliceti, P., Veronese, F. M. Pharmacokinetic and biodistribution properties of poly(ethylene glycol)-protein conjugates *Adv. Drug Delivery Rev.* **2003**, 55: 1261-1277.
274. Pasut, G., Veronese, F. M. Polymer-drug conjugation, recent achievements and general strategies *Prog. Polym. Sci.* **2007**, 32: 933-961.
275. Klok, H-A. Peptide/protein-synthetic polymer conjugates: quo vadis. *Macromolecules* **2009**, 42: 7990-8000.

REFERENCES

276. Caliceti, P., Salmaso, S., Walker, G., Bernkop-Schnurch, A. Development and in vivo evaluation of an oral insulin-PEG delivery system. *Eur. J. Pharm. Sci.* **2004**, 22: 315-323.
277. Johnson, L.M., Mortenson, D.E., Yun, H.G., Horne, W.S., Ketas, T.J., Lu, M., Moore, J.P., Gellmana, S.H. Enhancement of α -helix mimicry by an α/β -peptide foldamer via incorporation of a dense ionic side-chain array. *J. Am. Chem. Soc.* **2012**, 134: 7317-7320. doi:10.1021/ja302428d.
278. Ling, Y., Xue, H., Jiang, X., Cai, L., Liu, K. Increase of anti-HIV activity of C-peptide fusion inhibitors using a bivalent drug design approach. *Bioorg. and Med. Chem. Lett.* **2013**, 23: 4770-4773.
279. Allen, W.J., Rizzo, R.C. Computer-aided approaches for targeting HIVgp41. *Biology* **2012**, 1: 311-338. doi:10.3390/biology1020311
280. Yu, F., Lu, L., Du, L., Zhu, X., Debnath, A. K., Jiang, S. Approaches for identification of hiv-1 entry inhibitors targeting gp41 pocket. *Viruses* **2013**, 5, 127-149. doi:10.3390/v5010127
281. Nyakatura, E. Studying the interaction profiles of nonnatural amino acids - Towards predicting their specific applications at α -helical interfaces, **2013**. Dissertation FU Berlin www.diss.fu-berlin.de
282. Chong, H., Yao, X., Qiu, Z., Qin, B., Han, R., Waltersperger, S., Wang, M., Cui, S., He, Y. Discovery of critical residues for viral entry and inhibition through structural insight of HIV-1 fusion inhibitor CP621-652. *J. Biological Chemistry.* **2012**, 287: 20281-20289.
283. He, Y., Cheng, J., Li, J., Qi, Z., Lu, H., Dong, M., Jiang, S., Dai, Q. Identification of a critical motif for the human immunodeficiency virus type 1 (HIV-1) gp41 core structure: implications for designing novel anti-HIV fusion inhibitors. *Journal of Virology.* **2008**, 82: 6349-6358.
284. Tan, K., Liu, J., Wang, J., Shen, S., Lu, M. Atomic structure of a thermostable subdomain of HIV-1 gp41. *Proc. Natl. Acad. Sci. U. S. A.* **1997**, 94: 12303-12308.
285. Homola, J., Yee S.S., Gauglitz G. Surface plasmon resonance biosensors. *Optical Biosensors: Present and future* (Ligler, F.S., Rowe Taitt, C.A., et al. eds), Elsevier science, **2002**: 207-251.
286. Fagerstam, LG., Frostell, A., Karlsson, R., Kullman, M., Larsson, A., Malmqvist, M., Butt, H. Detection of antigen-antibody interactions by surface plasmon resonance. Application to epitope mapping. *J. Mol. Recog.* **1990**, 3: 208-214.
287. Ota A, Tanaka-Taya K, Ueda S. Cross-reactivity of anti-HIV-1-p17-derivative peptide (P30-52) antibody to Env V3 peptide. *Hybridoma, PubMed.* **1999**, 18: 149-157.
288. Kumar, S., Maiti, S. The effect of N-acetylation and N-methylation of lysine residue of Tat peptide on its interaction with HIV-1 TAR RNA. *PLoS ONE.* **2013**, 8: e77595. doi:10.1371/journal.pone.0077595
289. Ji, C., Kopetzki, E., Jekle, A., Stubenrauch, K.-G., Liu, X., Zhang, J., Rao, E., Schlothauer, T., Fischer, S., Cammack, N., Heilek, G., Ries S., Sankuratri, S. CD4-anchoring HIV-1 fusion inhibitor with enhanced potency and in vivo stability. *J. Biol. Chem.* **2009**, 284: 5175-5185. doi: 10.1074/jbc.M808745200.

REFERENCES

290. Wang, H., Qi, Z., Guo, A., Mao, Q., Lu, H., An, X., Xia, C., Li, X., Debnath, A.K., Wu, S. *Antimicrob. Agents Chemother.* **2009**, 53: 4987-4998.
291. Kovacs, J.M., Nkololac, J.P., Penga, H., Cheung, A., Perry, J. Miller, C.A., Seamanc, M.S., Barouch, D.H., Chen, Bing. HIV-1 envelope trimer elicits more potent neutralizing antibody responses than monomeric gp120. *Proc. Natl. Acad. Sci. USA.* **2012**, 109: 12111-12116. doi:10.1073/pnas.1204533109
292. Rich, R.L., Myszka, D.G. Spying on HIV with SPR. *Trends in Microbiology* **2003**, 11: 124-133. doi:10.1016/S0966-842X(03)00025-8
293. Welch, B.D., Van Demark, A.P., Heroux, A., Hill, C.P., Kay, M.S. Potent D-peptide inhibitors of HIV-1 entry. *Proc. Natl. Acad. Sci. USA* **2007**, 104: 16828-16833.
294. Danial, M., van Dulmen, T.H.H., Aleksandrowicz, J., Pötgens, A.J.G., Klok, H-A. Site-specific PEGylation of HR2 peptides: Effects of PEG conjugation position and chain length on HIV-1 membrane fusion inhibition and proteolytic degradation. *Bioconjugate Chem.* **2012**, 23: 1648-1660.
295. Bianchi, E., Joyc, J.G., Miller, M.D., Finnefrock, A.C., Liang, X., Finotto, M., Ingallinella, P., McKenna, P., Citron, M., Ottinger, E. Hepler, R.W., Hrin, R., Nahas, D., Wu, C., Montefiori, D., Shiver, J.W., Pessi, A., Kim, P.S. Vaccination with peptide mimetics of the gp41 prehairpin fusion intermediate yields neutralizing antisera against HIV-1 isolates. *Proc. Natl. Acad. Sci. USA* **2010**, 107, 10655-10660. doi: 10.1073/pnas.1004261107
296. Li, C., Pazgier, M., Li, J., Li, C., Liu, M., Zou, G., Li, Z., Chen, J., Tarasov, S.G., Lu, W.Y., Lu, W. Limitations of peptide retro-inverso isomerization in molecular mimicry. *J. Biol. Chem.* **2010**, 285: 19572-19581. doi: 10.1074/jbc.M110.116814
297. Alam, S.M., Paleos, C.A., Liao, H.X., Searce, R., Robinson, J., Haynes, B.F. An inducible HIV type 1 gp41 HR-2 peptide-binding site on HIV type 1 envelope gp120. *AIDS Res. Hum. Retroviruses.* **2004**, 20: 836-845.
298. Tam, J., Yu, Q. A facile ligation approach to prepare three-helix bundles of HIV fusion-state protein mimetics. *Org. Lett.* **2002**, 4: 4167-4170.
299. Nomura, W., Hashimoto, C., Ohya, A., Miyauchi, K., Urano, E., Tanaka, T., Narumi, T., Nakahara, T., Komano, J.A., Yamamoto, N., Tamamura, H. A synthetic C34 trimer of HIV-1 gp41 shows significant increase in inhibition potency. *ChemMedChem* **2012**, 7: 205.
300. Fasting, C., Schalley, C.A., Weber, M., Seitz, O., Hecht, S., Kokschi, B., Dervedde, J., Graf, C., Knapp, E-W., Haag, R. Multivalency as a chemical organization and action principle. *Angew. Chem. Int. Ed.* **2012**, 51: 10472-10498.
301. Asante, V., Mortier, J., Wolber, G., Kokschi, B. Impact of fluorination on proteolytic stability of peptides: a case study with α -chymotrypsin and pepsin. *Amino acids.* **2014**. doi: 10.1007/s00726-014-1819-7
302. Shenoy, D., Fu, W., Li, J., Crasto, C., Jones, G., DiMarzio, C., Sridhar, S., Amiji, M. Surface functionalization of gold nanoparticles using hetero-bifunctional poly(ethylene glycol) spacer for intracellular tracking and delivery. *Int. J. Nanomed.* **2006**, 1: 51-57. doi:10.2147/nano.2006.1.1.51

REFERENCES

303. Seitz, O., Kunz, H. HYCRON, an allylic anchor for high-efficiency solid phase synthesis of protected peptides and glycopeptides. *J. Org. Chem.* **1997**, 62: 813-826. doi: 10.1021/jo960743w
304. Wosnick, J.H., Mello, C.M., Swager, T.M. Synthesis and application of poly(phenylene ethynylene)s for bioconjugation: A conjugated polymer-based fluorogenic probe for proteases. *J. Am. Chem. Soc.* **2005**, 127: 3400-3405. doi: 10.1021/ja043134b
305. Herzner, H., Kunz, H. Spacer-separated sialyl LewisX cyclopeptide conjugates as potential E-selectin ligands. *Carbohydr. Res.* **2007**, 342: 541-557.
306. Miller, M.L., Roller, E.E., Zhao, R.Y., Leece, B.A., Ab, O., Baloglu, E., Goldmacher, V.S., Chari, R.V.J. Synthesis of taxoids with improved cytotoxicity and solubility for use in tumor-specific delivery. *J. Med. Chem.* **2004**, 47: 4802-4805.
307. Schoenhentz, J. PhD thesis: "Synthesis of perfluoroalkylated mucin-like glycolipopeptides for the purpose of multivalent antigen presentation" **2012**. Johannes Gutenberg-Universität Mainz.
308. Liu, Y., Shipton, M.K., Ryan, J., Kaufman, E.D., Franzen, S., Feldheim, D.L. Synthesis, stability, and cellular internalization of gold nanoparticles containing mixed peptide-poly(ethylene glycol) monolayers. *Anal. Chem.* **2007**, 79: 2221- 2229.
309. Bartz, M., Kuther, J., Nelles, G., Weber, N., Seshadri, R., Tremel, W. Monothiols derived from glycols as agents for stabilizing gold colloids in water: synthesis, self assembly and use as crystallization templates. *J. Mater. Chem.* **1999**, 9: 1121-1125.
310. Tsushima, T., Kawada, K., Ishihara, S., Uchida, N., Shiratori, O., Higaki, J., Hirata, M., *Tetrahedron* **1988**, 44: 5375-5387.
311. Chiu, H.-P., Suzuki, Y., Gullickson, D., Ahmad, R., Kokona, B., Fairman, R., Cheng, R.P. *J. Am. Chem. Soc.* **2006**, 128: 15556-15557.
312. Winkler, D., Burger, K. Synthesis of enantiomerically pure D- and L-armentomycin and its difluoro analogues from aspartic acid. *Synthesis.* **1996**, 1419-1421.
313. Fridkin, M., Patchornik, A. Peptide synthesis. *Annu. Rev. Biochem.* **1974**, 43: 419-443.
314. Vincent, H.L., Satish, D.K., George, M.G., Werner, R. Oral route of protein and peptide drug delivery. In: Vincent HL (Ed.) *Peptide and protein drug delivery*. Marcel Dekker, New York. **1991**, 691-738.
315. Shaji, J., Patole, V. Protein and peptide drug delivery: oral approaches. *Indian J. Pharm. Sci.* **2008**, 70: 269-277.
316. Berman, H.L., Westbrook, J., Feng, Z., Gilliland, G., Bhat, T.N., Weissig, H., Shindyalov, I.N., Bourne, P.E. The protein data bank. *Nucl. Acids Res.* **2000**, 28: 235-242.
317. Tsukada, H., Blow, D.M. Structure of α -chymotrypsin refined at 1.6 Å resolution. *J. Mol. Biol.* **1985**, 184: 703-711.
318. Chen, L., Erickson, J.W., Rydel, T.J., Park, C.H., Neidhart, D., Luly, J., Abad-Zapatero, C. Structure of a pepsin/renin inhibitor complex reveals a novel crystal packing induced by minor chemical alterations in the inhibitor. *Acta. Crystallogr. B.* **1992**, 48: 476-88.
319. Wolber, G., Dornhofer, A.A., Langer, T. Efficient overlay of small molecules using 3-D pharmacophores. *J. Comput-Aid. Mol. Des.* **2006**, 20: 773-788. doi:10.1007/s10822-006-9078-7

REFERENCES

320. Wolber, G., Langer, T. LigandScout: 3-D Pharmacophores derived from protein-bound ligands and their use as virtual screening filters. *J. Chem. Inf. Model.* **2005**, 45: 160-169. doi:10.1021/ci049885e
321. Seidel, T., Ibis, G., Bendix, F., Wolber, G. Strategies for 3D pharmacophore-based virtual screening. *Drug Discov. Today Technol.* **2010**, 7: 221-228. doi:10.1016/j.ddtec.2010.11.004